CONFIDENTIAL

UNCLASSIFIED

Studies in Radar Cross-Sections - XVII

Complete Scattering Matrices and Circular Polarization Cross-Sections for the B-47 Aircraft at S-Band (U)

by A. L. Maffett, M. L. Barasch, W. E. Burdick, R. F. Goodrich, W. C. Orthwein, C. E. Schensted, and K. M. Siegel

Contract AF 33(616)-2531

June 1955

2260-6-T

2260-6-T = RL-2046

The University of Michigan
Engineering Research Institute
Willow Run Laboratories
Willow Run Airport
Ypsilanti, Michigan

UNCLASSIFIED

CONFIDENTIAL

This document contains information affecting the national defense of the United States within the meaning of the Espionage Laws, (Title 18 U. S. C., Sections 793 and 794). Its transmission or the revelation of its contents in any manner to an unauthorized person is prohibited by law.

CONFIDENTIAL

STUDIES IN RADAR CROSS-SECTIONS

I Scattering by a Prolate Spheroid, F.V. Schultz (UMM-42, March 1950), W(038)-ac-14222. UNCLASSIFIED

II The Zeros of the Associated Legendre Functions $P_n^m(\mu')$ of Non-Integral Degree, K.M. Siegel, D.M. Brown, H.E. Hunter, H.A. Alperin, and C.W. Quillen (UMM-82, April 1951), W-33(038)-ac-14222. UNCLASSIFIED

III Scattering by a Cone, K.M. Siegel and H.A. Alperin (UMM-87, January 1952), AF 30(602)-9. UNCLASSIFIED

IV Comparison Between Theory and Experiment of the Cross-Section of a Cone, K.M. Siegel, H.A. Alperin, J.W. Crispin, H.E. Hunter, R.E. Kleinman, W.C. Orthwein, and C.E. Schensted (UMM-92, February 1953), AF 30(602)-9. UNCLASSIFIED

V An Examination of Bistatic Early Warning Radars, K.M. Siegel (UMM-98, August 1952), W-33(038)-ac-14222. SECRET

VI Cross-Sections of Corner Reflectors and Other Multiple Scatterers at Microwave Frequencies, R.R. Bonkowski, C.R. Lubitz, and C.E. Schensted (UMM-106, October 1953), AF 30(602)-9. SECRET (UNCLASSIFIED when Appendix is removed)

VII Summary of Radar Cross-Section Studies Under Project Wizard, K.M. Siegel, J.W. Crispin, and R.E. Kleinman (UMM-108, November 1952), W-33(038)-ac-14222. SECRET

VIII Theoretical Cross-Sections as a Function of Separation Angle Between Transmitter and Receiver at Small Wavelengths, K.M. Siegel, H.A. Alperin, R.R. Bonkowski, J.W. Crispin, A.L. Maffett, C.E. Schensted, and I.V. Schensted (UMM-115, October 1953), W-33(038)-ac-14222. UNCLASSIFIED

IX Electromagnetic Scattering by an Oblate Spheroid, L.M. Rauch (UMM-116, October 1953), AF 30(602)-9. UNCLASSIFIED

X The Radar Cross-Section of a Sphere, H. Weil (2144-6-T, to be published), DA 36(039)SC-52654. UNCLASSIFIED

XI The Numerical Determination of the Radar Cross-Section of a Prolate Spheroid, K.M. Siegel, B.H. Gere, I. Marx, and F.B. Sleator (UMM-126, December 1953), AF 30(603)-9. UNCLASSIFIED

XII Summary of Radar Cross-Section Studies Under Project MIRO, K.M. Siegel, M.E. Anderson, R.R. Bonkowski, and W.C. Orthwein (UMM-127, December 1953), AF 30(602)-9. SECRET

XIII Description of a Dynamic Measurement Program, K.M. Siegel and J.M. Wolf (UMM-128, May 1954) W-33(038)-ac-14222. CONFIDENTIAL

XIV Radar Cross-Section of a Ballistic Missile, K.M. Siegel, M.L. Barasch, J.W. Crispin, I.V. Schensted, W.C. Orthwein, and H. Weil (UMM-134, September 1954), W-33(038)-ac-14222. SECRET

XV Radar Cross-Sections of B-47 and B-52 Aircraft, C.E. Schensted, J.W. Crispin, and K.M. Siegel (2260-1-T, August 1954), AF 30(616)-2531. CONFIDENTIAL

XVI Microwave Reflection Characteristics of Buildings, H. Weil, R.R. Bonkowski, T.A. Kaplan, and M. Leichter (2255-12-T, May 1955), AF 30(602)-1070. SECRET

XVII Complete Scattering Matrices and Circular Polarization Cross-Sections for the B-47 Aircraft at S-Band, A.L. Maffett, M.L. Barasch, W.E. Burdick, R.F. Goodrich, W.C. Orthwein, C.E. Schensted, and K.M. Siegel, (2260-6-T, June 1955), AF 33(616)-2531. CONFIDENTIAL

UNCLASSIFIED

CONFIDENTIAL

CONFIDENTIAL UNCLASSIFIED

TABLE OF CONTENTS

(Unclassified)

UNCLASSIFIED

CONFIDENTIAL

TABLE OF CONTENTS (Continued)

LIST OF FIGURES

(Unclassified)

LIST OF FIGURES (Continued)

LIST OF FIGURES (Continued)

LIST OF FIGURES (Continued)

LIST OF FIGURES (Continued)

LIST OF FIGURES (Continued)

LIST OF TABLES

NOMENCLATURE

(AB) - arbitrary polarization basis

$\vec{a}$ - radius vector of constant magnitude

$\hat{b}$ - unit vector along the body axis

c - velocity of light

$\hat{d}$ - unit vector along an electric dipole

$\vec{E}$ - electric field vector

$\vec{E}_{\hat{k}}$ - electric field vector propagating in the direction k

$\vec{E}^s, \vec{E}^i$ - scattered and incident electric field vectors

$F(\xi), G(\xi)$ - Fock's current distribution functions

H - horizontal polarization

$\vec{H}$ - magnetic field vector

$\vec{H}_{\hat{k}}$ - magnetic field vector propagating in the direction k

$\vec{H}^s, \vec{H}^i$ - scattered and incident magnetic field vectors

$H_\mu^{(1)}(z), H_\mu^{(2)}(z)$ - Hankel functions of the first and second kinds

I, J - arbitrary polarization indices

i - imaginary element, $\sqrt{-1}$

$\hat{i}$ - unit vector along the x-axis

$\hat{i}^*$ - unit vector along the x^*-axis

$\hat{j}$ - unit vector along the y-axis

$\hat{j}^*$ - unit vector along the y^*-axis

$K_\mu^{(2)}$ - modified Hankel function, $-i\frac{\pi}{2} e^{-i\mu\frac{\pi}{2}} H_\mu(ze^{-i\frac{\pi}{2}})$

k - wave number, $k = 2\pi/\lambda$

NOMENCLATURE (Continued)

$\hat{k}$ - unit vector along the z-axis, or in the direction of propagation

k^* - unit vector along the z^*-axis

$\vec{k}$ - vector wave number, $k\hat{k}$

L - left circular polarization

$\hat{n}$ - unit vector normal to a surface

$\hat{n}_w$ - unit vector normal to the wing

$\hat{n}_b$ - unit vector normal to a body

$\hat{p}(A), \hat{p}(B)$ - unit vectors forming the polarization basis (AB)

R - right circular polarization

R - radial distance

R_o - radius of curvature

R_w - radius of curvature of the wing

R_b - radius of curvature of the body

r - radial distance

$\hat{r}$ - unit radius vector

$\vec{r}$ - radius vector

$S(\hat{k}, \hat{k}')$ - scattering matrix referred to the directions of propagation

S(AB;A'B') - back scattering matrix referred to the polarization bases (AB) and (A'B')

s(IJ) - scattering matrix element

U(AB;A'B') - 2 × 2 unitary transformation referred to the polarization bases (AB) and (A'B')

u(IJ) - matrix element of U

V - vertical polarization

NOMENCLATURE (Continued)

$w(\xi)$ - Airy integral

x, y, z - Cartesian coordinates

α - angle

α = (IJ), β = (I'J'), polarization "pairs"

β - angle

γ - angle

θ - angle

$\theta(IJ)$ - phase of the scattering matrix element s(IJ)

$\theta, \theta^{\star}$ - polar angles

Λ - left elliptical polarization

λ - wavelength

ξ - reduced length measured from the shadow boundary

P - right elliptical polarization

$\sigma(IJ)$ - cross-section referred to the polarizations I and J

ϕ, ϕ_o - angles

$\phi, \phi^{\star}$ - azimuthal angles

ψ - solution of the scalar wave equation

ω - angular frequency, $2\pi c/\lambda$

$\otimes$ - direct (or Kronecker) matrix product

PREFACE

(Unclassified)

This paper is the seventeenth in a series of reports growing out of Studies in Radar Cross-Sections at the Engineering Research Institute of The University of Michigan. The primary aims of this program are:

1. To show that radar cross-sections can be determined analytically.
2. To elaborate means for computing cross-sections of objects of military interest.
3. To demonstrate that these theoretical cross-sections are in agreement with experimentally determined values.

Intermediate objectives are:

1. To compute the exact theoretical cross-sections of various simple bodies by solution of the appropriate boundary-value problems arising from Maxwell's equations.
2. To examine the various approximations possible in this problem, and determine the limits of their validity and utility.
3. To find means of combining the simple body solutions in order to determine the cross-sections of composite bodies.
4. To tabulate various formulas and functions necessary to enable such computations to be done quickly for arbitrary objects.
5. To collect, summarize, and evaluate existing experimental data.

Titles of the papers already published or presently in process of publication are listed on the back of the title page.

K. M. Siegel

PART I--THEORY

1

INTRODUCTION AND SUMMARY

(Confidential)

This is the seventeenth in a series of reports aimed primarily at finding the radar cross-sections of aircraft. In the fifteenth report in this series (Ref. 1), the monostatic radar cross-sections of B-47 and B-52 aircraft were found for horizontal and vertical polarizations at seven different wavelengths. This report contains the natural extension of the methods employed in Reference 1 to methods of finding the monostatic radar cross-sections of aircraft at any polarization, and specifically to finding the circular polarization cross-section of a B-47 aircraft at a wavelength of 0.4 ft $\cong$ 12 cm (S-band).

The present report is a companion report to Reference 1. Hence, much of the notation and some of the computations are common to both reports.

There are two Parts to this report. Part I deals with the theory of finding the scattering matrices and the cross-polarization cross-sections for certain simple geometric shapes which approximate aircraft parts (e.g., wedges and loops). It is shown that the cross-polarization cross-section for arbitrary incident and received polarization can be obtained from nine basic cross-polarization cross-sections. Furthermore, it is shown how the cross-sections obtained for the simple geometric shapes can be combined to obtain the cross-polarization cross-sections for a complex body such as the B-47.

In Section A of Part II, the methods of Part I are used to find the monostatic S-band cross-polarization radar cross-sections

$$\sigma(HH),\ \sigma(VV),\ \sigma(HV),\ \sigma(LH),\ \sigma(LV),$$

$$\sigma(+H),\ \sigma(+V),\ \sigma(LR),\ \sigma(\Delta P),\ \sigma(RR),\ \sigma(LL),$$

of a B-47 aircraft. The results are presented graphically.

These graphs are shown to be in good agreement with results of recent dynamic experiments made by the Hughes Aircraft Company (Part II, Sec. B), and indicate the amount of degradation to be expected for a B-47, using circular polarization on a clear day.

The interest in cross-polarization radar cross-sections has been fostered in part by much recent dynamic radar cross-section measurement which utilized circular polarization as a means of ground clutter rejection, and as a means of improving aircraft discrimination in rain; indeed, with regard to the latter point, it has long been postulated (e.g., Ref. 2) that in rain, snow, and cloud cover a circularly polarized radar could obtain higher signal-to-noise ratios than a linearly polarized radar when viewing complex targets. In Section C of Part II there is a discussion of experiments by the Airborne Instruments Laboratory (Ref. 3), The Ohio State University (Ref. 4), Lincoln Laboratory of the Massachusetts Institute of Technology (Ref. 5), and the Raytheon Manufacturing Company (Ref. 18), all of which deal with comparisons of returns from real and simulated weather and from aircraft, using circularly and linearly polarized radiation. These experiments indicate that circularly polarized energy yields minimum reflection from rain and maximum discrimination of jet aircraft in rain.

2

SCATTERING MATRICES

(Unclassified)

The scattering of electromagnetic radiation may be described quite generally as follows: For simplicity, assume an incident plane wave and choose a coordinate system such that the negative z-axis is in the direction of propagation of the incident wave (Fig. 2-1). Since the incident electric and magnetic vectors lie in a plane perpendicular to the direction of propagation, the incident radiation is completely specified in free space by the direction of propagation and the x- and y-components of either the electric or magnetic fields. After impinging on an obstacle the scattered radiation in the "far zone" is then completely determined by the configuration of the scatterer, its electrical properties, and by the incident radiation. If $\hat{k}_o$ is a unit vector in the direction of the incident wave, and $\hat{k}$ is a unit vector in the direction in which the scattered wave is observed, the far field in the direction $\hat{k}$ is determined by the type of obstacle and the incident radiation, or, in symbols,

$$\vec{E}^{s}_{\hat{k}} = S(\hat{k}, \hat{k}_o)\, \vec{E}^{i}_{\hat{k}_o} \quad , \tag{2-1}$$

where $\vec{E}^{i}_{\hat{k}_o}$ is the incident field moving in the direction $\hat{k}_o$, $\vec{E}^{s}_{\hat{k}}$ is the scattered field moving in the direction $\hat{k}$, and $S(\hat{k}, \hat{k}_o)$ is a matrix with continuous indices $\hat{k}$ and $\hat{k}_o$ which depends on the obstacle and the wavelength of the radiation. From its analog in quantum mechanics, the matrix S is called the scattering matrix or, more briefly, S-matrix.

2.1 SCATTERED FIELD IN S-MATRIX NOTATION

If the coordinate system is rotated such that the new z-axis lies along the direction $\hat{k}$, the incident field will be specified by three components, but the scattered field in the direction $\hat{k}$ will be specified simply by the x- and y-components since the radiation field is transverse. Symbolically, this rotation R is expressed as

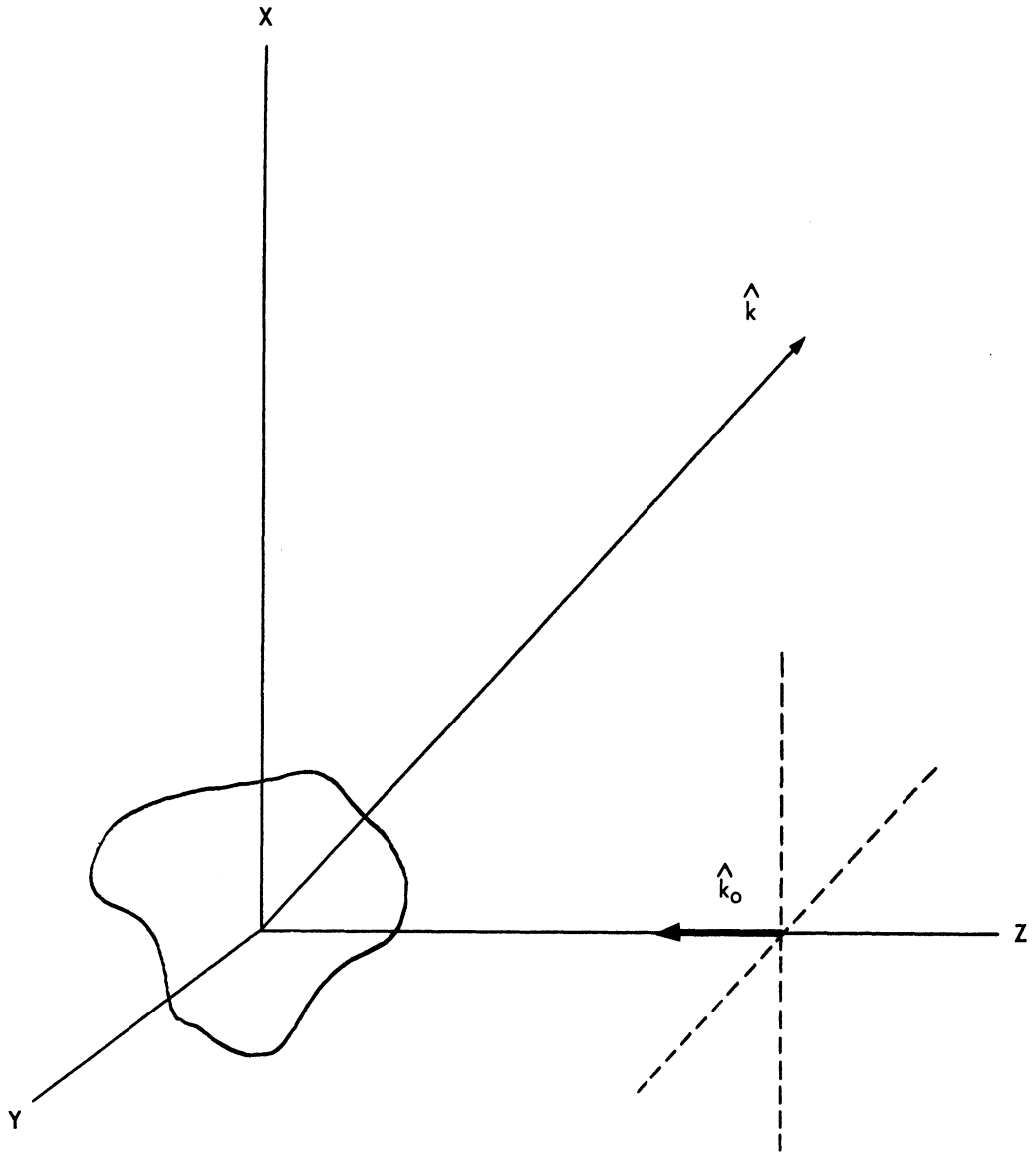

FIG. 2-1 ASSUMED GEOMETRY FOR $\hat{k}$ AND $\hat{k}_o$

$$R\,\vec{E}^{s}_{\hat{k}} = \begin{pmatrix} \alpha \\ \beta \\ 0 \end{pmatrix} = R\,S(\hat{k},\ \hat{k}_o)\,R^{-1}\left(R\,\vec{E}^{i}_{\hat{k}_o}\right) \quad . \tag{2.1-1}$$

An immediate condition on the new S-matrix RSR^{-1} is then that it lead to zero z-component of the scattered field.

The maximum advantage of using the S-matrix notation is obtained when circularly or elliptically polarized incident radiation is considered. Before going into this, however, it is desirable to give a brief review of the polarization phenomenon.

Consider a plane wave moving along the z-axis as in Figure 2.1-1. If the electric vector is restricted to lie in one plane through the z-axis, say the yz-plane, the wave is said to be plane or linearly polarized since the projection of the locus of the electric vector on the xy-plane is a straight line.

If the electric vector is no longer required to lie in a single plane, then its projection on the xy-plane will no longer be a straight line but will in general describe an ellipse in time as shown in Figure 2.1-2. The case of circular polarization occurs when the ellipse degenerates into a circle as shown in Figure 2.1-3.

In particular, for back-scattering, $\hat{k} = -\hat{k}_o$. An incident elliptically polarized field can be expressed in terms of Cartesian coordinates and hence, as before:

$$\vec{E}^{s}_{-\hat{k}_o} = S(-\hat{k}_o,\ \hat{k}_o)\,\vec{E}^{i}_{\hat{k}_o} \quad . \tag{2.1-2}$$

It is possible to express the fields in terms of an elliptic basis by a coordinate transformation, U, such that

$$\vec{\mathcal{E}}^{i}_{\hat{k}_o} = U\,\vec{E}^{i}_{\hat{k}_o} \quad , \tag{2.1-3}$$

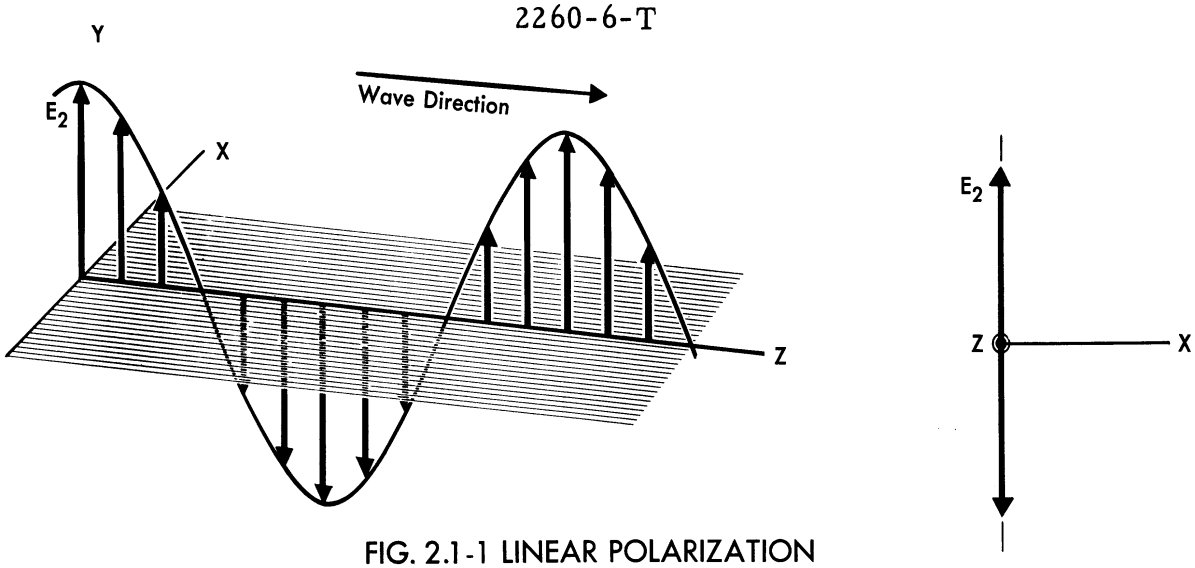

FIG. 2.1-1 LINEAR POLARIZATION

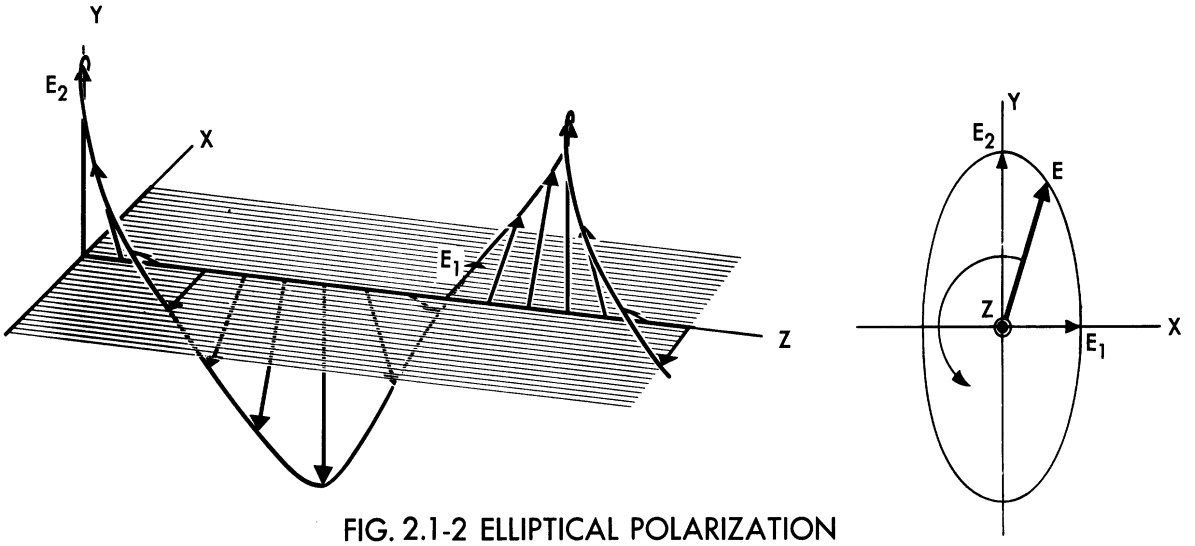

FIG. 2.1-2 ELLIPTICAL POLARIZATION

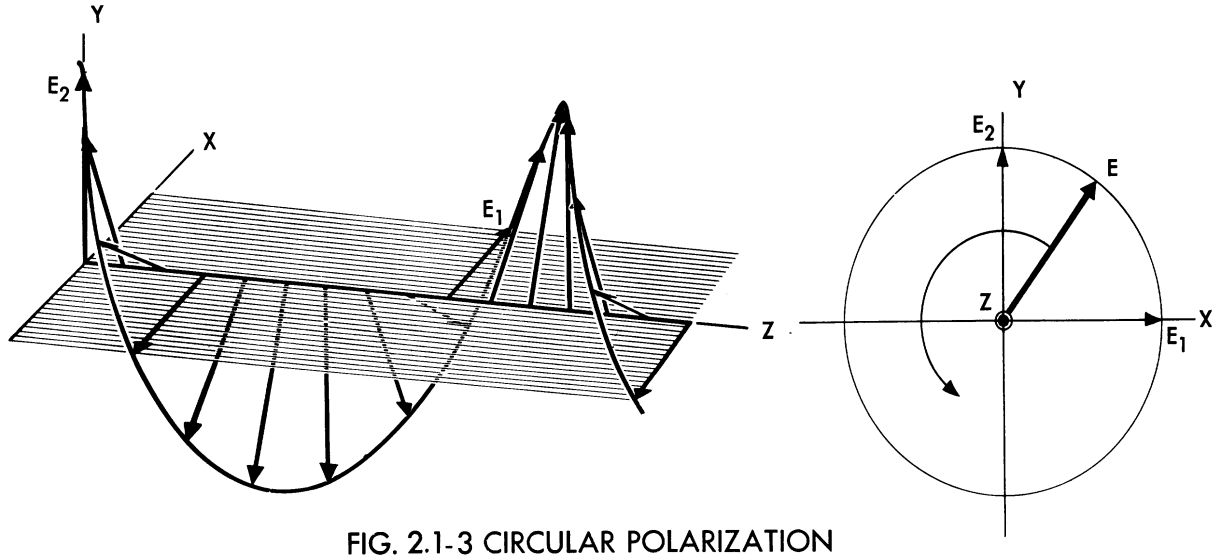

FIG. 2.1-3 CIRCULAR POLARIZATION

where $\vec{\varepsilon}^{\,i}$ is the incident vector in an elliptic basis. Then

$$\vec{E}^{\,s}_{-\hat{k}_o} = S(-\hat{k}_o, \hat{k}_o)\, U^{-1}\, U\, \vec{E}^{\,i}_{\hat{k}_o} = S(-\hat{k}_o, \hat{k}_o)\, U^{-1}\, \vec{\varepsilon}^{\,i}_{\hat{k}_o} \quad . \tag{2.1-4}$$

The scattered field is transformed by the same transformation so that in the elliptic basis,

$$\vec{\varepsilon}^{\,s}_{-\hat{k}_o} = U\, \vec{E}^{\,s}_{-\hat{k}_o} = U\, S(-\hat{k}_o, \hat{k}_o)\, U^{-1}\, \vec{\varepsilon}^{\,i}_{\hat{k}_o} \quad . \tag{2.1-5}$$

This then gives a new scattering matrix $U\,S\,U^{-1}$ which is used for the case in which the incident and scattered fields are referred to an elliptic basis. Since the fields describing the incident and back-scattered radiation lie in the same plane the two-dimensional transformation U gives the change of basis from linear to elliptic for both the incident and back scattered fields.

Thus, by using the S-matrix formalism, it is necessary to determine only the scattering for linear polarization and the transformation giving the change of basis to the particular basis of interest.

2.2 S-MATRIX IN TERMS OF FIXED BUT ARBITRARY BASIS

In order to be explicit, let $\hat{p}(H)$ and $\hat{p}(V)$ be unit orthogonal vectors; these vectors define, respectively, directions of horizontal[1] and vertical polarization of an electric vector. A vector $\vec{E}$ may be written in terms of this basis as

$$\vec{E} = E(H)\,\hat{p}(H) + E(V)\,\hat{p}(V) = \Big(E(H),\ E(V)\Big) \begin{pmatrix} \hat{p}(H) \\ \hat{p}(V) \end{pmatrix} = E'(HV)\,\hat{p}(HV),$$

where $E'(HV)$ designates the transpose of the column $\begin{pmatrix} E(H) \\ E(V) \end{pmatrix}$.

[1]Horizontal will mean tangent to the earth with horizontal, vertical, and direction of propagation being mutually orthogonal.

If $\hat{p}(A)$ and $\hat{p}(B)$ are an arbitrary pair of unit orthogonal[1] vectors co-planar with $\hat{p}(H)$ and $\hat{p}(V)$, then they must be obtainable from $\hat{p}(H)$ and $\hat{p}(V)$ by a unitary transformation[2]

$$\begin{pmatrix} u(AH) & u(AV) \\ u(BH) & u(BV) \end{pmatrix} = U(AB;\, HV),\quad U^{-1}(AB;\, HV) = U^{*\prime}(AB;\, HV) = U(HV;\, AB),$$

i.e., $\hat{p}(AB) = U(AB;\, HV)\, \hat{p}(HV)$, where the asterisk indicates complex conjugate of each element of the matrix and the prime indicates the transpose of the matrix.

Since the AB system will in general be used to describe some elliptical polarization, it is preferable to use distinct systems of unit vectors to specify the incident and scattered fields. This is done so that right-hand elliptical polarization may have the same sense with regard to the coordinate system for incident radiation as it does with regard to the coordinate system for scattered radiation. So if

$$\hat{p}^{i}(AB) = U(AB;\, HV)\, \hat{p}(HV)$$

is prescribed for the incident system, the desired similarity of sense for the two coordinate systems is accomplished by writing

$$\hat{p}^{s}(AB) = U^{*}(AB;\, HV)\, \hat{p}(HV)$$

for the scattered system. Thus $\hat{p}^{s}(AB) = \hat{p}^{i*}(AB)$.

---

[1]Orthogonal is to be interpreted in the sense that two vectors $\hat{p}(A)$ and $\hat{p}(B)$ are orthogonal if their product $\hat{p}(A) \cdot \hat{p}^{*}(B)$ is zero, where the asterisk indicates complex conjugate; unit in the sense that a vector $\hat{p}(A)$ is a unit vector if the product $\hat{p}(A) \cdot \hat{p}^{*}(A)$ is 1.

[2]$u(IJ)$ is defined by the product $u(IJ) = \hat{p}(I) \cdot \hat{p}^{*}(J)$. Note here also that $u^{*}(IJ) = u(JI)$.

An incident vector $\vec{E}^i$ may be written in terms of either the basis $\hat{p}(HV)$ or the basis $\hat{p}^i(AB)$:

$$\vec{E}^i = E'^i(HV)\,\hat{p}(HV) = E'^i(AB)\,\hat{p}^i(AB).$$

From this relation it easily follows that the two sets of components of $\vec{E}^i$ are connected by

$$E^i(AB) = U^*(AB;\,HV)\,E^i(HV). \qquad (2.2\text{-}1a)$$

Similarly for a scattered vector $\vec{E}^s$ the relation between components is

$$E^s(AB) = U(AB;\,HV)\,E^s(HV). \qquad (2.2\text{-}1b)$$

Since both the incident and scattered electric vectors are expressible in terms of either unit vector basis, there will be four transformations, i.e., scattering matrices, relating the components of the incident vector for either basis to the components of the scattered vector for either basis.

$$E^s(HV) = S(HV;\,HV)\,E^i(HV), \qquad (2.2\text{-}2)$$

$$E^s(AB) = S(AB;\,HV)\,E^i(HV), \qquad (2.2\text{-}3)$$

$$E^s(HV) = S(HV;\,AB)\,E^i(AB), \qquad (2.2\text{-}4)$$

$$E^s(AB) = S(AB;\,AB)\,E^i(AB), \qquad (2.2\text{-}5)$$

where the two subscripts in front of, and following, the semicolon indicate respectively rows and columns of the scattering matrix. For example, if Equation (2.2-3) were written in detail, it would read[1]

$$\begin{pmatrix} E^s(A) \\ E^s(B) \end{pmatrix} = \begin{pmatrix} s(AH) & s(AV) \\ s(BH) & s(BV) \end{pmatrix} \begin{pmatrix} E^i(H) \\ E^i(V) \end{pmatrix}.$$

[1] In $s(IJ)$, $\hat{p}(J)$ designates the incident polarization.

The elements of these matrices are associated with effective radar cross-section σ by the following definition:

$$\sigma = \lim_{r \to \infty} 4\pi r^2 \left| \frac{\vec{E}^s \cdot \hat{p}}{\vec{E}^i} \right|^2 , \qquad (2.2\text{-}6)$$

where $\hat{p}$ is a unit vector denoting receiver polarization. For example, if $\vec{E}^i = \hat{p}(H)$ and $\hat{p} = \hat{p}(V)$, then

$$\vec{E}^s = E^s(H)\,\hat{p}(H) + E^s(V)\,\hat{p}(V) = s(HH)\,\hat{p}(H) + s(VH)\,\hat{p}(V) ,$$

and

$$\sigma(VH) = \lim_{r \to \infty} 4\pi r^2 \left| \frac{\vec{E}^s \cdot \hat{p}(V)}{\hat{p}(H)} \right|^2 = \lim_{r \to \infty} 4\pi r^2 \left| s(VH) \right|^2 . \qquad (2.2\text{-}7a)$$

In a similar fashion it can be shown that

$$\sigma(IJ) = \lim_{r \to \infty} 4\pi r^2 \left| s(IJ) \right|^2 . \qquad (2.2\text{-}7b)$$

These $\sigma(IJ)$ will be called CROSS-POLARIZATION cross-sections.

Using Equation (2.2-1) in conjunction with Equations (2.2-2) through (2.2-5), it follows that any three of the scattering matrices can be expressed in terms of the fourth. Thus, for example,

$$S(AB; HV) = U(AB; HV)\, S(HV; HV)\, U^*(HV; HV), \qquad (2.2\text{-}8)$$

$$S(HV; AB) = U(HV; HV)\, S(HV; HV)\, U^*(HV; AB), \qquad (2.2\text{-}9)$$

$$S(AB; AB) = U(AB; HV)\, S(HV; HV)\, U^*(HV; AB).^{1} \qquad (2.2\text{-}10)$$

[1] More generally, $S(AB; JK) = U(AB; HV)\, S(HV; HV)\, U^*(HV; JK)$, where JK indicates an arbitrary basis. $U(HV; HV)$ and $U^*(HV; HV)$ have been included above for consistency. (They are each equal to the identity matrix).

This means that if S(HV; HV) is known completely any scattering matrix can be calculated from it. Since the elements of S(HV; HV) are complex numbers, there will be eight real numbers (four magnitudes, four phases) required to specify S(HV; HV) completely. This is reduced from eight to seven because only relative phase differences can be calculated. It is further reduced to five for back-scattering because of the reciprocity theorem[1] and the conservation of energy principle[2].

To recapitulate, assume that $|s(HH)|$, $|s(HV)|$, $|s(VV)|$, $|s(AH)|$, $|s(AV)|$ are known; from these quantities the differences of phases (or relative arguments) of s(HH), s(HV), s(VH), and s(VV) can be determined, i.e., the complete matrix

$$S(HV;\,HV) = \begin{pmatrix} s(HH) & s(HV) \\ s(VH) & s(VV) \end{pmatrix} \qquad (2.2\text{-}11)$$

can be found.

---

[1]If $\vec{E}_1^i$ and $\vec{E}_2^i$ are two given incident electric vectors, and $\vec{E}_1^s$ and $\vec{E}_2^s$ are the respective scattered electric vectors, then the reciprocity theorem states that

$$\vec{E}_1^s \cdot \vec{E}_2^i = \vec{E}_2^s \cdot \vec{E}_1^i \quad , \text{ or}$$

$$E_1^s(H)\, E_2^i(H) + E_1^s(V)\, E_2^i(V) = E_2^s(H)\, E_1^i(H) + E_2^s(V)\, E_1^i(V).$$

If Equation (2.2-2) is used to state this theorem entirely in terms of the components of the incident vectors, it follows that

$$s(HV)\left(E_1^i(V)\, E_2^i(H) - E_2^i(V)\, E_1^i(H)\right) = s(VH)\left(E_1^i(V)\, E_2^i(H) - E_2^i(V)\, E_1^i(H)\right) \quad ,$$

or

$$s(HV) = s(VH).$$

From this equality and Equations (2.2-8), (2.2-9), and (2.2-10), it follows that s(IJ) = s(JI) for $I \neq J$.

[2]Because energy must be conserved it follows that

$$\sigma(KA) + \sigma(KB) = \sigma(KH) + \sigma(KV),$$

where K may be H, V, A, or B.

Since s(IJ) and u(IJ) may be written:

$$s(IJ) = \left|s(IJ)\right| e^{i\theta(IJ)} ,$$
$$u(IJ) = \left|u(IJ)\right| e^{i\phi(IJ)} , \qquad (2.2\text{-}12)$$

it follows from Equation (2.2-8) that

$$\left|s(AH)\right|^2 = \left|u(AH)\,s(HH) + u(AV)\,s(VH)\right|^2$$
$$= \left|u(AH)\,s(HH)\right|^2 + \left|u(AV)\,s(VH)\right|^2 + 2\left|u(AH)\,u(AV)\,s(HH)\,s(VH)\right|$$
$$\times \cos\left[\theta(HH) - \theta(VH) + \phi(AH) - \phi(AV)\right] . \qquad (2.2\text{-}13)$$

Therefore,

$$\cos\left[\theta(HH) - \theta(VH) + \phi(AH) - \phi(AV)\right] = \frac{\left|s(AH)\right|^2 - \left|u(AH)\,s(HH)\right|^2 - \left|u(AV)\,s(VH)\right|^2}{2\left|u(AH)\,u(AV)\,s(HH)\,s(VH)\right|} , \qquad (2.2\text{-}14)$$

where $\theta(IJ) = \arg s(IJ)$ and $\phi(IJ) = \arg u(IJ)$.

Similarly,

$$\cos\left[\theta(HV) - \theta(VV) + \phi(AH) - \phi(AV)\right] = \frac{\left|s(AV)\right|^2 - \left|u(AH)\,s(HV)\right|^2 - \left|u(AV)\,s(VV)\right|^2}{2\left|u(AH)\,u(AV)\,s(HV)\,s(VV)\right|} . \qquad (2.2\text{-}15)$$

An expression for the difference $\theta(HH) - \theta(VV)$ may be obtained from Equations (2.2-14) and (2.2-15). A check for this difference can be obtained by assuming that $\sigma(AA)$ is known; then the difference $\theta(HH) - \theta(VV)$ can be calculated directly as a function of $\left|s(AA)\right|$, $\left|s(HH)\right|$, $\left|s(VV)\right|$, and the u(IJ).

The above argument may be summarized in the theorem: If $\sigma(HH)$, $\sigma(HV)$, $\sigma(VV)$, $\sigma(AH)$, and $\sigma(AV)$ are given, then the matrix S(HV; HV) can be determined to within an arbitrary phase factor; and from S(HV; HV) any scattering matrix can be found.

3

APPROACH TO THE MULTIPLE-COMPONENT BODY PROBLEM

(Unclassified)

In Section 2 it was shown that for a single simple geometric shape, or a complex shape considered as a unit, the scattering matrix S(HV ; HV) can be completely specified from a knowledge of the five radar cross-sections σ(HH), σ(HV), σ(VV), σ(AH), and σ(AV).

However, in an analytic treatment of the scattering matrix for a complex configuration consisting of many components, each of which is a simple geometric shape, a somewhat different approach must be used since component-wise calculation of cross-sections does not furnish information as to phase differences between different parts of the target. It is reasonable to assume that for each component of the scattering body expressions for certain of the s(IJ) may be obtained directly from expressions for the scattered fields in terms of the incident fields. Then, to find certain σ(IJ) [to be given below] as fairly smooth functions of aspect, and to minimize computational labor, an average with respect to phase is made over the set of components of the scatterer. Such an averaging procedure assumes random phase relations among scattered fields of the components, and requires a knowledge of nine[1] real numbers for the determination of arbitrary σ(IJ).

That only nine real numbers are needed may be seen as follows: Let

$$s(IJ) = \big(u(IH)\ u(IV)\big)\ S(HV\ ;\ HV) \begin{pmatrix} u^{*}(HJ) \\ u^{*}(VJ) \end{pmatrix} \qquad (3\text{-}1)$$

represent, for the entire scattering body, any of the linear relations among elements indicated by Equations (2.2-8), (2.2-9), or (2.2-10). The

[1]By the reciprocity relation; without reciprocity, 16 real numbers would have to be known.

averaged quantity $\overline{\left|s(IJ)\right|^2}$ is then

$$\overline{\left|s(IJ)\right|^2} = \overline{s(IJ)\, s^*(IJ)}$$

$$= \left(u(IH)u(IV)\right) \otimes \left(u^*(IH)u^*(IV)\right) \overline{S(HV\,;\,HV) \otimes S^*(HV\,;\,HV)}$$

$$\begin{pmatrix} u^*(HJ) \\ u^*(VJ) \end{pmatrix} \otimes \begin{pmatrix} u(HJ) \\ u(VJ) \end{pmatrix} \qquad (3\text{-}2)$$

where $\otimes$ indicates a direct (or Kronecker) matrix product[1, 2] and the bar indicates phase-averaged matrix elements. Let α, β denote any of the values HH, HV, VH, VV; if $s(\alpha) = \sum_m s_m(\alpha)$ where the sum is taken over the set of components of the entire scattering body, then the expressions $\overline{s(\alpha)s^*(\beta)}$ in the right hand member of Equation (3-2) are given by

---

[1]The definition of a direct (or Kronecker) matrix product is illustrated by the example

$$\begin{bmatrix} a_{11} & a_{12} & a_{13} \\ a_{21} & a_{22} & a_{23} \end{bmatrix} \otimes \begin{bmatrix} b_{11} & b_{12} \\ b_{21} & b_{22} \end{bmatrix} = \begin{bmatrix} a_{11}b_{11} & a_{11}b_{12} & a_{12}b_{11} & a_{12}b_{12} & a_{13}b_{11} & a_{13}b_{12} \\ a_{11}b_{21} & a_{11}b_{22} & a_{12}b_{21} & a_{12}b_{22} & a_{13}b_{21} & a_{13}b_{22} \\ a_{21}b_{11} & a_{21}b_{12} & a_{22}b_{11} & a_{22}b_{12} & a_{23}b_{11} & a_{23}b_{12} \\ a_{21}b_{21} & a_{21}b_{22} & a_{22}b_{21} & a_{22}b_{22} & a_{23}b_{21} & a_{23}b_{22} \end{bmatrix}$$

[2]In Equation (3-2) the following theorem has been used:

$$(ABC) \otimes (DEF) = (A \otimes D)(B \otimes E)(C \otimes F)$$

where A, B, C, D, E, F are matrices of suitable dimensions. As applied in Equation (3-2) it should be noted that $s(IJ)s^*(IJ) = s(IJ) \otimes s^*(IJ)$.

$$\overline{s(\alpha)s^{*}(\beta)} = \overline{\sum_{m,n} s_m(\alpha)s_n^{*}(\beta)} = \sum_{m,n} \overline{s_m(\alpha)s_n^{*}(\beta)}$$

$$= \sum_{m,n} \left| s_m(\alpha)s_n(\beta) \right| \overline{e^{\,i\left[\theta_m(\alpha) - \theta_n(\beta)\right]}} \,. \qquad (3\text{-}3)$$

Since it is assumed that random phase relations obtain among scattered fields of the components, the last sum is zero for $m \neq n$. Hence, Equation (3-3) becomes

$$\overline{s(\alpha)s^{*}(\beta)} = \sum_{n} s_n(\alpha)s_n^{*}(\beta) \,. \qquad (3\text{-}4)$$

Thus to obtain an element of the form $\overline{|s(IJ)|^2} = \overline{\sigma(IJ)}$ it is necessary and sufficient to know a certain set of quantities $s_n(\alpha)s_n^{*}(\beta)$ for each component. Since α and β may take any of the values HH, HV, VH, VV it will be necessary to know a set of six quantities, three of which are real, three complex (Eq. 3-5).

The matrix

$$\overline{S(HV\,;\,HV) \otimes S^{*}(HV\,;\,HV)}$$

$$= \begin{bmatrix} \overline{s(HH)s^{*}(HH)} & \overline{s(HH)s^{*}(HV)} & \overline{s(HV)s^{*}(HH)} & \overline{s(HV)s^{*}(HV)} \\ \overline{s(HH)s^{*}(VH)} & \overline{s(HH)s^{*}(VV)} & \overline{s(HV)s^{*}(VH)} & \overline{s(HV)s^{*}(VV)} \\ \overline{s(VH)s^{*}(HH)} & \overline{s(VH)s^{*}(HV)} & \overline{s(VV)s^{*}(HH)} & \overline{s(VV)s^{*}(HV)} \\ \overline{s(VH)s^{*}(VH)} & \overline{s(VH)s^{*}(VV)} & \overline{s(VV)s^{*}(VH)} & \overline{s(VV)s^{*}(VV)} \end{bmatrix} \qquad (3\text{-}5)$$

is of course not a scattering matrix. It is made up of the direct product of two scattering matrices, and will be called an $\overline{S \otimes S^{*}}$ - MATRIX.

Assuming reciprocity, and taking into account that $[s_n(\alpha)s_n^*(\beta)]^* = s_n^*(\alpha)s_n(\beta)$, it follows from Equations (3-4) and (3-5) that is necessary and sufficient to know the six numbers

$$s_n(HH)s_n^*(HH),\quad s_n(VH)s_n^*(VH),\quad s_n(VV)s_n^*(VV),$$

$$s_n(HH)s_n^*(VH),\quad s_n(HH)s_n^*(VV),\quad s_n(VV)s_n^*(VH)$$

for each n (component of the body) in order to determine an $\overline{S \circledast S^*}$ - matrix and hence the elements $\overline{|s(IJ)|^2}$.

A numerical example of an $\overline{S \circledast S^*}$ - matrix and of its use in finding arbitrary cross-polarization radar cross-sections is given in Part II, Section A.4.

4

INDEPENDENT CROSS-SECTIONS APPROPRIATE TO MULTIPLE-COMPONENT BODIES

(Unclassified)

It was shown in Section 3 that $\overline{\sigma(IJ)}$ could be obtained from the independent set $\overline{|s(HH)|^2}$, $\overline{|s(HV)|^2}$, $\overline{|s(VV)|^2}$, $\overline{s(HH)\,s^*(HV)}$, $\overline{s(HV)\,s^*(VV)}$, and $\overline{s(VV)\,s^*(HH)}$. In this section it will be shown how $\overline{\sigma(IJ)}$ can be obtained from a basic set of nine average effective cross-sections.

To do so, it is necessary to determine the most general set of basis vectors $\hat{p}(A)$, $\hat{p}(B)$, in terms of $\hat{p}(H)$ and $\hat{p}(V)$. The orthogonality of $\hat{p}(A)$ and $\hat{p}(B)$ requires that $\hat{p}(A) \cdot \hat{p}^*(A) = 1$ and $\hat{p}(B) \cdot \hat{p}^*(B) = 1$. The most general vectors satisfying these requirements are:

$$\hat{p}(A) = e^{i\phi_1} \cos\alpha\, \hat{p}(H) + e^{i\phi_2} \sin\alpha\, \hat{p}(V) \quad ,$$

$$\hat{p}(B) = -e^{i\phi_3} \sin\beta\, \hat{p}(H) + e^{i\phi_4} \cos\beta\, \hat{p}(V) \quad .$$

There is the additional requirement $\hat{p}(A) \cdot \hat{p}^*(B) = 0$, or

$$-e^{i(\phi_1 - \phi_3)} \cos\alpha \sin\beta + e^{i(\phi_2 - \phi_4)} \sin\alpha \cos\beta = 0.$$

Thus, $\phi_1 - \phi_3 = \phi_2 - \phi_4$, and $\alpha = \beta$[1]. The values of the cross-sections $\sigma(AJ)$ and $\sigma(BJ)$ are not affected by multiplying $\hat{p}(A)$ and $\hat{p}(B)$ by $e^{-i\phi_1}$ and $e^{-i\phi_3}$ respectively. As a result, the most general basis vectors which need be considered are of the form

$$\hat{p}(A) = \cos\alpha\, \hat{p}(H) + e^{i\gamma} \sin\alpha\, \hat{p}(V) \quad ,$$

$$\hat{p}(B) = -\sin\alpha\, \hat{p}(H) + e^{i\gamma} \cos\alpha\, \hat{p}(V) \quad . \qquad (4\text{-}1)$$

[1]Actually there are other solutions but they do not result in increased generality.

The corresponding transformation matrices are:

$$U(AB;\,HV) = \begin{pmatrix} \cos\alpha & e^{i\gamma}\sin\alpha \\ -\sin\alpha & e^{i\gamma}\cos\alpha \end{pmatrix} ;\; U(HV;\,AB) = \begin{pmatrix} \cos\alpha & -\sin\alpha \\ e^{-i\gamma}\sin\alpha & e^{-i\gamma}\cos\alpha \end{pmatrix}. \tag{4-2}$$

Using Equations (2.2-8), (2.2-9), and (2.2-10), it follows that

$$s(AH) = \cos\alpha\, s(HH) + e^{i\gamma}\sin\alpha\, s(HV),$$

$$s(AV) = \cos\alpha\, s(HV) + e^{i\gamma}\sin\alpha\, s(VV),$$

$$s(AB) = -\frac{1}{2}\sin 2\alpha\, s(HH) + e^{i\gamma}\cos 2\alpha\, s(HV) + \frac{1}{2}e^{2i\gamma}\sin 2\alpha\, s(VV)\ . \tag{4-3}$$

Taking the squares of the magnitudes of Equation (4-3) yields:

$$\begin{aligned}
|s(AH)|^2 &= \cos^2\alpha\,|s(HH)|^2 + \sin^2\alpha\,|s(HV)|^2 + \sin 2\alpha\cos\gamma\ \mathrm{Re}\, s^*(HH)\, s(HV) \\
&\quad - \sin 2\alpha\sin\gamma\ \mathrm{Im}\, s^*(HH)\, s(HV), \\
|s(AV)|^2 &= \cos^2\alpha\,|s(HV)|^2 + \sin^2\alpha\,|s(VV)|^2 + \sin 2\alpha\cos\gamma\ \mathrm{Re}\, s^*(HV)\, s(VV) \\
&\quad - \sin 2\alpha\sin\gamma\ \mathrm{Im}\, s^*(HV)\, s(VV), \\
|s(AB)|^2 &= \frac{1}{4}\sin^2 2\alpha\,|s(HH)|^2 + \cos^2 2\alpha\,|s(HV)|^2 + \frac{1}{4}\sin^2 2\alpha\,|s(VV)|^2 \\
&\quad - \frac{1}{2}\sin 4\alpha\cos\gamma\ \mathrm{Re}\, s^*(HH)\, s(HV) + \frac{1}{2}\sin 4\alpha\sin\gamma\ \mathrm{Im}\, s^*(HH)\, s(HV) \\
&\quad - \frac{1}{2}\sin^2 2\alpha\cos 2\gamma\ \mathrm{Re}\, s^*(HH)\, s(VV) + \frac{1}{2}\sin^2 2\alpha\sin 2\gamma\ \mathrm{Im}\, s^*(HH)\, s(VV) \\
&\quad + \frac{1}{2}\sin 4\alpha\cos\gamma\ \mathrm{Re}\, s^*(HV)\, s(VV) - \frac{1}{2}\sin 4\alpha\sin\gamma\ \mathrm{Im}\, s^*(HV)\, s(VV)\ ,
\end{aligned} \tag{4-4}$$

where Re and Im refer respectively to the real and imaginary part of the quantity they precede.

The squares of the magnitudes of the other elements are obtained from the conservation of energy relations, together with the reciprocity relation s(IJ) = s(JI):

$$|s(BH)|^2 = |s(HH)|^2 + |s(HV)|^2 - |s(AH)|^2$$

$$|s(BV)|^2 = |s(HV)|^2 + |s(VV)|^2 - |s(AV)|^2$$

$$|s(AA)|^2 = |s(AH)|^2 + |s(AV)|^2 - |s(AB)|^2$$

$$|s(BB)|^2 = |s(BH)|^2 + |s(BV)|^2 - |s(AB)|^2 \quad . \qquad (4\text{-}5)$$

For $\alpha = 45^\circ$, $\gamma = 90^\circ$, let A = L and B = R. For $\alpha = 45^\circ$, $\gamma = 0^\circ$, let A = + and B = -. For $\alpha = 45^\circ$, $\gamma = 45^\circ$, let A = Λ, B = P. The polarizations H, V, L, R, +, -, Λ, P, being considered are shown in Figure 4-1.

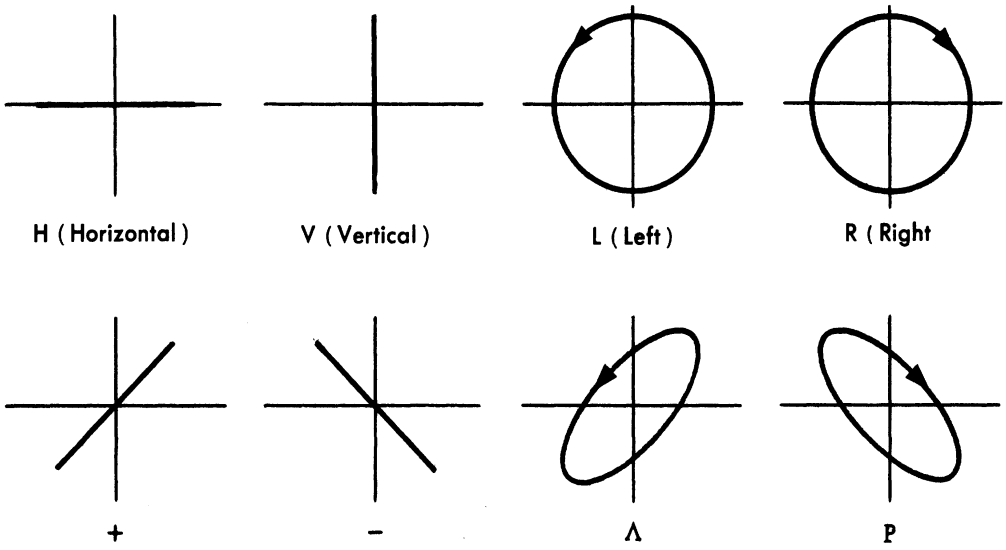

FIG. 4-1 POLARIZATIONS H, V, L, R, +, −, Λ, P

Then it follows from Equation (4-4) that

$$|s(LH)|^2 = \frac{1}{2}|s(HH)|^2 + \frac{1}{2}|s(HV)|^2 - \text{Im } s^*(HH)\, s(HV)$$

$$|s(LV)|^2 = \frac{1}{2}|s(HV)|^2 + \frac{1}{2}|s(VV)|^2 - \text{Im } s^*(HV)\, s(VV)$$

$$|s(LR)|^2 = \frac{1}{4}|s(HH)|^2 + \frac{1}{4}|s(VV)|^2 + \frac{1}{2}\text{Re } s^*(HH)\, s(VV)$$

$$|s(+H)|^2 = \frac{1}{2}|s(HH)|^2 + \frac{1}{2}|s(HV)|^2 + \text{Re } s^*(HH)\, s(HV)$$

$$|s(+V)|^2 = \frac{1}{2}|s(HV)|^2 + \frac{1}{2}|s(VV)|^2 + \text{Re } s^*(HV)\, s(VV)$$

$$|s(\Lambda P)|^2 = \frac{1}{4}|s(HH)|^2 + \frac{1}{4}|s(VV)|^2 + \frac{1}{2}\text{Im } s^*(HH)\, s(VV) \quad . \qquad (4\text{-}6)$$

If the scattering matrix S(HV; HV) has been obtained, then from S and Equation (4-6), the cross-sections $\sigma(HH)$, $\sigma(HV)$, $\sigma(VV)$, $\sigma(LH)$, $\sigma(LV)$, $\sigma(LR)$, $\sigma(+H)$, $\sigma(+V)$, and $\sigma(\Lambda P)$ can be found. From these nine cross-sections the cross-sections for all other polarization combinations may be obtained by using Equations (4-4), (4-5), and (4-6). Use of Equation (4-6) in Equation (4-4) gives

$$\sigma(AH) = \left[\cos^2\alpha - \frac{1}{2}\sin 2\alpha\,(\sin\gamma + \cos\gamma)\right]\sigma(HH)$$
$$+ \left[\sin^2\alpha - \frac{1}{2}\sin 2\alpha\,(\sin\gamma + \cos\gamma)\right]\sigma(HV)$$
$$+ \sin 2\alpha\cos\gamma\,\sigma(+H) + \sin 2\alpha\sin\gamma\,\sigma(LH) \quad ,$$

$$\sigma(AV) = \left[\cos^2\alpha - \frac{1}{2}\sin 2\alpha(\sin\gamma + \cos\gamma)\right]\sigma(HV)$$
$$+ \left[\sin^2\alpha - \frac{1}{2}\sin 2\alpha(\sin\gamma + \cos\gamma)\right]\sigma(VV)$$
$$+ \sin 2\alpha\cos\gamma\,\sigma(+V) + \sin 2\alpha\sin\gamma\,\sigma(LV) \quad , \qquad (4\text{-}7)$$

$$\sigma(AB) = \frac{1}{4}\sin^2 2\alpha\,(1+\cos 2\gamma - \sin 2\gamma)\left[\sigma(HH)+\sigma(VV)\right]$$

$$+\frac{1}{4}\sin 4\alpha\,(\sin\gamma+\cos\gamma)\left[\sigma(HH)-\sigma(VV)\right]+\frac{1}{2}\sin 4\alpha\cos\gamma\left[\sigma(+V)-\sigma(+H)\right]$$

$$+\frac{1}{2}\sin 4\alpha\sin\gamma\left[\sigma(LV)-\sigma(LH)\right]+\cos^2 2\alpha\,\sigma(HV)+\sin^2 2\alpha\sin 2\gamma\;\sigma(\Lambda P)$$

$$-\sin^2 2\alpha\cos 2\gamma\;\sigma(LR).$$

From Equation (4-5):

$$\sigma(BH) = \sigma(HH) + \sigma(HV) - \sigma(AH)\,,$$

$$\sigma(BV) = \sigma(HV) + \sigma(VV) - \sigma(AV)\,,$$

$$\sigma(AA) = \sigma(AH) + \sigma(AV) - \sigma(AB)\,,$$

$$\sigma(BB) = \sigma(BH) + \sigma(BV) - \sigma(AB); \qquad (4\text{-}8)$$

and by reciprocity,

$$\sigma(HA) = \sigma(AH), \qquad \sigma(HB) = \sigma(BH),$$

$$\sigma(VA) = \sigma(AV), \qquad \sigma(VB) = \sigma(BV),$$

$$\sigma(BA) = \sigma(AB)\,. \qquad (4\text{-}9)$$

Equations (4-7), (4-8), and (4-9) give all of the cross-polarization cross-sections of interest except ones of the form $\sigma(AJ)$ where A and J are polarization vectors from different bases. These can be obtained by using the $\overline{S \otimes S^{*}}$ - matrix defined in the preceding section. The elements of the $\overline{S \otimes S^{*}}$ - matrix can be obtained from Equation (4-6) and the cross-section can be obtained from the $\overline{S \otimes S^{*}}$ - matrix defined in Equation (3-5).

5

POLARIZATION EFFECTS AND THE PHYSICAL OPTICS APPROXIMATION

(Unclassified)

No REPOLARIZATION[1] effects obtain when physical optics is used in computing the monostatic single scattering cross-sections. However, the physical optics approximation does yield repolarization effects for monostatic multiple scattering cross-sections.

Since the assumptions[2,3] of physical optics are employed in this report, according to the methods of Reference 1, to obtain cross-sections for many simple shapes representing component parts of an aircraft, it is necessary to consider the degree to which the physical optics approximation agrees with experiment and with exact solutions when available.

For arbitrary directions of incidence on a general body, if any radius of curvature of the body is of the order of a wavelength in the neighborhood of a stationary phase point, neither the physical optics prediction of no repolarization nor its prediction of magnitude should be accepted without further investigation. Likewise in those cases where any radius of

---

[1]Repolarization is said to occur when S(HV; HV) is not of the form $\begin{pmatrix} q & o \\ o & q \end{pmatrix}$.

[2]A simple and commonly used assumption for a body possessing principal radii of curvature R_1 and R_2 which are everywhere large compared to a wavelength is, as stated in Reference 2, p. 462, that "... the induced currents and fields radiated from any infinitesimal unit of area are very nearly those which would be obtained from the same area if it were part of an infinite plane, tangent to the surface at the location of the element of area. The currents and fields on the surface are determined by the boundary condition that the surface magnetic field is entirely tangential and is twice the tangential component of the magnetic field of the incident wave."

[3]For a detailed discussion of the assumptions of physical optics see Reference 16, p. 9.

curvature is less than the wavelength, the assumptions of physical optics make the results suspect, although other considerations for a particular case may show the results to be quite acceptable. For example, for the Poynting vector incident along the axis of symmetry of a perfectly conducting surface of revolution, the physical optics indications of no repolarization are valid. Such validity may most easily be seen from an analysis of the boundary value problem involved.

Since the boundary conditions may be given in terms of $\vec{E}$ alone, and since $\vec{H}$ is given in terms of $\vec{E}$ by Maxwell's equations, the problem of a perfect conductor may be stated in terms of $\vec{E}$ alone. The wave equation for $\vec{E}$ and the boundary conditions are unchanged by reflection in the plane P containing the incident Poynting vector and the incident electric field. Therefore, to any solution for $\vec{E}^s$ with components normal to P, there must correspond another solution with normal components cancelling these. Since two solutions are impossible by uniqueness, $\vec{E}^s$ must lie in P. Thus there is no repolarization. So the validity of the application of physical optics for the Poynting vector incident along the axis of symmetry of a perfectly conducting surface of revolution will be a question of magnitude only.

It has been observed that for the case of a cone or a paraboloid of revolution with the transmitter and receiver on the axis of symmetry the physical optics answer agrees both with experimental results and with the exact theory, as illustrated in References 7 and 16. Further, it has been found (Ref. 8) that the geometric optics fields for the infinite dihedral agree with the exact fields for dihedral angles of π/n, $n = 1, 2, \ldots$, and that the geometric and physical optics fields are in agreement for these cases.

These results suggest that the physical optics cross-section may be expected to agree fairly well with the exact solution for a wider range of objects than the large-principal-radii criterion would indicate.

It is, of course, not necessary to be limited to the particular method discussed above. A different assumption (as in Kerr's example of the finite cylinder) is that the exact solution for a similar problem (in Kerr's

case the infinite cylinder) may be used as a guide for the assumed field at the surface of the scatterer. It would seem reasonable to expect this solution to be a good approximation as long as it is used advisedly.

Another approximate method has been suggested by Fock (Ref. 9). It is limited only by the restrictions that the scatterer be convex and the radii of curvature be much greater than the wavelength, so that it is applicable to a wide variety of scatterers and will yield both scattered magnitude and polarization information.

For those components of a scattering body to which physical optics applies it may be assumed that the scattering matrix S(HV; HV) has the form

$$S(HV;\,HV) = \begin{pmatrix} 1 & 0 \\ 0 & 1 \end{pmatrix} s(HH)\ . \qquad (5\text{-}1)$$

From this relation the scattering matrices S(LR; HV), S(HV; LR), and S(LR; LR) may be determined from Equations (2.2-8), (2.2-9), (2.2-10), and (4-2) by putting A = L, B = R, $\alpha = 45^{\circ}$ and $\gamma = 90^{\circ}$. The unitary transformation matrices U(LR; HV) and U(HV; LR) involved here are given by [from Equation (4-2) with $\alpha = 45^{\circ}$, $\gamma = 90^{\circ}$] ,

$$U(LR;\,HV) = \frac{1}{\sqrt{2}}\begin{pmatrix} 1 & i \\ -1 & i \end{pmatrix};\quad U(HV;\,LR) = \frac{1}{\sqrt{2}}\begin{pmatrix} 1 & -1 \\ -i & -i \end{pmatrix}. \qquad (5\text{-}2)$$

Hence,

$$S(LR;\,HV) = \begin{pmatrix} 1 & i \\ -1 & i \end{pmatrix}\frac{s(HH)}{\sqrt{2}}\ , \qquad (5\text{-}3a)$$

$$S(HV;\,LR) = \begin{pmatrix} 1 & -1 \\ i & i \end{pmatrix}\frac{s(HH)}{\sqrt{2}}\ , \qquad (5\text{-}3b)$$

$$S(LR;\,LR) = \begin{pmatrix} 0 & -1 \\ -1 & 0 \end{pmatrix} s(HH)\ . \qquad (5\text{-}3c)$$

It follows from Equations (5-3 and 4-6) that, for the nine cross-sections of interest (as given in Sec. 4), the following relations hold where physical optics reasoning is applied:

$$\sigma(HH) = \sigma(VV) = \sigma(LR), \tag{5-4a}$$

$$\sigma(HV) = 0, \quad \left[\sigma(RR) = \sigma(LL) = 0 \text{ also}\right], \tag{5-4b}$$

$$\sigma(LH) = \sigma(LV) = \sigma(+H) = \sigma(+V) = \sigma(\Delta P) = \frac{1}{2}\sigma(HH). \tag{5-4c}$$

6

CROSS-POLARIZATION CROSS-SECTIONS OF WEDGES

(Unclassified)

The trailing edges of wing and tail assemblies of modern aircraft, in particular the B-47 aircraft, are thin and sharp enough to warrant simulation by wedge, or tapered wedge, shapes. Since sharp edges will, in general, give rise to repolarization, such edges are considered in this section.

6.1 GENERAL THEORY

Consider an infinite perfectly conducting wedge whose edge lies along the z-axis and whose intersection with the xy-plane makes an angle ϕ_o with the positive x-axis.

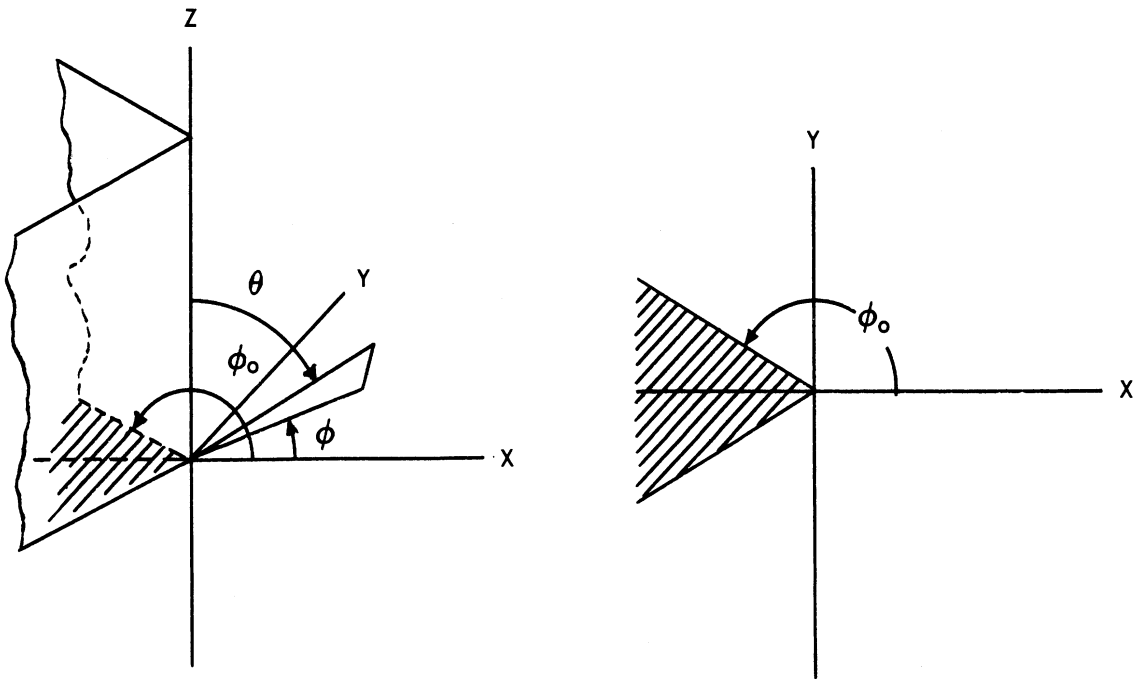

FIG. 6.1-1 WEDGE COORDINATE SYSTEM

To find the total electric field for arbitrary incidence it is necessary to solve the equation[1]

$$(\nabla^2 + k^2)\,\vec{E} = 0, \tag{6.1-1}$$

subject to a radiation condition at infinity and to the conditions

$$\nabla \cdot \vec{E} = 0, \quad \text{in space,} \tag{6.1-2}$$

$$\hat{n} \times \vec{E} = 0, \quad \text{at the body,} \tag{6.1-3}$$

where $\hat{n}$ is a unit exterior normal to the body.

---

[1]In free space the electric and magnetic fields $\vec{E}$ and $\vec{H}$ satisfy Maxwell's equations

$$\nabla \times \vec{E} = -\frac{1}{c}\frac{\partial \vec{H}}{\partial t}, \quad \nabla \cdot \vec{E} = 0 \qquad \nabla \times \vec{H} = \frac{1}{c}\frac{\partial \vec{E}}{\partial t}, \quad \nabla \cdot \vec{H} = 0$$

where c is the velocity of light. These equations can, of course, be reduced to

$$\nabla^2 \vec{E} = \frac{1}{c^2}\frac{\partial^2 \vec{E}}{\partial t^2}, \quad \nabla \cdot \vec{E} = 0 \qquad \nabla^2 \vec{H} = \frac{1}{c^2}\frac{\partial^2 \vec{H}}{\partial t^2}, \quad \nabla \cdot \vec{H} = 0\,.$$

If $\vec{E}$ is time harmonic, i.e., $\vec{E}(x, y, z, t) = \vec{E}(x, y, z)\, e^{-i\omega t}$, the equations for $\vec{E}$ reduce to Equations (6.1-1) and (6.1-2) with

$$k = \frac{\omega}{c} = \frac{2\pi}{\lambda},$$

where λ is wavelength. If the scattering body is perfectly conducting, then $\vec{E}$ obeys Equation (6.1-3).

Let the direction of incidence be restricted to the xy-plane with polarizations (a) perpendicular to, and (b) parallel to the edge of the wedge. Then Equations (6.1-1) and (6.1-2) are satisfied if $\vec{E}$ has the form

$$\hat{k}\,\psi(r,\phi)$$

or

$$-\frac{1}{ik}\,\mathrm{curl}\,\hat{k}\,\psi(r,\phi)\,,$$

where

$$(\nabla^2 + k^2)\;\psi(r,\phi) = 0^1\,. \qquad (6.1\text{-}4)$$

The form $\vec{E} = -1/ik\ \mathrm{curl}\ \hat{k}\,\psi(r,\phi)$ suffices for case (a) with Equation (6.1-3) implying the condition

$$\frac{\partial}{\partial n}\,\psi(r,\pm\phi_o) = 0\,. \qquad (6.1\text{-}5)$$

Case (b) requires the form $\vec{E} = \hat{k}\,\psi(r,\phi)$ with Equation (6.1-3) implying the condition

$$\psi(r,\pm\phi_o) = 0\,. \qquad (6.1\text{-}6)$$

In a recent paper (Ref. 10) F. Oberhettinger obtained expressions for the Green's functions for the wave equation for the conditions (6.1-5) and (6.1-6). Let $Q(\rho, \gamma + \phi_o)$ be the intersection with the xy-plane

---

[1] A cylindrical coordinate system, r, ϕ, z, is used throughout this section. Unit vectors for these directions are $\hat{r}$, $\hat{\phi}$, $\hat{k}$. The unit vector designating polarization perpendicular to the edge of the wedge is $\hat{p}(a) = \hat{\phi}$, and the unit vector designating polarization parallel to the edge of the wedge is $\hat{p}(b) = \hat{k}$.

of a line source parallel to the edge of the wedge and $P(r, \phi + \phi_o)$ be a point outside the wedge. Oberhettinger expresses the incident cylindrical wave in the form

$$\psi_{(i)} = H_o^{(2)}(-kR) = \frac{2i}{\pi} K_o(\beta R) = \frac{2i}{\pi} K_o \left[\beta \left(r^2 + \rho^2 - 2r\rho \cos(\phi - \gamma) \right)^{1/2} \right] \tag{6.1-7}$$

where k has been put equal to $i\beta$. This equation is expanded in the form

$$\psi_{(i)} = \frac{4i}{\pi^2} \int_0^\infty K_{i\zeta}(\beta r) K_{i\zeta}(\beta \rho) \cosh \left[\zeta (\pi - |\phi - \gamma|) \right] d\zeta, \tag{6.1-8}$$

where $K_\mu(Z)$ is the modified Hankel function defined by

$$K_\mu(Z) = -\frac{1}{2} i\pi e^{\frac{-i\mu\pi}{2}} H_\mu^{(2)}\left(Z e^{-\frac{i\pi}{2}} \right).$$

The total field $\psi_{(t)}$ is given as the sum of the incident field $\psi_{(i)}$ and the reflected field ψ:

$$\psi_{(t)} = \psi_{(i)} + \psi . \tag{6.1-9}$$

The reflected field can be represented in a form similar to Equation (6.1-8)

$$\psi = \frac{4i}{\pi^2} \int_0^\infty K_{i\zeta}(\beta r) K_{i\zeta}(\beta \rho) \left[f_1(\zeta) e^{\zeta(\phi + \phi_o)} + f_2(\zeta) e^{-\zeta(\phi + \phi_o)} \right] d\zeta, \tag{6.1-10}$$

where, by using Equations (6.1-8) and (6.1-9), f_1 and f_2 are given by

$$\begin{aligned} f_1(\zeta) - f_2(\zeta) &= -\sinh\left[\zeta(\pi - \gamma - \phi_o) \right] \\ f_1(\zeta)\, e^{2\zeta\phi_o} - f_2(\zeta)\, e^{-2\zeta\phi_o} &= \sinh\left[\zeta(\pi + \gamma - \phi_o) \right] , \end{aligned} \tag{6.1-11}$$

for condition (6.1-5), and by

$$f_1(\zeta) + f_2(\zeta) = -\cosh\left[\zeta(\pi - \gamma - \phi_o)\right]$$
$$f_1(\zeta)\, e^{2\zeta\phi_o} + f_2(\zeta)\, e^{-2\zeta\phi_o} = -\cosh\left[\zeta(\pi + \gamma - \phi_o)\right] , \qquad (6.1\text{-}12)$$

for condition (6.1-6).

To determine radar cross-sections, the reflected fields must be found for conditions (6.1-5) and (6.1-6). In particular for condition (6.1-6) it follows from Equation (6.1-12) that

$$\psi = -\frac{4i}{\pi^2} \int_0^\infty K_{i\zeta}(\beta r) K_{i\zeta}(\beta\rho)\, A(\zeta)\, d\zeta ,$$

where

$$A(\zeta) = \frac{1}{\sinh 2\zeta\phi_o} \left\{ \sinh \zeta\pi \cosh \zeta(\phi + \gamma) + \sinh \zeta(2\phi_o - \pi) \cosh \zeta(\phi - \gamma) \right\}$$

or

$$\psi = i \int_0^\infty e^{-\zeta\pi} H_{i\zeta}^{(1)}(kr) H_{i\zeta}^{(1)}(k\rho)\, A(\zeta)\, d\zeta . \qquad (6.1\text{-}13)$$

If the point $Q(\rho, \gamma + \phi_o)$ defined above is moved to infinity, the Hankel function $H_{i\zeta}^{(1)}(k\rho)$ may be replaced[1] by its asymptotic value

$$\sqrt{\frac{2}{\pi k\rho}}\, e^{ik\rho + \frac{\pi\zeta}{2} - \frac{i\pi}{4}} .$$

[1]This is justified in Section 6.2.

To express Equation (6.1-13) in a manner appropriate to the form $e^{-ikr\cos(\phi-\gamma)}$ for an incoming plane wave, the asymptotic expansion of $H_{i\zeta}^{(1)}(k\rho)$ must be divided by the asymptotic expression

$$-\sqrt{\frac{2}{\pi k\rho}}\, e^{ik\rho - \frac{\pi i}{4} - ikr\cos(\phi-\gamma)}$$

of Equation (6.1-7) and multiplied by $e^{-ikr\cos(\phi-\gamma)}$. Thus Equation (6.1-13) becomes for incident polarization (b) parallel to the edge of the wedge,

$$\psi^{(b)} \approx -i\int_0^\infty e^{-\frac{\zeta\pi}{2}} H_{i\zeta}^{(1)}(kr)\,A(\zeta)\,d\zeta \quad . \tag{6.1-14}$$

If it is further assumed that the value of r is very large, an asymptotic expansion can be substituted for the Hankel function in Equation (6.1-14) giving[1]

$$\psi^{(b)} \approx -\sqrt{\frac{2}{\pi kr}}\, e^{ikr + \frac{\pi i}{4}} \int_0^\infty A(\zeta)\,d\zeta \quad .$$

The remaining integral is convergent and may be evaluated for

$$2\phi_o > \pi + \left|\phi + \gamma\right|$$

$$2\phi_o > \left|2\phi_o - \pi\right| + \left|\phi - \gamma\right|$$

to give (Ref. 11, page 55),

$$\psi^{(b)} \approx -\frac{1}{4\phi_o}\sqrt{\frac{2\pi}{kr}}\, e^{ikr + \frac{\pi i}{4}} \left[\frac{1}{A} + \frac{1}{B}\right] \sin\frac{\pi^2}{2\phi_o} \tag{6.1-15}$$

---

[1]This is justified in Section 6.2.

where $$A = \cos \frac{\pi(\phi + \gamma)}{2\phi_o} + \cos \frac{\pi^2}{2\phi_o}$$

and $$B = \cos \frac{\pi(\phi - \gamma)}{2\phi_o} - \cos \frac{\pi^2}{2\phi_o} \quad .$$

Using condition (6.1-5) and Equation (6.1-11) it can be shown for incident polarization (a) perpendicular to the edge of the wedge that

$$\psi^{(a)} \approx \frac{1}{4\phi_o} \sqrt{\frac{2\pi}{kr}}\, e^{ikr + \frac{\pi i}{4}} \left[\frac{1}{A} - \frac{1}{B}\right] \sin \frac{\pi^2}{2\phi_o} \quad . \qquad (6.1\text{-}16)$$

6.2 REMARK ON THE USE OF ASYMPTOTIC EXPANSIONS OF HANKEL FUNCTIONS IN THE INTEGRAL REPRESENTATION OF THE SCATTERED FIELD FOR A WEDGE

The purpose of this section is the justification of the replacement of the Hankel functions by their asymptotic expansions in the integral

$$\int_0^\infty e^{-\zeta\pi} H_{i\zeta}^{(1)}(kr)\, H_{i\zeta}^{(1)}(k\rho)\, A(\zeta)\, d\zeta \quad . \qquad (6.2\text{-}1)$$

Since the Hankel function $H_{i\zeta}^{(1)}(kr)$ has the representation

$$H_{i\zeta}^{(1)}(kr) = \frac{2\, e^{\frac{\zeta\pi}{2}}}{\pi i} \int_0^\infty e^{ikr \cosh t} \cos \zeta t\, dt, \qquad (6.2\text{-}2)$$

and since the asymptotic form

$$\sqrt{\frac{2}{\pi kr}}\, e^{ikr + \frac{\zeta\pi}{2} - \frac{\pi i}{4}} \quad \text{of} \quad H_{i\zeta}^{(1)}(kr)$$

has the representation

$$\sqrt{\frac{2}{\pi kr}}\, e^{ikr + \frac{\zeta\pi}{2} - \frac{\pi i}{4}} = e^{\frac{\zeta\pi}{2} + \frac{i\pi}{4}}\, H_{1/2}^{(1)}(kr) = \frac{2\, e^{\frac{\zeta\pi}{2}}}{\pi i} \int_0^\infty e^{ikr \cosh t} \cosh \frac{1}{2} t\, dt, \qquad (6.2\text{-}3)$$

it will suffice to consider the problem of obtaining a bound for the expression

$$\left| \int_0^\infty e^{ikr \cosh t} (\cosh t/2 - \cos \zeta t)\, dt \right| . \qquad (6.2\text{-}4)$$

More generally, if f(t) and g(t) are real valued functions such that g(t)/f'(t) is of bounded variation and such that g(∞)/f'(∞) = 0, then

$$\left| \int_0^\infty e^{if(t)} g(t)\,dt - ie^{if(0)} \frac{g(0)}{f'(0)} \right| = \left| \int_0^\infty e^{if(t)} \frac{d}{dt}\left[\frac{g(t)}{f'(t)}\right] dt \right| \le \int_0^\infty \left| \frac{d}{dt}\left[\frac{g(t)}{f'(t)}\right] \right| dt. \qquad (6.2\text{-}5)$$

Taking f(t) = kr cosh t and g(t) = cosh 1/2t - cos ζ t it follows that the problem of bounding the expression (6.2-4) becomes the problem of bounding

$$I = \frac{1}{kr} \int_0^\infty \left| \frac{d}{dt}\left[\frac{\cosh t/2 - \cos \zeta t}{\sinh t}\right] \right| dt; \qquad (6.2\text{-}6)$$

and this is done as follows:

$$kr\, I = \int_0^\infty \left| \frac{\sinh t\left(\frac{1}{2}\sinh\frac{1}{2}t + \zeta \sin \zeta t\right) - \cosh t\left(\cosh\frac{1}{2}t - \cos \zeta t\right)}{\sinh^2 t} \right| dt$$

$$\le \int_0^\infty \frac{\left|\frac{1}{2}\sinh\frac{1}{2}t\right| + \left|\zeta \sin \zeta t\right|}{\sinh t}\, dt + \int_0^\infty \frac{\left|\cosh\frac{1}{2}t - \cos \zeta t\right| \cosh t}{\sinh^2 t}\, dt$$

$$\le \int_0^\infty \frac{\frac{1}{2}\sinh\frac{1}{2}t\, dt}{2\sinh\frac{1}{2}t\cosh\frac{1}{2}t} + \int_0^\infty \frac{\left|\zeta \sin \zeta t\right| dt}{2\sinh\frac{1}{2}t\cosh\frac{1}{2}t}$$

$$+ \int_0^\infty \frac{\left|\cosh\frac{1}{2}t - \cos \zeta t\right| \cosh t\, dt}{\sinh^2 t} = I_1 + I_2 + I_3 . \qquad (6.2\text{-}7)$$

Each of I_1, I_2, I_3 may be either bounded or evaluated in finite form:

$$I_1 = \frac{1}{4}\int_0^\infty \frac{dt}{\cosh\frac{t}{2}} = \frac{\pi}{8} ; \qquad I_2 \le \zeta^2 \int_0^\infty \frac{t\, dt}{t\cosh\frac{1}{2}t} = \frac{\zeta^2\pi}{2} ;$$

$$I_3 = \int_0^\infty \frac{\left(\cosh\frac{1}{2}t - \cos\zeta t\right)\cosh t\, dt}{\sinh^2 t} = \frac{\pi}{4} + \frac{\zeta\pi}{2}\tanh\frac{\zeta\pi}{2}\,^{1} \leq \frac{\pi}{4} + \frac{\zeta\pi}{2}.$$

Therefore,

$$\left| e^{-\frac{\zeta\pi}{2}} H_{i\zeta}^{(1)}(kr) - \sqrt{\frac{2}{\pi kr}}\, e^{ikr - \frac{\zeta\pi}{2} - \frac{\pi i}{4}} \right| \leq I \leq \frac{\pi}{8kr}(3 + 4\zeta + 4\zeta^2) . \qquad (6.2\text{-}8)$$

A similar bound can be given in the case of the remaining Hankel function of Equation (6.2-1) for the difference between it and its asymptotic expansion.

Finally, since every term of $A(\zeta)$ is of the form

$$\frac{e^{\mu\zeta} - e^{-\mu\zeta}}{e^{\nu\zeta} - e^{-\nu\zeta}}, \quad \nu > \mu \geq 0 ,$$

it can be seen that by using Equation (6.2-8) a bound which goes to zero as $1/r\rho$ for large r and ρ may be given for

$$\left| \int_0^\infty e^{-\zeta\pi} \left(H_{i\zeta}^{(1)}(kr) - \sqrt{\frac{2}{\pi kr}}\, e^{ikr + \frac{\zeta\pi}{2} - \frac{\pi i}{4}} \right) \left(H_{i\zeta}^{(1)}(k\rho) - \sqrt{\frac{2}{\pi k\rho}}\, e^{ik\rho + \frac{\zeta\pi}{2} - \frac{\pi i}{4}} \right) A(\zeta)\, d\zeta \right| .$$

---

[1] This integration is performed as follows: on pages 142 and 163 of Reference 11 the integrals

$$\int_0^\infty \frac{\cos ax - \cos bx}{\sinh cx}\frac{dx}{x} = \log\frac{\cosh\frac{b\pi}{2c}}{\cosh\frac{a\pi}{2c}}, \quad c > 0 ,$$

$$\int_0^\infty \frac{\cosh ax - 1}{\sinh cx}\frac{dx}{x} = -\log\left(\cos\frac{a\pi}{2c}\right), \quad c > |a| , \quad \text{are given} .$$

Put $a = 0$ in the first of these formulas and add:

$$\int_0^\infty \frac{\cosh ax - \cos bx}{\sinh cx}\frac{dx}{x} = \log\frac{\cosh\frac{b\pi}{2c}}{\cos\frac{a\pi}{2c}} ;$$

differentiate with respect to c and set $a = 1/2$, $b = \zeta$, $c = 1$:

$$\int_0^\infty \frac{\left(\cosh\frac{1}{2}t - \cos\zeta t\right)\cosh t}{\sinh^2 t}\, dt = \frac{\pi}{4} + \frac{\zeta\pi}{2}\tanh\frac{\zeta\pi}{2} .$$

6.3 ELECTRIC FIELDS FOR LINEAR POLARIZATIONS

Let the incident field be polarized perpendicular to the edge of the wedge. Then the scattered electric field for the infinite wedge is given by

$$\vec{E}^{s(a)} = \frac{1}{ik}\hat{k}\times\nabla\psi^{(a)} \cong \left\{\frac{1}{4\phi_o}\sqrt{\frac{2\pi}{kr}}\, e^{ikr+\frac{\pi i}{4}} \sin\frac{\pi^2}{2\phi_o}\left[\frac{1}{A}-\frac{1}{B}\right]\right\}\hat{\phi} \qquad (6.3\text{-}1a)$$

where A and B are given by Equation (6.1-15).

If $\psi^{(a)}$ is written as $\psi^{(a)} = D\sqrt{\frac{2\pi}{kr}}\, e^{ikr+\frac{\pi i}{4}} f(\phi)$, then

$$\nabla\psi^{(a)} = D\, f(\phi)\left[ik\sqrt{\frac{2\pi}{kr}}\, e^{ikr+\frac{\pi i}{4}} - \frac{1}{2}\sqrt{\frac{2\pi}{k}}\, r^{-\frac{3}{2}}\, e^{ikr+\frac{\pi i}{4}}\right]\hat{r}$$

$$+ D\sqrt{\frac{2\pi}{k}}\, r^{-\frac{3}{2}}\, e^{ikr+\frac{\pi i}{4}} f'(\phi)\hat{\phi}$$

can be approximated, for very large r, by

$$\nabla\psi^{(a)} \cong ikD\sqrt{\frac{2\pi}{kr}}\, e^{ikr+\frac{\pi i}{4}} f(\phi)\hat{r} = ik\psi^{(a)}\hat{r}$$

in Equation (6.3-1a).

If the incident field is polarized parallel to the edge of the wedge, the scattered electric field for the infinite wedge is given by

$$\vec{E}^{s(b)} = \hat{k}\psi^{(b)} \cong \left\{\frac{-1}{4\phi_o}\sqrt{\frac{2\pi}{kr}}\, e^{ikr+\frac{\pi i}{4}} \sin\frac{\pi^2}{2\phi_o}\left[\frac{1}{A}+\frac{1}{B}\right]\right\}\hat{k}. \qquad (6.3\text{-}1b)$$

6.4 ELECTRIC FIELDS FOR ARBITRARY POLARIZATIONS

If the incident field, with direction of incidence in a plane normal to the edge of the wedge, has an arbitrary polarization, i.e., if

$$\vec{E}^i = E(a)(-\hat{i}\sin\gamma + \hat{j}\cos\gamma) + E(b)\hat{k} = E(a)\hat{\phi} + E(b)\hat{k}, \qquad (6.4\text{-}1a)$$

the scattered field is a linear combination of Equations (6.3-1a) and (6.3-1b):

$$\vec{E}^s = \frac{1}{4\phi_o}\sqrt{\frac{2\pi}{kr}}\, e^{ikr + \frac{\pi i}{4}} \sin\frac{\pi^2}{2\phi_o}\left[\frac{E(a)\hat{\phi} - E(b)\hat{k}}{A} - \frac{E(a)\hat{\phi} - E(b)\hat{k}}{B}\right]. \qquad (6.4\text{-}1b)$$

It was shown in Section A.2.8 of Reference 1 that to go from the field for an infinite wedge to the field for the class of finite wedges whose current distributions are the same near the vertex involves only the multiplicative factor $\frac{L\, e^{-i\pi/4}}{\sqrt{r\lambda}}$, where L is the length of the finite wedge. Thus, if the incident electric field is of the form (6.4-1a), Equation (6.4-1b) becomes for a wedge of length L:

$$\vec{E}^s = \frac{L e^{ikr}}{4r\phi_o}\sin\frac{\pi^2}{2\phi_o}\left[\frac{E(a)\hat{\phi} - E(b)\hat{k}}{A} - \frac{E(a)\hat{\phi} + E(b)\hat{k}}{B}\right]. \qquad (6.4\text{-}2)$$

6.5 CROSS-SECTIONS FOR LINEAR POLARIZATIONS

The effective cross-sections σ for the finite wedge can now be given for the cases where the transmitted and received radiation is of arbitrary polarization and the direction of incidence still in a plane perpendicular to the edge of the wedge. The definition of effective cross-section is, as given before by Equation (2-6),

$$\sigma = \lim_{r\to\infty} 4\pi r^2 \left|\frac{\vec{E}^s \cdot \hat{p}}{\vec{E}^i}\right|^2, \qquad (6.5\text{-}1)$$

where $\hat{p}$ is a unit vector denoting the receiver polarization.

For example, if $\vec{E}^i = E(b)\hat{k}$ and $\hat{p} = \hat{p}(b) = \hat{k}$, then

$$\vec{E}^s = -\frac{Le^{ikr}}{4\phi_o r} \sin \frac{\pi^2}{2\phi_o}\left[\frac{1}{A}+\frac{1}{B}\right] E(b)\hat{k} \qquad (6.5\text{-}2)$$

and

$$\sigma(bb) = \frac{\pi L^2}{4\phi_o^2} \sin^2 \frac{\pi^2}{2\phi_o}\left[\frac{1}{A}+\frac{1}{B}\right]^2 , \qquad (6.5\text{-}3)$$

where $\sigma(bb)$ indicates that both the transmitted and received polarizations are in a direction parallel to the edge of the wedge.

If $\vec{E}^i = E(b)\hat{k}$ and $\hat{p} = \hat{p}(a) = -\hat{i}\sin\gamma + \hat{j}\cos\gamma$, then $\vec{E}^s$ is as in Equation (6.5-2) and

$$\sigma(ab) = 0 , \qquad (6.5\text{-}4)$$

where $\sigma(ab)$ means that the transmitted and received polarizations are respectively parallel and perpendicular to the edge of the wedge. When the transmitted and received polarizations are both in a direction perpendicular to the edge of the wedge, i.e., when $\vec{E}^i = E(a)(-\hat{i}\sin\gamma + \hat{j}\cos\gamma)$ and $\hat{p} = \hat{p}(a) = -\hat{i}\sin\gamma + \hat{j}\cos\gamma$, then

$$\vec{E}^s = \frac{Le^{ikr}}{4\phi_o r} \sin \frac{\pi^2}{2\phi_o}\left[\frac{1}{A}-\frac{1}{B}\right] E(a)\hat{\phi} \qquad (6.5\text{-}5)$$

and

$$\sigma(aa) = \frac{\pi L^2}{4\phi_o^2} \sin^2 \frac{\pi^2}{2\phi_o}\left[\frac{1}{A}-\frac{1}{B}\right]^2 \cos^2(\phi-\gamma) . \qquad (6.5\text{-}6)$$

6.6 CROSS-SECTIONS FOR CIRCULAR POLARIZATIONS

For circularly polarized transmitted and received polarizations it suffices to find $\sigma(Rb)$, $\sigma(Ra)$, and $\sigma(RR)$, where R indicates right circular polarization. For incident radiation, unit vectors indicating right and left circular polarization are respectively,

$$\hat{i}(R) = \frac{1}{\sqrt{2}}\left[(-\hat{i}\sin\gamma + \hat{j}\cos\gamma) + \sqrt{-1}\,\hat{k}\right], \qquad (6.6\text{-}1a)$$

$$\hat{i}(L) = \frac{1}{\sqrt{2}}\left[(-\hat{i}\sin\gamma + \hat{j}\cos\gamma) - \sqrt{-1}\,\hat{k}\right]. \qquad (6.6\text{-}1b)$$

For scattered radiation, the unit vector system is interchanged, i.e., $\hat{i}^s(R) = \hat{i}(L)$ and $\hat{i}^s(L) = \hat{i}(R)$.

If $\vec{E}^i = E(R)\hat{i}(R)$ and $\hat{p} = \hat{p}(R) = \hat{i}^s(R)$, then

$$\vec{E}^s = \frac{E(R)}{\sqrt{2}} \cdot \frac{Le^{ikr}}{4\phi_o r} \sin\frac{\pi^2}{2\phi_o}\left\{\hat{\phi}\left[\frac{1}{A} - \frac{1}{B}\right] - \sqrt{-1}\,\hat{k}\left[\frac{1}{A} + \frac{1}{B}\right]\right\} \qquad (6.6\text{-}2)$$

and

$$\sigma(RR) = \frac{\pi L^2}{16\phi_o^2}\sin^2\frac{\pi^2}{2\phi_o}\left[\left(\frac{1}{A} - \frac{1}{B}\right)\cos(\phi - \gamma) + \left(\frac{1}{A} + \frac{1}{B}\right)\right]^2. \qquad (6.6\text{-}3)$$

If $\vec{E}^i = E(b)\hat{k}$ and $\hat{p} = \hat{p}^s(R) = \left[(-\hat{i}\sin\gamma + \hat{j}\cos\gamma) - i\hat{k}\right]\sqrt{\frac{1}{2}}$, then $\vec{E}^s$ is as in Equation (6.5-2) and

$$\sigma(Rb) = \frac{\pi L^2}{8\phi_o^2}\sin^2\frac{\pi^2}{2\phi_o}\left[\frac{1}{A} + \frac{1}{B}\right]^2 = \frac{1}{2}\sigma(bb). \qquad (6.6\text{-}4)$$

Finally, if $\vec{E}^i$ is given by $\vec{E}^i = E(a)(-\hat{i}\sin\gamma + \hat{j}\cos\gamma)$ and $\hat{p}$ by $\hat{p}(R) = 1/\sqrt{2}\,[(-\hat{i}\sin\gamma + \hat{j}\cos\gamma) - i\hat{k}]$, then $\vec{E}^s$ is given by Equation (6.5-5) and

$$\sigma(Ra) = \frac{\pi L^2}{8\phi_o^2}\sin^2\frac{\pi^2}{2\phi_o}\left[\frac{1}{A} - \frac{1}{B}\right]^2\cos^2(\phi - \gamma) = \frac{1}{2}\sigma(aa). \qquad (6.6\text{-}5)$$

6.7 SUMMARY OF FORMULAS

For back-scattering, $\phi = \gamma$ (direction of incidence still perpendicular to the edge of the wedge) the effective cross-sections obtained in Sections 6.5 and 6.6 become:

$$
\left.
\begin{aligned}
&1.\quad \sigma(bb) = M\left[\frac{1}{C}+\frac{1}{D}\right]^2 \\
&2.\quad \sigma(ab) = 0 \\
&3.\quad \sigma(aa) = M\left[\frac{1}{C}-\frac{1}{D}\right]^2 \\
&4.\quad \sigma(RR) = \frac{M}{4C^2} \\
&5.\quad \sigma(Rb) = \frac{1}{2}\sigma(bb) \\
&6.\quad \sigma(Ra) = \frac{1}{2}\sigma(aa)
\end{aligned}
\right\}
\qquad
\begin{aligned}
M &= \frac{\pi L^2}{4\phi_o^2}\sin^2\frac{\pi^2}{2\phi_o} \\
C &= \cos\frac{\pi\gamma}{\phi_o}+\cos\frac{\pi^2}{2\phi_o} \qquad (6.7\text{-}1) \\
D &= 1-\cos\frac{\pi^2}{2\phi_o}
\end{aligned}
$$

C and D are respectively the values of A and B of Equation (6.1-15) for $\phi = \gamma$.

6.8 COORDINATE SYSTEMS

To apply the formulas of section 6.7 to wedge-shaped components of an airplane, the relations between the polar angles of the wedge and of the airplane coordinate systems must be known. These relations are derived in this section.

Let $\hat{i}^*$, $\hat{j}^*$, $\hat{k}^*$ be a unit orthogonal set describing the airplane x^*, y^*, z^*-axes, with ϕ^* and θ^* as polar angles in this system. Let $\hat{i}$, $\hat{j}$, $\hat{k}$ be a unit orthogonal set describing the wedge axes, with ϕ and θ as polar angles in this system; and suppose that the edge of the wedge lies along the z-axis and that the wedge is symmetric with regard to the xz-plane.

For a fixed aspect θ^* it is desired to find the azimuth, $\phi_\perp^*$, for which the direction of incidence, $\phi = \gamma$, is perpendicular to the edge of the wedge.

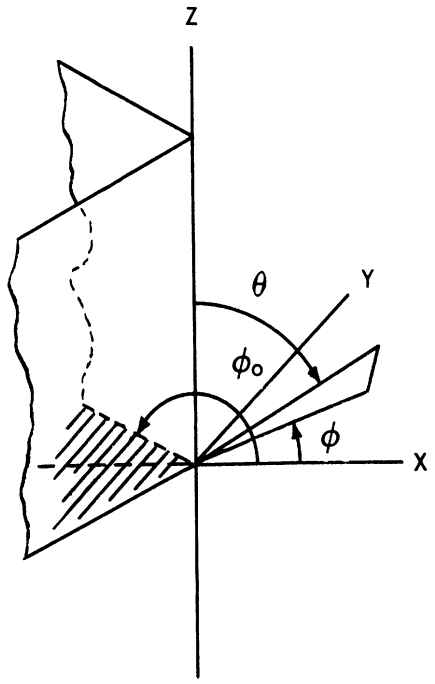

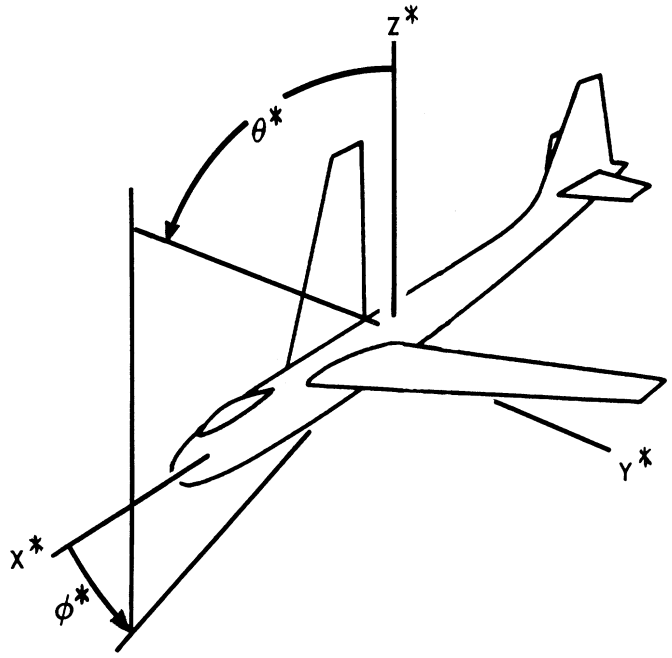

FIG. 6.8-1 WEDGE COORDINATE SYSTEM FIG. 6.8-2 AIRCRAFT COORDINATE SYSTEM

Let

$$\hat{i}^* = a_{11}\hat{i} + a_{12}\hat{j} + a_{13}\hat{k}$$

$$\hat{j}^* = a_{21}\hat{i} + a_{22}\hat{j} + a_{23}\hat{k} \qquad (6.8\text{-}1)$$

$$\hat{k}^* = a_{31}\hat{i} + a_{32}\hat{j} + a_{33}\hat{k} \ .$$

Let the unit vector $\hat{k}$ in the direction of the edge of the wedge be given by

$$\hat{k} = \sin\alpha\cos\beta\,\hat{i}^* + \sin\alpha\sin\beta\,\hat{j}^* + \cos\alpha\,\hat{k}^*$$

$$= a_{13}\hat{i}^* + a_{23}\hat{j}^* + a_{33}\hat{k}^* . \qquad (6.8\text{-}2)$$

If the direction $\hat{v}$ of incidence is expressed by

$$\hat{v} = \sin\theta^{\star} \cos\phi^{\star}\,\hat{i}^{\star} + \sin\theta^{\star}\sin\phi^{\star}\,\hat{j}^{\star} + \cos\theta^{\star}\,\hat{k}^{\star}, \qquad (6.8\text{-}3)$$

then for some specified aspect $\theta^{\star}$, the azimuth $\phi_{\perp}^{\star}$ for which incidence is perpendicular to the edge of the wedge ($\hat{k} \cdot \hat{v} = 0$) is

$$\cos(\phi_{\perp}^{\star} - \beta) = -\cot\theta^{\star}\cot\alpha, \qquad (6.8\text{-}4)$$

where $\alpha = \arccos a_{33}$ and $\beta = \arctan a_{23}/a_{13}$.

The angle $\phi = \gamma$ for which incidence is perpendicular to the edge of the wedge is given by

$$\tan\gamma = \frac{a_{12}\sin\theta^{\star}\cos\phi_{\perp}^{\star} + a_{22}\sin\theta^{\star}\sin\phi_{\perp}^{\star} + a_{32}\cos\theta^{\star}}{a_{11}\sin\theta^{\star}\cos\phi_{\perp}^{\star} + a_{21}\sin\theta^{\star}\sin\phi_{\perp}^{\star} + a_{31}\cos\theta^{\star}}. \qquad (6.8\text{-}5)$$

For incidence slightly out of the normal plane, say by an amount δu, the cross-section will drop off approximately $\lambda^2/8\pi^2L^2(\delta u)^2$ (Cf. Ref. 1, p. 129), that is

$$\frac{\sigma_{\text{non-normal}}}{\sigma_{\text{normal}}} = g^2 \cong \frac{\lambda^2}{8\pi^2L^2(\delta u)^2}. \qquad (6.8\text{-}6)$$

Thus it is possible to find δu for which σ_{normal} drops off by a given amount[1]; it is from Equation (6.8-6)

$$\delta u \cong \frac{\lambda}{2\sqrt{2}\,\pi L g}. \qquad (6.8\text{-}7)$$

It is now necessary to find the change in azimuth angle $\delta\phi^{\star}$ for which σ_{normal} drops off by the fraction g^2, that is, find $\delta\phi^{\star}$ in terms of δu.

---

[1]The amounts used for the computations later are $g^2 = 1/2, 1/10, 1/100$.

From

$$\sin \delta u = a_{13} \sin\theta^{\star} \cos(\phi^{\star}_{\perp} + \delta\phi^{\star}) + a_{23} \sin\theta^{\star} \sin(\phi^{\star}_{\perp} + \delta\phi^{\star}) + a_{33} \cos\theta^{\star}, \tag{6.8-8}$$

it follows that

$$\delta u \cong a_{13} \sin\theta^{\star} \cos\phi^{\star}_{\perp} \left(1 - \frac{\delta\phi^{\star 2}}{2}\right) - a_{13} \sin\theta^{\star} \sin\phi^{\star}_{\perp} \delta\phi^{\star}$$

$$+ a_{23} \sin\theta^{\star} \sin\phi^{\star}_{\perp} \left(1 - \frac{\delta\phi^{\star 2}}{2}\right) + a_{23} \sin\theta^{\star} \cos\phi^{\star}_{\perp} \delta\phi^{\star} + a_{33} \cos\theta^{\star}$$

$$\cong a_{33} \cos\theta^{\star} \frac{\delta\phi^{\star 2}}{2} + \delta\phi^{\star} \left[- a_{13} \sin\theta^{\star} \sin\phi^{\star}_{\perp} + a_{23} \sin\theta^{\star} \cos\phi^{\star}_{\perp} \right]$$

$$\delta u \cong a_{33} \cos\theta^{\star} \frac{\delta\phi^{\star 2}}{2} + \delta\phi^{\star} \sqrt{\sin^2\theta^{\star} - a_{33}^2} \,. \tag{6.8-9}$$

Solving Equation (6.8-9) for $\delta\phi^{\star}$ yields

$$\delta\phi^{\star} \cong \frac{- \sqrt{\sin^2\theta^{\star} - a_{33}^2} + \sqrt{\sin^2\theta^{\star} - a_{33}^2 + 2 a_{33} \cos\theta^{\star} (\delta u)}}{a_{33} \cos\theta^{\star}}, \tag{6.8-10}$$

and if $\sin^2\theta^{\star} - a_{33}^2 >> 2 a_{33} \cos\theta^{\star} (\delta u)$, Equation (6.8-10) gives

$$\delta\phi^{\star} \cong \frac{\delta u}{\sqrt{\sin^2\theta^{\star} - a_{33}^2}} \,. \tag{6.8-11}$$

6.9 WEDGE S-MATRICES IN THE AIRPLANE COORDINATE SYSTEM

Let the designation of axes be as given in Section 6.8 and the direction of incidence of energy on the airplane be as given by Equation (6.8-3). Horizontal polarization is taken to be polarization parallel to the ground, i.e., in the xy-plane of the airplane coordinate system:

$$\hat{p}(H) = -\hat{i}^{\star} \sin\phi^{\star} + \hat{j}^{\star} \cos\phi^{\star} \ . \qquad (6.9\text{-}1)$$

Vertical polarization is perpendicular to horizontal polarization; hence

$$\hat{p}(V) = \hat{v} \times \hat{p}(H) = -\cos\theta^{\star} \cos\phi^{\star}\, \hat{i}^{\star} - \cos\theta^{\star} \sin\phi^{\star}\, \hat{j}^{\star} + \sin\theta^{\star}\, \hat{k}^{\star} \ . \qquad (6.9\text{-}2)$$

The polarization directions $\hat{p}(a)$ and $\hat{p}(b)$ of Section 6.5 may be written in the airplane system as

$$\hat{p}(b) = \sin\alpha \cos\beta\, \hat{i}^{\star} + \sin\alpha \sin\beta\, \hat{j}^{\star} + \cos\alpha\, \hat{k}^{\star} \left[= \hat{k} = a_{13}\hat{i}^{\star} + a_{23}\hat{j}^{\star} + a_{33}\hat{k}^{\star} \right], \qquad (6.9\text{-}3)$$

$$\begin{aligned} \hat{p}(a) = \hat{v} \times \hat{p}(b) = {} & (\sin\theta^{\star} \sin\phi^{\star} \cos\alpha - \cos\theta^{\star} \sin\alpha \sin\beta)\, \hat{i}^{\star} \\ & + (\cos\theta^{\star} \sin\alpha \cos\beta - \sin\theta^{\star} \cos\phi^{\star} \cos\alpha)\, \hat{j}^{\star} \\ & + (\sin\theta^{\star} \cos\phi^{\star} \sin\alpha \sin\beta - \sin\theta^{\star} \sin\phi^{\star} \sin\alpha \cos\beta)\, \hat{k}^{\star}. \end{aligned} \qquad (6.9\text{-}4)$$

The matrix $U = \begin{pmatrix} u(Ha) & u(Hb) \\ u(Va) & u(Vb) \end{pmatrix}$

can now be given explicitly as

$$U = \begin{pmatrix} -\sin\theta^{\star} \cos\alpha + \cos\theta^{\star} \sin\alpha \cos(\phi^{\star} - \beta) & -\sin\alpha \sin(\phi^{\star} - \beta) \\ -\sin\alpha \sin(\phi^{\star} - \beta) & \sin\theta^{\star} \cos\alpha - \cos\theta^{\star} \sin\alpha \cos(\phi^{\star} - \beta) \end{pmatrix}, \qquad (6.9\text{-}5)$$

where the elements u(IJ) of the matrix are determined from the previously given relation $u(IJ) = p(I) \cdot p^{\star}(J)$. Since the direction of incidence is to be perpendicular to the edge of the wedge, i.e., $\hat{v}$ is perpendicular to $\hat{p}(b)$, the angle $\phi^{\star}_{\perp}$ for which such perpendicularity occurs (for fixed $\theta^{\star}$, α, β) is given by Equation (6.8-4)

$$\cos(\phi^{\star}_{\perp} - \beta) = -\cot\theta^{\star}\cot\alpha \,. \qquad (6.8\text{-}4)$$

For each such angle $\phi^{\star}_{\perp}$, U reduces to

$$U = \begin{pmatrix} -\cos\alpha \csc\theta^{\star} & -\sin\alpha \sin(\phi^{\star}_{\perp} - \beta) \\ -\sin\alpha \sin(\phi^{\star}_{\perp} - \beta) & \cos\alpha \csc\theta^{\star} \end{pmatrix} . \qquad (6.9\text{-}6)$$

From Equation (6.4-2) the S-matrix S(ab ; ab) can be read off as

$$S(ab\,;\,ab) = \frac{L e^{ikr}}{4r\phi_o} \sin\frac{\pi^2}{2\phi_o} \begin{bmatrix} \left(\frac{1}{C} - \frac{1}{D}\right) & 0 \\ 0 & -\left(\frac{1}{C} + \frac{1}{D}\right) \end{bmatrix} . \qquad (6.9\text{-}7)$$

Using Equation (6.9-7) in conjunction with Equations (6.9-5)and (2-10), the matrix S(HV ; HV) = U S(ab ; ab)U' in the airplane coordinate system for any wedge component of the airplane is

$$S(HV\,;\,HV) = \frac{1}{2}\left(\frac{M}{\pi}\right)^{\frac{1}{2}} \frac{e^{ikr}}{r} \begin{bmatrix} \frac{2\cos^2\alpha}{C\sin^2\theta^{\star}} - \left(\frac{1}{C} + \frac{1}{D}\right) & \frac{\sin\alpha\cos\alpha\sin(\phi^{\star} - \beta)}{C\sin\theta^{\star}} \\ \frac{\sin\alpha\cos\alpha\sin(\phi^{\star} - \beta)}{C\sin\theta^{\star}} & \left(\frac{1}{C} - \frac{1}{D}\right) - \frac{2\cos^2\alpha}{C\sin^2\theta^{\star}} \end{bmatrix} , \qquad (6.9\text{-}8)$$

where M, C, D, are given by Equation (6.7-1).

7

CROSS-POLARIZATION CROSS-SECTIONS OF WIRE LOOPS

(Unclassified)

In addition to those sharp edges on an aircraft which must be represented by wedges there are, particularly for jet aircraft, sharp edges of a circular or loop shape. Such circular sharp edges are represented by wire loops which are discussed in this section.

7.1 GENERAL THEORY

As pointed out in Section A.2.10 of Reference 1, the scattered field from a small straight piece of thin wire is similar to the field of a dipole. It is of the form

$$\vec{E}^s = K \frac{\hat{r} \times (\hat{r} \times \hat{d})}{r} e^{ikr} \, d\ell \quad , \qquad (7.1\text{-}1)$$

where $d\ell$ is the length of the wire, $\hat{r}$ is the unit vector to the field point, r is the distance to the field point, and $\hat{d}$ is a unit vector along the wire. K is a proportionality factor given by,

$$K = K_1 (\hat{p}^i \cdot \hat{d}) \quad , \qquad (7.1\text{-}2)$$

where $\hat{p}^i$ is a unit vector giving the direction of polarization of the incident electric field and K_1 is a constant to be determined.

From the definition of cross-section given by Equation (2-6) the cross-section of a small straight piece of thin wire is

$$\sigma = 4\pi r^2 \frac{K_1^2 (\hat{p}^i \cdot d)^2}{|\vec{E}^i|^2} \frac{(\hat{p}^r \cdot \hat{d})^2}{r^2} (d\ell)^2 \quad , \qquad (7.1\text{-}3)$$

where superscripts i and r denote transmitter and receiver polarizations

respectively. If $\hat{p}$ (for both i and r) is parallel to the wire, $(\hat{p} \cdot \hat{d}) = 1$; for this case ($\phi_o = \pi$, $\gamma = 0$) Equation (6.5-3) gives for the cross-section

$$\sigma = \frac{(d\ell)^2}{\pi} \quad , \tag{7.1-4}$$

where, in Equation (6.5-3), L has been replaced by $d\ell$. Comparison of Equations (7.1-3 and 7.1-4) for this case (i.e., $\hat{p}$ parallel to wire) yields:

$$K_1 = \frac{\left|\vec{E}^i\right|}{2\pi} \quad .$$

Hence the field Equation (7.1-1) may be written as

$$\vec{E}^s_{d\ell} = \frac{\left|\vec{E}^i\right| (\hat{p}^i \cdot \hat{d})}{2\pi} \cdot \frac{\hat{r} \times (\hat{r} \times \hat{d})}{r} \cdot e^{2ikr} \, d\ell \quad .^1 \tag{7.1-5}$$

To find the scattered field for a wire loop, an integration is made over the loop;

$$\vec{E}^s = \frac{\left|\vec{E}^i\right|}{2\pi} \int_{\text{loop}} (\hat{p}^i \cdot \hat{d}) \frac{\hat{r} \times (\hat{r} \times \hat{d})}{r} e^{2ikr} \, d\ell \quad .$$

The effective cross-section of a wire loop is then, since $\hat{p} \cdot \hat{r} = 0$,

$$\sigma = 4\pi r^2 \left| \frac{\vec{E}^s \cdot \hat{p}^r}{\vec{E}^i} \right|^2 = \frac{1}{\pi} \left| \int_{\text{loop}} (\hat{p}^i \cdot \hat{d}) (\hat{p}^r \cdot \hat{d}) e^{2ik\rho} \, d\ell \right|^2 \quad , \tag{7.1-6}$$

where ρ is the distance measured in the direction of incidence.

---

[1] To take into account the phase lag in making the round trip from radar to wire and back, Equation (7.1-1) has been multiplied by e^{ikr} to obtain Equation (7.1-5).

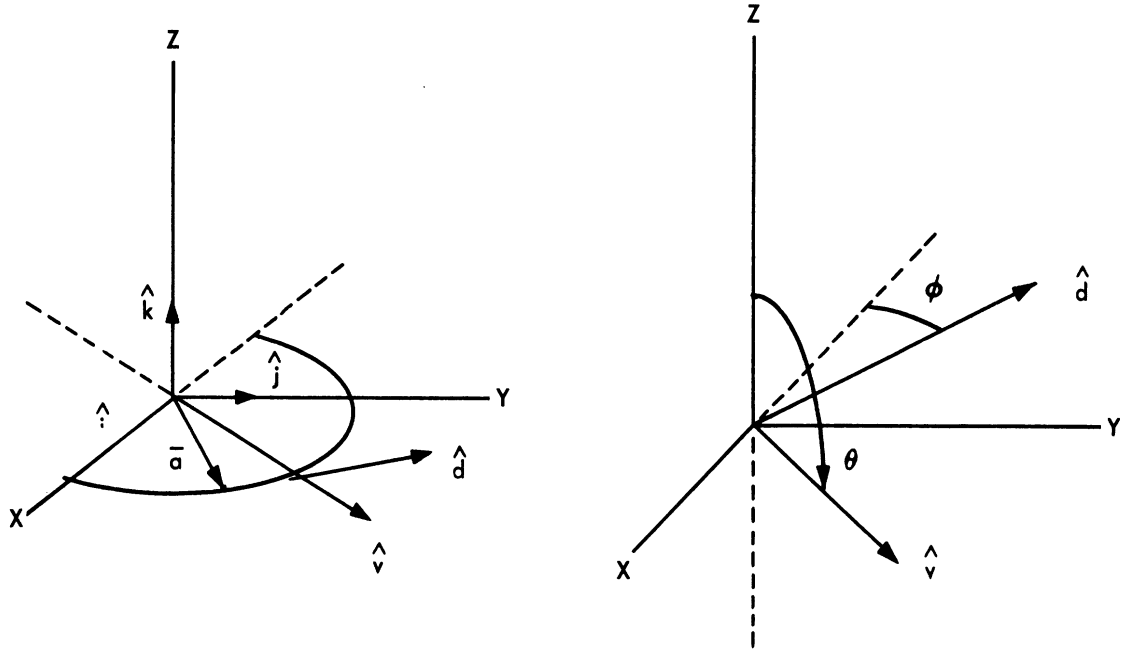

$\bar{a}$ = radius of loop

$\hat{d}$ = direction of dipole

$\hat{v}$ = direction of propagation of incident plane wave

$\hat{d} = -\hat{i}\sin\phi + \hat{j}\cos\phi$

$\hat{v} = -\hat{i}\sin\theta + \hat{k}\cos\theta$

$\bar{a} = a(\hat{i}\cos\phi + \hat{j}\sin\phi)$

FIG. 7.1-1 COORDINATE SYSTEMS FOR A WIRE LOOP

Consider a loop of radius a in the xy-plane with center at the origin Figure 7.1-1. On the wire $x = a\cos\phi$, $y = a\sin\phi$; thus $d\ell = a\,d\phi$; and the direction of the dipole is $\hat{d} = -\hat{i}\sin\phi + \hat{j}\cos\phi$. Let the direction of incidence be in the xz-plane and be given by $\hat{v} = \hat{i}\sin\theta - \hat{k}\cos\theta$; this makes $\rho = (x\hat{i} + y\hat{j})\cdot\hat{v} = a\sin\theta\cos\phi$. Let two perpendicular directions of polarization be given by:

$$\hat{p}(A) = \hat{i}\cos\theta\sin\gamma + \hat{j}\cos\gamma + \hat{k}\sin\theta\sin\gamma \ , \qquad (7.1\text{-}7)$$

$$\hat{p}(B) = \hat{i}\cos\theta\cos\gamma - \hat{j}\sin\gamma + \hat{k}\sin\theta\cos\gamma \ , \qquad (7.1\text{-}8)$$

where γ is the angle between the polarization vector and the y-axis. Right- and left-circular polarization directions can then be given respectively by:

$$\hat{p}(R) = \frac{1}{\sqrt{2}} e^{-i\gamma}\left[\hat{i}(i\cos\theta) + \hat{j} + \hat{k}(i\sin\theta)\right] \ , \qquad (7.1\text{-}9)$$

$$\hat{p}(L) = \frac{1}{\sqrt{2}} e^{i\gamma}\left[-\hat{i}(i\cos\theta) + \hat{j} - \hat{k}(i\sin\theta)\right] \ . \qquad (7.1\text{-}10)$$

7.2 CROSS-SECTION FORMULAS

Formulas for the following effective cross-sections have been determined: $\sigma(AA)$, $\sigma(BB)$, $\sigma(AB)$, $\sigma(AR)$, $\sigma(BR)$, and $\sigma(RR)$; in $\sigma(IJ)$, I and J denote receiver and transmitter polarization respectively. For example, using Equations (7.1-6) and (7.1-7), $\sigma(AA)$ is given by:

$$\sigma(AA) = \frac{a^2}{\pi}\left|\int_0^{2\pi} (\cos\phi\cos\gamma - \sin\phi\sin\gamma\cos\theta)^2 \, e^{2ika\sin\theta\cos\phi} \, d\phi\right|^2$$

$$= \pi a^2 \Big|(\sin^2\gamma\cos^2\theta + \cos^2\gamma)\, J_0(2ka\sin\theta)$$

$$+ (\sin^2\gamma\cos^2\theta - \cos^2\gamma)\, J_2(2ka\sin\theta)\Big|^2 \ . \qquad (7.2\text{-}1)$$

In a similar fashion the remaining formulas are found to be

$$\sigma(BB) = \pi a^2 \Big|(\cos^2\theta\cos^2\gamma - \sin^2\gamma)\, J_2(2ka\sin\theta)$$

$$+ (\cos^2\theta\cos^2\gamma + \sin^2\gamma)\, J_0(2ka\sin\theta)\Big|^2 \ , \qquad (7.2\text{-}2)$$

$$\sigma(AB) = \pi a^2 \sin^2\gamma \cos^2\gamma \left| (1 + \cos^2\theta)\, J_2(2ka \sin\theta) - \sin^2\theta\, J_0(2ka \sin\theta) \right|^2 , \tag{7.2-3}$$

$$\sigma(AR) = \frac{\pi a^2}{2} \left| (i \cos^2\theta \sin\gamma - \cos\gamma)\, J_2(2ka \sin\theta) + (i \cos^2\theta \sin\gamma + \cos\gamma)\, J_0(2ka \sin\theta) \right|^2 , \tag{7.2-4}$$

$$\sigma(BR) = \frac{\pi a^2}{2} \left| (i \cos^2\theta \cos\gamma + \sin\gamma)\, J_2(2ka \sin\theta) + (i \cos^2\theta \cos\gamma - \sin\gamma)\, J_0(2ka \sin\theta) \right|^2 , \tag{7.2-5}$$

$$\sigma(RR) = \frac{\pi a^2}{4} \left| (-\cos^2\theta - 1)\, J_2(2ka \sin\theta) + (-\cos^2\theta + 1)\, J_0(2ka \sin\theta) \right|^2 . \tag{7.2-6}$$

8

DIHEDRAL SCATTERING

(Unclassified)

8.1 WING-BODY DIHEDRAL SCATTERING IN THE DIHEDRAL COORDINATE SYSTEM

Let the surfaces representing the wing and body be such that for each surface one of the two principal radii of curvature is infinite and the other is neither infinite nor zero. The scattered field is computed in this section for the dihedral formed by the wing and body by Fock's formulation of geometric optics (Ref. 17).

Consider the conditions on a ray which is reflected back to the point whence it came: Let $\hat{v}$ be the initial direction of the ray and let $\hat{n}_w$ and $\hat{n}_b$ be the normals of the wing and body, respectively, at the points where the ray hits them. Suppose the ray hits the wing first. After hitting the wing the ray is traveling in a direction

$$\hat{v} - 2(\hat{v} \cdot \hat{n}_w)\, \hat{n}_w \; ; \tag{8.1-1}$$

after hitting the body the ray will be traveling in a direction

$$\hat{v} - 2(\hat{v} \cdot \hat{n}_w)\, \hat{n}_w - 2\left\{\left[\hat{v} - 2(\hat{v} \cdot \hat{n}_w)\, \hat{n}_w\right] \cdot \hat{n}_b\right\} \hat{n}_b = -\hat{v} \; . \tag{8.1-2}$$

The equality is required in order that the ray be reflected back to the source. Since Equation (8.1-2) may be rewritten as:

$$\hat{v} + 2(\hat{v} \cdot \hat{n}_w)\, (\hat{n}_w \cdot \hat{n}_b)\, \hat{n}_b = (\hat{v} \cdot \hat{n}_w)\, \hat{n}_w + (\hat{v} \cdot \hat{n}_b)\, \hat{n}_b \; , \tag{8.1-3}$$

it is apparent that $\hat{v}$ is a linear combination of $\hat{n}_w$ and $\hat{n}_b$, and thus lies in the plane of these two vectors. Further, the scalar product of Equation (8.1-3) with $\hat{n}_w$ and $\hat{n}_b$ respectively yields:

$$(\hat{n}_w \cdot \hat{n}_b)\left[2(\hat{v} \cdot \hat{n}_w)(\hat{n}_w \cdot \hat{n}_b) - (\hat{v} \cdot \hat{n}_b)\right] = 0,$$

$$(\hat{v} \cdot \hat{n}_w)(\hat{n}_w \cdot \hat{n}_b) = 0 \; . \tag{8.1-4}$$

Thus, $\hat{n}_w \cdot \hat{n}_b = 0$. The same conclusions would have been reached if the ray had hit the body first.

The above results allow a coordinate system to be chosen such that $\hat{n}_w = \hat{k}$ and $\hat{n}_b = \hat{i}$ (Fig. 8.1-1). The ray is reflected from the xy-plane at $x = R \sin\theta$, from the yz-plane at $z = R \cos\theta$, where R is the distance between the two points from which the ray is reflected.

Since the geometric optics field depends only on local properties of the scatterer, the wing and body surfaces may be replaced by parabolic cylinders having the same radii of curvature. These are, for the wing and body, respectively,

$$z = -\frac{(y\cos\beta - x\sin\beta + R\sin\theta\sin\beta)^2}{2R_w} ,$$

$$x = -\frac{(z\cos\alpha - y\cos\alpha - R\cos\theta\cos\alpha)^2}{2R_b} , \qquad (8.1\text{-}5)$$

where R_w and R_b are the radii of curvature of the wing and the body.

Fock's formulation of geometric optics will be used. Since the pertinent formulas are given in Section 3.1 of Reference 17, the detail involved to obtain reflected fields will be omitted.

Consider the case shown in Figure 8-1-1 where the ray hits the wing before it hits the body. (The reverse case can then be obtained from the symmetries of the problem.) If the incident electric field is taken to be

$$\vec{E}^i = \left[\hat{j}\cos\gamma + (-\hat{i}\cos\theta + \hat{k}\sin\theta)\sin\gamma\right] e^{-ik(x\sin\theta + z\cos\theta)} , \qquad (8.1\text{-}6)$$

the field reflected from the wing at the reflection point on the body is (following the procedure of the above mentioned reference),

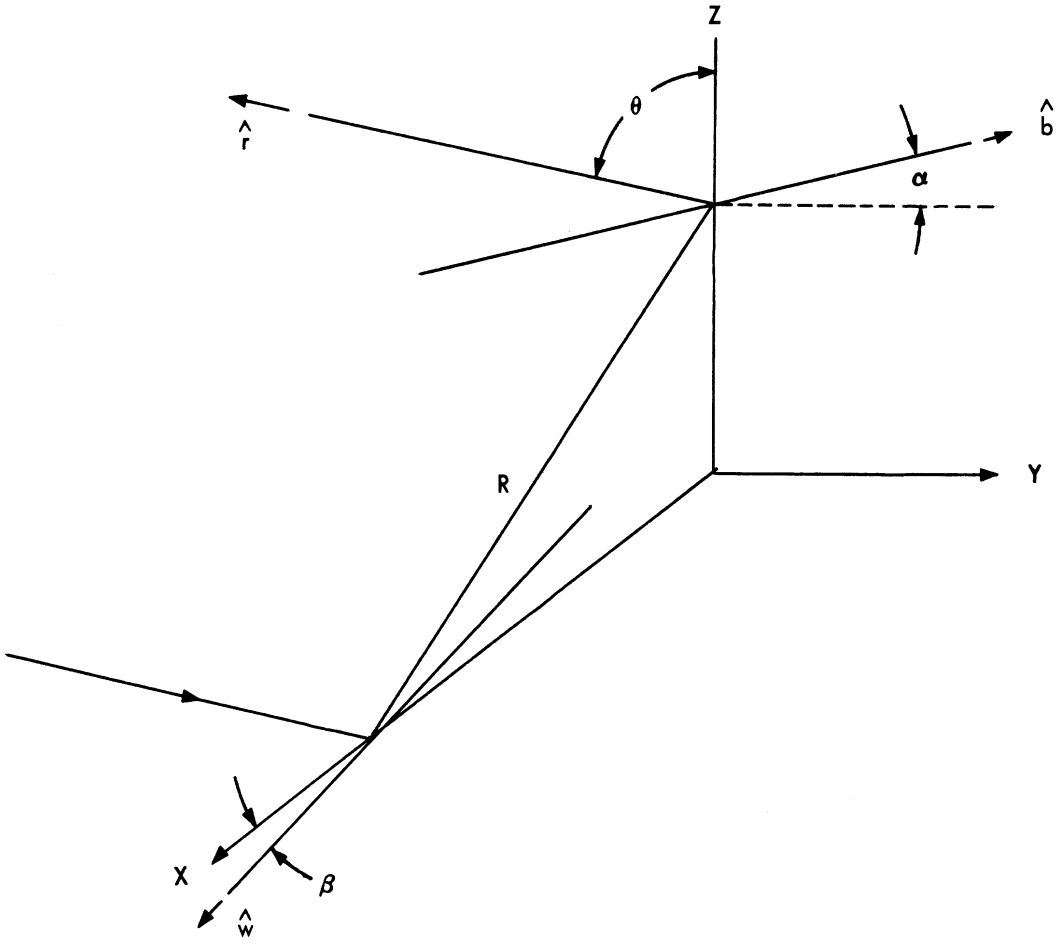

Incidence in xz-Plane

$\hat{r}$ = direction to radar = $\sin\theta\,\hat{i} + \cos\theta\,\hat{k}$

$\hat{b}$ = direction of body axis = $\cos\alpha\,\hat{j} + \sin\alpha\,\hat{k}$

$\hat{w}$ = direction of wing axis = $\cos\beta\,\hat{i} + \sin\beta\,\hat{j}$

θ = measured in xz-plane

α = measured in yz-plane

β = measured in xy-plane

FIG. 8.1-1 COORDINATE SYSTEM FOR WING-BODY DIHEDRAL

$$\vec{E} = (\sin\gamma\cos\theta\,\hat{i} - \cos\gamma\,\hat{j} + \sin\gamma\sin\theta\,\hat{k}\,\frac{ikR\cos^2\theta}{\sqrt{1+2\frac{R}{R_w}\frac{1-\sin^2\theta\cos^2\beta}{\cos\theta}}}. \quad (8.1\text{-}7)$$

After reflection from the body the scattered field for large R_o is

$$\vec{E}^s = \frac{\sqrt{R_w R_b \sin\theta\cos\theta}\,(\sin\gamma\cos\theta\,\hat{i} + \cos\gamma\,\hat{j} - \sin\gamma\sin\theta\,\hat{k})}{2R_o\,|\cos\alpha\cos\beta\cos\theta - \sin\alpha\sin\beta\sin\theta|}\,e^{ik(R\cos^2\theta + R_o)},$$

where R_o is the distance from the reflector to the radar. Thus the scattered field of wing-to-body plus body-to-wing is

$$\vec{E}^s = \frac{\sqrt{R_w R_b \sin\theta\cos\theta}\,(\sin\gamma\cos\theta\,\hat{i} + \cos\gamma\,\hat{j} - \sin\gamma\sin\theta\,\hat{k})\,e^{ik(R\cos^2\theta + R_o}}{R_o\,|\cos\alpha\cos\beta\cos\theta - \sin\alpha\sin\beta\sin\theta|}.$$

(8.1-1)

If the polarization basis vectors are taken to be

$$\hat{p}(A) = \hat{j},$$

$$\hat{p}(B) = -\cos\theta\,\hat{i} + \sin\theta\,\hat{k}, \quad (8.1\text{-}9)$$

then the scattering matrix S(AB; AB) is given by:

$$S(AB;\,AB) = \frac{Q\,e^{i\mu}}{R_o}\begin{pmatrix} 1 & 0 \\ 0 & -1 \end{pmatrix}, \quad (8.1\text{-}10)$$

where

$$Q = \frac{\sqrt{R_w R_b \sin\theta\cos\theta}}{|\cos\alpha\cos\beta\cos\theta - \sin\alpha\sin\beta\sin\theta|},$$

and μ is a phase factor which is unimportant for the calculation of cross-sections. The form of Equation (8.1-10) indicates that the incident wave has been repolarized (Sec. 5) by the wing-body dihedral.

8.2 TRANSFORMATION TO THE AIRCRAFT COORDINATE SYSTEM

In Figure 8.1-1 let $\hat{r}$ be the direction to the radar, $\hat{b}$ be the direction of the body axis, and $\hat{w}$ be the direction of the wing axis. The direction of incidence is taken to be in the xz-plane so that θ is measured in the xz-plane; α and β are measured in the yz- and xy-planes, respectively.

Put

$$\begin{aligned}\hat{w} &= \cos\beta\,\hat{i} + \sin\beta\,\hat{j}\,,\\ \hat{b} &= \cos\alpha\,\hat{j} + \sin\alpha\,\hat{k}\,,\\ \hat{r} &= \sin\theta\,\hat{i} + \cos\theta\,\hat{k}\,.\end{aligned} \qquad (8.2\text{-}1)$$

As before asterisks are used to denote the aircraft coordinate system.

The tie-up between the two coordinate systems is made through $\hat{r}$, $\hat{b}$, and $\hat{w}$ which can be expressed in both coordinate systems. In the aircraft coordinate system $\hat{b}$ and $\hat{w}$ are constant vectors for a given aircraft while

$$\hat{r} = \sin\theta^* \cos\phi^*\,\hat{i}^* + \sin\theta^* \sin\phi^*\,\hat{j}^* + \cos\theta^*\,\hat{k}^*\,. \qquad (8.2\text{-}2)$$

The expressions of Equation (8.2-1) for $\hat{w}$, $\hat{b}$, and $\hat{r}$ can be inverted to give

$$\hat{i} = \frac{\cos\alpha\cos\theta\,\hat{w} - \sin\beta\cos\theta\,\hat{b} + \sin\alpha\sin\beta\,\hat{r}}{\hat{w}\cdot\hat{b}\times\hat{r}}$$

$$\hat{j} = \frac{\sin\alpha\sin\theta\,\hat{w} + \cos\beta\cos\theta\,\hat{b} - \sin\alpha\cos\beta\,\hat{r}}{\hat{w}\cdot\hat{b}\times\hat{r}}$$

$$\hat{k} = \frac{-\sin\theta\cos\alpha\,\hat{w} + \sin\beta\sin\theta\,\hat{b} + \cos\alpha\cos\beta\,\hat{r}}{\hat{w}\cdot\hat{b}\times\hat{r}} \qquad (8.2\text{-}3)$$

where $\cos\alpha\cos\beta\cos\theta + \sin\alpha\sin\beta\sin\theta$ has been replaced by $\hat{w}\cdot\hat{b}\times\hat{r}$. If the expressions for $\hat{w}$, $\hat{b}$, and $\hat{r}$ in terms of $\hat{i}^*$, $\hat{j}^*$, $\hat{k}^*$ are substituted into Equation (8.2-3), the vectors $\hat{i}$, $\hat{j}$, and $\hat{k}$ will be given in terms of $\hat{i}^*$, $\hat{j}^*$, and $\hat{k}^*$ except that α, β, and θ are unknown. These angles can be determined from

$$\hat{w}\cdot\hat{b} = \sin\beta\cos\alpha = s,$$

$$\hat{b}\cdot\hat{r} = \sin\alpha\cos\theta = t,$$

$$\hat{r}\cdot\hat{w} = \sin\theta\cos\beta = u; \qquad (8.2\text{-}4)$$

they are

$$\cos 2\alpha = \frac{s^2 - t^2 + D}{1 - u^2},$$

$$\cos 2\beta = \frac{u^2 - s^2 + D}{1 - t^2},$$

$$\cos 2\gamma = \frac{t^2 - u^2 + D}{1 - s^2}, \qquad (8.2\text{-}5)$$

where $D^2 = (1 - s^2 - t^2 - u^2)^2 - (2stu)^2$. The sign of D must be chosen so as to obtain the correct physical setup of the wing-body combination. α, β, and θ are used not only in the expressions for $\hat{i}$, $\hat{j}$, and $\hat{k}$, but also in the expression for Q.

The transformation from the scattering matrix for the AB basis to that for the HV basis is accomplished by:

$$S(HV; HV) = U(HV; AB)\, S(AB; AB)\, U'(HV; AB), \qquad (8.2\text{-}6)$$

where

$$U(HV; AB) = \begin{pmatrix} \hat{p}(H) \cdot \hat{p}(A) & \hat{p}(H) \cdot \hat{p}(B) \\ \hat{p}(V) \cdot \hat{p}(A) & \hat{p}(V) \cdot \hat{p}(B) \end{pmatrix} , \qquad (8.2\text{-}7)$$

since $\hat{p}(A)$ and $\hat{p}(B)$ are real. Here,

$$\hat{p}(H) = -\sin\phi^{\star}\,\hat{i}^{\star} + \cos\phi^{\star}\,\hat{j}^{\star} ,$$

$$\hat{p}(V) = -\cos\theta^{\star}\cos\phi^{\star}\,\hat{i}^{\star} - \cos\theta^{\star}\sin\phi^{\star}\,\hat{j}^{\star} + \sin\theta^{\star}\,\hat{k}^{\star} . \qquad (8.2\text{-}8)$$

The only unknowns remaining in the determination of S(HV; HV) are R_w and R_b. From Figure 8.1-1 the normals to the wing and body at the reflection point are:

$$\hat{n}_w = \hat{k} ,$$

$$\hat{n}_b = \hat{i} ,$$

which are known in terms of $\hat{i}^{\star}$, $\hat{j}^{\star}$, and $\hat{k}^{\star}$. From the direction of the normal at the reflection point the radius of curvature can be determined from the formula

$$\text{radius of curvature} = \frac{a^2 b^2}{\left[(a\hat{n}\cdot\hat{M})^2 + (b\hat{n}\cdot\hat{m})^2\right]^{3/2}} , \qquad (8.2\text{-}9)$$

where a and b are the semi-major and semi-minor ellipse axes and $\hat{M}$ and $\hat{m}$ are unit vectors along these axes, respectively.

9

CROSS-POLARIZATION CROSS-SECTIONS FOR CYLINDERS

(Unclassified)

In this section the limitations on the use of the physical optics current distribution method are considered. That such limitations exist is evident from the fact that there is no repolarization of incident radiation in monostatic single reflection situations according to physical optics. However, this is not an essential limitation in computing the cross-sections for various of the aircraft components.

For example, consider the scattering from the wing-fuselage combination illustrated in Figure 9-1.

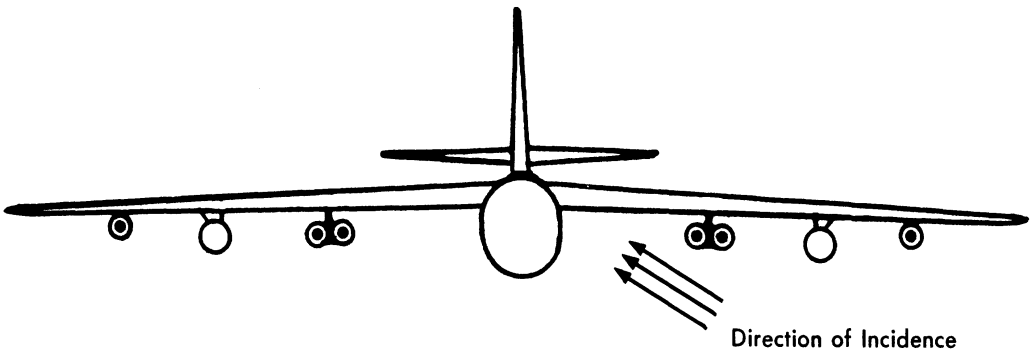

FIG. 9-1 WING-BODY DIHEDRAL

For broadside aspects the wing-fuselage combination was treated as a dihedral which gives rise to double scattering (Sec. 8). Moreover, the single scattering contributions, principally from the fuselage, have been included.

In the case of circularly polarized radiation, an analysis in terms of the characteristic dimensions of the wing and fuselage for the aspects considered indicates that for double scattering the dominant components will be $\sigma(RR)$ and $\sigma(LL)$, while for single scattering the dominant components are $\sigma(RL)$ and $\sigma(LR)$. That is, the characteristic dimensions are such as to insure the validity of the physical optics approximation. It is then possible to set up the following rule of thumb for the application of the physical optics approximation in determining the scattering properties of a target for circularly polarized radiation:

1. The double scattering contribution to $\sigma(RR)$ must be much greater than that of single scattering to $\sigma(RR)$, i.e., the repolarization effect of the single scattering is small with respect to the double scattering.
2. The single scattering contribution to $\sigma(RL)$ must be much greater than that of double scattering to $\sigma(RL)$.

On the other hand, viewing, for example, the leading edge of the wing there may be a measurable contribution to $\sigma(RR)$ arising principally from a single scattering repolarization effect. Although in this case the physical optics approximation may give a sufficiently accurate measure of $\sigma(HH)$ and $\sigma(VV)$, it can give no indication of the contribution to $\sigma(RR)$. To take into account such cases the polarization dependent current distribution method of V. A. Fock (Ref. 9) is introduced. It is, in effect, a modification of the physical optics method and can best be illustrated by a comparison with physical optics.

In the physical optics approximation, the tangential component of the magnetic field on the surface is taken to be twice the tangential component of the incident field on the illuminated side and zero on the shadow side of the scatterers. Thus, the tangential component of the incident magnetic field can be written:

$$H_t = H_t^o \, G(\xi), \tag{9-1}$$

where $G(\xi)$ is a function of a certain reduced distance from the shadow boundary; ξ is positive on the shadow side, negative on the illuminated side of the scatterer. Hence, for the physical optics approximation

$$G(\xi) = 2 \text{ for } \xi < 0,$$
$$= 0 \text{ for } \xi > 0. \tag{9-2}$$

By considering the local fields on the shadow boundary, Fock had obtained a continuous function $G(\xi)$ such that

$$G(\xi) \xrightarrow[\xi \to +\infty]{} 0,$$

$$G(\xi) \xrightarrow[\xi \to -\infty]{} 2. \tag{9-3}$$

Fock's value for the field on the surface becomes the first approximation of the method of Franz and Depperman (Refs. 12 and 13) applied to the circular cylinder or sphere.

The details of Fock's method applied to the particular surface chosen to approximate the wing surface are given below.

Consider a finite cylinder whose cross-section is made up of one-half an ellipse and one-half an ogive. Let the major and minor semi-axes of the ellipse be designated by a and b respectively. Let the ogive have radius of curvature a^2/b, and a semi-minor axis b.

Attach the half ogive at the point of maximum radius of curvature of the ellipse, i.e., at the minor axis. The cross-section is then a smooth curve having an elliptic "nose" and a ogival "tail." Let the length of the cylinder be L.

Under the assumption that plane radiation is incident at or near "nose-on," i.e., the direction of propagation $\hat{k}$ is in the X Y-plane making a small angle α with the negative X-axis, the cross-section is computed using a current distribution method as follows:

After Fock (Ref. 9) it is assumed that the characteristic dimensions of the cylinder are sufficiently large with respect to the wavelength of the incident radiation that the current on the surface is given by the geometrical optics current modified by a shape factor which is a universal function of a certain reduced distance from the shadow boundary. It is further assumed that the cylinder is of sufficient length L that edge effects may be neglected and that the same current distribution can be used along the entire length of the cylinder.

In general the magnetic field scattered from a finite perfectly conducting closed surface is given by the expression (Ref. 1),

$$\vec{H}^s = \frac{1}{4\pi} \int_S (\hat{n} \times \vec{H}_t) \times \nabla \frac{e^{ikr}}{r} \, dS, \tag{9-4}$$

where S is the surface of the cylinder, $\hat{n}$ is the unit outward normal vector to S, r is the distance from the integration element on S to the field point, and $\vec{H}_t$ is the tangential component of the total magnetic field on the surface. In particular, for the back-scattered far field,

$$\vec{H}^s = \frac{ik}{4\pi R} \int_S \hat{n}_o \times (\hat{n} \times \vec{H}_t) \, e^{ikr} \, dS, \tag{9-5}$$

where R is the distance from the field point to the center of the scatterer and $\hat{n}_o$ is a unit vector in the direction of propagation of the incident plane wave.

For the scatterer under consideration put the origin of coordinates on the upper shadow boundary midway between the ends of the cylinder. Let the X-axis be in the direction of the incoming radiation, the Z-axis perpendicular to the cylinder surface and the Y-axis in the direction of the cylinder axis (Fig. 9-2).

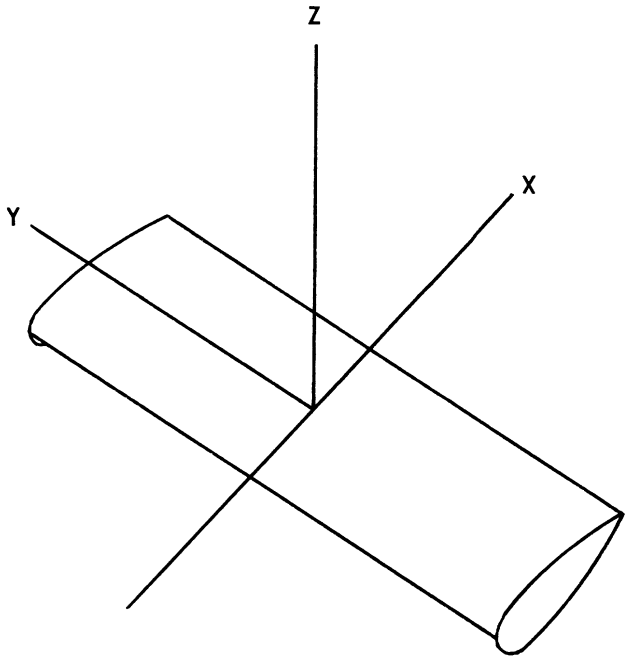

FIG. 9-2 ORIENTATION OF COORDINATE AXES

First consider the case of incidence along the X-axis and the electric vector polarized perpendicular to the cylinder axis (Fig. 9-3).

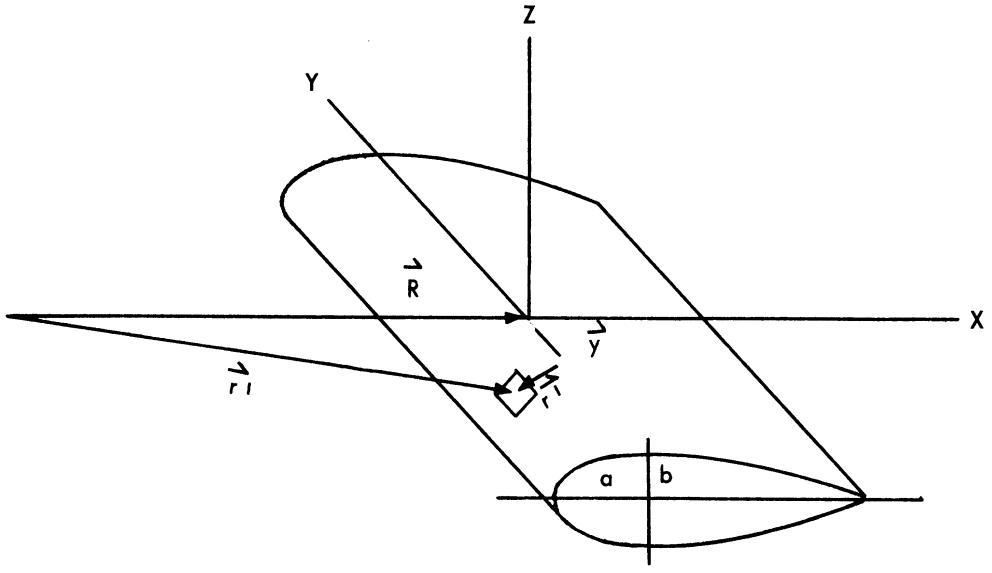

FIG. 9-3 DEFINITION OF PARAMETERS

In this case

$$\vec{H}_t = (0,\ H_t,\ 0); \tag{9-6}$$

hence,

$$\hat{n}_o \times (\hat{n} \times \vec{H}_t) = (0,\ n_x H_t,\ 0), \text{ and} \tag{9-7}$$

$$e^{ikr} \cong e^{ikR}\, e^{i\vec{k}\cdot\vec{r}'}, \tag{9-8}$$

where,

$$\vec{k} = \hat{n}_o k, \tag{9-9}$$

so that

$$H^s = \frac{ik}{4\pi} \frac{e^{ikR}}{R} \int_S n_x H_t\, e^{i\vec{k}\cdot\vec{r}'}\, dS. \tag{9-10}$$

After Fock (Ref. 9), write

$$H_t = H_t^o\, G(\xi), \tag{9-11}$$

where $H_t^o = e^{i\vec{k}\cdot\vec{r}}$. The function $G(\xi)$ is determined numerically and tabulated for $\xi = -4.5\ (0.1)\ 4.5$ by Fock (Ref. 9).

The integration over the y direction of the integral gives simply

$$H^s = \frac{ikL}{4} \frac{e^{2ikR}}{R} \int n_x\, e^{2i\vec{k}\cdot\vec{r}'}\, G(\xi)\, d\ell, \tag{9-12}$$

where $d\ell$ is the element of path around the cross-section of the cylinder.

To facilitate the computation divide the integral into two parts, that over the ellipse, and that over the ogive. Let these parts be designated by I_e and I_o for the integration over the ellipse and ogive respectively. Because of the symmetry of the nose-on case, only the integral over 1/2 the cross-section, from nose to tail need be calculated. Thus,

$$H^s = \frac{ikL}{4\pi} \frac{e^{ikR}}{R} (2\, I_e + 2\, I_o) , \tag{9-13}$$

where,

$$I_{\substack{e \\ o}} = \int_{\ell_{\substack{e \\ o}}} n_x\, e^{2i\vec{k}\cdot\vec{r}'}\, G(\xi)\, d\ell \ . \tag{9-14}$$

Now

$$n_x\, d\ell = -\frac{bx}{a^2} \frac{dx}{\sqrt{1 - \frac{x^2}{a^2}}} \text{ on } \ell_e \ , \text{ and} \tag{9-15}$$

$$\xi = \left(\frac{kb^2}{2a}\right)^{1/3} \frac{x}{a} \ ; \tag{9-16}$$

hence,

$$I_e = \int_{-\left(\frac{kb^2}{2a}\right)^{1/3}}^{0} \frac{\xi\, d\xi}{\sqrt{1 - \left(\frac{2a}{kb^2}\right)^{2/3} \xi^2}} e^{i\left(\frac{4ka^2}{b}\right)^{2/3} \xi} G(\xi) \left(\frac{4a^2}{k^2 b}\right)^{1/3} , \tag{9-17}$$

while $n_x \, d\ell = \frac{a^2}{b} \cos\theta \, d\theta$ on ℓ_o and ξ is given above; hence

$$I_o = \left(4\frac{a^2}{bk^2}\right)^{1/3} \int_o^{\left(\frac{ka^2}{2b}\right)^{1/3}} \frac{\xi \, d\xi}{\sqrt{1 - \left(\frac{2b}{ka^2}\right)^{2/3} \xi^2}} e^{i\left(\frac{4ka^2}{b}\right)^{2/3} \xi} G(\xi). \quad (9\text{-}18)$$

The cross-section is then given by:

$$\sigma = \left(\frac{Lk^2}{\pi}\right)^2 \left(\frac{4a^2}{k^2 b}\right)^{2/3} \left| I_e + I_o \right|^2 ,$$

$$= \frac{L^2}{\pi^2} (4kR_o)^{2/3} \left| I_e + I_o \right|^2 . \quad (9\text{-}19)$$

For incidence at some angle α to the X-axis, the same current distribution technique is applicable provided:

1. The radius of curvature at the shadow boundary remains sufficiently large,

2. The minimum distance from the shadow boundary to the "tail" is large enough for the shape factors to assume the asymptotic value, zero.

It is required that the radius of curvature at A be much larger than a wavelength and that the reduced distance from the shadow curve at B to the tail C be so great as to be in the asymptotic range of the function $G(\xi)$.

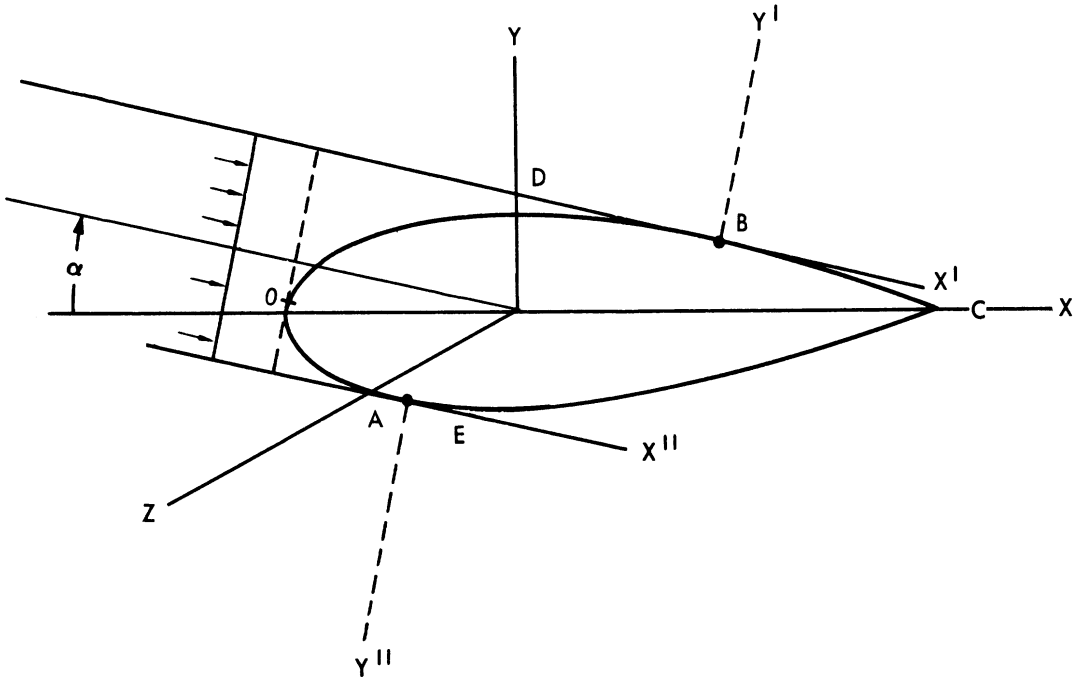

FIG. 9-4 COORDINATE AXES FOR INCIDENCE AT ANGLES α

As before erect the coordinate axis with the shadow boundary as the origin. Since there is no longer the symmetry of the "nose-on" case, it is necessary to divide the surface into two parts and determine the contributions from the two sides of the specular reflection point separately. With this in mind two coordinate systems as indicated are used and the procedure is the same as before.

In the case of parallel polarization, after Fock (Ref. 9), make the approximation that on the surface

$$H_z = 0 , \tag{9-20}$$

$$H_x = \frac{i}{m} H_z^o e^{ikx} F(\xi) , \tag{9-21}$$

where

$$m = \left(\frac{ka^2}{2b}\right)^{1/3} = \left(\frac{kR_o}{2}\right)^{1/3} ,$$

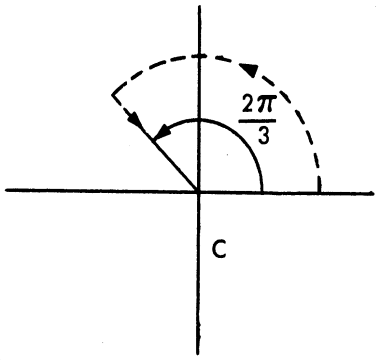

$$F(\xi) = \frac{1}{\sqrt{\pi}} e^{\frac{i\xi^3}{3}} \int_C \frac{e^{i\xi t}}{w(t)} dt,$$

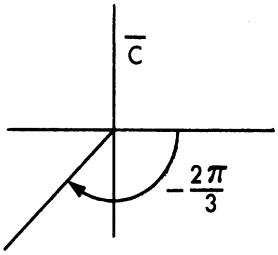

$$w(t) = \frac{1}{\sqrt{\pi}} \int_{\bar{C}} e^{zt - \frac{1}{3}z^3} dz . \qquad (9\text{-}22)$$

Asymptotically for large negative ξ, $F(\xi)$ is evaluated by the method of stationary phase; thus,

$$\left| F(\xi) \right| \cong 2\xi , \qquad (9\text{-}23)$$

which gives the geometrical optic field

$$H_x = 2i\, e^{ikx}\, H_z^o \frac{xb}{a^2} = 2i\, H_z^o\, e^{ikx} \frac{x}{R_o} . \qquad (9\text{-}24)$$

For positive ξ, the function $F(\xi)$ may be evaluated by closing the contour C and obtaining the sum of residues,

$$F(\xi) = 2\pi i \sum \frac{e^{i\xi t_s}}{w'(t_s)} , \qquad (9\text{-}25)$$

where the t_s are the zeros of $w(t)$.

The zeros of w(t) are given by Fock (Ref. 9) and by Franz (Ref. 13). The values of $w'(t_s)$ are given by Franz in the form of those of a related function. The function $F(\xi)$ must be evaluated by quadratures for $\xi < 0$ and as is indicated above, may be evaluated by the method of stationary phase for $\xi << -1$. The function $F(\xi)$ has been computed and appears in Tables 9-1 and 9-2.

By an analysis analogous to the above the scattered magnetic field is found to be in the Z-direction, and is given by

$$H^S = \frac{ik}{4\pi} \frac{e^{ikR}}{R} \int n_z H_x e^{i\vec{k} \cdot \vec{r}'} dS . \qquad (9\text{-}26)$$

Substituting for H_x,

$$H^S = \left(\frac{ik}{4\pi}\right)\left(\frac{i}{m}\right)\frac{e^{ikR}}{R} \int_S e^{2ikx} n_z F(\xi) dS , \qquad (9\text{-}27)$$

where $n_z = \sqrt{1 - n_x^2}$ and n_x is given above.

TABLE 9-1

VALUES OF $F(\xi)$, 0(0.1)2.1

ξ	Re[F(ξ)] Numerical Integration	Re[F(ξ)] Residues	Im[F(ξ)] Numerical Integration	Im[F(ξ)] Residues
0	0.38791		-0.67188	
.1	0.38569		-0.56098	
.2	0.37880		-0.45779	
.3	0.36699		-0.36257	
.4	0.35013	0.34876	-0.27557	-0.27526
.5	0.32825	0.32747	-0.19712	-0.19747
.6	0.30153	0.30120	-0.12754	-0.12793
.7	0.27040	0.27027	-0.06721	-0.06291
.8	0.23547	0.23550	-0.01648	-0.01665
.9	0.19762	0.19768	+0.02432	+0.02432
1.0	0.15799	0.15777	0.05496	0.05480
1.1	0.11797	0.11793	0.07539	0.07526
1.2	0.07918	0.07920	0.08582	0.08575
1.3	0.04341	0.04343	0.08683	0.08681
1.4	0.01247	0.01249	0.07951	0.07950
1.5		-0.01193		0.06546
1.6		-0.02852		0.04689
1.7		-0.03660		0.02651
1.8		-0.03644		0.00722
1.9		-0.02937		-0.00815
2.0		-0.01785		-0.01748
2.1		-0.00512		-0.01986
2.2				
2.3				
2.4				
2.5				
2.6				
2.7				

TABLE 9-2

VALUES OF F(ξ), -2.7(0.1)0

ξ	Re[F(ξ)]		Im[F(ξ)]	
	Numerical Integration	Asymptotic	Numerical Integration	Asymptotic
0	0.38791		-0.67188	
-.1	0.38582		-0.79024	
-.2	0.37987		-0.91585	
-.3	0.37052		-1.04845	
-.4	0.35838		-1.18775	
-.5	0.34392		-1.33347	
-.6	0.32771		-1.48526	
-.7	0.31027		-1.64276	
-.8	0.29209		-1.80557	
-.9	0.27355		-1.97328	
-1.0	0.25509	0.15972	-2.14544	-2.13348
-1.1	0.23697	0.16006	-2.32164	-2.30150
-1.2	0.21948	0.15162	-2.50144	-2.47517
-1.3	0.20285	0.13924	-2.68455	-2.65543
-1.4	0.18718	0.12599	-2.87050	-2.84129
-1.5		0.11340		-3.03128
-1.6		0.10205		-3.22414
-1.7		0.09207		-3.41898
-1.8		0.08336		-3.61514
-1.9		0.07576		-3.81216
-2.0		0.06912		-4.00998
-2.1		0.06328		-4.20819
-2.2		0.05810		-4.40675
-2.3		0.05352		-4.60557
-2.4		0.04942		-4.80461
-2.5		0.04575		-5.00388
-2.6		0.04245		-5.20322
-2.7		0.03947		-5.40270

PART II--APPLICATIONS

A

B-47 CROSS-POLARIZATION RADAR CROSS-SECTIONS AS A FUNCTION OF ASPECT AT S-BAND

(Confidential)

In this Part the results of Part I are used to obtain information about the form of $\overline{S \circledast S^{\star}}$ -matrices for the B-47 aircraft as functions of the aspect of the aircraft. These $\overline{S \circledast S^{\star}}$ -matrices are presented in the form of graphs of the cross-polarization radar cross-sections[1]

$\sigma(HH)$, $\sigma(VV)$, $\sigma(HV)$, $\sigma(+H)$, $\sigma(+V)$, $\sigma(LH)$, $\sigma(LV)$,

$\sigma(LR)$, $\sigma(\Lambda P)$, $\sigma(RR)$, $\sigma(LL)$,[2]

as functions of azimuth angle $\phi^{\star}$ for the polar angles,

$$\theta^{\star} = 86^{\circ}, 90^{\circ}, 94^{\circ}, 98^{\circ}, 102^{\circ}, 120^{\circ}, 150^{\circ},$$

and the wavelength[3] $\lambda \cong 12$ cm. From these cross-polarization cross-sections an $\overline{S \circledast S^{\star}}$ -matrix as function of aspect can be deduced for the B-47 aircraft by the methods of Sections 3 and 4.

---

[1]The last two cross-sections are included for the convenience of the reader; only the first nine cross-sections are needed to compute an $\overline{S \circledast S^{\star}}$-matrix for a complex configuration (Sec. 3 and 4).

[2]These cross-polarization cross-sections are defined by Equation (2.2-7b). The various polarizations are illustrated in Figure 4-1.

[3]This wavelength was chosen so that use could be made of certain computations already in hand from the companion volume Studies XV (Ref. 1). These computations are for those B-47 components (mainly conical and ellipsoidal shapes) for which no new theory was needed.

To further elaborate, the following sections will contain more detailed discussions on how the above-mentioned cross-sections, and in some cases the scattering matrices themselves, are obtained for particular components of the B-47 aircraft.

In every case the break-down of the B-47 into individual components is that given by Figure A-1 used in Reference 1. Moreover, the simulation of these components by simple geometric shapes is understood to be that of Figure A-2 used in Reference 1.

A.1 COMPONENTS OF THE B-47 AIRCRAFT SIMULATED BY WEDGE SHAPES

The components of the B-47 aircraft which have been simulated by wedge shapes are the trailing edges of the wings and the trailing edges of the horizontal and vertical tail sections; the tapered wedges used to simulate these components have respective edge lengths L of 18 meters, 4.8 meters, and 5.5 meters.

The following cross-sections have been obtained by applying Equation (6.9-8) for the scattering matrix S(HV; HV):

$$\sigma(HH) = M\left[\frac{2\cos^2\alpha}{C\sin^2\theta^{\star}} - \left(\frac{1}{C}+\frac{1}{D}\right)\right]^2 , \qquad (A.1\text{-}1)$$

$$\sigma(VV) = M\left[\left(\frac{1}{C}-\frac{1}{D}\right) - \frac{2\cos^2\alpha}{C\sin^2\theta^{\star}}\right]^2 , \qquad (A.1\text{-}2)$$

$$\sigma(HV) = M\left[\frac{\sin\alpha\cos\alpha\,\sin(\phi_{\perp}^{\star}-\beta)}{C\sin\theta^{\star}}\right]^2 , \qquad (A.1\text{-}3)$$

where C, D, M are given by Equation (6.7-1), $\cos\alpha = a_{33}$, $\tan\beta = a_{23}/a_{13}$, and the a_{ij} are given by Equation (6.8-1). By the formulas of Section 4 the remaining six cross-sections for the wedge shapes can be given in terms of the above three:

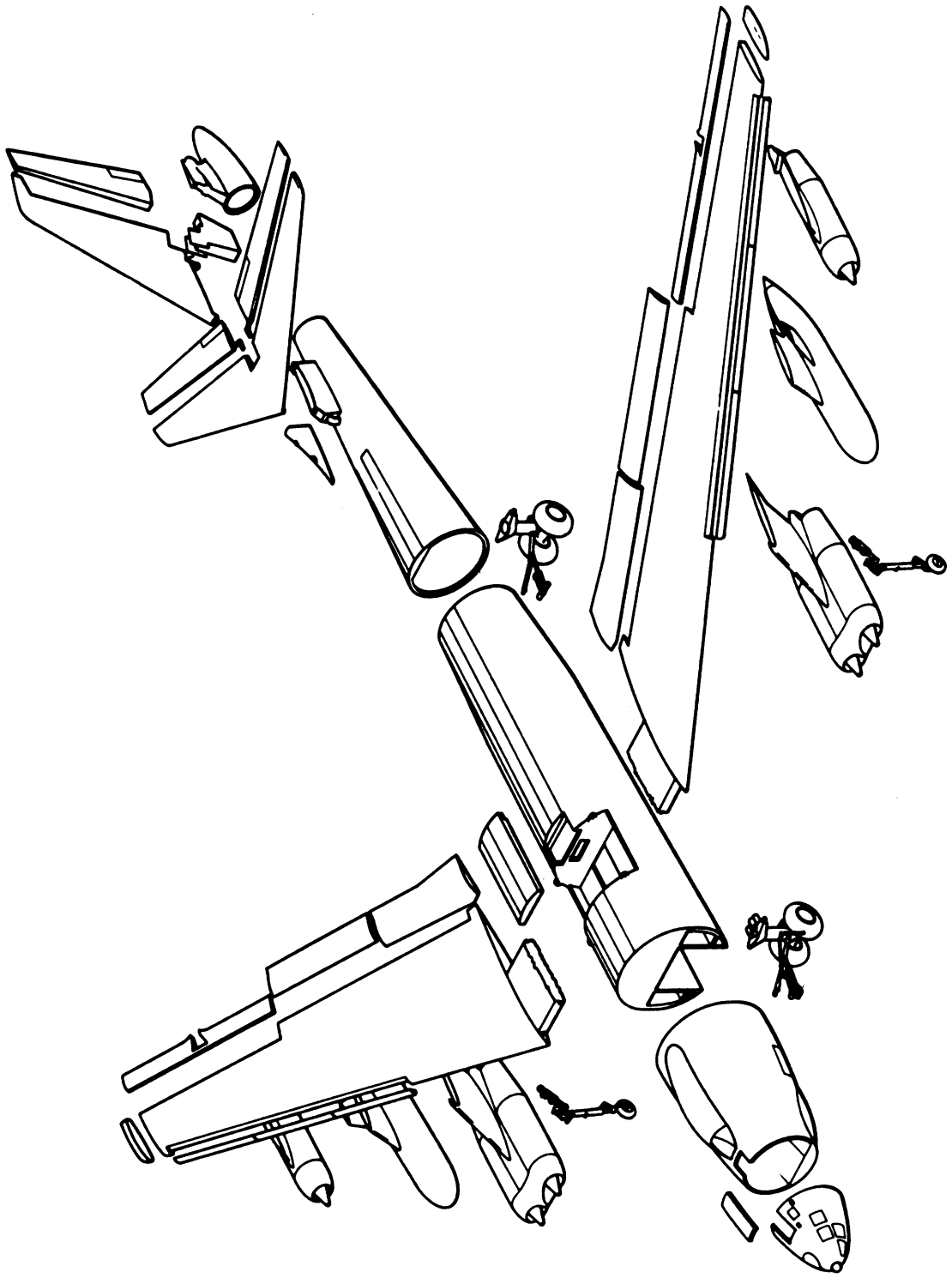

FIG. A-1 STRUCTURAL BREAKDOWN OF THE B-47

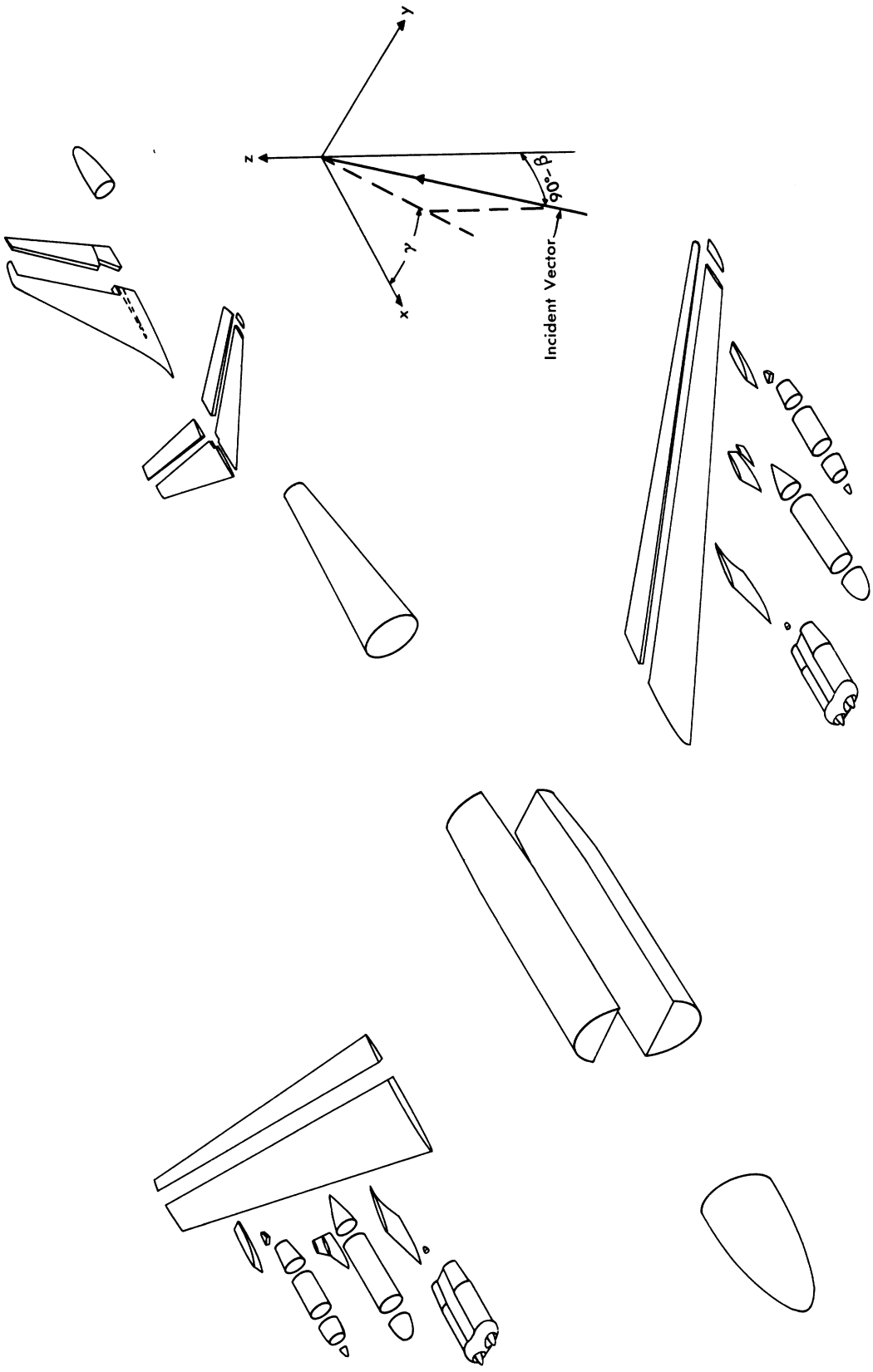

FIG. A-2 ILLUSTRATIVE EXAMPLE OF THE BREAKDOWN USED FOR THE B-47

$$\sigma(+H) = \frac{1}{2}\sigma(HH) + \frac{1}{2}\sigma(HV) + \frac{1}{4\pi}\sqrt{\sigma(HH)\,\sigma(HV)}, \qquad \text{(A.1-4)}$$

$$\sigma(+V) = \frac{1}{2}\sigma(HV) + \frac{1}{2}\sigma(VV) + \frac{1}{4\pi}\sqrt{\sigma(HV)\,\sigma(VV)}, \qquad \text{(A.1-5)}$$

$$\sigma(LH) = \frac{1}{2}\sigma(HH) + \frac{1}{2}\sigma(HV), \qquad \text{(A.1-6)}$$

$$\sigma(LV) = \frac{1}{2}\sigma(HV) + \frac{1}{2}\sigma(VV), \qquad \text{(A.1-7)}$$

$$\sigma(LR) = \frac{1}{4}\sigma(HH) + \frac{1}{4}\sigma(VV) + \frac{1}{8\pi}\sqrt{\sigma(HH)\,\sigma(VV)}, \qquad \text{(A.1-8)}$$

$$\sigma(\Lambda P) = \frac{1}{4}\sigma(HH) + \frac{1}{4}\sigma(VV). \qquad \text{(A.1-9)}$$

Following the methods of Sections 6.8 and 6.9, peak values of the cross-sections, and the azimuths $\phi^{\star}$ at which they occur, can be computed for fixed polar angles $\theta^{\star}$. Widths of peaks are determined by finding the azimuth values for which the cross-sections have decreased by factors $1/g^2$ of 2, 10, and 100.

To illustrate the contribution to the total B-47 aircraft cross-section due to a component represented by a tapered wedge of edge length L = 18 meters (trailing edge of wing), four graphs (cross-sections vs. azimuth for $\theta^{\star} = 86^{\circ}, 90^{\circ}, 94^{\circ}, 98^{\circ}, 120^{\circ}, 150^{\circ}$) are presented in Figures A.1-1 through A.1-4.

A.2 COMPONENTS OF THE B-47 AIRCRAFT SIMULATED BY WIRE LOOPS

It was pointed out in Section 2.2 that, if scattering matrices are to be calculated for a single component, only the five numbers $\sigma(HH)$, $\sigma(VV)$, $\sigma(HV)$, $\sigma(HR)$, $\sigma(VR)$ are required. But in Sections 3 and 4, it was shown that if $\overline{S \otimes S^{\star}}$-matrices are to be found for a B-47, it is necessary to

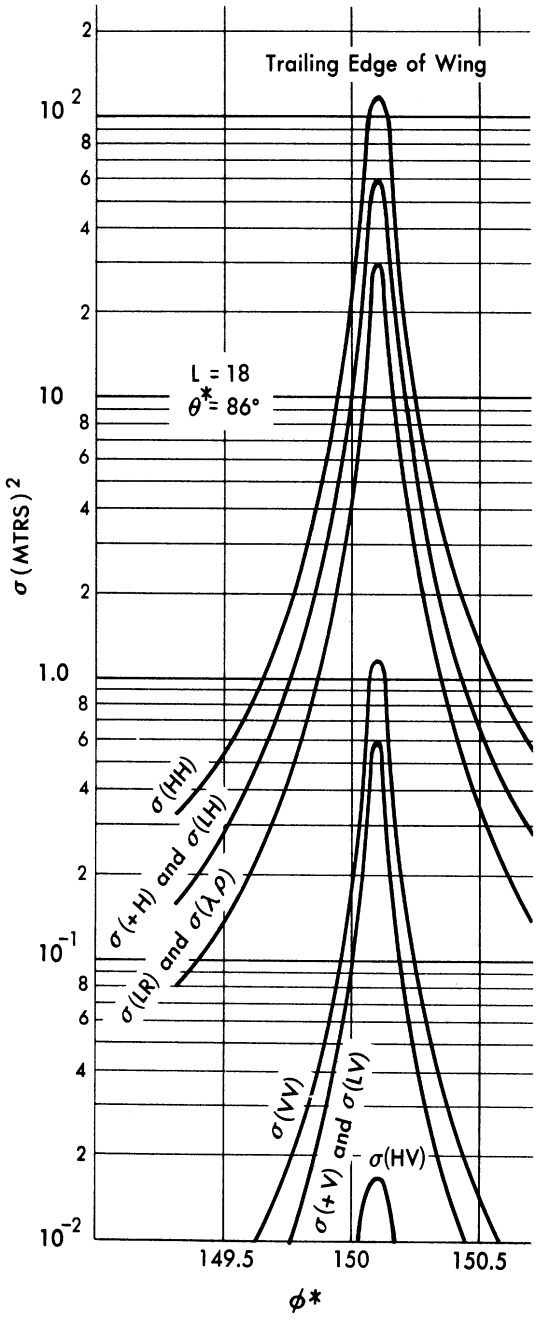

FIG. A.1-1 CROSS-SECTIONS vs. AZIMUTH ϕ^* FOR A TAPERED WEDGE OF EDGE LENGTH L = 18m FOR THE ASPECT $\theta^* = 86°$ (Trailing Edge of Wing)

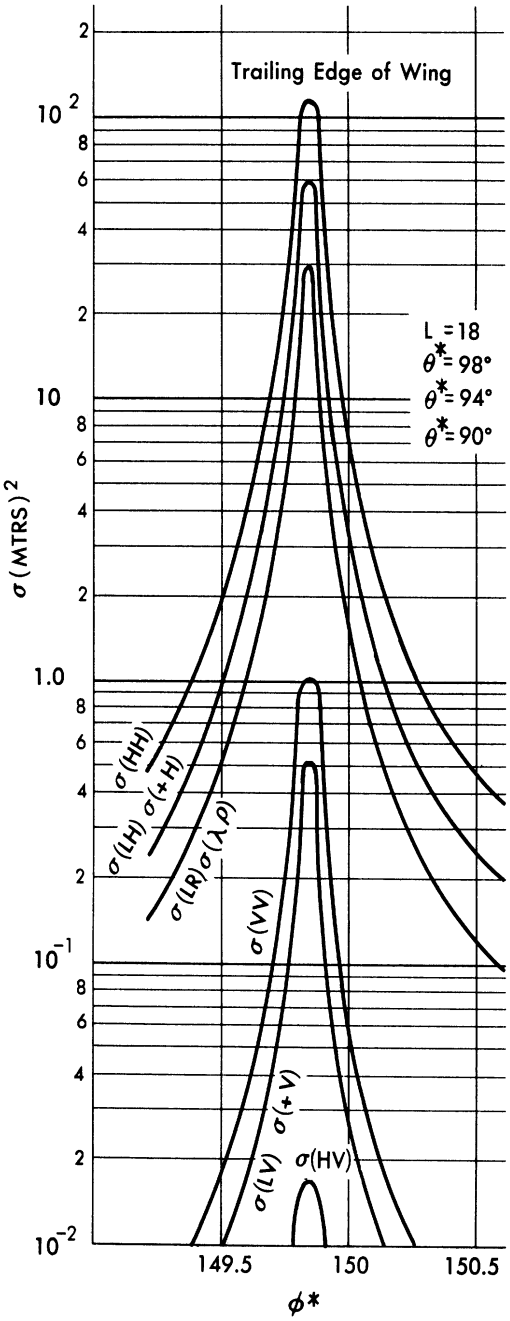

FIG. A.1-2 CROSS-SECTIONS vs. AZIMUTH ϕ^* FOR A TAPERED WEDGE OF EDGE LENGTH L = 18m FOR THE ASPECT $\theta^* = 90°, 94°, 98°$ (Trailing Edge of Wing)

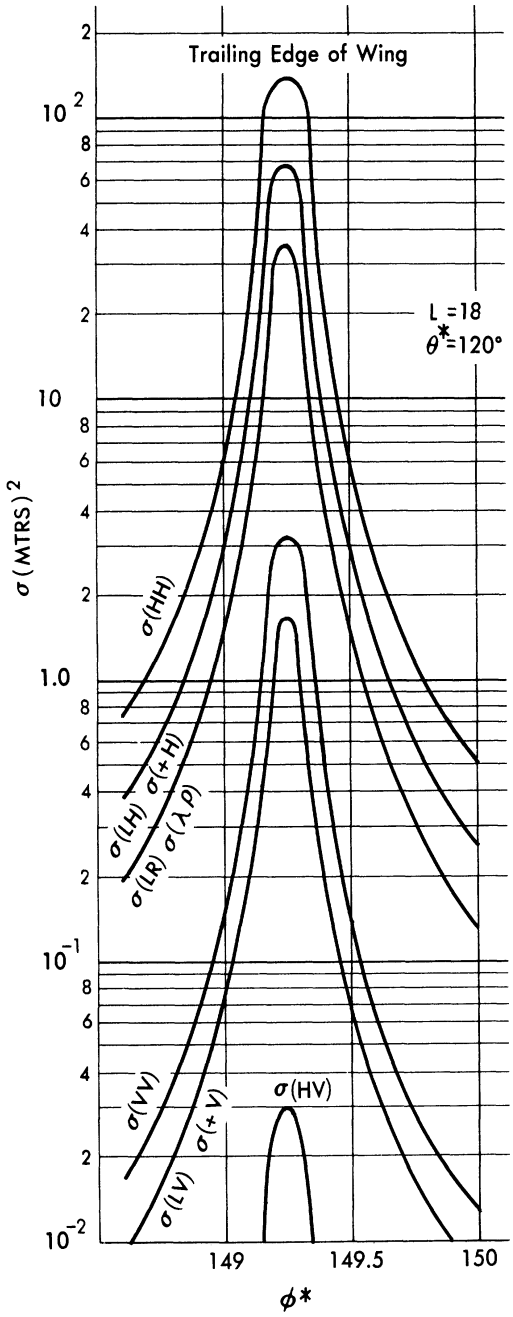

FIG. A.1-3 CROSS-SECTIONS vs. AZIMUTH ϕ^* FOR A TAPERED WEDGE OF EDGE LENGTH L = 18m FOR THE ASPECT θ^* =120° (Trailing Edge of Wing)

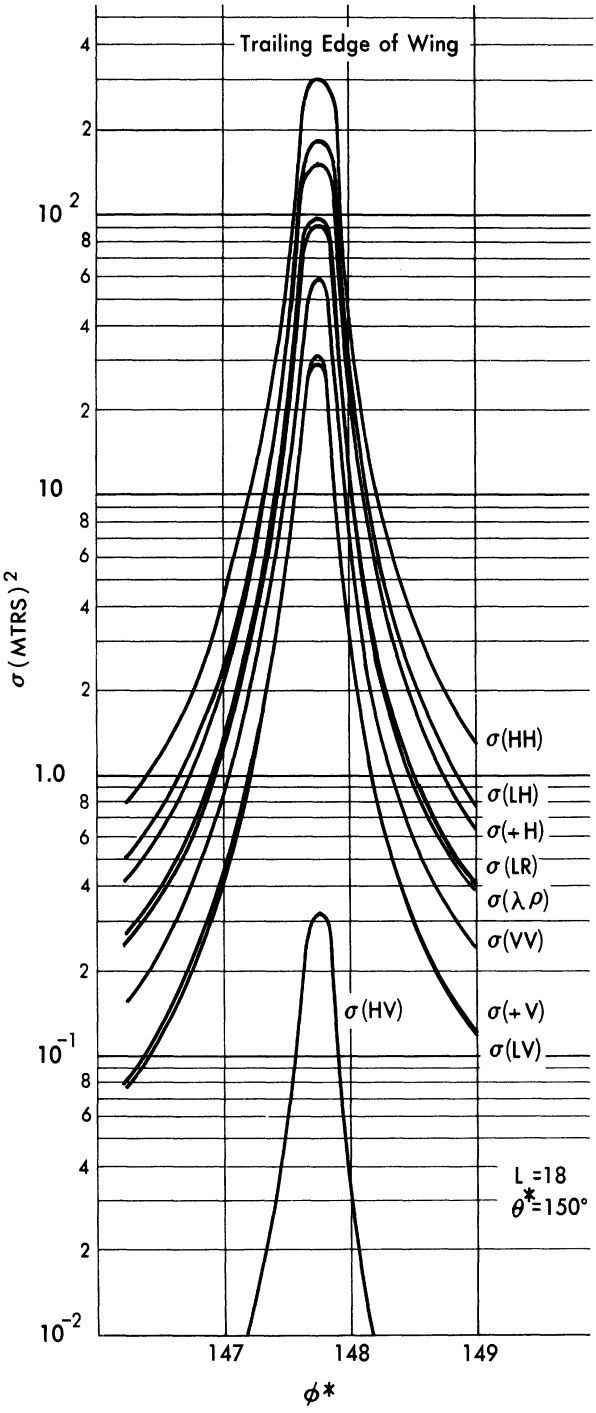

FIG. A.1-4 CROSS-SECTIONS vs. AZIMUTH ϕ^* FOR A TAPERED WEDGE OF EDGE LENGTH L = 18m FOR THE ASPECT θ^* =150° (Trailing Edge of Wing)

know the nine cross-polarization cross-sections given at the beginning of Section A so that techniques involving phase averaging over all components of the B-47 can be used.

To illustrate how the nine numbers just mentioned can be obtained at once from the five listed above by means of the considerations of Sections 2, 3, 4, consider the following example.

It follows immediately from the conservation of energy relation (footnote 2, p. 11) that

$$\text{(a)}\quad \sigma(LV) = \sigma(HV) + \sigma(VV) - \sigma(VR) = \sigma(VR),$$

$$\text{(b)}\quad \sigma(LH) = \sigma(HH) + \sigma(VH) - \sigma(HR) = \sigma(HR),$$

$$\text{(c)}\quad \sigma(LR) = \sigma(HR) + \sigma(VR) - \sigma(RR). \qquad \text{(A.2-1)}$$

The final three cross-sections desired may be obtained from Equation (4-6) using Equations (2-14) and (2-15); they are:

$$\text{(a)}\quad \sigma(+H) = \frac{1}{2}\sigma(HH) + \frac{1}{2}\sigma(HV) + \sqrt{\sigma(HR)\,\sigma(HL) - \frac{1}{4}\left[\sigma(HH) - \sigma(HV)\right]^2},$$

$$= \sigma(HR) + \sqrt{\sigma(HH)\,\sigma(HV)} = \frac{1}{2}\left(\sqrt{\sigma(HH)} + \sqrt{\sigma(HV)}\right)^2,$$

$$\text{(b)}\quad \sigma(+V) = \frac{1}{2}\sigma(HV) + \frac{1}{2}\sigma(VV) + \sqrt{\sigma(VR)\,\sigma(VL) - \frac{1}{4}\left[\sigma(HV) - \sigma(VV)\right]^2},$$

$$= \sigma(VR) + \sqrt{\sigma(VV)\,\sigma(HV)} = \frac{1}{2}\left(\sqrt{\sigma(VV)} + \sqrt{\sigma(HV)}\right)^2,$$

$$\text{(c)}\quad \sigma(\Delta P) = \frac{1}{4}\sigma(HH) + \frac{1}{4}\sigma(VV) + \frac{1}{4}\sqrt{4\,\sigma(HH)\,\sigma(VV) - \left[\sigma(HH) + \sigma(VV) - 4\,\sigma(LR)\right]^2},$$

$$= \frac{1}{4}\sigma(HH) + \frac{1}{4}\sigma(VV). \qquad \text{(A.2-2)}$$

For purposes of illustration the method of obtaining Formula (A.2-2a) is presented here in detail. From Equation (4-6),

$$\left| S(+H) \right|^2 = \frac{1}{2} \left| S(HH) \right|^2 + \frac{1}{2} \left| S(HV) \right|^2 + \text{Re } S^{*}(HH)\, S(HV); \qquad \text{(A.2-3)}$$

or, if the form of the scattering matrix S(HV; HV) is assumed to be

$$S(HV; HV) = \begin{bmatrix} \sqrt{\sigma(HH)}\, e^{i[\theta(HH) - \theta(HV)]}, & \sqrt{\sigma(HV)} \\ \sqrt{\sigma(HV)}, & \sqrt{\sigma(VV)}\, e^{i[\theta(VV) - \theta(HV)]} \end{bmatrix}, \qquad \text{(A.2-4)}$$

Equation (A.2-3) may be written as:

$$\sigma(+H) = \frac{1}{2}\sigma(HH) + \frac{1}{2}\sigma(HV) + \sqrt{\sigma(HH)\,\sigma(HV)}\cos[\theta(HH) - \theta(HV)]\,. \qquad \text{(A.2-5)}$$

Here the value of $\cos[\theta(HH) - \theta(HV)]$ is obtainable from Equation (2.2-14) provided the matrix U(HV; RL) is known. Using the values of $\hat{p}(H)$, $\hat{p}(V)$, $\hat{p}(R)$, $\hat{p}(L)$, given respectively by Equations (7.1-7), (7.1-8), (7.1-9), and (7.1-10), the matrix U(HV; RL) is obtainable from the transformation

$$\hat{p}(HV) = U(HV; RL)\, \hat{p}(RL)$$

as

$$U(HV; RL) = \frac{1}{\sqrt{2}} \begin{pmatrix} 1 & 1 \\ -i & i \end{pmatrix}.$$

Thus from Equation (2.2-14),

$$\cos\left[\theta(HH) - \theta(HV) - \frac{\pi}{2}\right] = \frac{\sigma(HR) - \frac{1}{2}\sigma(HH) - \frac{1}{2}\sigma(HV)}{\sqrt{\sigma(HH)\,\sigma(HV)}},$$

and hence,

$$\cos\left[\theta(HH) - \theta(HV)\right] = \frac{\sqrt{\sigma(HR)\,\sigma(HL) - \frac{1}{4}\left[\sigma(HH) - \sigma(HV)\right]^2}}{\sigma(HH)\,\sigma(HV)}. \qquad (A.2\text{-}6)$$

Substitution of Equation (A.2-6) into Equation (A.2-5) finally yields Equation (A.2-2a).

The nine cross-sections obtained above are used in the computation of cross-sections of the B-47 aircraft.

To illustrate contributions from components represented by wire loops (such as the front of engine nacelles) graphs of the above nine cross-sections as functions of θ for a wire loop of radius 39 cm are shown in Figure A.2-2 and Figure A.2-3. The coordinate system shown in Figure A.2-1 applies.

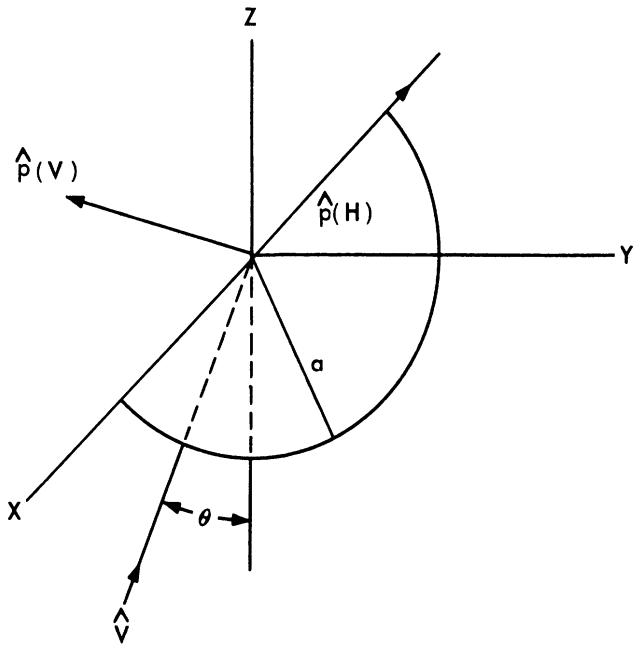

FIG. A.2-1 COORDINATE SYSTEM FOR A LOOP

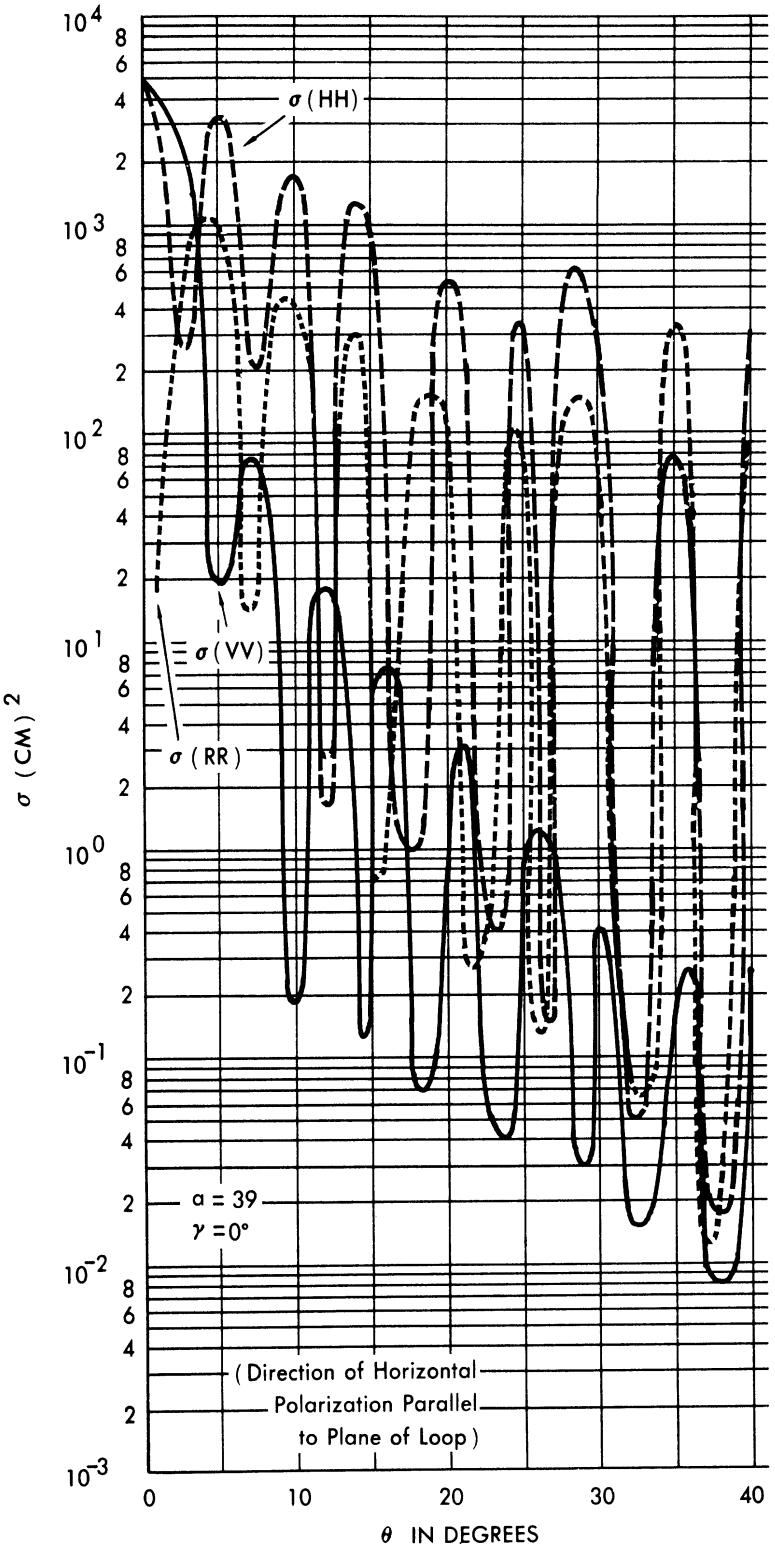

FIG. A.2-2 σ(HH), σ(VV), σ(RR) VERSUS ANGLE OF INCIDENCE θ MEASURED FROM THE NORMAL TO THE PLANE OF A WIRE LOOP OF RADIUS 39 CM.

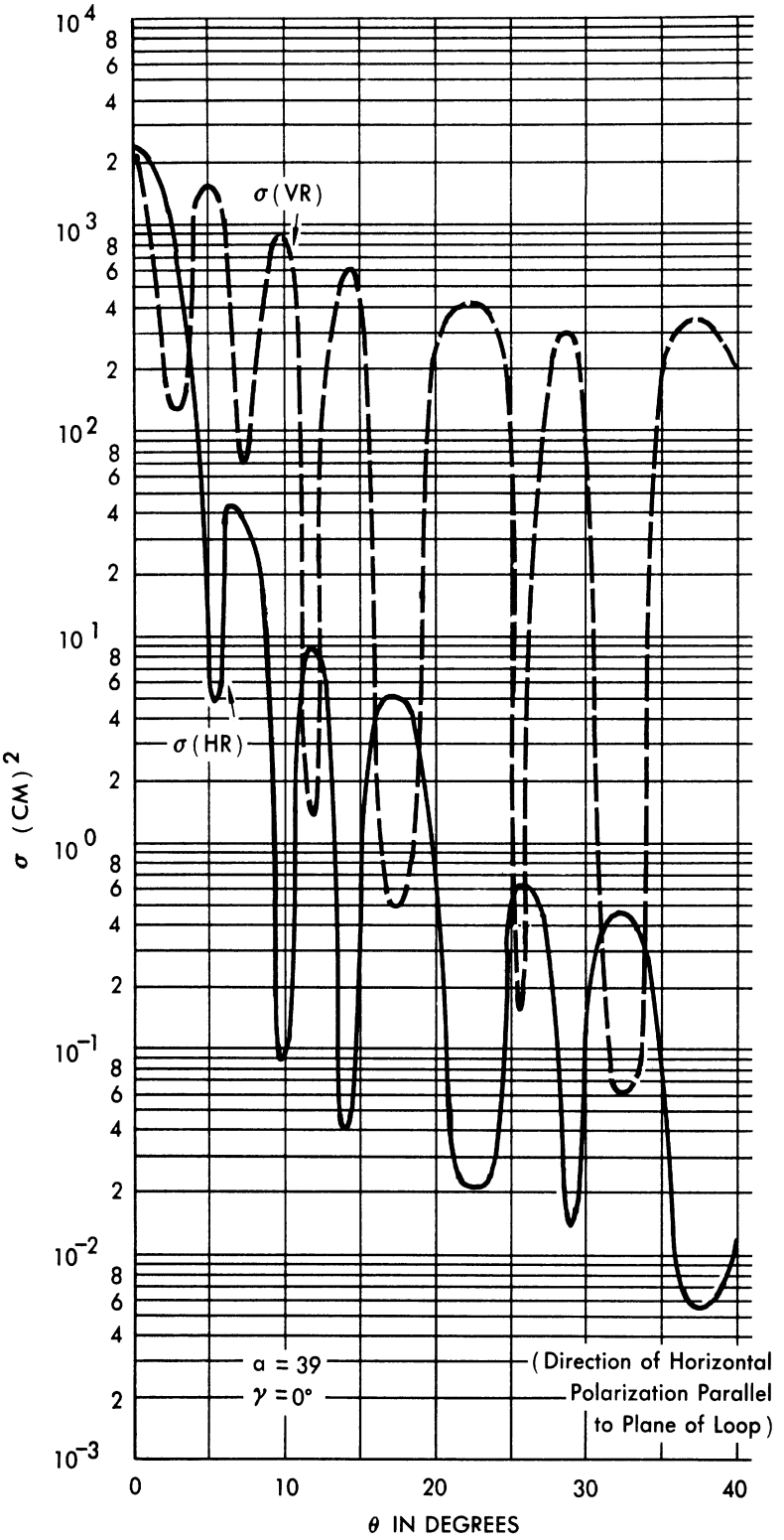

FIG. A.2-3 σ (HR), σ (VR) VERSUS ANGLE OF INCIDENCE θ MEASURED FROM THE NORMAL TO THE PLANE OF A WIRE LOOP OF RADIUS 39 CM.

The direction of horizontal polarization is the y-direction, i.e., the angle γ is zero for all graphs (Eq. 7.1-7 through 7.1-10). In this case $\sigma(HV) = 0$. It is to be noted that these curves have not been smoothed.

A.3 DIHEDRAL SCATTERING

In computing the radar cross-sections of the B-47, it was assumed that the fuselage (represented by a circular cylinder) and the wing (represented by an elliptical cylinder) form a dihedral scattering surface. The method of calculating the return from this dihedral is described in this subsection.

The wing-body orientation of the B-47 chosen for the computation is:

$$\hat{b} = \hat{i}^{\star},$$

$$\hat{w} = \hat{i}^{\star} \cos 125^{o} + \hat{j}^{\star} \sin 125^{o};$$

as before the direction of incident radiation is

$$\hat{r} = \hat{i}^{\star} \sin\theta^{\star} \cos\phi^{\star} + \hat{j}^{\star} \sin\theta^{\star} \sin\phi^{\star} + \hat{k}^{\star} \sin\theta^{\star}.$$

These specifications yield for s, t, and u of Equations (8-14) and 8-15) the values,

$$s = \cos 125^{o},$$

$$t = \sin\theta^{\star} \cos\phi^{\star},$$

$$u = \sin\theta^{\star} \cos(125^{o} - \phi^{\star});$$

hence the angles α, β, and θ can be determined by Equation (8.2-5) in terms of given values of $\theta^{\star}$ and $\phi^{\star}$. Further, the transformation between the $\hat{i}$, $\hat{j}$, $\hat{k}$, and the $\hat{i}^{\star}$, $\hat{j}^{\star}$, $\hat{k}^{\star}$ systems can now be given explicitly:

$$\hat{i} = \frac{1}{ccc+sss}\Big[(\cos\alpha\cos\theta\cos 125^{o} - \sin\beta\cos\theta + \sin\alpha\sin\beta\sin\theta^{*}\cos\phi^{*})\hat{i}^{*}$$
$$+ (\cos\alpha\cos\theta\sin 125^{o} + \sin\alpha\sin\beta\sin\theta^{*}\sin\phi^{*})\hat{j}^{*}$$
$$+ (\sin\alpha\sin\beta\sin\theta^{*})\hat{k}^{*}\Big],$$

$$\hat{j} = \frac{1}{ccc+sss}\Big[(\sin\alpha\sin\theta\cos 125^{o} + \cos\beta\cos\theta - \sin\alpha\cos\beta\sin\theta^{*}\cos\phi^{*})\hat{i}^{*}$$
$$+ (\sin\alpha\sin\theta\sin 125^{o} - \sin\alpha\cos\beta\sin\theta^{*}\sin\phi^{*})\hat{j}^{*}$$
$$- (\sin\alpha\cos\beta\sin\theta^{*})\hat{k}^{*}\Big],$$

$$\hat{k} = \frac{1}{ccc+sss}\Big[(-\sin\theta\cos\alpha\cos 125^{o} + \sin\beta\sin\theta + \cos\alpha\cos\beta\sin\theta^{*}\cos\phi^{*})\hat{i}^{*}$$
$$+ (-\sin\theta\cos\alpha\sin 125^{o} + \cos\alpha\cos\beta\sin\theta^{*}\sin\phi^{*})\hat{j}^{*}$$
$$+ (\cos\alpha\cos\beta\sin\theta^{*})\hat{k}^{*}\Big],$$

where ccc and sss designate respectively $\cos\alpha\cos\beta\cos\theta$ and $\sin\alpha\sin\beta\sin\theta$.

Knowledge of these equations permits the transformation (Eq. 8.2-7),

$$U(HV;AB) = \begin{pmatrix} u(HA) & u(HB) \\ u(VA) & u(VB) \end{pmatrix} = \begin{pmatrix} \hat{p}(H)\cdot\hat{p}(A) & \hat{p}(H)\cdot\hat{p}(B) \\ \hat{p}(V)\cdot\hat{p}(A) & \hat{p}(V)\cdot\hat{p}(B) \end{pmatrix},$$

to be given explicitly with the aid of Equations (8.1-9) and (8.2-8) for $\hat{p}(A)$, $\hat{p}(B)$, $\hat{p}(H)$, and $\hat{p}(V)$:

$$u(HA) = \frac{1}{ccc+sss}\Big[-\sin\alpha\sin\theta\sin(\phi^{*} - 125^{o}) - \cos\beta\cos\theta\sin\phi^{*}\Big],$$

$$u(HB) = \frac{1}{ccc+sss}\left[-\sin\phi^* \sin\beta + \cos\alpha \sin(\phi^* - 125^o)\right],$$

$$u(VA) = \frac{1}{ccc+sss}\left[\sin\alpha \cos\beta \sin\theta^* \cos\theta^* - \sin\alpha \sin\theta \cos\theta^* \cos(\phi^* - 125^o)\right.$$

$$\left. - \cos\theta^* \cos\phi^* \cos\beta \cos\theta\right],$$

$$u(VB) = \frac{1}{ccc+sss}\left[\cos\alpha \cos\theta^* \cos(\phi^* - 125^o)\right.$$

$$+ \sin\theta^* \cos\theta^* (\cos\theta \sin\alpha \sin\beta - \sin\theta \cos\alpha \cos\beta)$$

$$\left. - \cos\theta^* \cos\phi^* \sin\beta + \sin^2\theta^* (\sin\theta \cos\alpha \cos\beta - \cos\theta \sin\alpha \sin\beta)\right].$$

These values together with Equations (8.1-10 and 8.2-6) give the scattering matrix S(HV; HV) as:

$$S(HV;HV) = \frac{Q e^{i\mu}}{R_o}\begin{pmatrix} u^2(HV) - u^2(HB) & u(HA)\,u(VA) - u(HB)\,u(VB) \\ u(HA)\,u(VA) - u(HB)\,u(VB) & u^2(VA) - u^2(VB) \end{pmatrix}.$$

In the expression for Q (Eq. 8.1-10) the radius of curvature of the B-47 body (represented by a circular cylinder) is $R_b = 1.57$ m; the radius of curvature R_w of the B-47 wing is computed from Equation (8.2-9); and the semi-major and semi-minor axes of a right section of a wing are respectively 2.92 m and 0.58 m with unit vectors along those axes given by:

$$\hat{M} = \cos 5^o \cos 35^o \hat{i}^* + \cos 5^o \sin 35^o \hat{j}^* + \sin 5^o \hat{k}^*,$$

$$\hat{m} = -\sin 5^o \cos 35^o \hat{i}^* - \sin 5^o \sin 35^o \hat{j}^* + \cos 5^o \hat{k}^*.$$

A.4 S-BAND CROSS-POLARIZATION RADAR CROSS-SECTIONS FOR A B-47 AIRCRAFT

On the following pages a set of cross-section graphs for the B-47 aircraft is presented in groups of five according to a given polar angle. Thus, for the polar angle $\theta^{\star}$ = constant the group of five graphs is arranged in this sequence:

1st group: $\sigma(HH)$, $\sigma(VV)$, $\sigma(HV)$ vs azimuth $\phi^{\star}$,

2nd group: $\sigma(LH)$, $\sigma(LV)$ vs azimuth $\phi^{\star}$,

3rd group: $\sigma(RR)$, $\sigma(LL)$ vs azimuth $\phi^{\star}$,

4th group: $\sigma(LR)$, $\sigma(\Lambda P)$ vs azimuth $\phi^{\star}$,

5th group: $\sigma(+H)$, $\sigma(+V)$ vs azimuth $\phi^{\star}$.

In Figures A.4-36 and A.4-37 composites of all cross-sections are given for $\theta^{\star} = 94^{\circ}$ and $\theta^{\star} = 120^{\circ}$.

As an example of how to use the $\overline{S \otimes S^{\star}}$-matrix for a fixed aspect to find a particular $\sigma(IJ)$, say $\sigma(RR)$, consider the aspect $\theta^{\star} = 98^{\circ}$, $\phi^{\star} = 70^{\circ}$. From Figures A.4-16, 17, 19, and 20, the values of the nine basic cross-polarization cross-sections are:

$\sigma(HH) = 32$, $\sigma(HV) = 8$, $\sigma(VV) = 32$,

$\sigma(LH) = 20$, $\sigma(LV) = 20$, $\sigma(LR) = 27$,

$\sigma(+H) = 15$, $\sigma(+V) = 23$, $\sigma(\Lambda P) = 17$,

where all values are in square meters. From these numbers it follows that,

$s(HH)\, s^{\star}(HH) = 32$
$s(VH)\, s^{\star}(VH) = 8$
$s(VV)\, s^{\star}(VV) = 32$
$s(HH)\, s^{\star}(VH) = -5$
$s(HH)\, s^{\star}(VV) = 22-2i$
$s(VV)\, s^{\star}(VH) = 3$

where the latter three of these values have been determined from Equation (4-6). The $\overline{S \circledast S^*}$-matrix may now be read off from Equation (3-5) as:

$$\overline{S \circledast S^*} = \begin{bmatrix} 32 & -5 & -5 & 8 \\ -5 & 22-2i & 8 & 3 \\ -5 & 8 & 22-2i & 3 \\ 8 & 3 & 3 & 32 \end{bmatrix} .$$

To find $\sigma(RR)$ it is only necessary to perform the multiplication indicated in Equation (3-2) taking I = J = R. The expressions,

$$(u(RH)\ u(RV)) = \left(-\frac{1}{\sqrt{2}} \quad \frac{i}{\sqrt{2}}\right) = M,$$

$$\begin{pmatrix} u^*(HR) \\ u^*(VR) \end{pmatrix} = \begin{pmatrix} -\frac{1}{\sqrt{2}} \\ \frac{i}{\sqrt{2}} \end{pmatrix} = M'$$

are obtained by putting A = L, B = R, $\alpha = 45^o$, $\gamma = 90^o$ in the matrices of Equation (4-2).

Utilization of $\overline{S \circledast S^*}$, M, and M' in Equation (3-2) yields:

$$\sigma(RR) = (M \circledast M^*)\ \overline{S \circledast S^*}\ (M' \circledast M'^*) = 13\,m^2$$

for the aspect $\theta^* = 98^o$, $\phi^* = 70^o$.

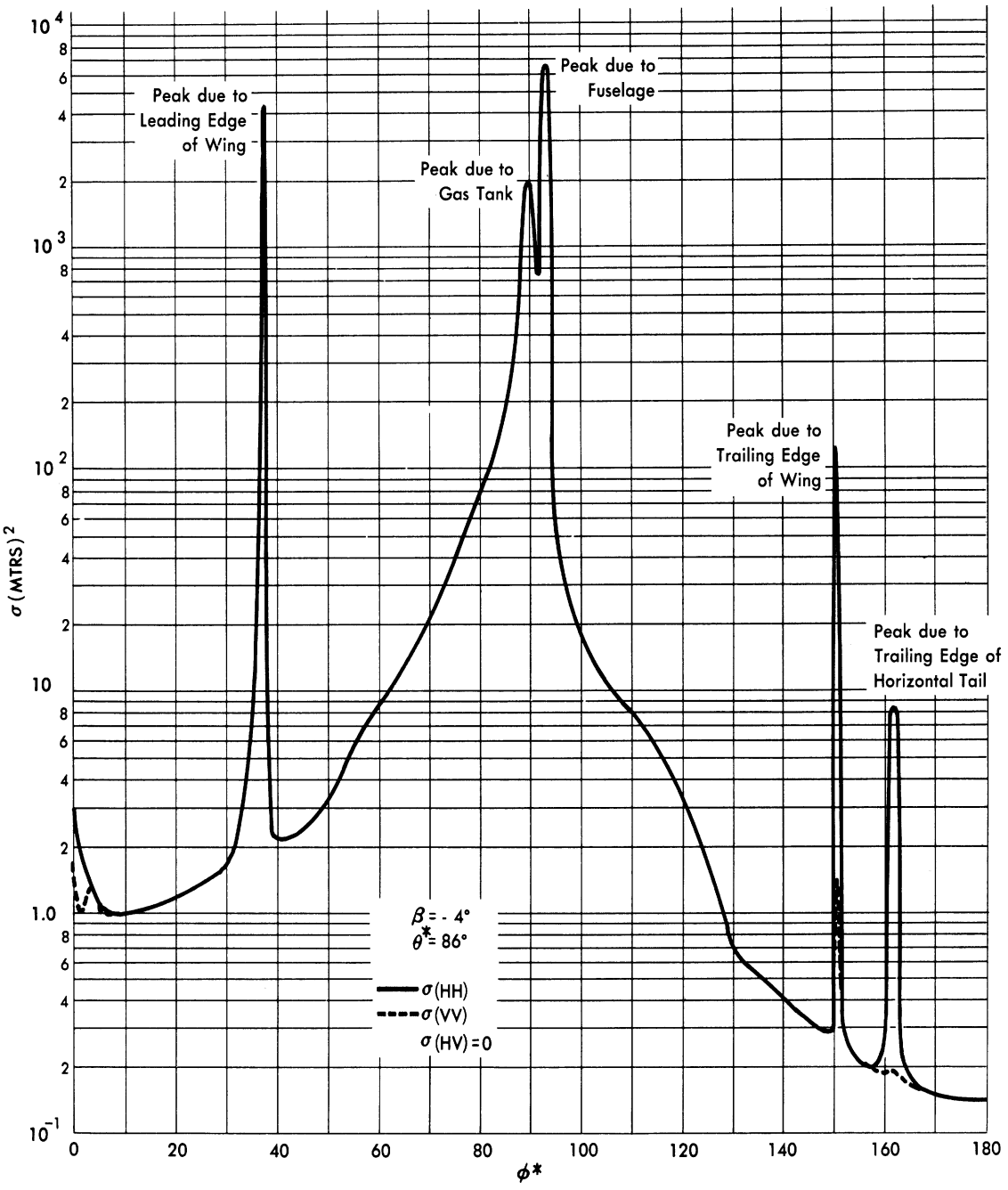

FIG. A.4-1 THEORETICAL CROSS-SECTIONS AT S-BAND FOR THE B-47 FOR ELEVATION - 4°

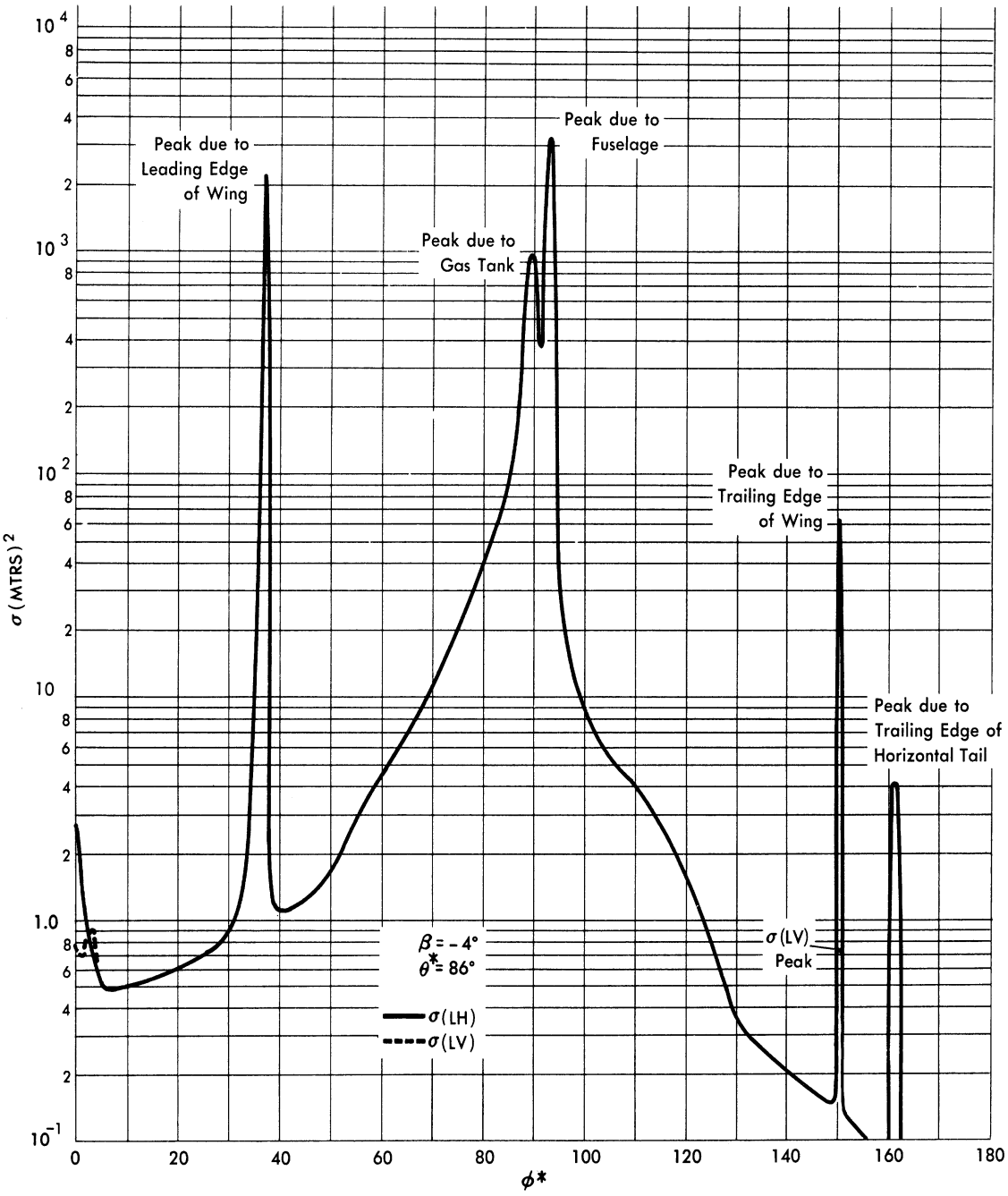

FIG. A.4-2 THEORETICAL CROSS-SECTIONS AT S-BAND FOR THE B-47 FOR ELEVATION - 4°

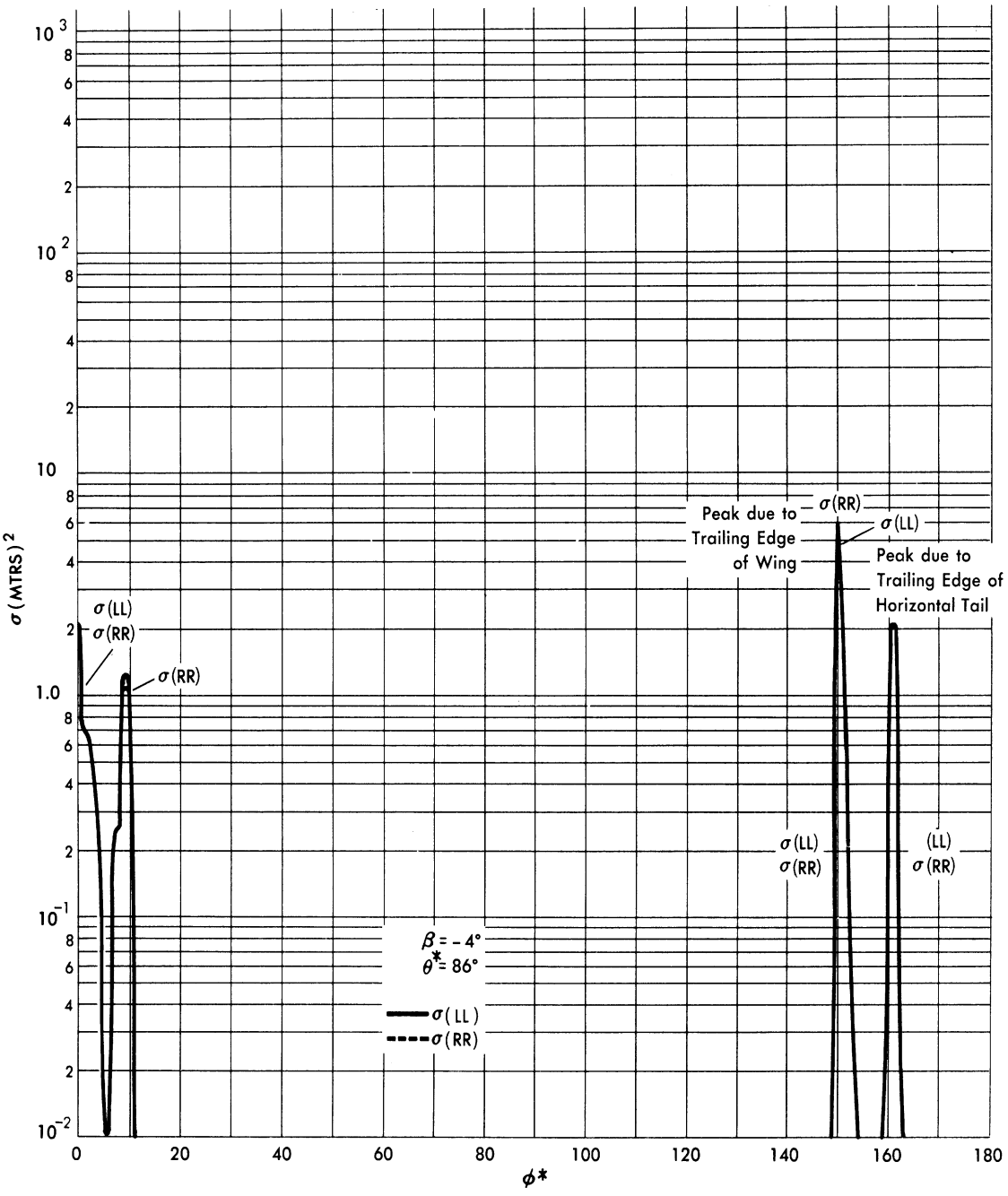

FIG. A.4-3 THEORETICAL CROSS-SECTIONS AT S-BAND FOR THE B-47 FOR ELEVATION - 4°

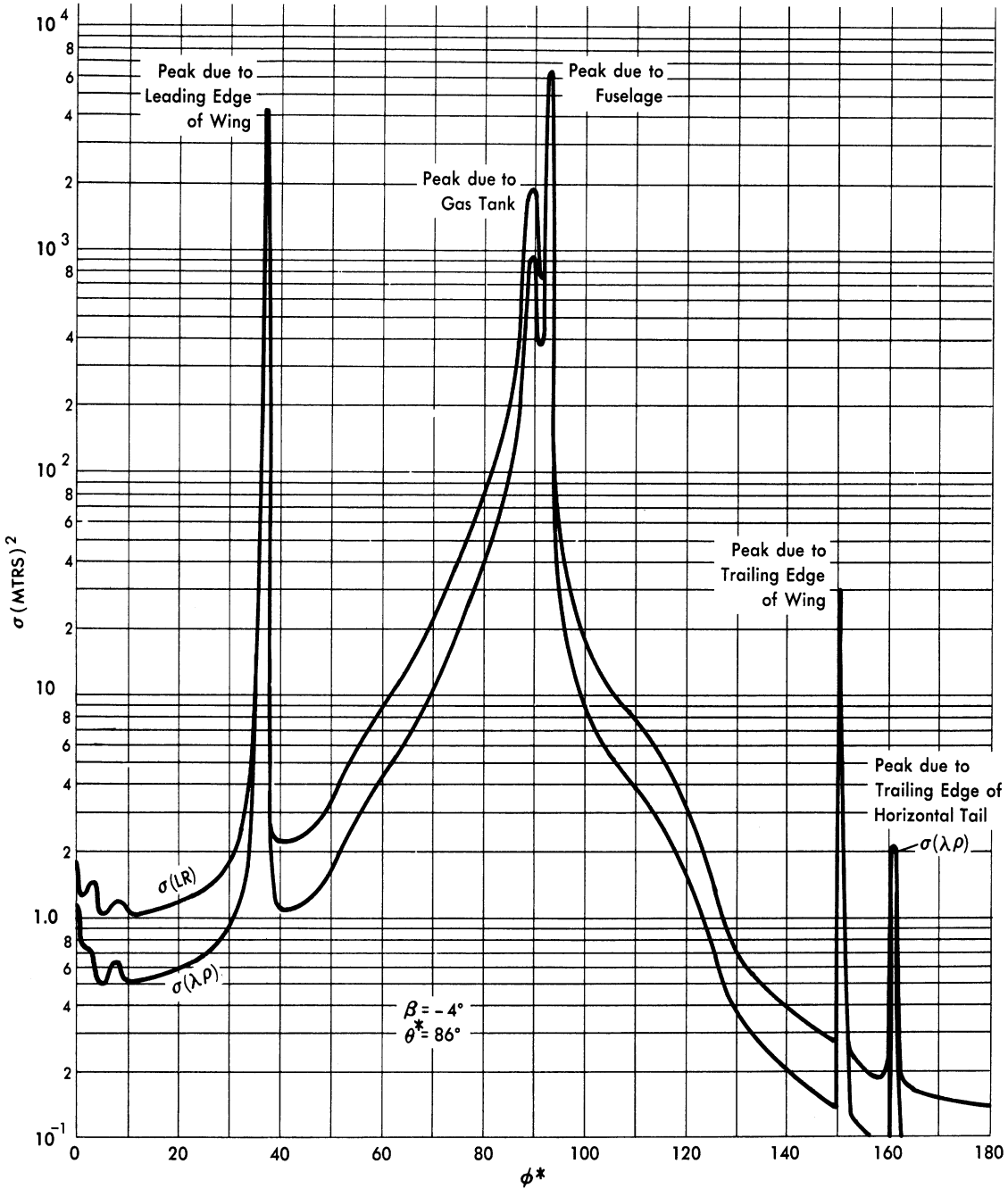

FIG. A.4-4 THEORETICAL CROSS-SECTIONS AT S-BAND FOR THE B-47 FOR ELEVATION - 4°

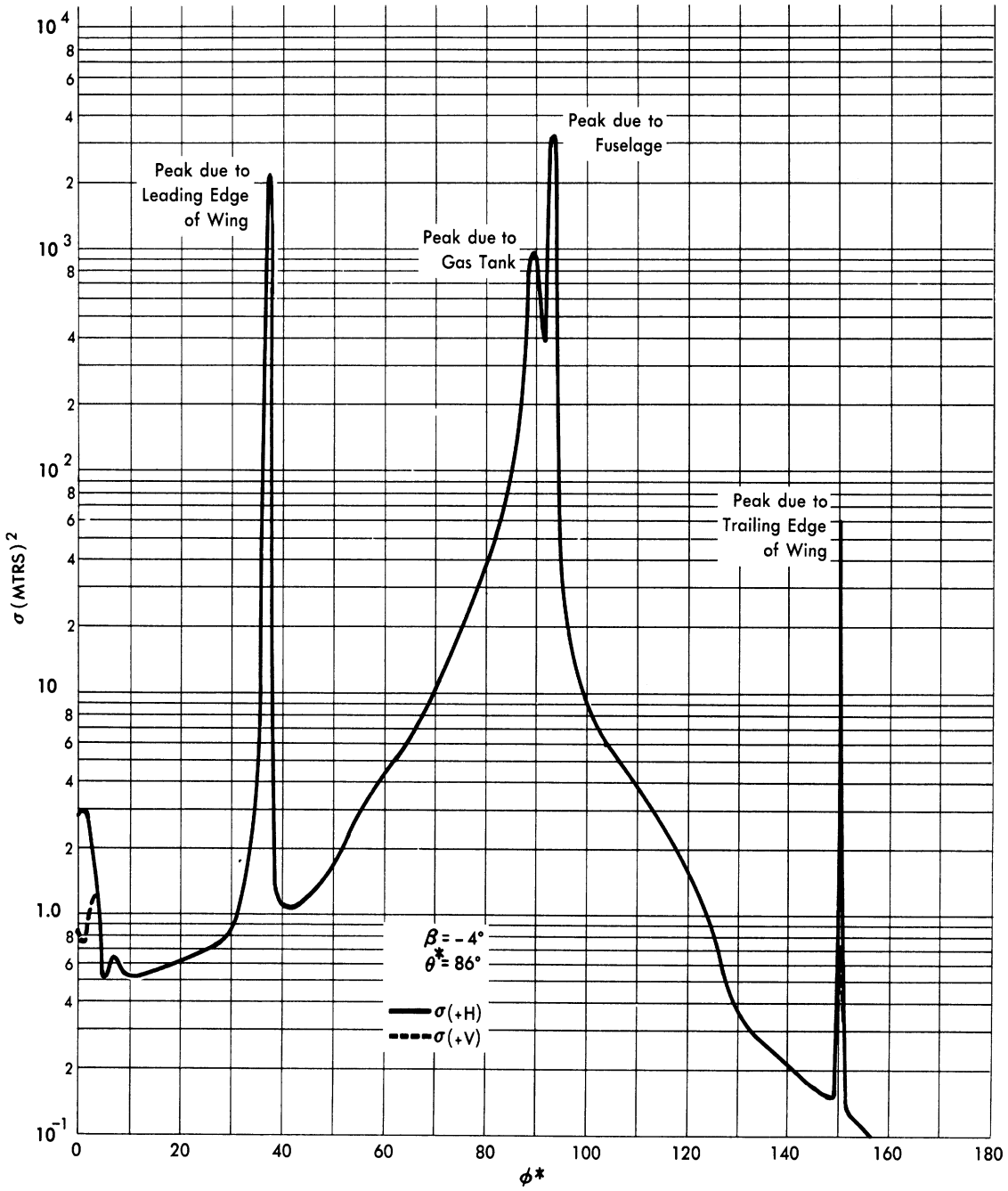

FIG. A.4-5 THEORETICAL CROSS-SECTIONS AT S-BAND FOR THE B-47 FOR ELEVATION - 4°

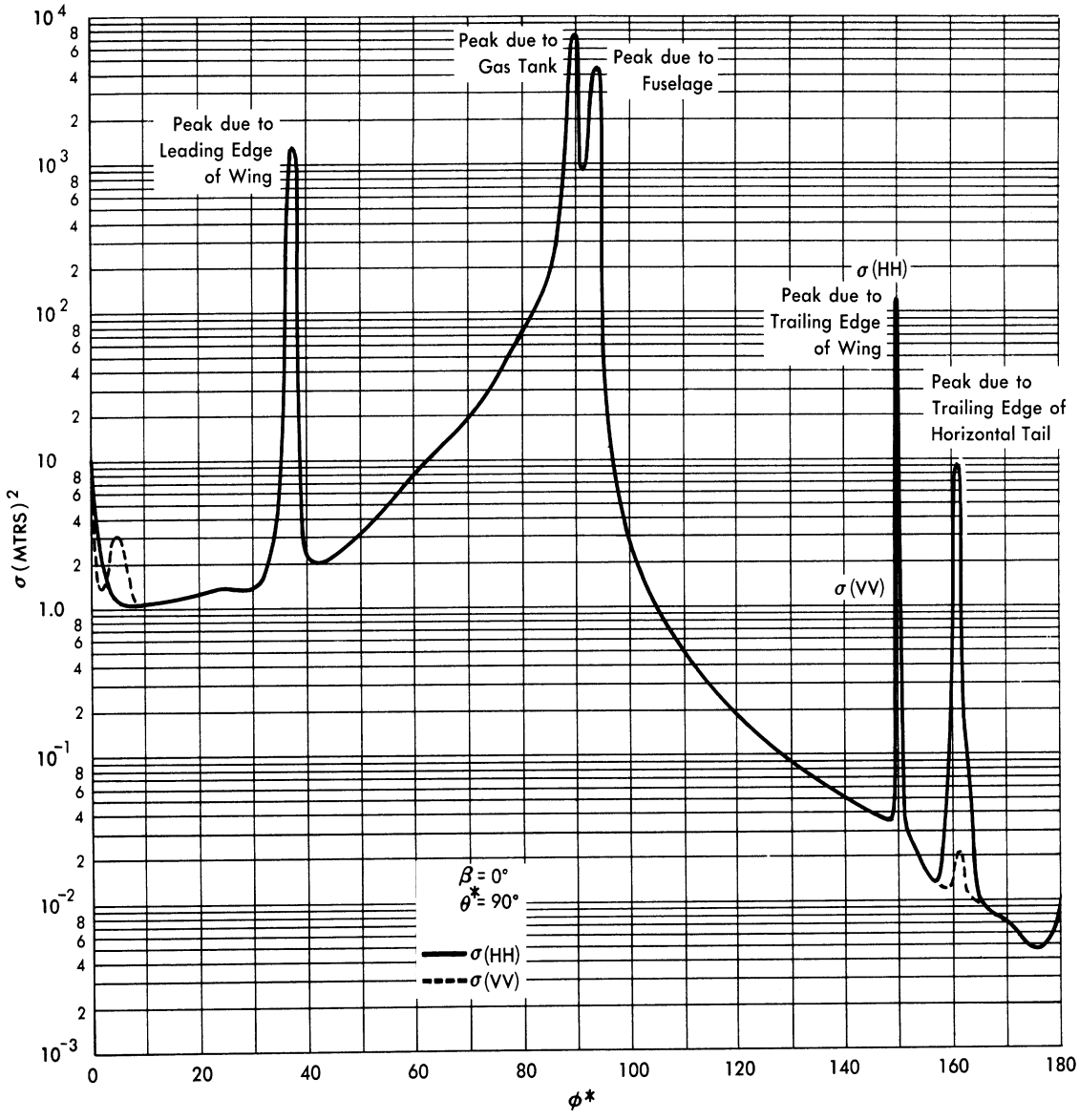

FIG. A.4-6 THEORETICAL CROSS-SECTIONS AT S-BAND FOR THE B-47 FOR ELEVATION 0°

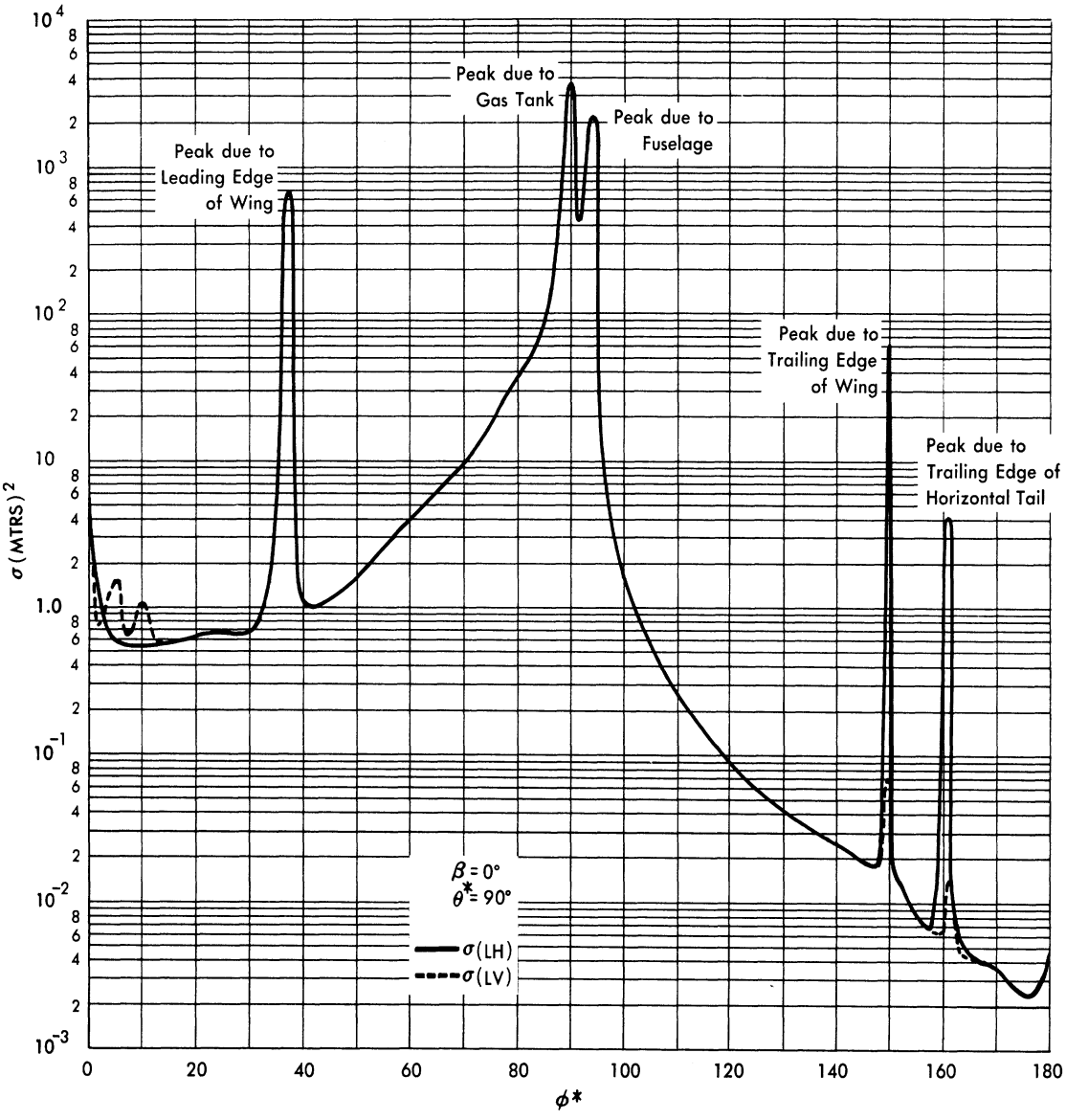

FIG. A.4-7 THEORETICAL CROSS-SECTIONS AT S-BAND FOR THE B-47 FOR ELEVATION 0°

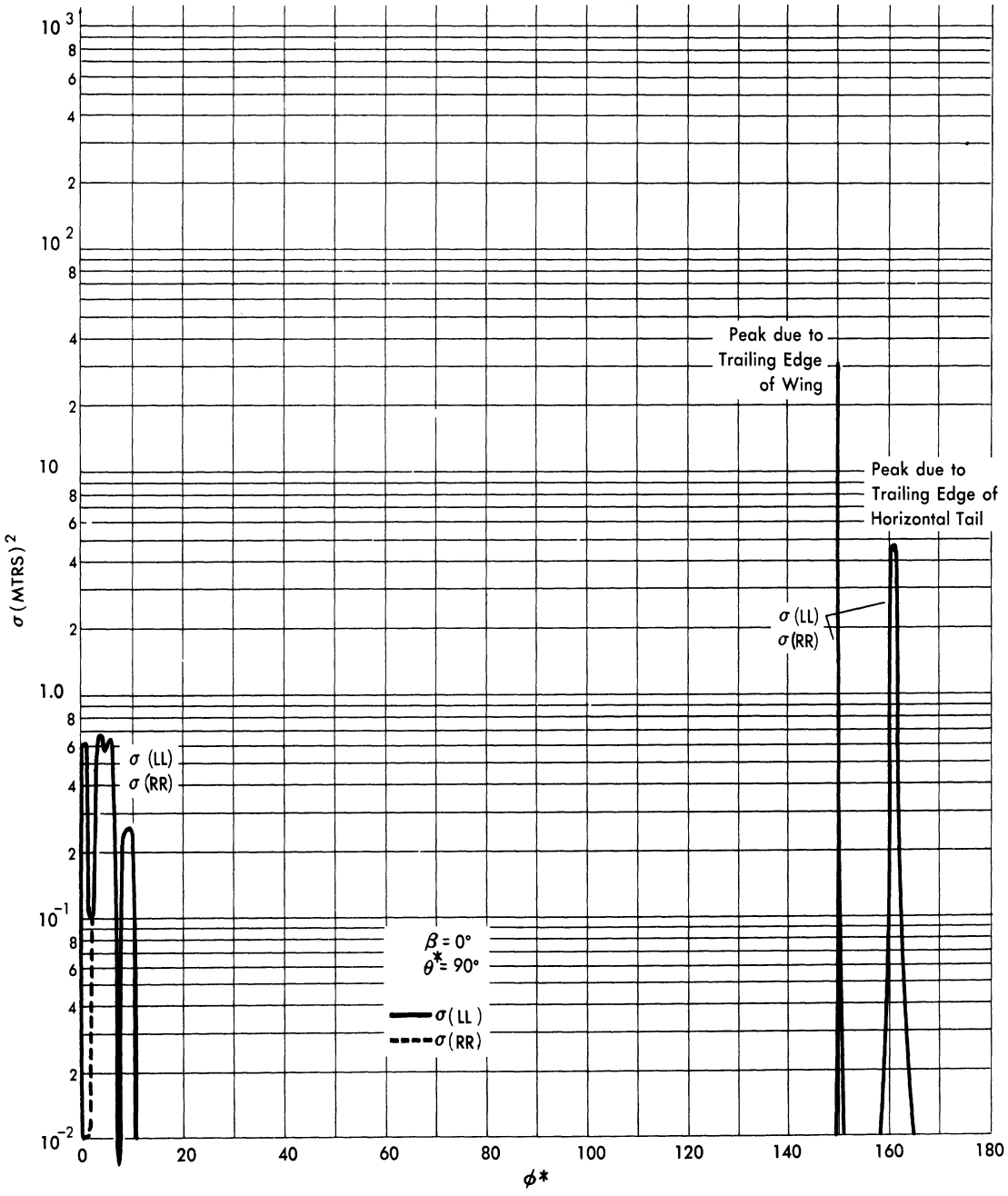

FIG. A.4-8 THEORETICAL CROSS-SECTIONS AT S-BAND FOR THE B-47 FOR ELEVATION 0°

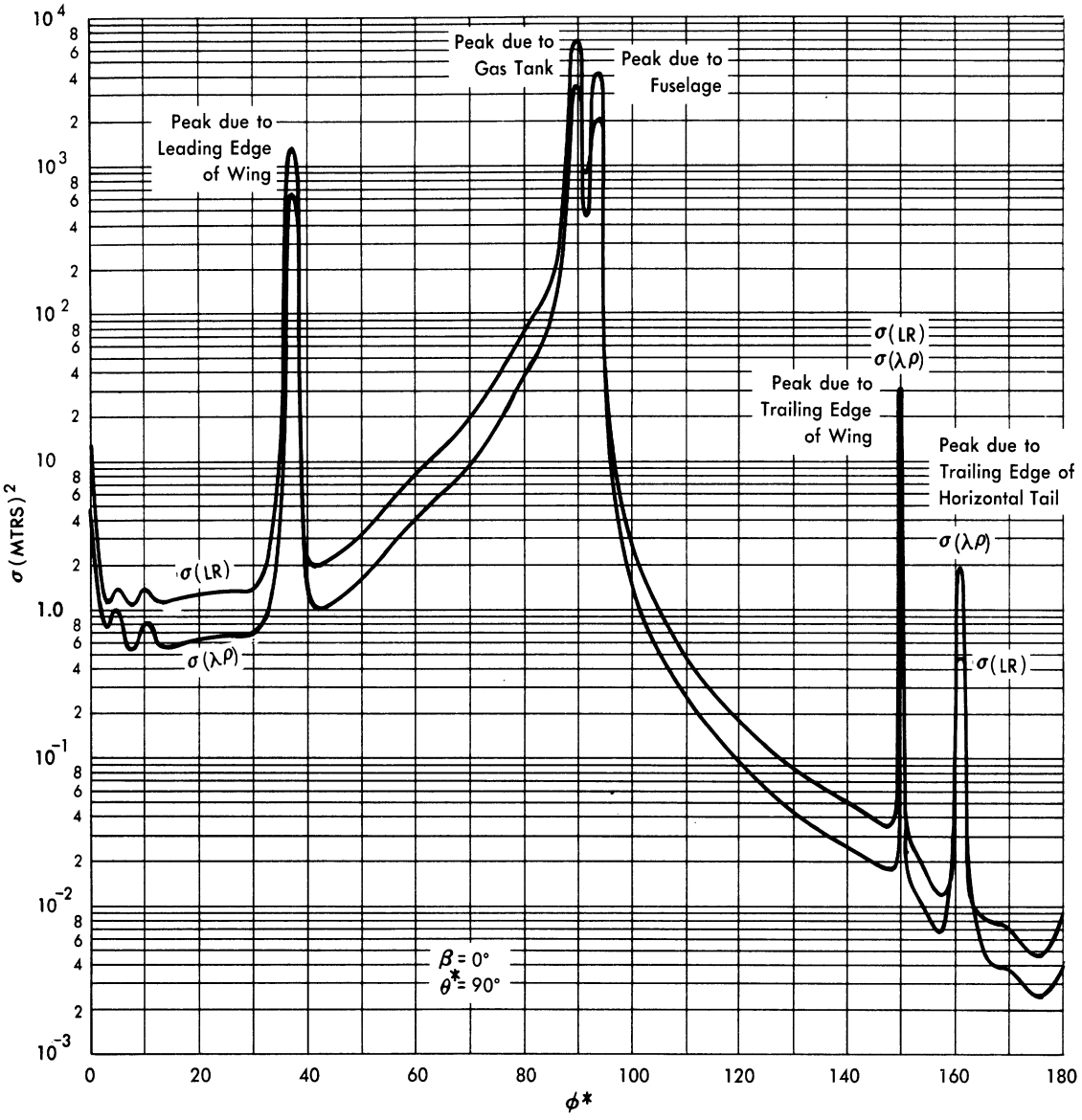

FIG. A.4-9 THEORETICAL CROSS-SECTIONS AT S-BAND FOR THE B-47 FOR ELEVATION 0°

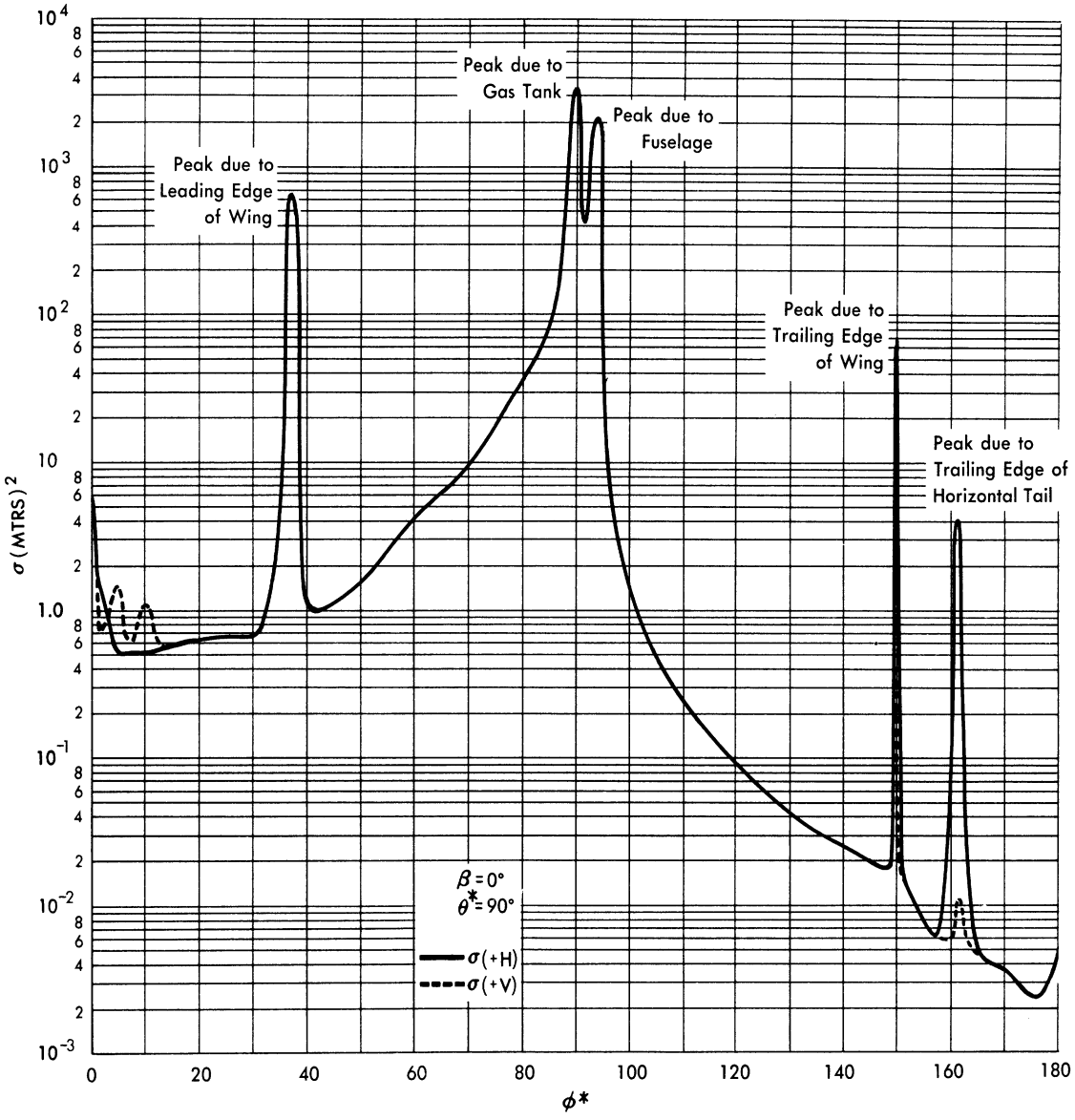

FIG. A.4-10 THEORETICAL CROSS-SECTIONS AT S-BAND FOR THE B-47 FOR ELEVATION 0°

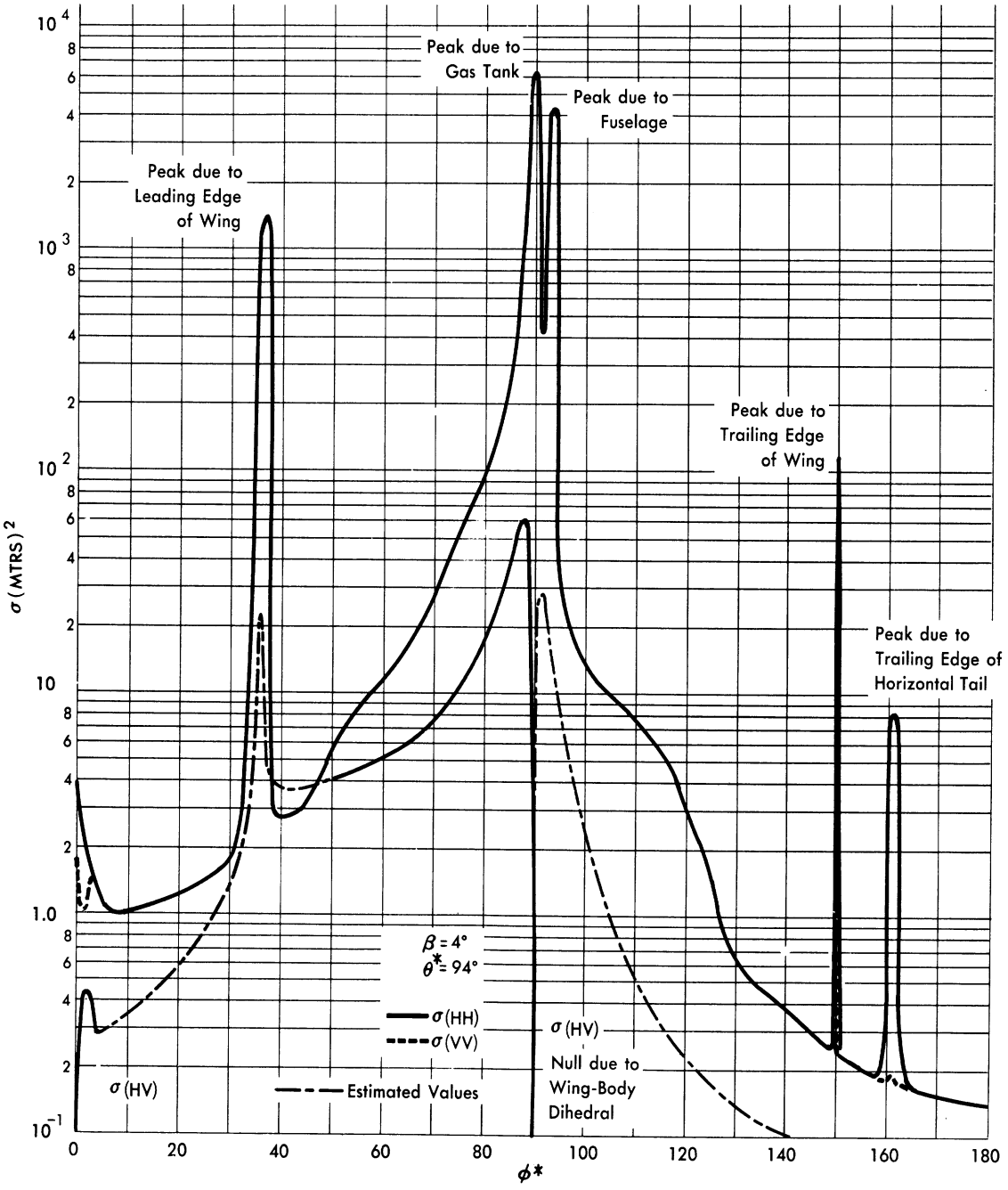

FIG. A.4-11 THEORETICAL CROSS-SECTIONS AT S-BAND FOR THE B-47 FOR ELEVATION 4°

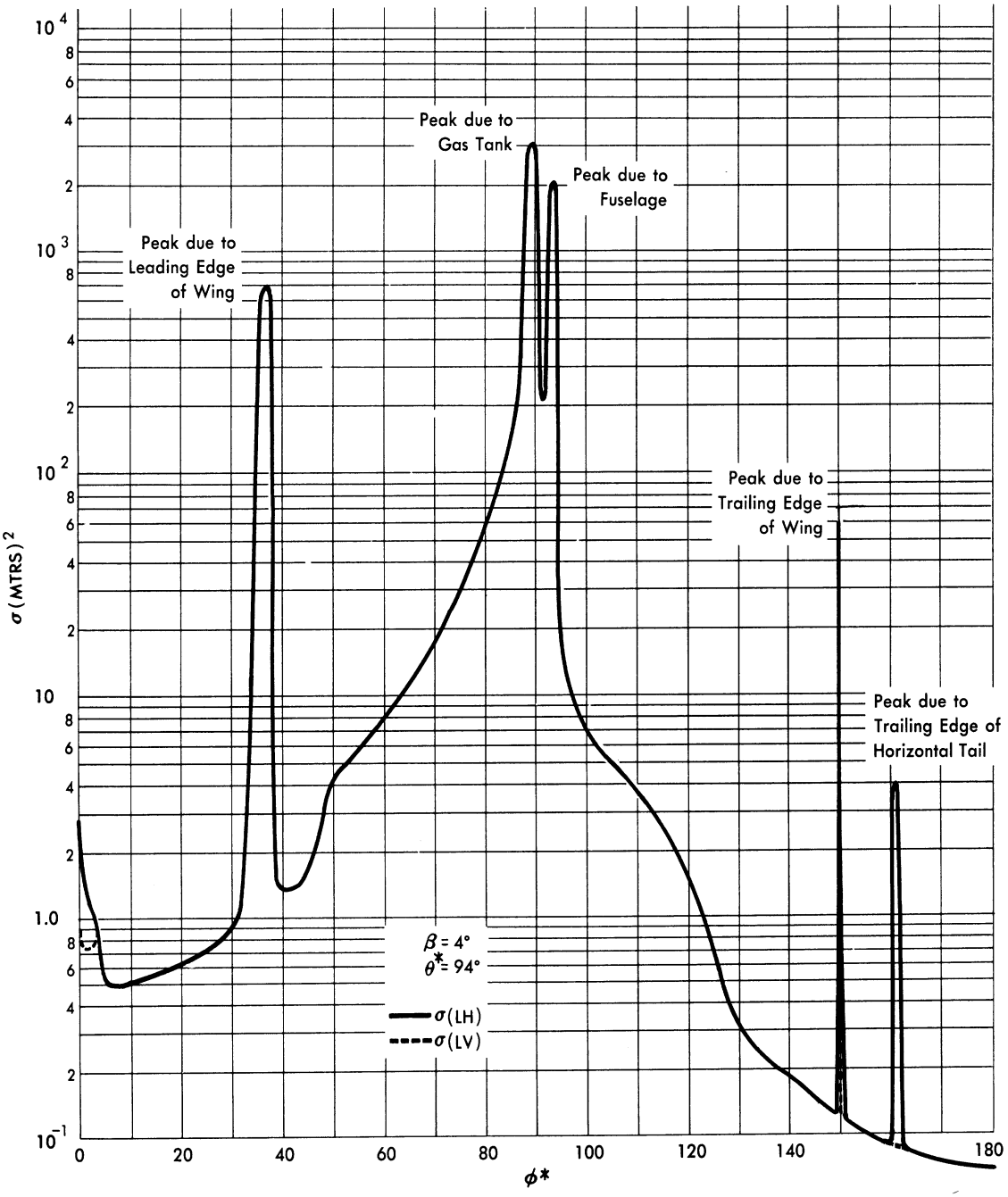

FIG. A.4-12 THEORETICAL CROSS-SECTIONS AT S-BAND FOR THE B-47 FOR ELEVATION 4°

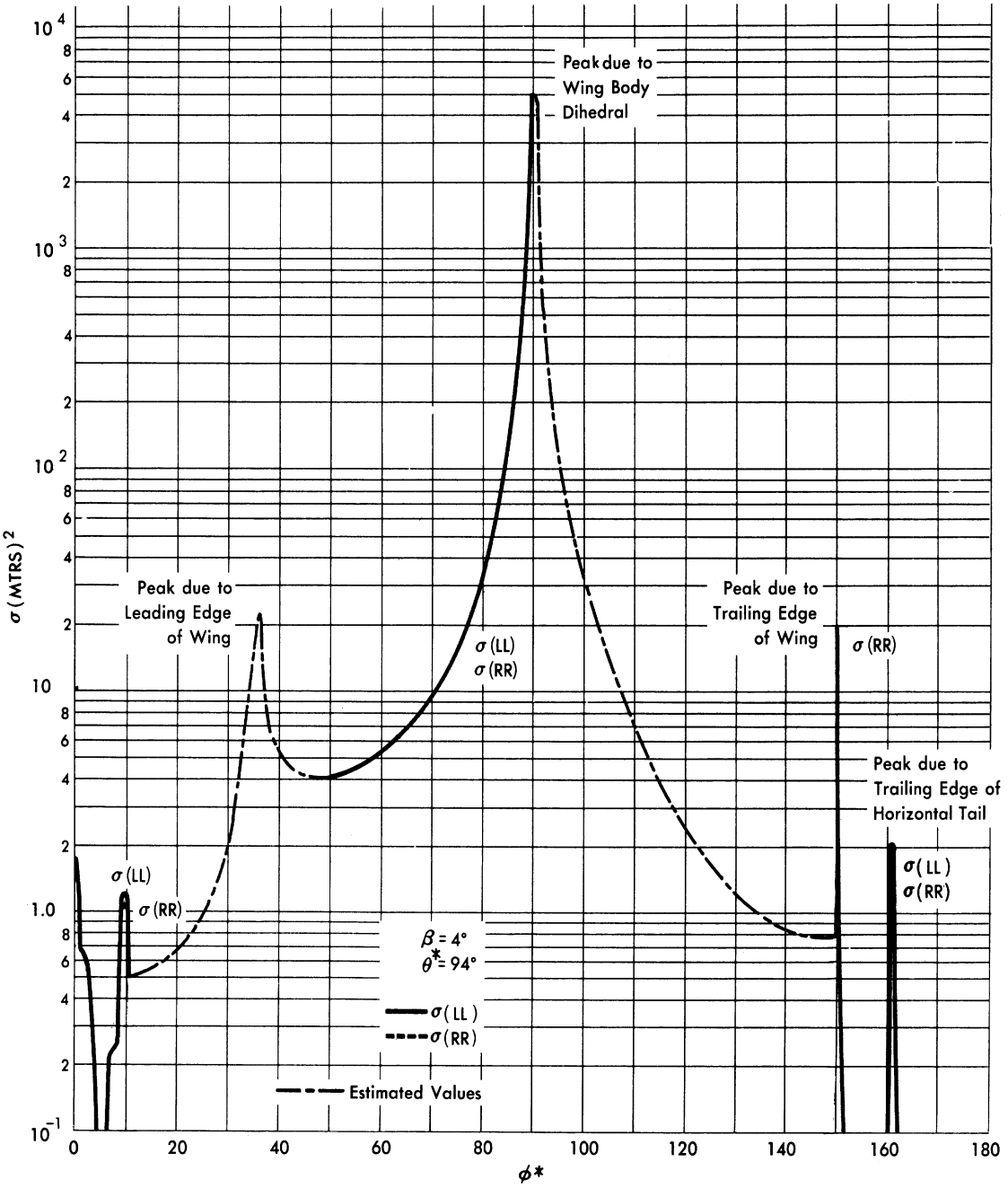

FIG. A.4-13 THEORETICAL CROSS-SECTIONS AT S-BAND FOR THE B-47 FOR ELEVATION 4°

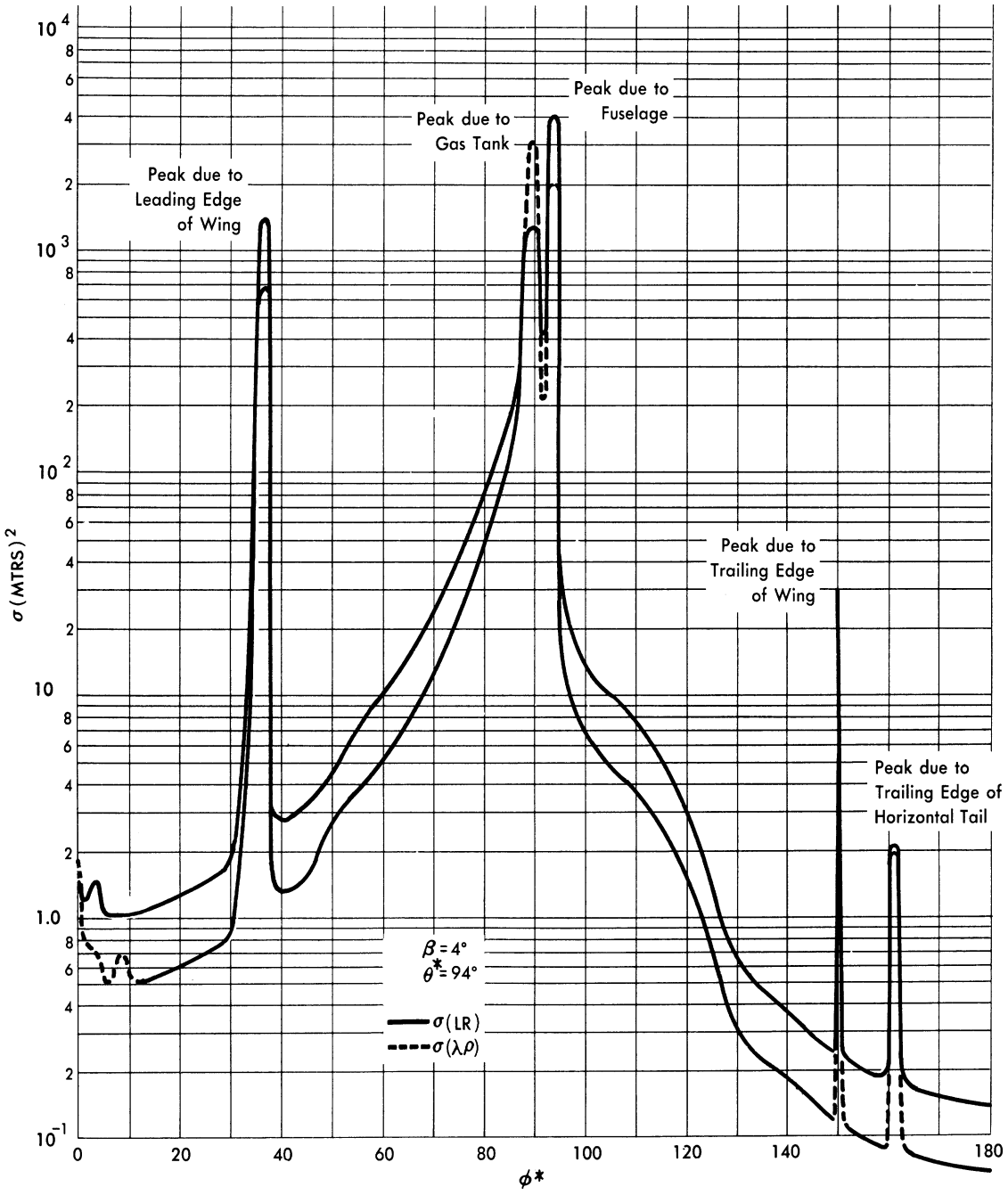

FIG. A.4-14 THEORETICAL CROSS-SECTIONS AT S-BAND FOR THE B-47 FOR ELEVATION 4°

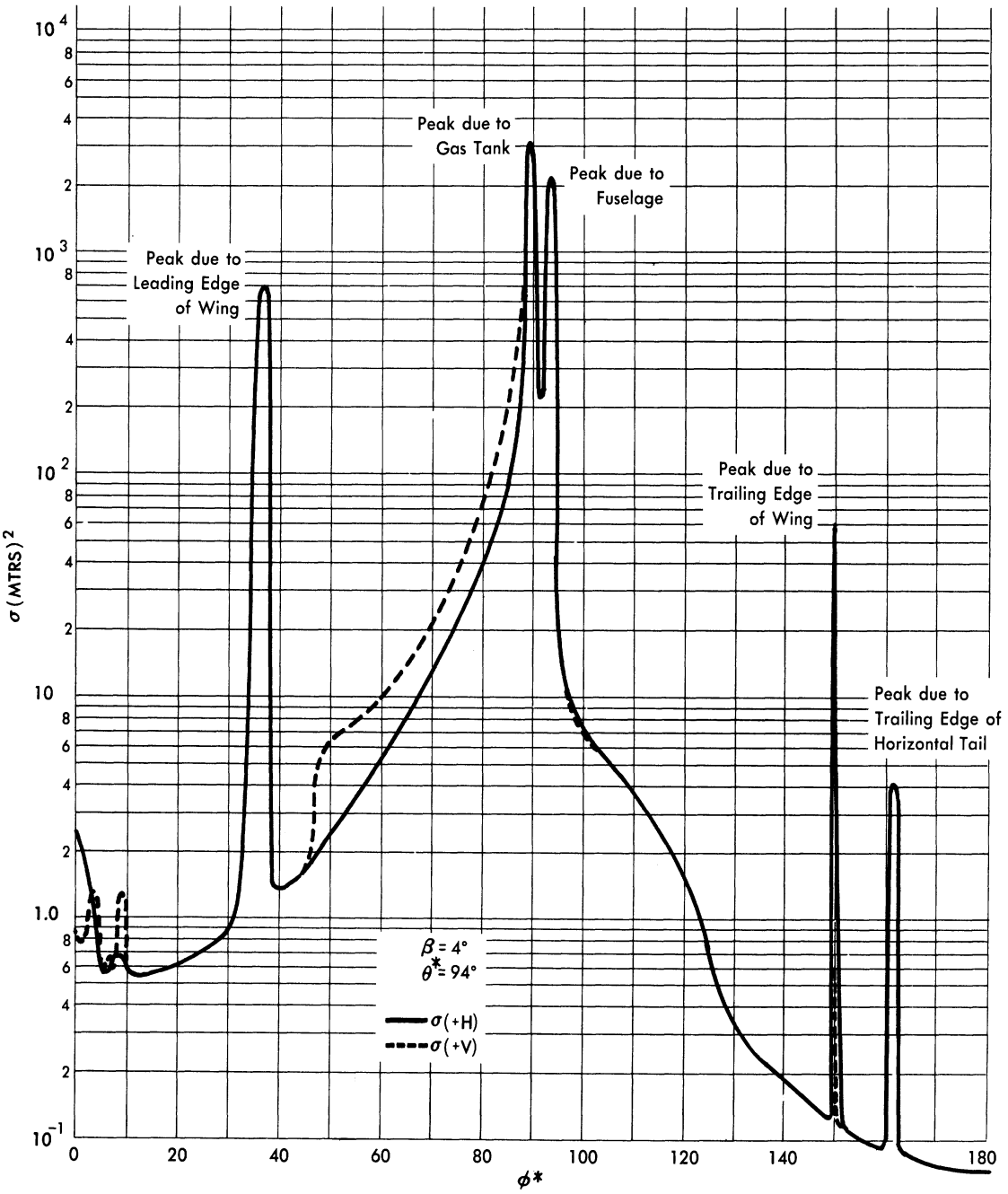

FIG. A.4-15 THEORETICAL CROSS-SECTIONS AT S-BAND FOR THE B-47 FOR ELEVATION 4°

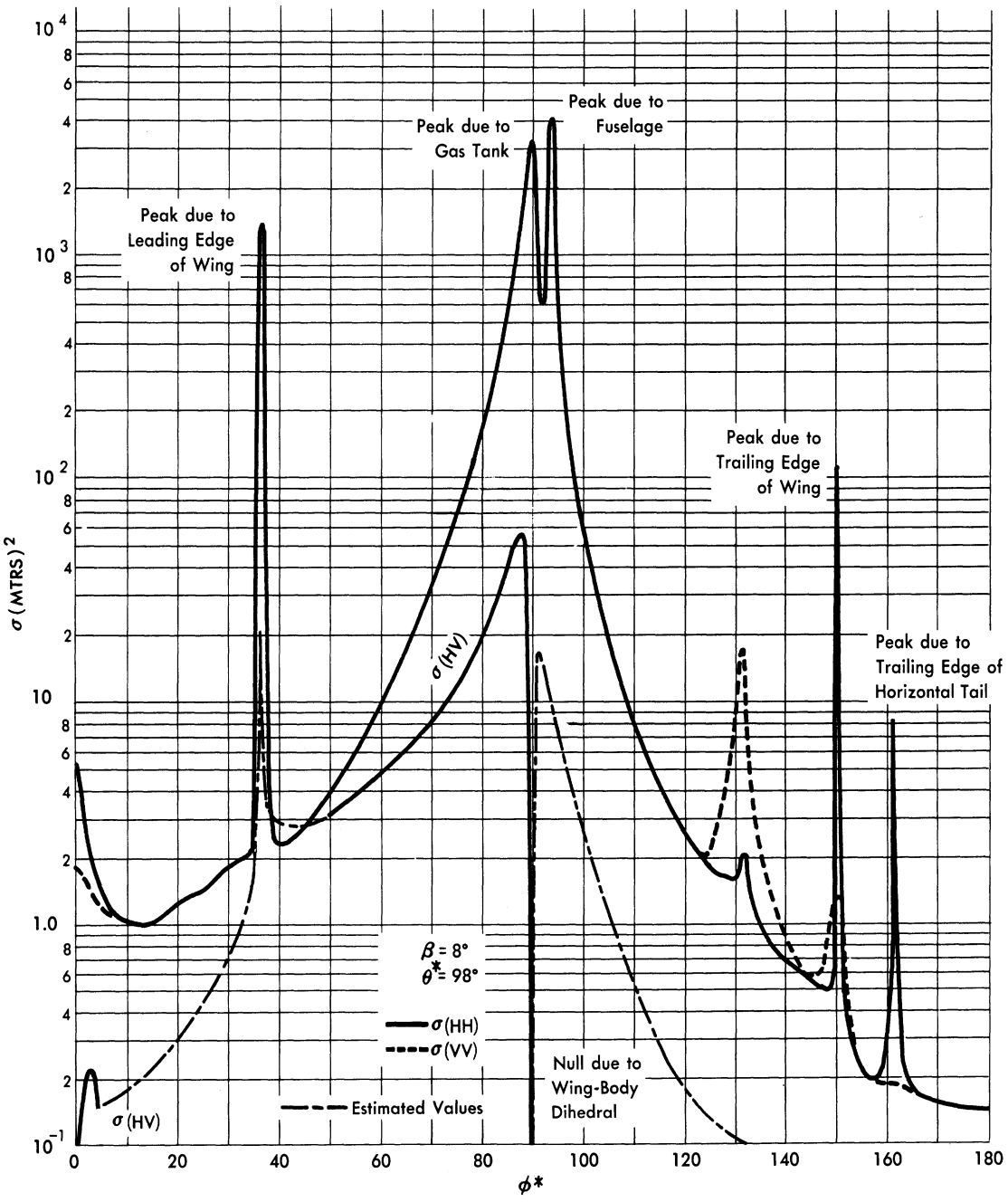

FIG. A.4-16 THEORETICAL CROSS-SECTIONS AT S-BAND FOR THE B-47 FOR ELEVATION 8°

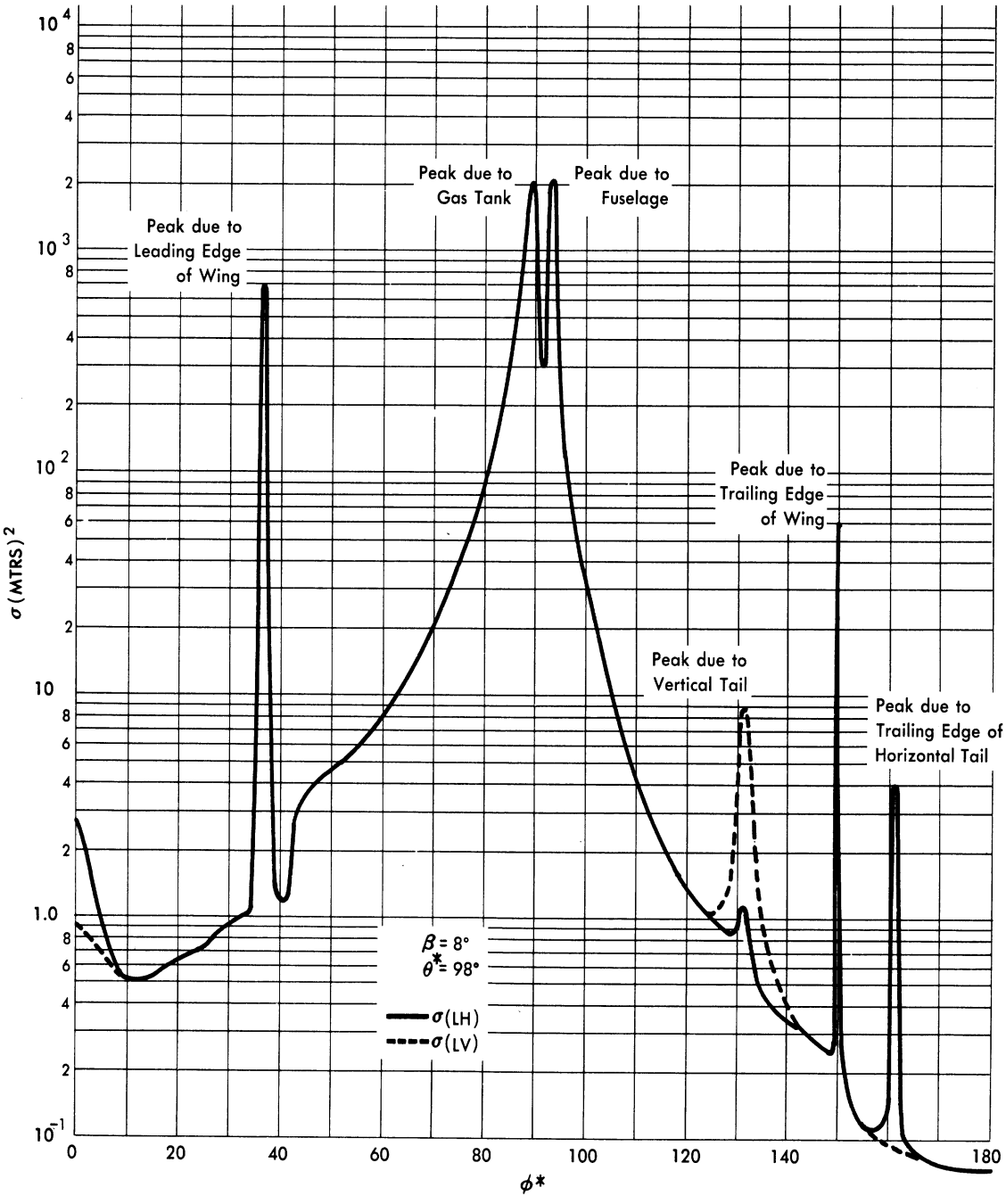

FIG. A.4-17 THEORETICAL CROSS-SECTIONS AT S-BAND FOR THE B-47 FOR ELEVATION 8°

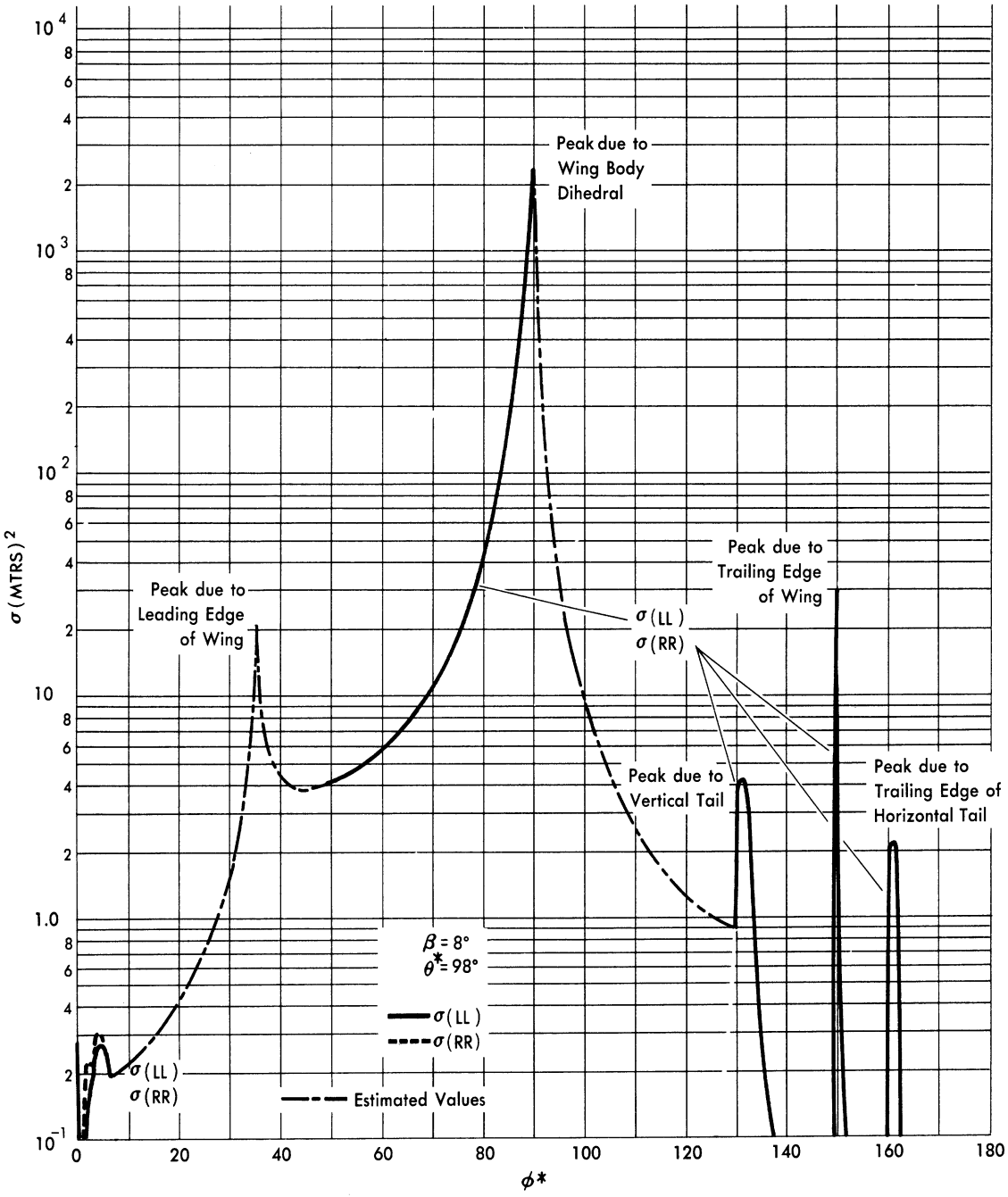

FIG. A.4-18 THEORETICAL CROSS-SECTIONS AT S-BAND FOR THE B-47 FOR ELEVATION 8°

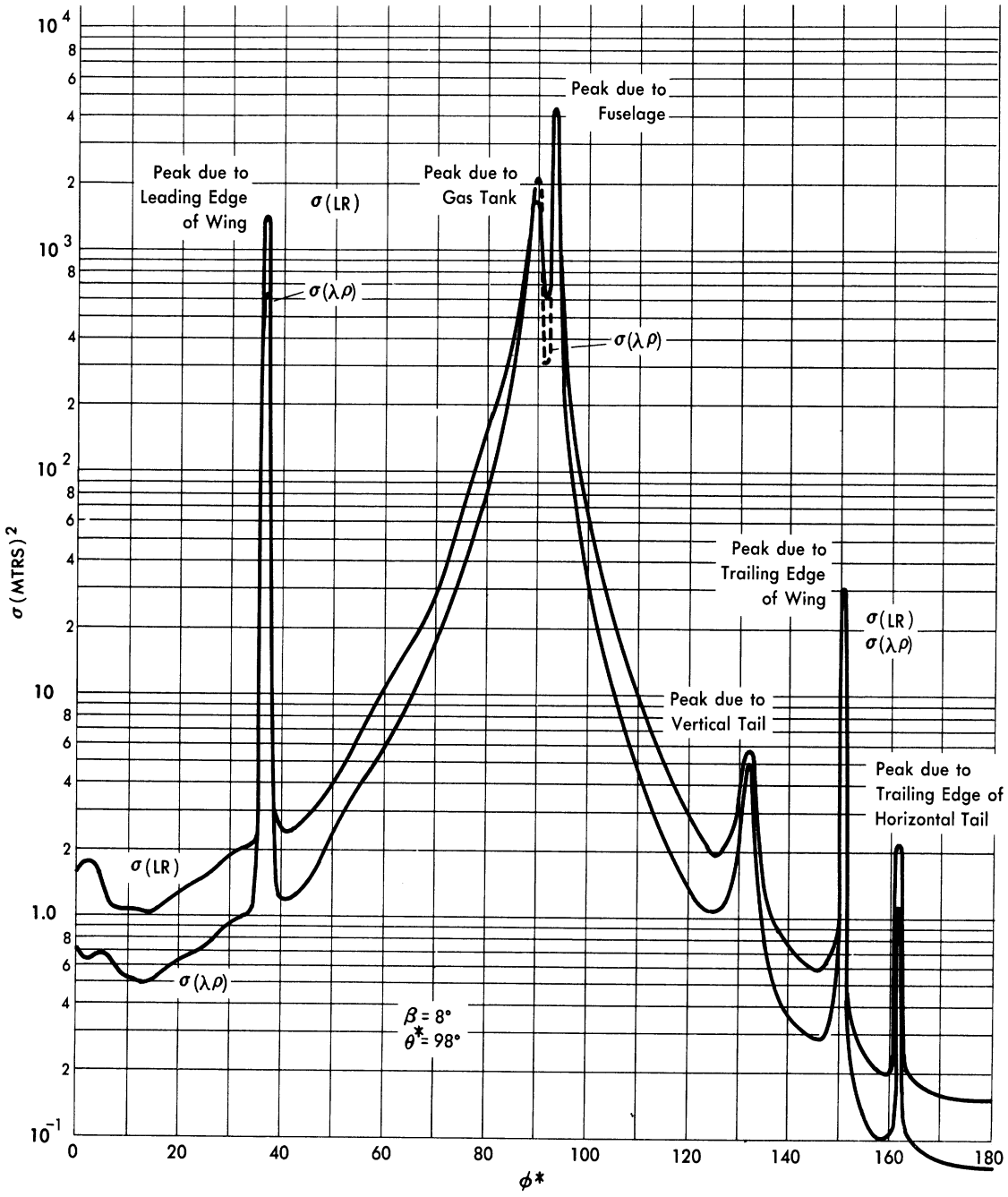

FIG. A.4-19 THEORETICAL CROSS-SECTIONS AT S-BAND FOR THE B-47 FOR ELEVATION 8°

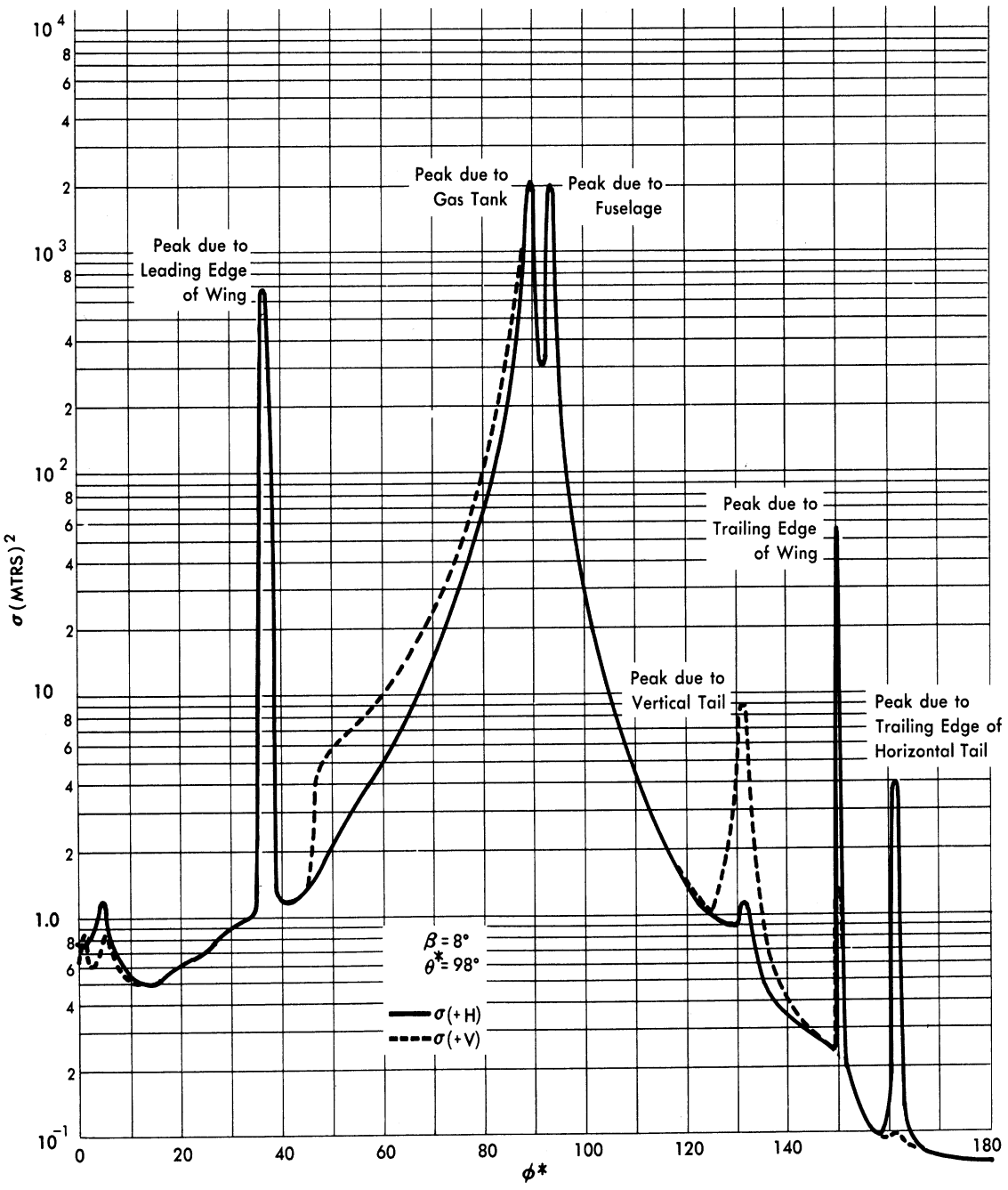

FIG. A.4-20 THEORETICAL CROSS-SECTIONS AT S-BAND FOR THE B-47 FOR ELEVATION 8°

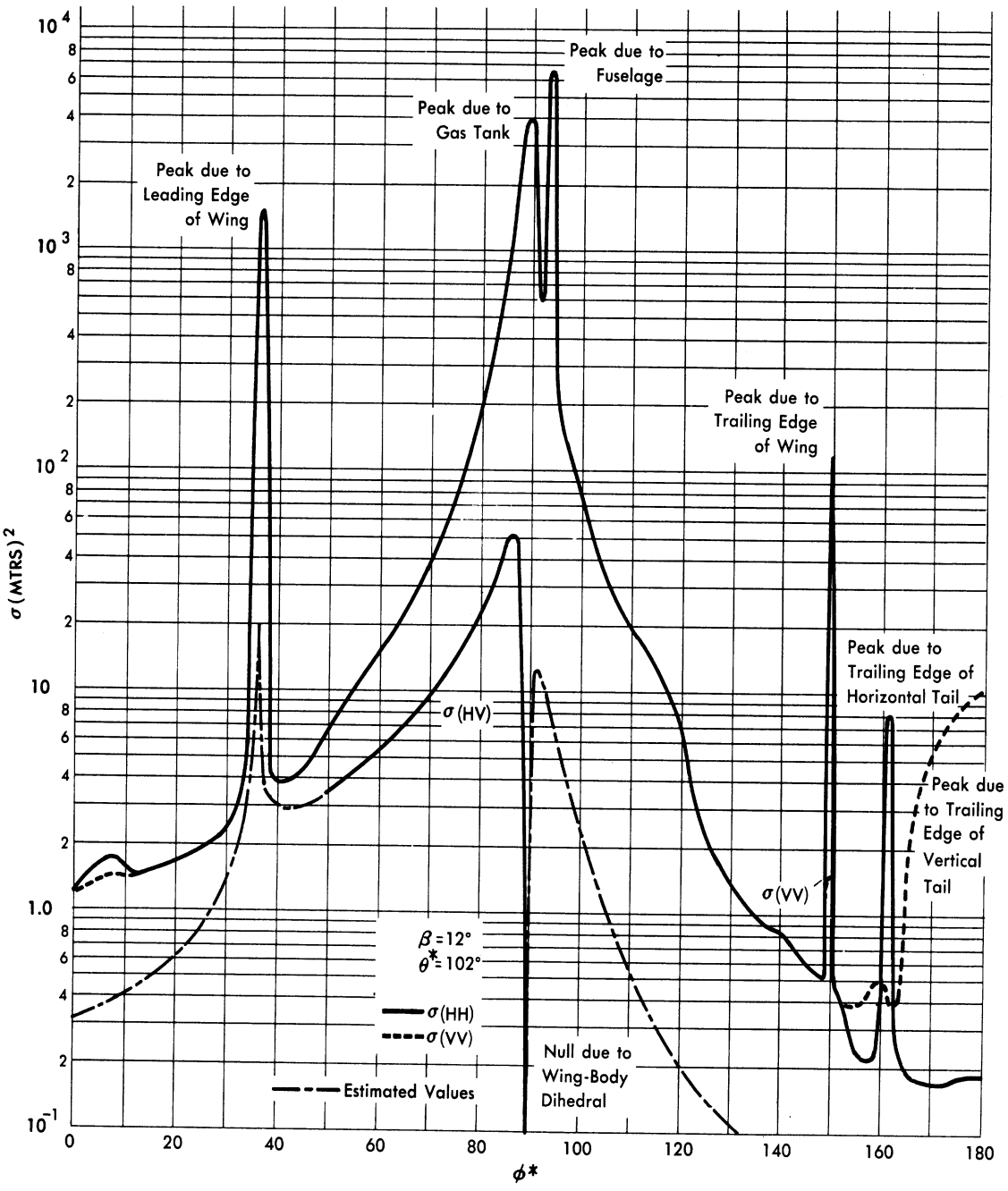

FIG. A.4-21 THEORETICAL CROSS-SECTIONS AT S-BAND FOR THE B-47 FOR ELEVATION 12°

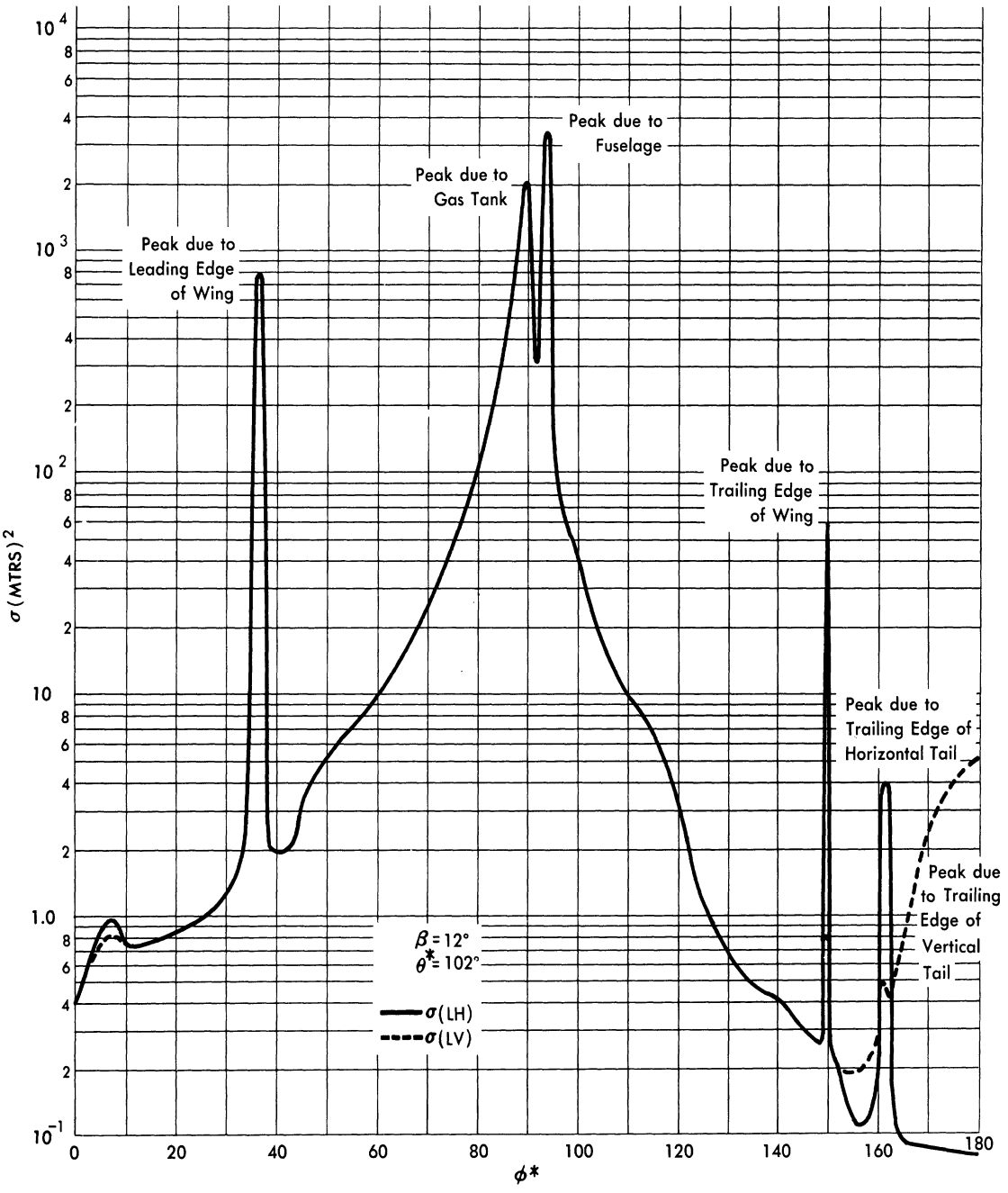

FIG. A.4-22 THEORETICAL CROSS-SECTIONS AT S-BAND FOR THE B-47 FOR ELEVATION 12°

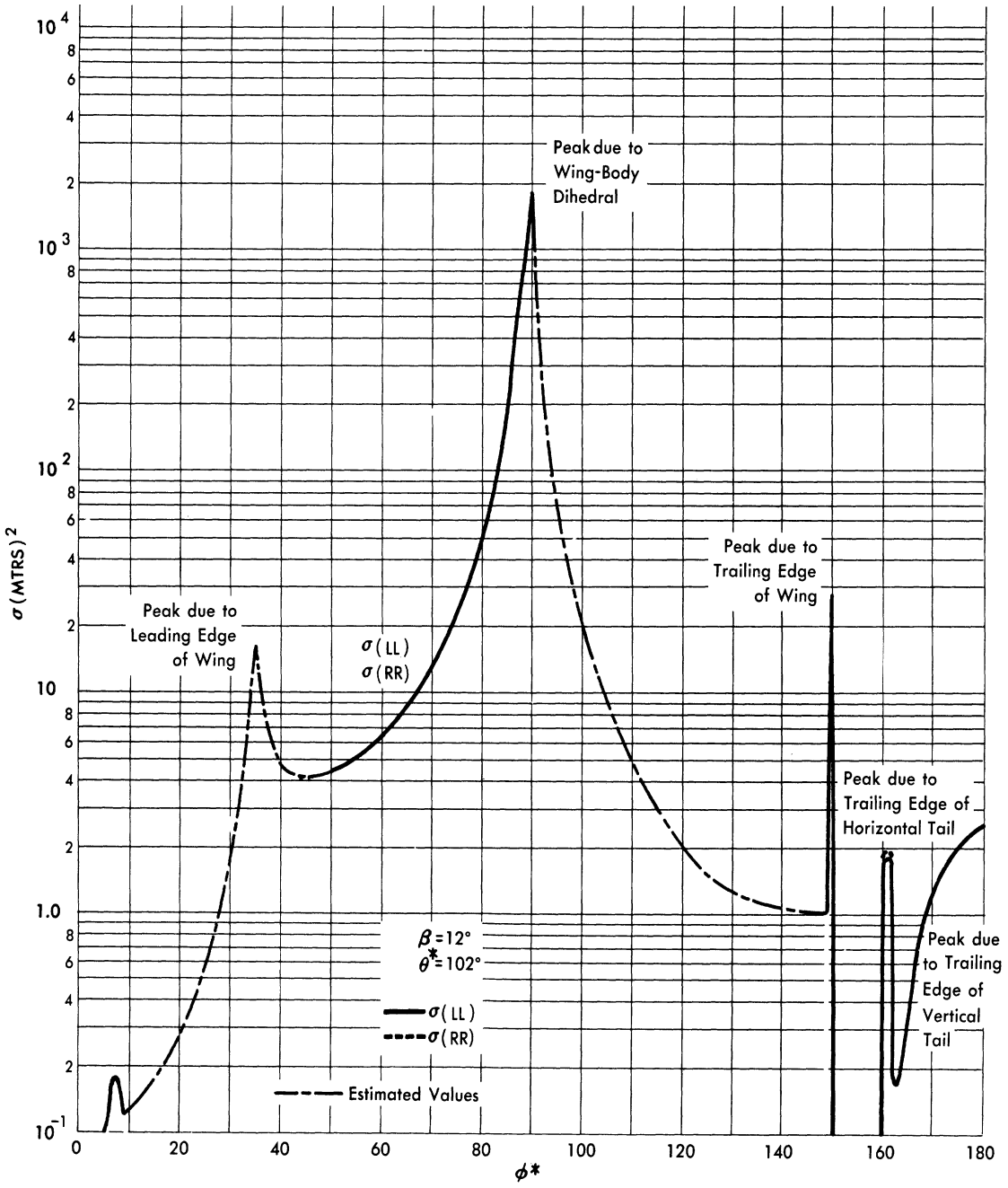

FIG. A.4-23 THEORETICAL CROSS-SECTIONS AT S-BAND FOR THE B-47 FOR ELEVATION 12°

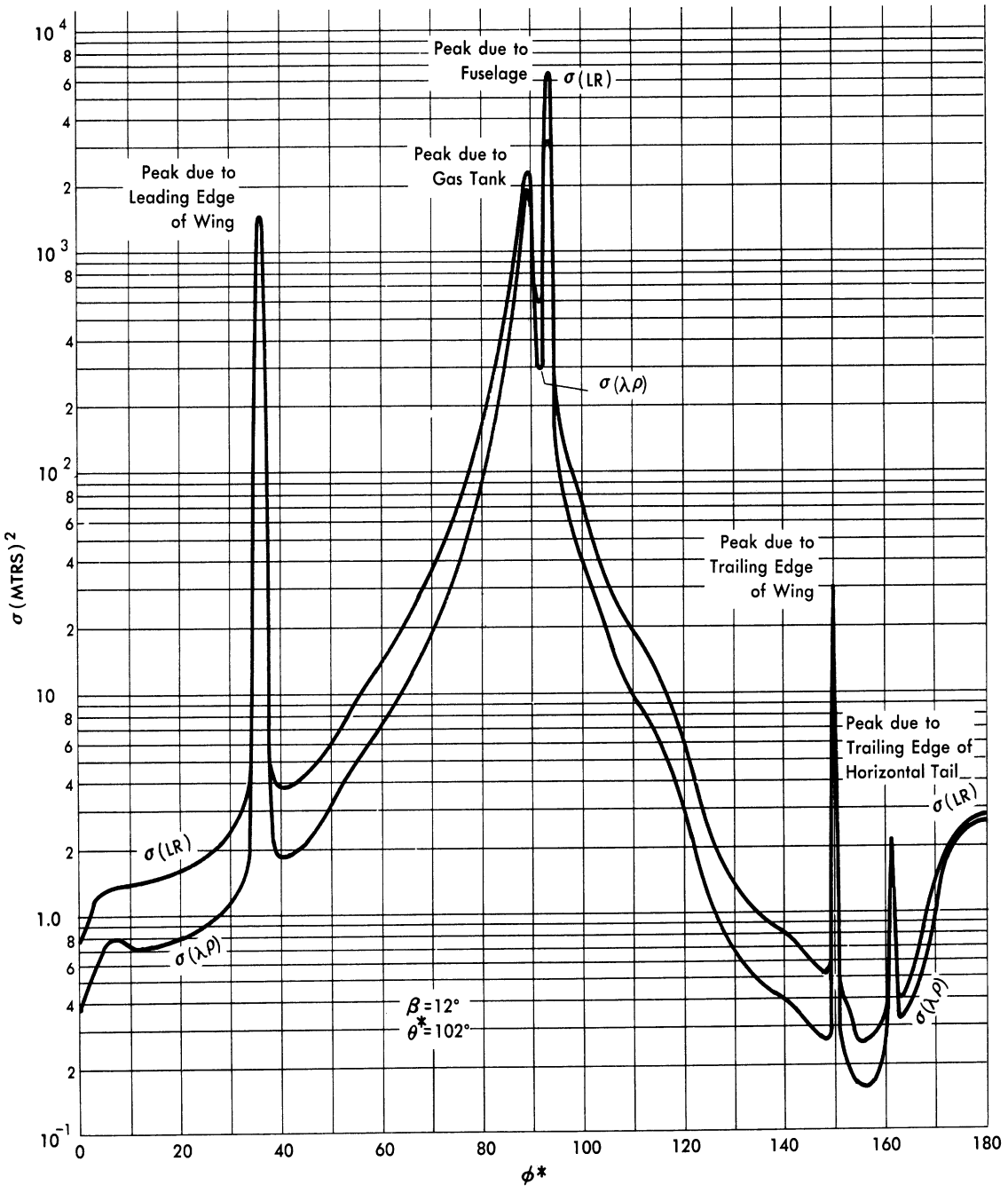

FIG. A.4-24 THEORETICAL CROSS-SECTIONS AT S-BAND FOR THE B-47 FOR ELEVATION 12°

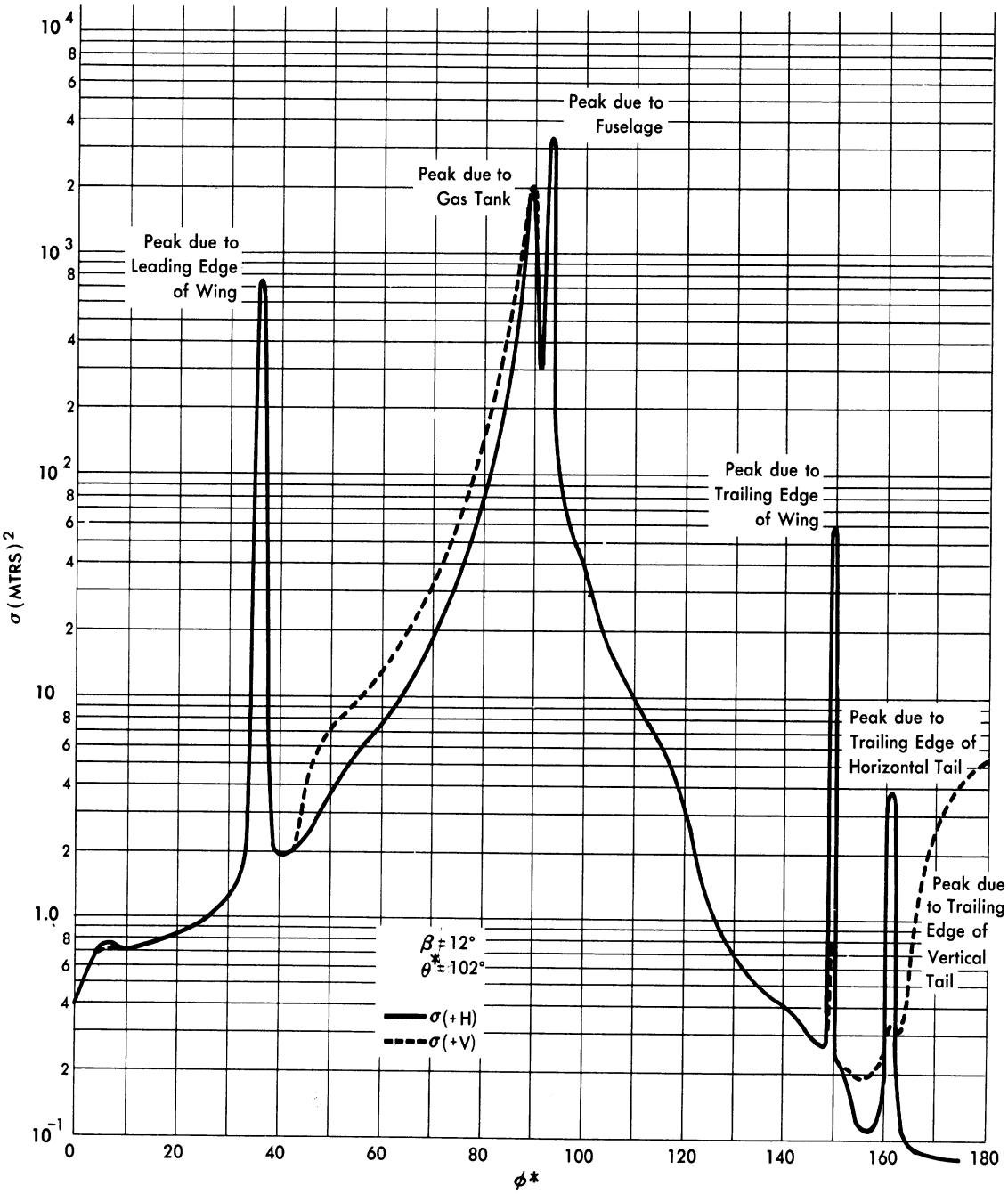

FIG. A.4-25 THEORETICAL CROSS-SECTIONS AT S-BAND FOR THE B-47 FOR ELEVATION 12°

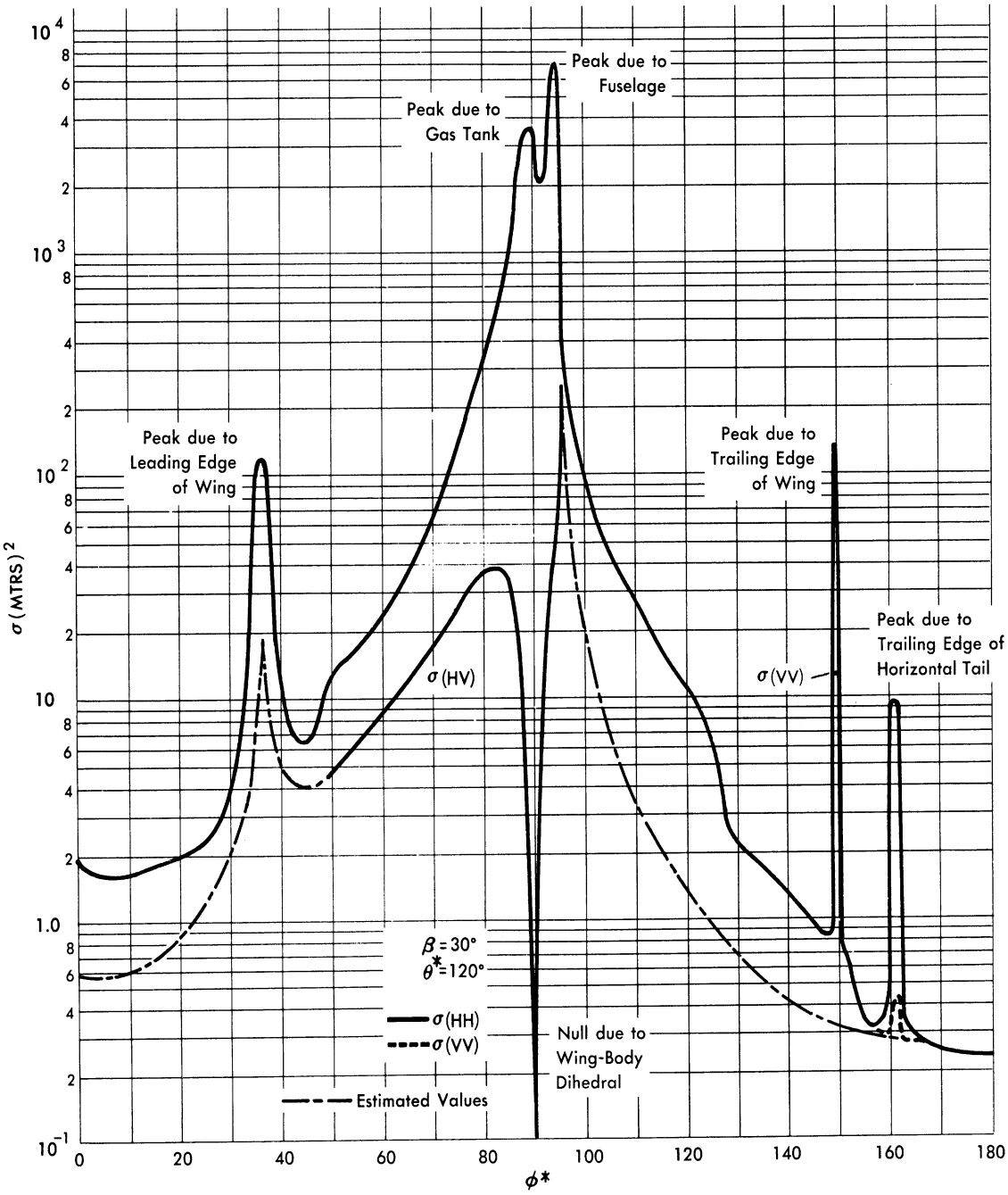

FIG. A.4-26 THEORETICAL CROSS-SECTIONS AT S-BAND FOR THE B 47 FOR ELEVATION 30°

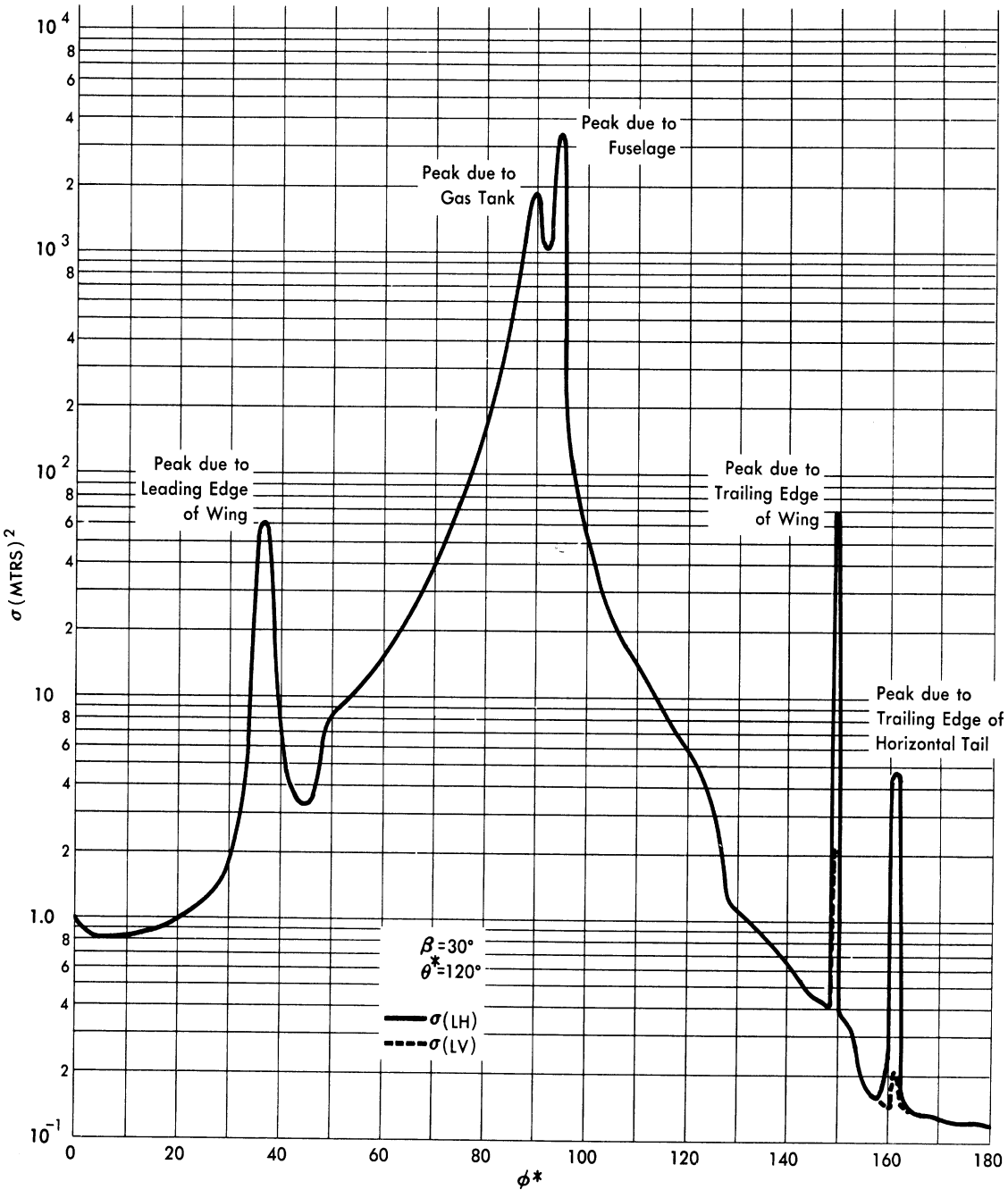

FIG. A.4-27 THEORETICAL CROSS-SECTIONS AT S-BAND FOR THE B-47 FOR ELEVATION 30°

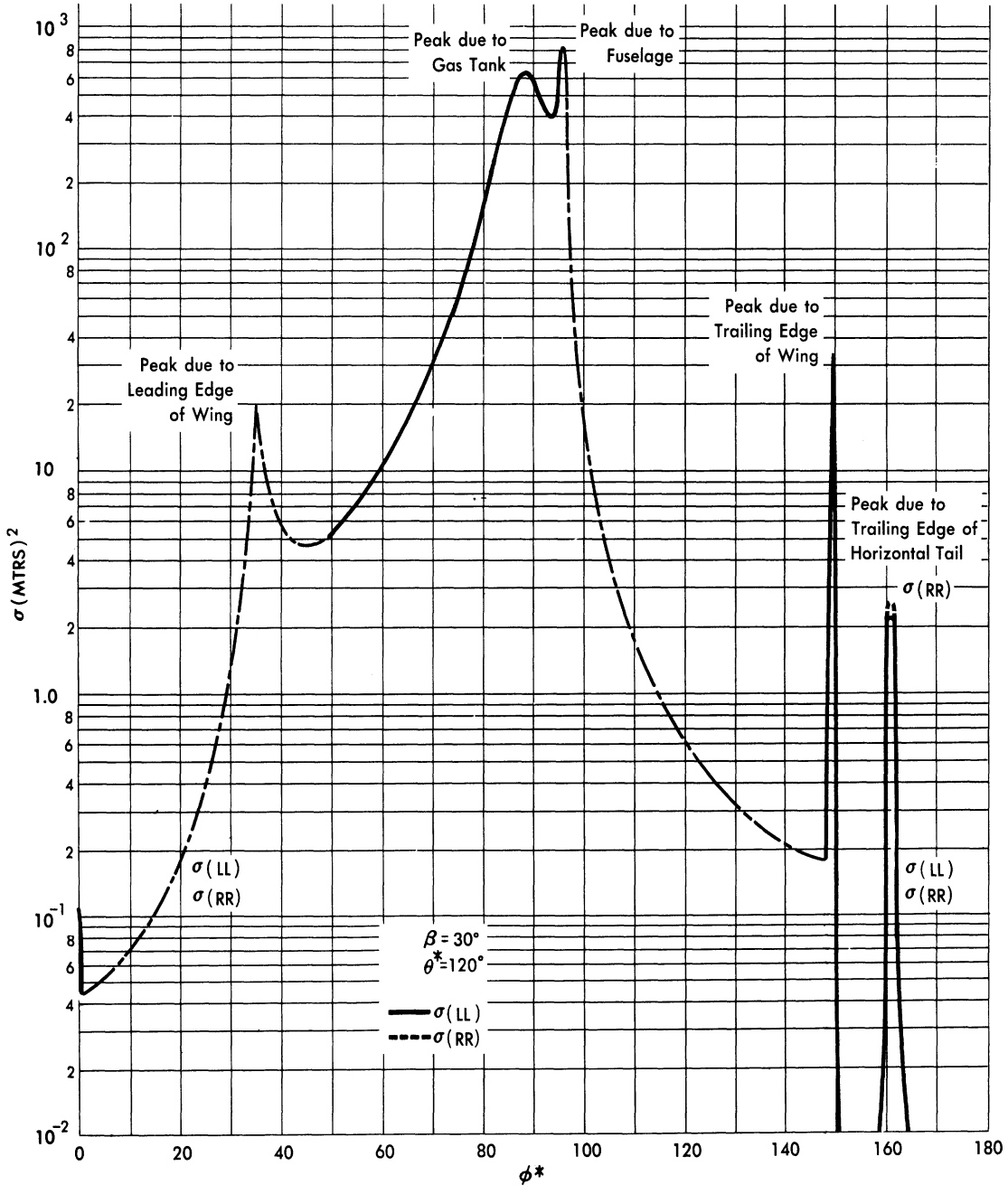

FIG. A.4-28 THEORETICAL CROSS-SECTIONS AT S-BAND FOR THE B-47 FOR ELEVATION 30°

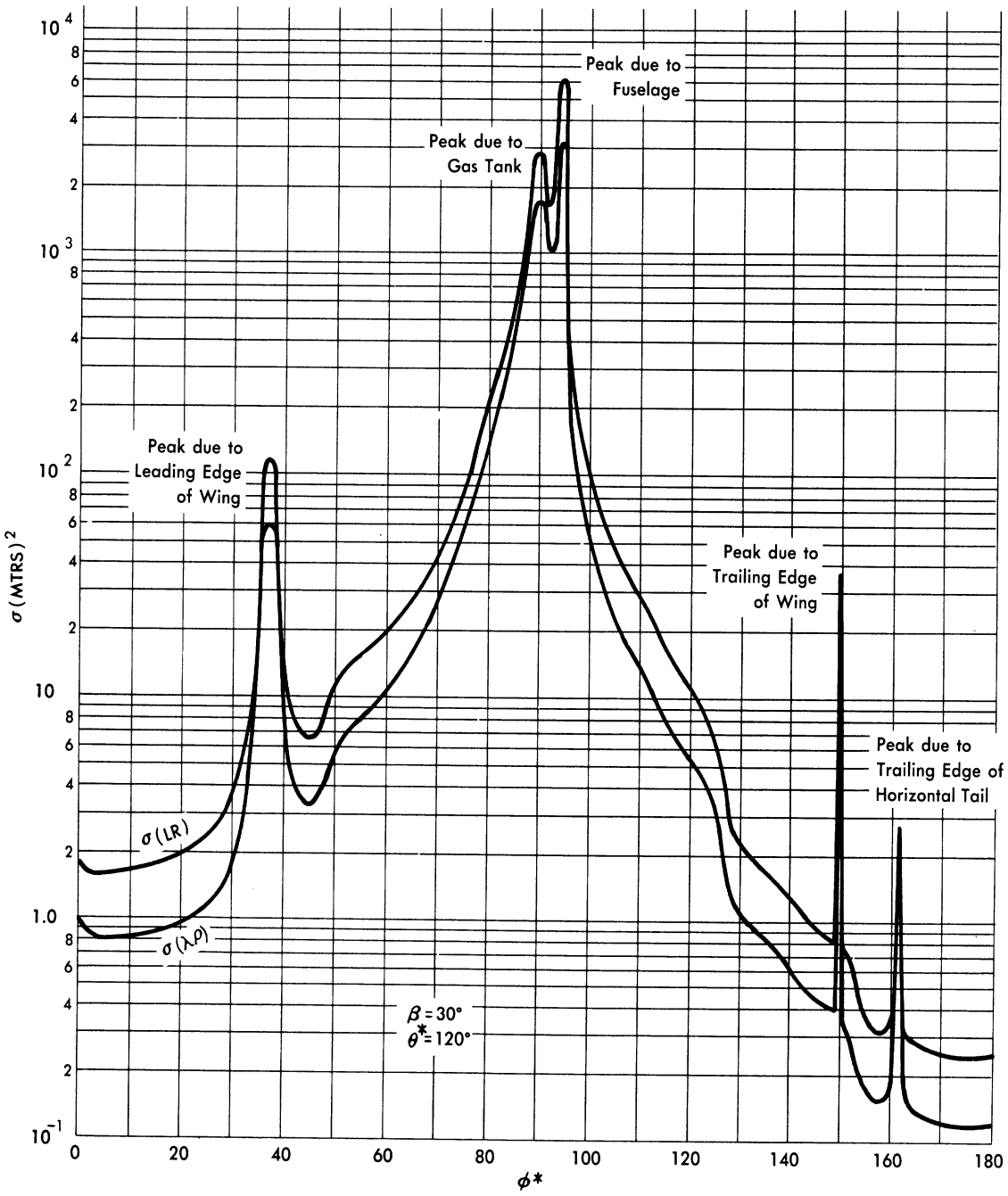

FIG. A.4-29 THEORETICAL CROSS-SECTIONS AT S-BAND FOR THE B-47 FOR ELEVATION 30°

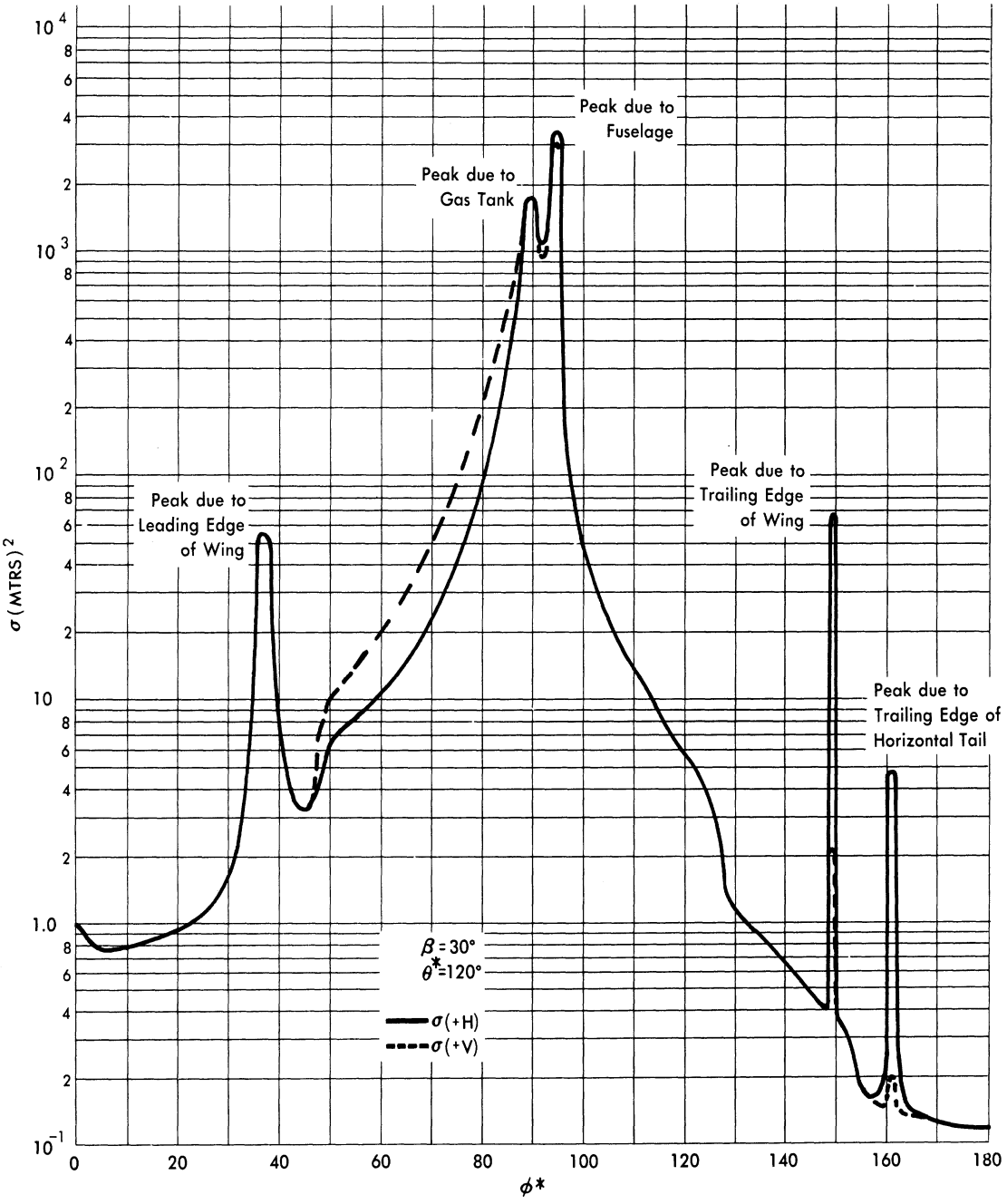

FIG. A.4-30 THEORETICAL CROSS-SECTIONS AT S-BAND FOR THE B-47 FOR ELEVATION 30°

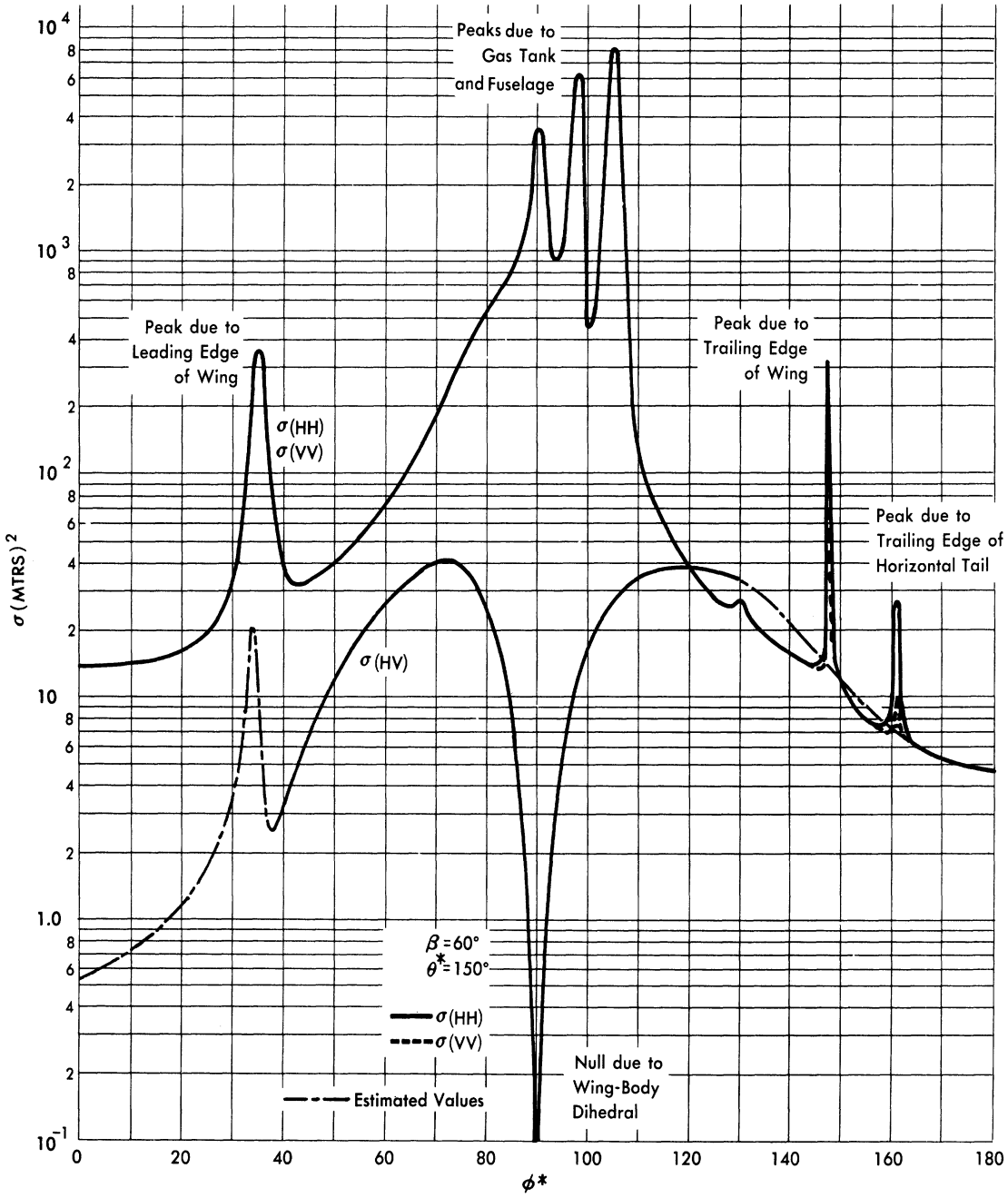

FIG. A.4-31 THEORETICAL CROSS-SECTIONS AT S-BAND FOR THE B-47 FOR ELEVATION 60°

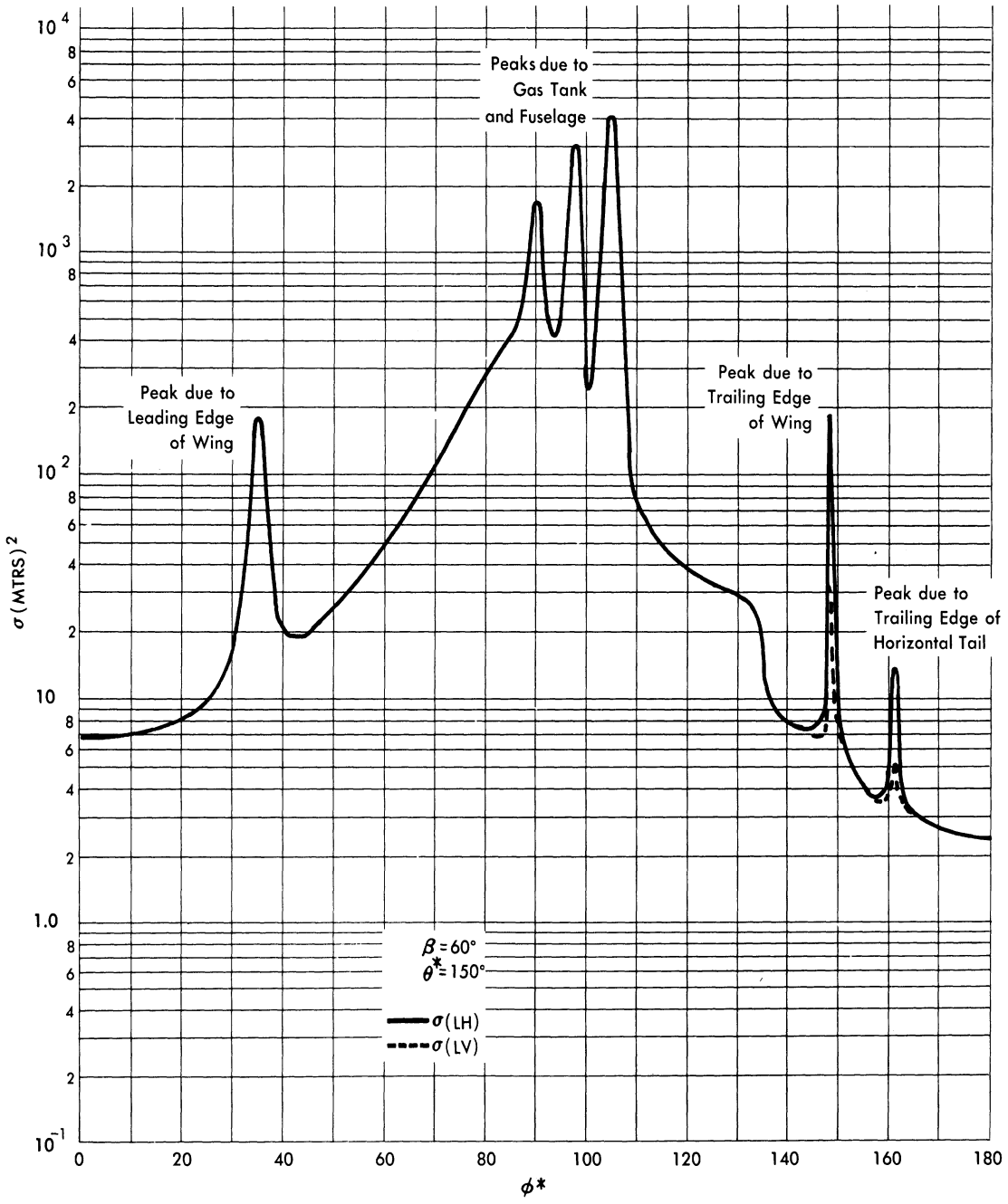

FIG. A.4-32 THEORETICAL CROSS-SECTIONS AT S-BAND FOR THE B-47 FOR ELEVATION 60°

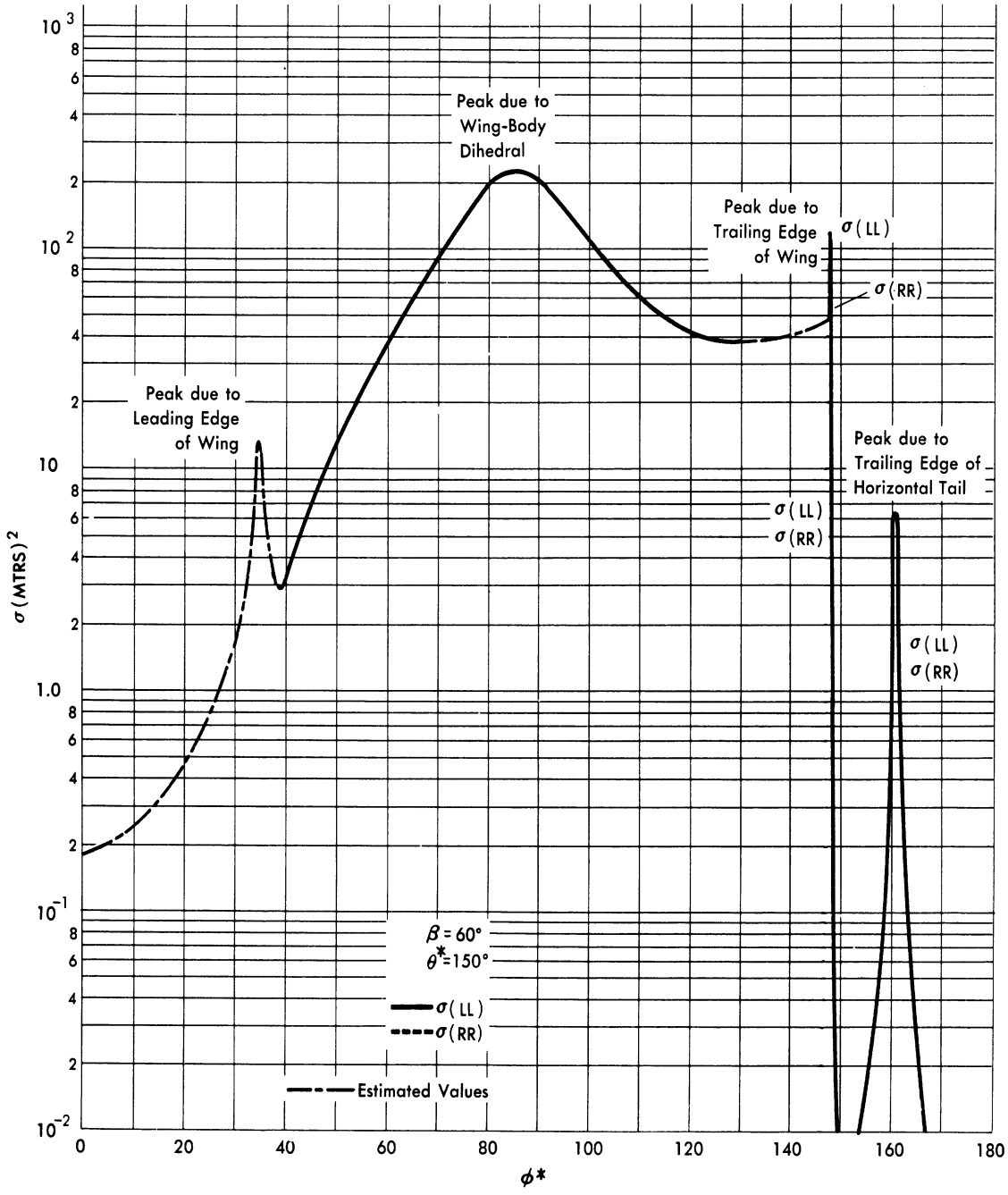

FIG. A.4-33 THEORETICAL CROSS-SECTIONS AT S-BAND FOR THE B-47 FOR ELEVATION 60°

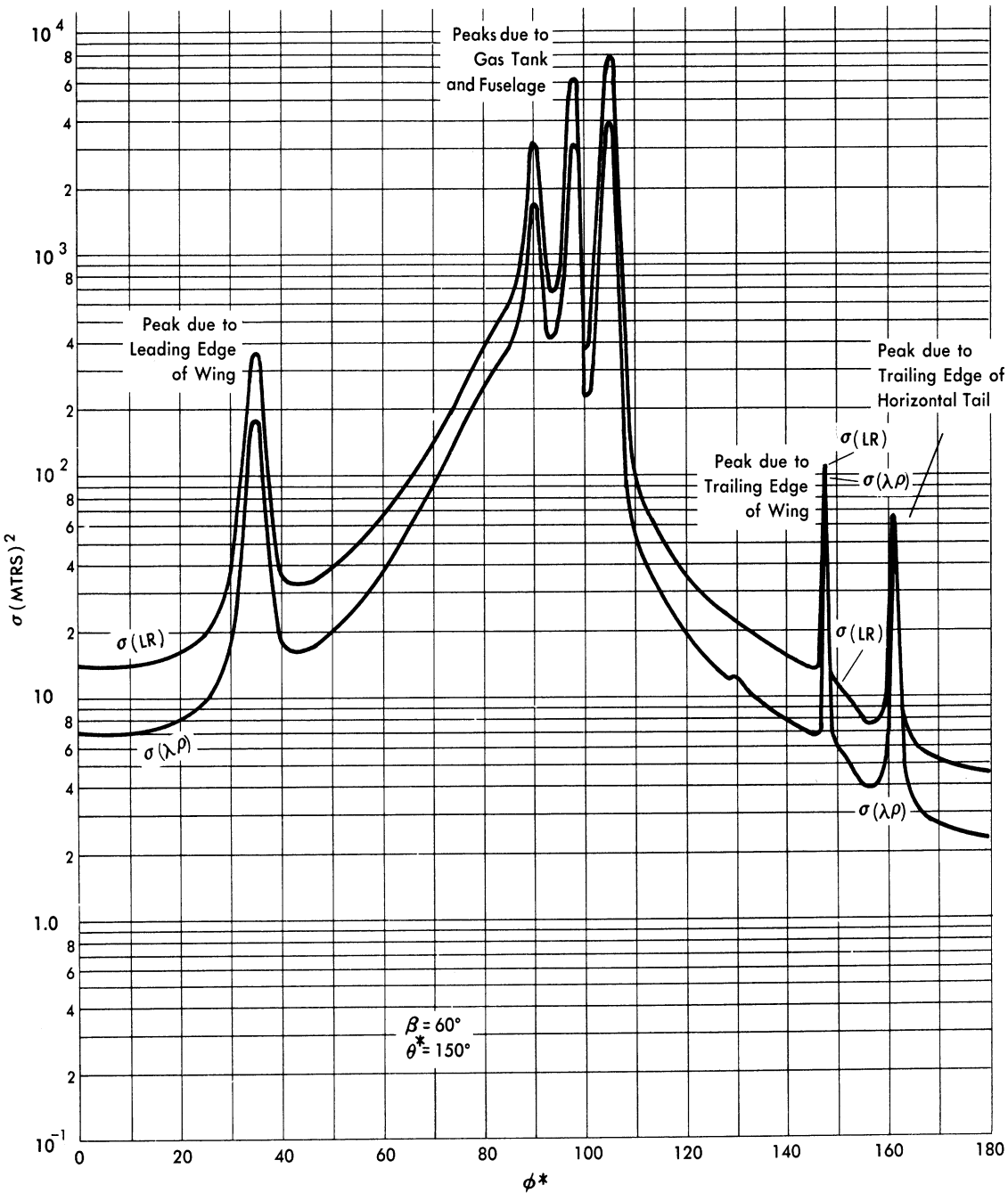

FIG. A.4-34 THEORETICAL CROSS-SECTIONS AT S-BAND FOR THE B-47 FOR ELEVATION 60°

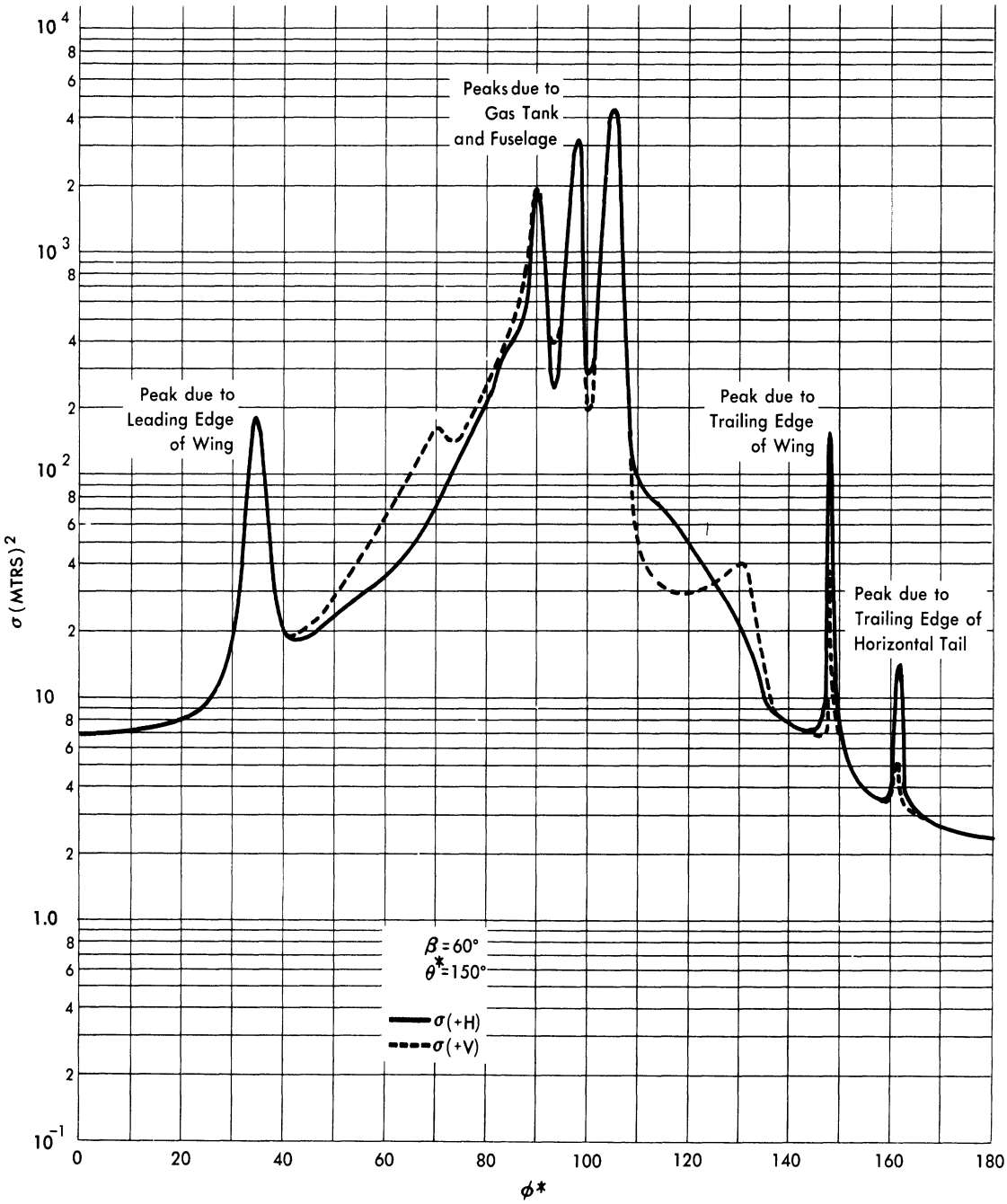

FIG. A.4-35 THEORETICAL CROSS-SECTIONS AT S-BAND FOR THE B-47 FOR ELEVATION 60°

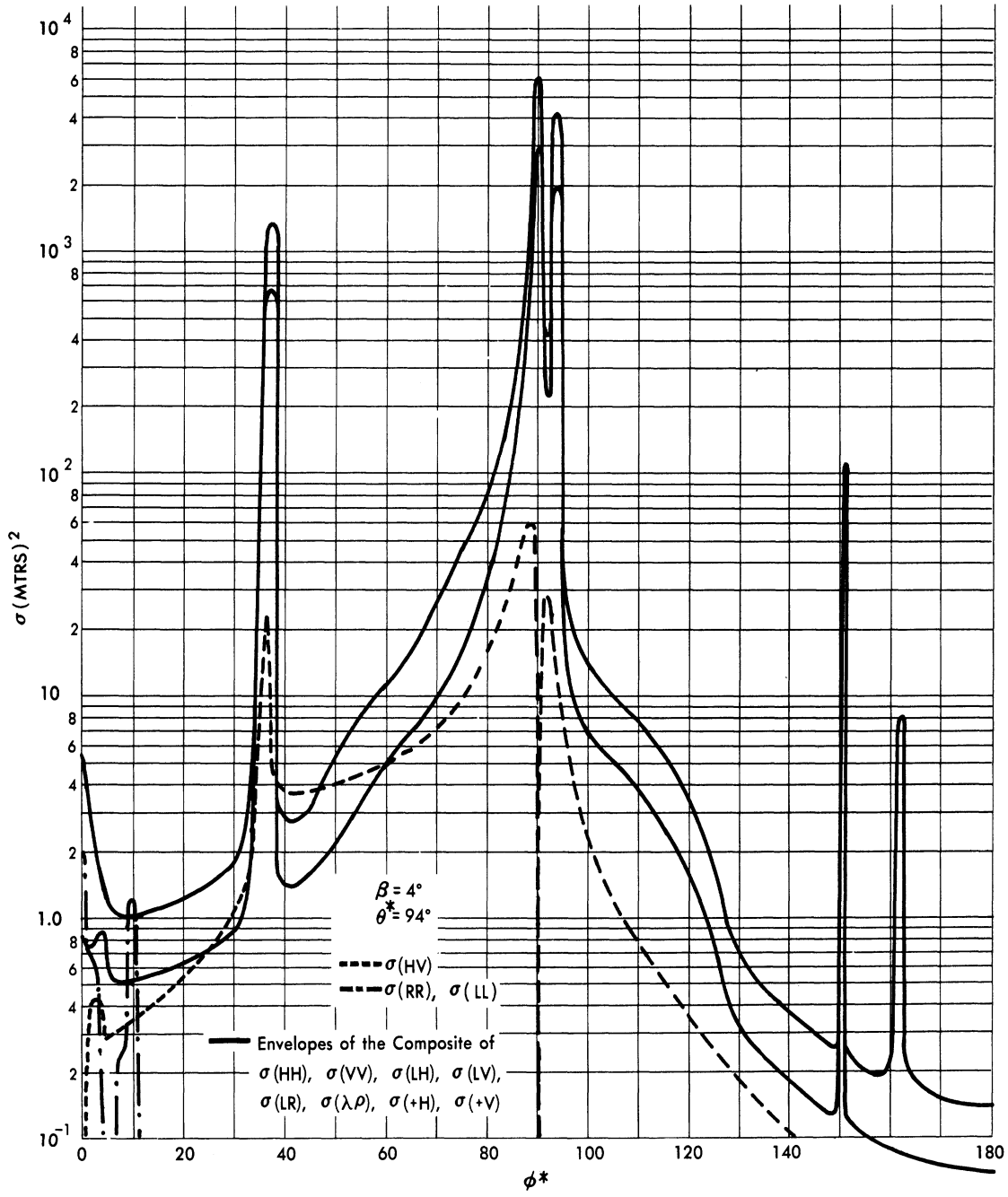

FIG. A.4-36 COMPOSITE OF THEORETICAL CROSS-SECTIONS AT S-BAND FOR THE B-47 FOR ELEVATION 4°

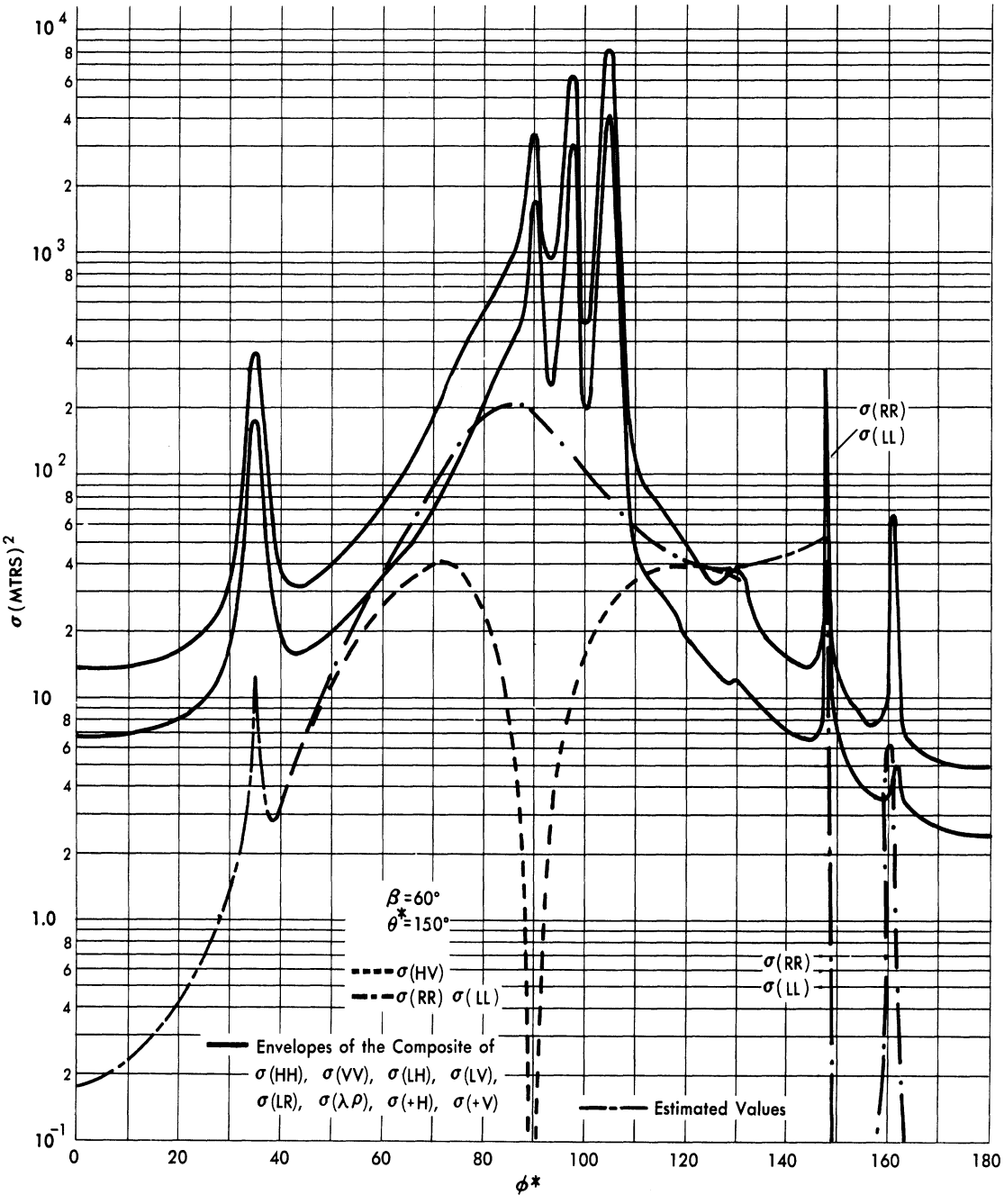

FIG. A.4-37 COMPOSITE OF THEORETICAL CROSS-SECTIONS AT S-BAND FOR THE B-47 FOR ELEVATION 60°

B

COMPARISON BETWEEN THEORY AND EXPERIMENT

(Confidential)

Measured values of the radar cross-section of the B-47 aircraft for the polarizations (HH), (VV), (VH), (HL), (VL), (LR), and (LL) at a limited number of aspect and elevation angles are reported by the Hughes Aircraft Company of Culver City, California in Reference 15. These data were obtained from four constant-bearing, constant-altitude flights of a B-47B. The ranges of azimuth and elevation angles covered were:

Flight	Azimuth	Elevation
1	20^{o} to 160^{o}	8^{o} to 22^{o}
2	20^{o} to 160^{o}	32^{o} to 61^{o}
3	20^{o} to 160^{o}	46^{o} to 72^{o}
4	180^{o}	10^{o} to 35^{o}

All cross-section values reported are average values[1] over a $\pm 5^{o}$ range in azimuth except for Flight 4, where the averages were taken over a $\pm 5^{o}$ range for 20^{o} and 30^{o} elevations, and over $\pm 2\frac{1}{2}^{o}$ range for the $12\frac{1}{2}^{o}$ elevation.

[1]Averages of experimental data were made in two steps. First, the video and AGC data were averaged over one second intervals. Second, additional smoothing was introduced into the cross-section measurements by averaging the data over finite amounts of target aspect, as pointed out above. In the first case the averaging was arithmetic (performed electronically by means of a boxcar circuit) with the quantities video and AGC data being directly proportional to cross-section. In the second case the averaging was also arithmetic.

The phase-averaging technique which was used to get the theoretical cross-sections is also an arithmetic average comparable to the types mentioned above. However, since the experimental data was averaged over much greater ranges than the theoretical calculations, the experimental curves will not exhibit the sharp peaks and nulls of the theoretical curves.

To compare the above data with the theoretical curves for the B-47 only those portions of each flight were used which gave elevation angles close to the ones used for the theoretical computations. Thus, there are no experimental data which correspond to the theoretical curves for $\theta^* = 86^\circ$, 90°, and 94°. For the other theoretical curves experimental values were used as follows:

Figure	Elevation Angled Theoretical Curve	Elevation Range Experimental Data	Azimuth Points used for Comparison
B-1 through B-4	$\theta^* = 98^\circ$	$97^\circ < \theta^* < 99^\circ$	$\phi^* = 20^\circ$ and 160°.
B-5 through B-8	$\theta^* = 102^\circ$	$100^\circ < \theta^* < 104^\circ$	$\phi^* = 30^\circ$, 40°, 140°, 150°, and 180°.
B-9 through B-12	$\theta^* = 120^\circ$	$117^\circ < \theta^* < 123^\circ$	$\phi^* = 20^\circ$, 160°, 180°.
B-13 through B-16	$\theta^* = 150^\circ$	$147^\circ < \theta^* < 153^\circ$	$\phi^* = 40^\circ$, 60°, 70°, 80°, 90°, 100°, 110°, 120°, and 140°.

The Hughes data and the theoretical curves for $\theta^* = 150^\circ$ agree to within a factor of ten for all polarizations except (HV) and (LL) and to within a factor of four for (HH), (VV), (HL), and (VL). For the regions where the theoretical curves show sharp peaks this agreement would be improved if the theoretical curves were averaged over $\pm 5^\circ$ ranges at the same values of ϕ^* where the Hughes averages were made. In particular this procedure would improve the agreement at (LR) polarization from a factor of ten to a factor of five.

The Hughes data points for the other elevation angles ($\theta^* = 98^\circ$, 102°, and 120°) are too few to allow much comparison. In the case of (HV) polarization there is an experimental peak on looking at the leading edge of the wing at $\theta^* = 98^\circ$. This peak is not to be taken as showing a discrepancy between theory and experiment since in a dynamic test the wings

do not remain horizontal. In fact if the wings are rotated through an angle ψ from the horizontal the cross-section σ(HV) goes from the theoretical value zero to roughly,

$$\sigma(\mathrm{HV}) \cong \sin^2\psi \ \sigma(\mathrm{HH}).$$

In the $\theta^{\star} = 102^{\circ}$ curves where there are five Hughes data points on each curve, four of these fall in the vicinity of high peaks on the theoretical curves and the apparent disagreement could well be due to the Hughes points being averages.

Since modern day aircraft have major parts which have surfaces either parallel or perpendicular to each other and since such aircraft fly courses which are parallel to the ground (often great circle routes) it is expected that σ(HV) or σ(VH) (the same by the reciprocity theorem) will give negligibly small results. Thus, σ(HV) only plays a small role in the computing of σ(LR). Since these latter cross-sections were of most interest, little theoretical emphasis was placed on obtaining small, but not zero, results from the components which required lengthy analysis. As a result it was not expected to obtain good agreement between theory and experiment for σ(HV) but it is expected that good agreement will be obtained between theory and experiment for σ(RL) and σ(LR).

On the other hand, as has been indicated above, there is considerable interest in the behavior of the cross-section σ(LL). For this reason Fock's current distribution method (Sec. 9) has been applied to the wings for the elevation angle $\theta^{\star} = 90^{\circ}$ and the azimuth angle $\phi^{\star} = 36^{\circ}$. The resulting cross-section σ(LL) is approximately 25 square meters. This is to be compared with the experimental values σ(LL) = 5.4 square meters at $\theta^{\star} = 98^{\circ}$, $\phi^{\star} = 20^{\circ}$, σ(LL) = 7.0 square meters at $\theta^{\star} = 102^{\circ}$, $\phi^{\star} = 30^{\circ}$, and σ(LL) = 8.0 square meters at $\theta^{\star} = 102^{\circ}$, $\phi^{\star} = 40^{\circ}$. This comparison indicates that Fock's method can predict the repolarization effects to within at least a factor of three even through the wing dimensions do not lie strictly within the region of validity for the application of the method.

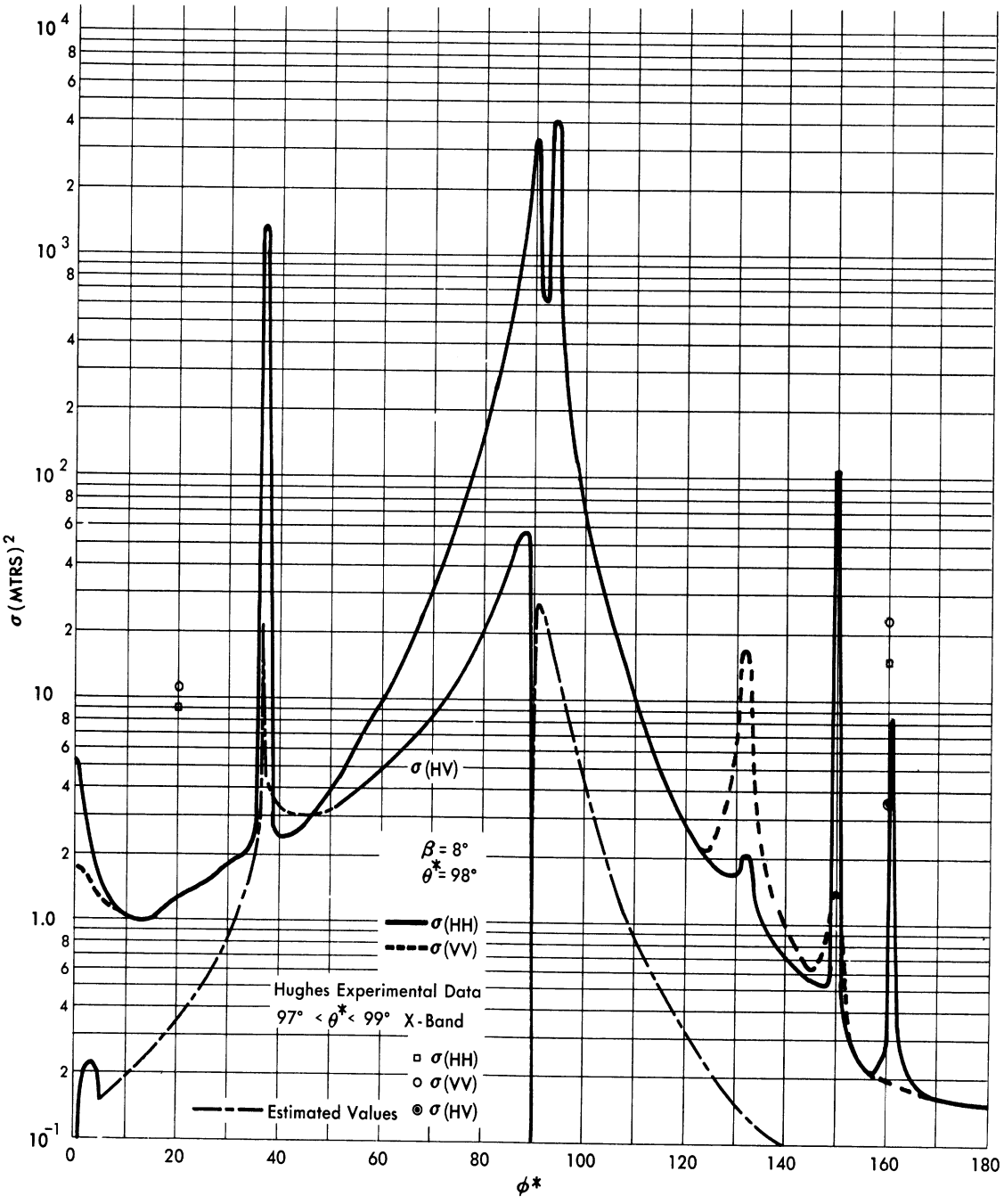

FIG. B-1 COMPARISON OF THEORY vs. EXPERIMENT FOR B-47 CROSS-SECTIONS FOR ELEVATION 8°

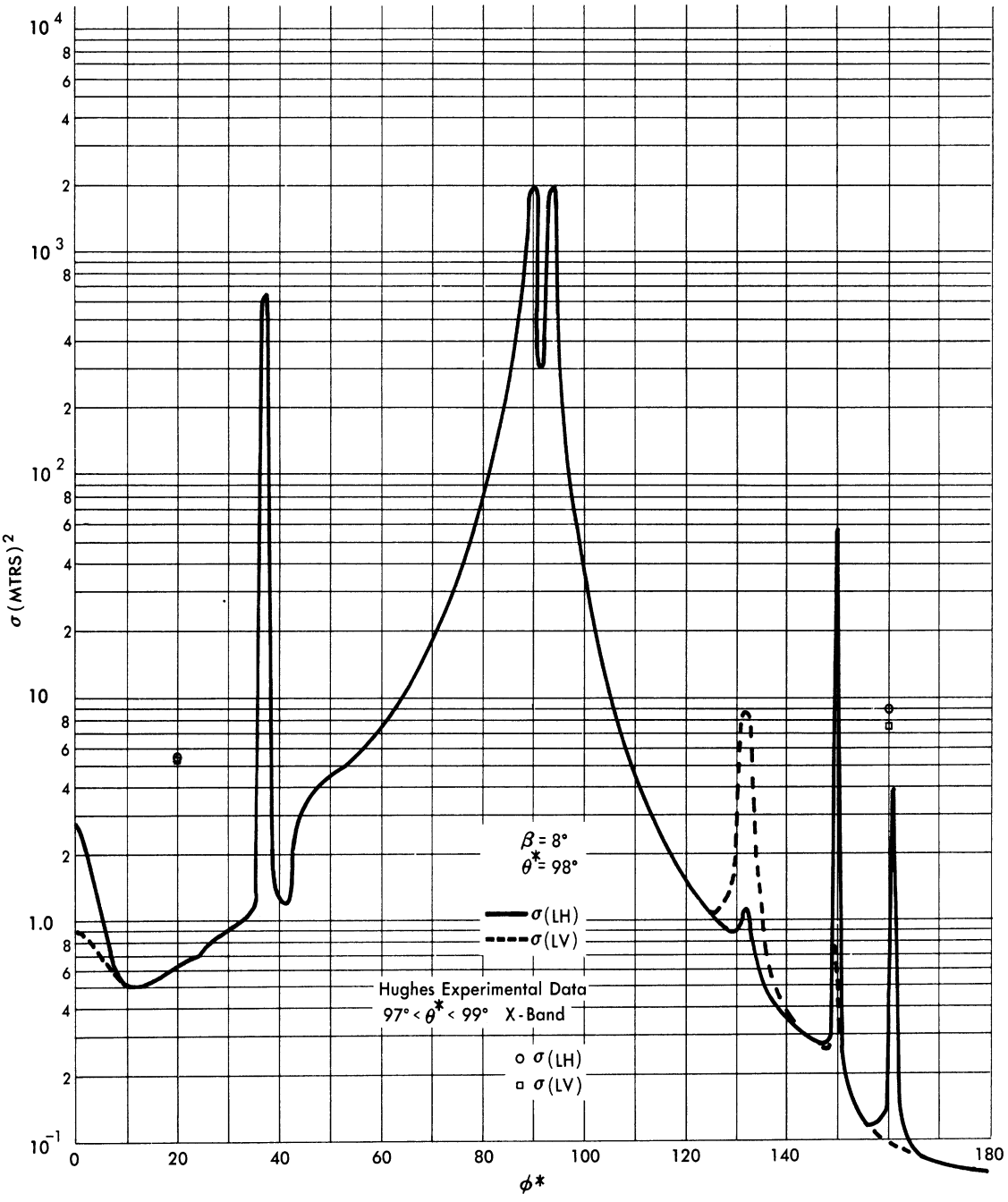

FIG. B-2 COMPARISON OF THEORY vs. EXPERIMENT FOR B-47 CROSS-SECTIONS FOR ELEVATION 8°

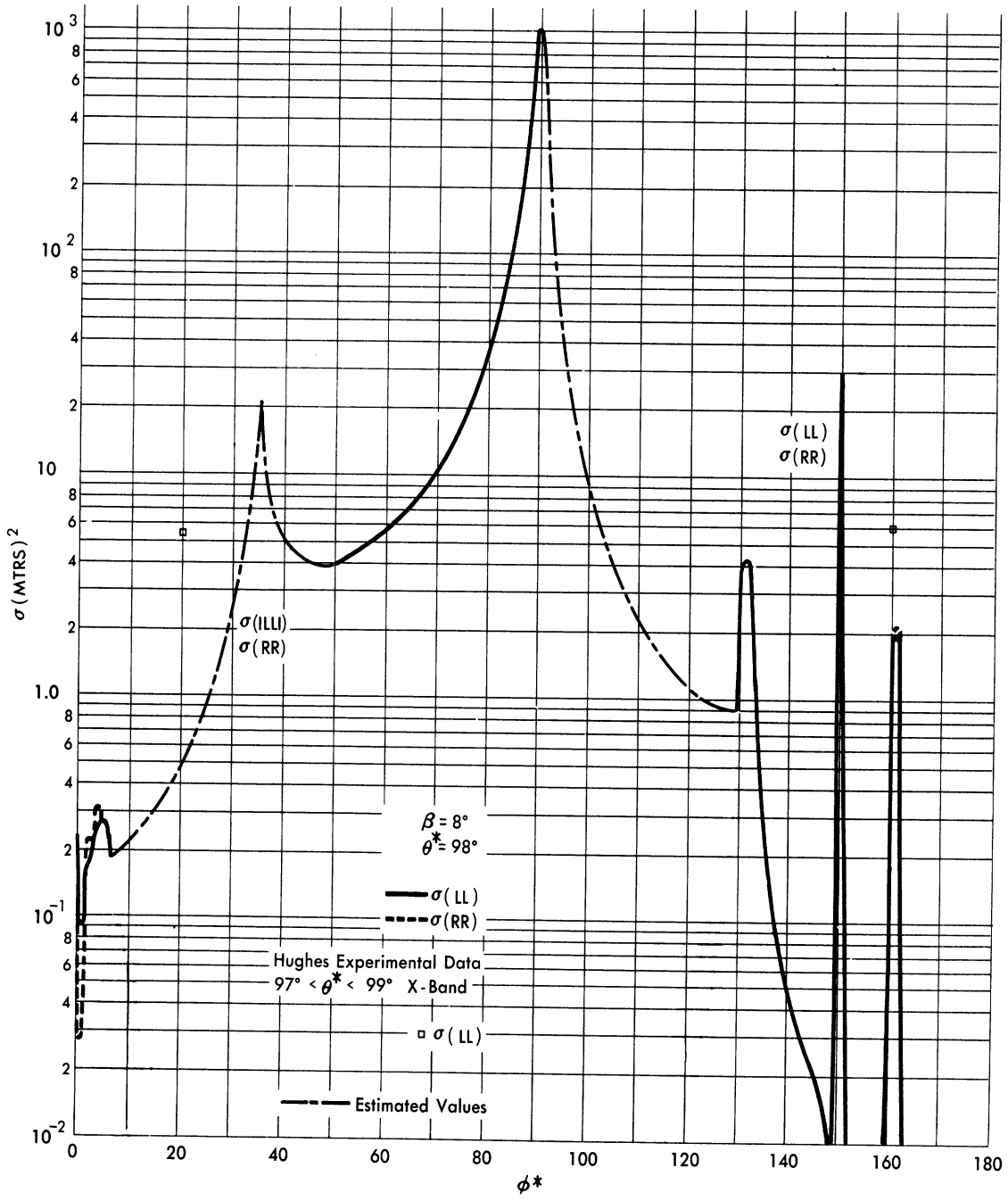

FIG. B-3 COMPARISON OF THEORY vs. EXPERIMENT FOR B-47 CROSS-SECTIONS FOR ELEVATION 8°

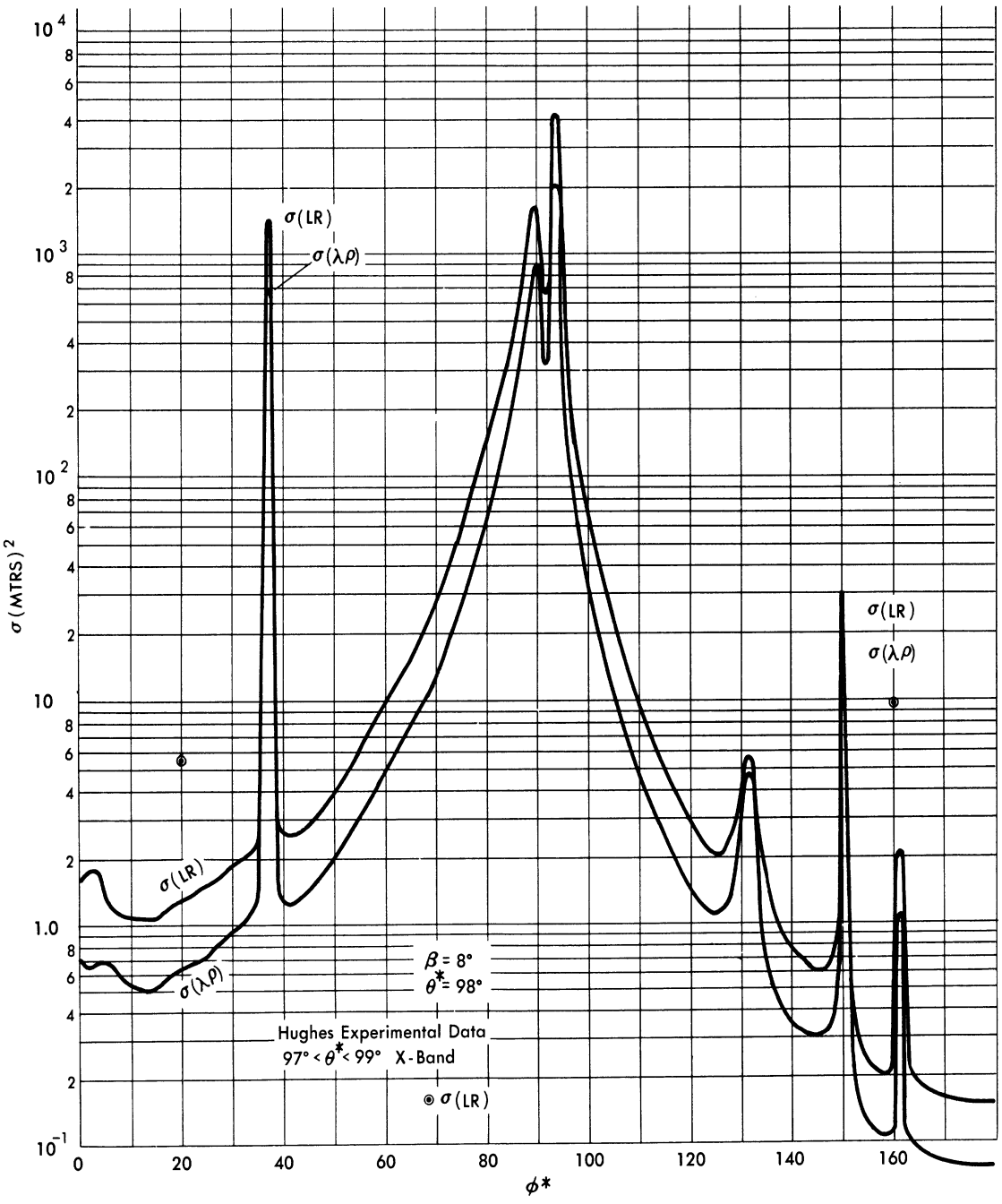

FIG. B-4 COMPARISON OF THEORY vs. EXPERIMENT FOR B-47 CROSS-SECTIONS FOR ELEVATION 8°

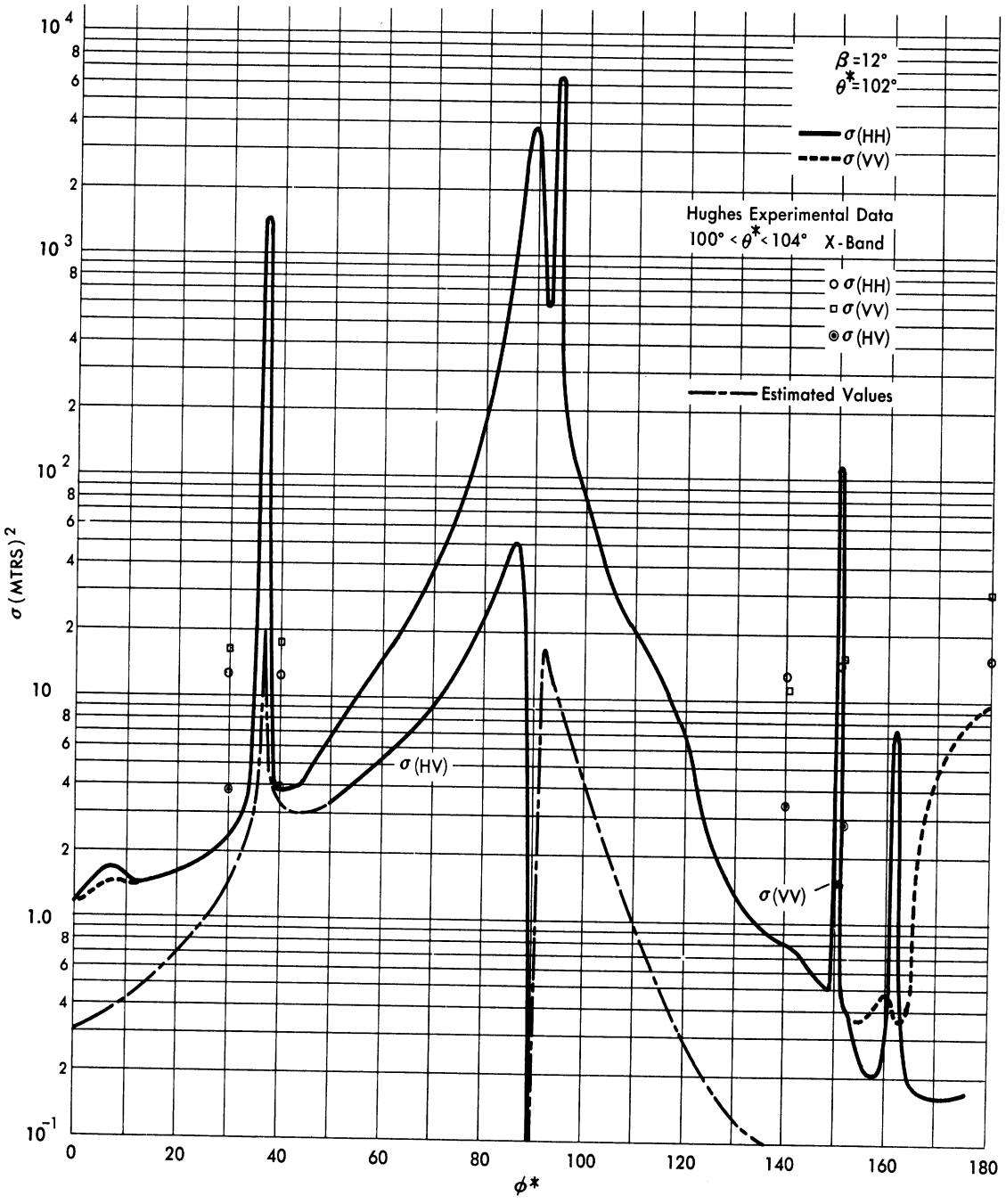

FIG. B-5 COMPARISON OF THEORY vs. EXPERIMENT FOR B-47 CROSS-SECTIONS FOR ELEVATION 12°

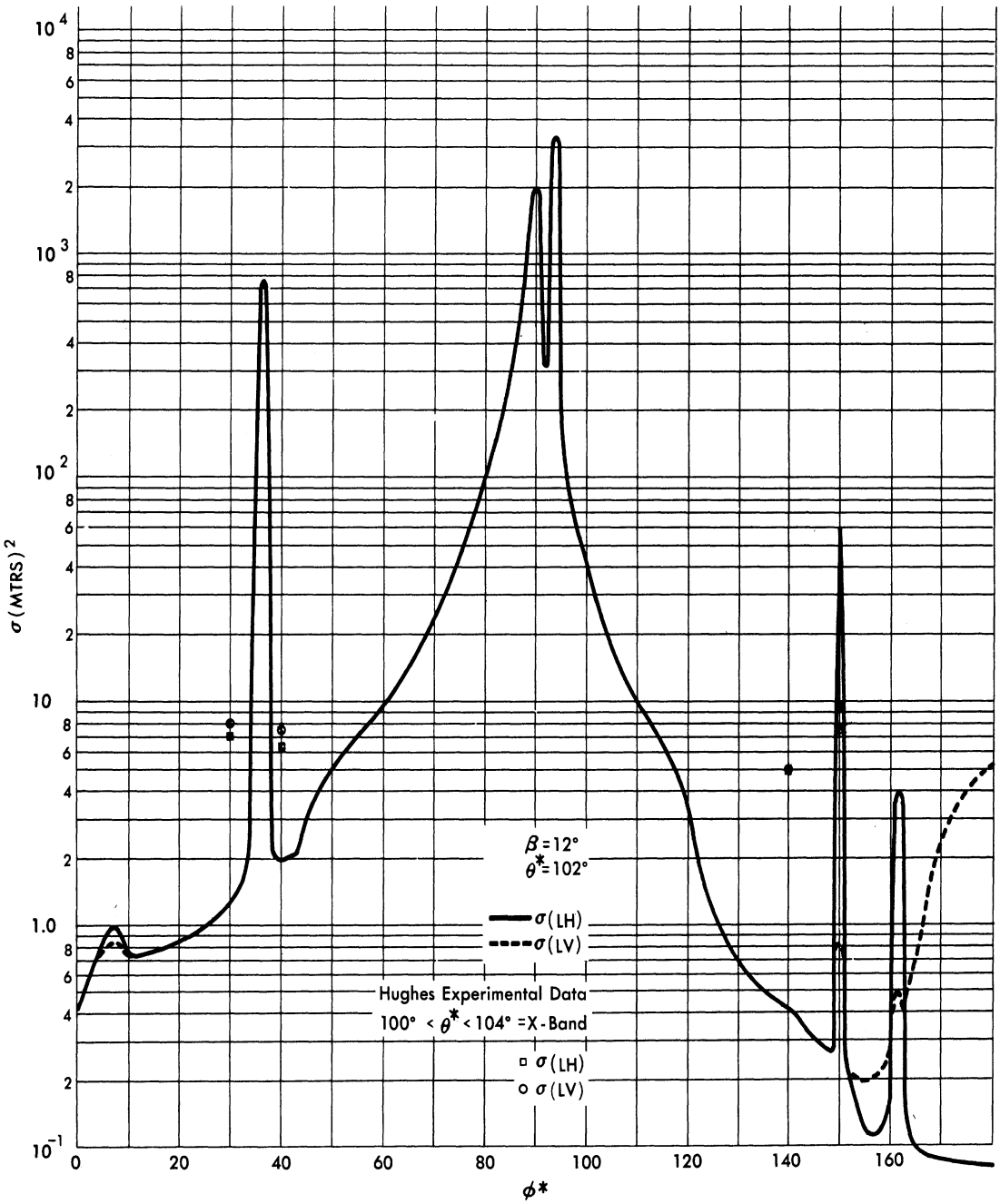

FIG. B-6 COMPARISON OF THEORY vs. EXPERIMENT FOR B-47 CROSS-SECTIONS FOR ELEVATION 12°

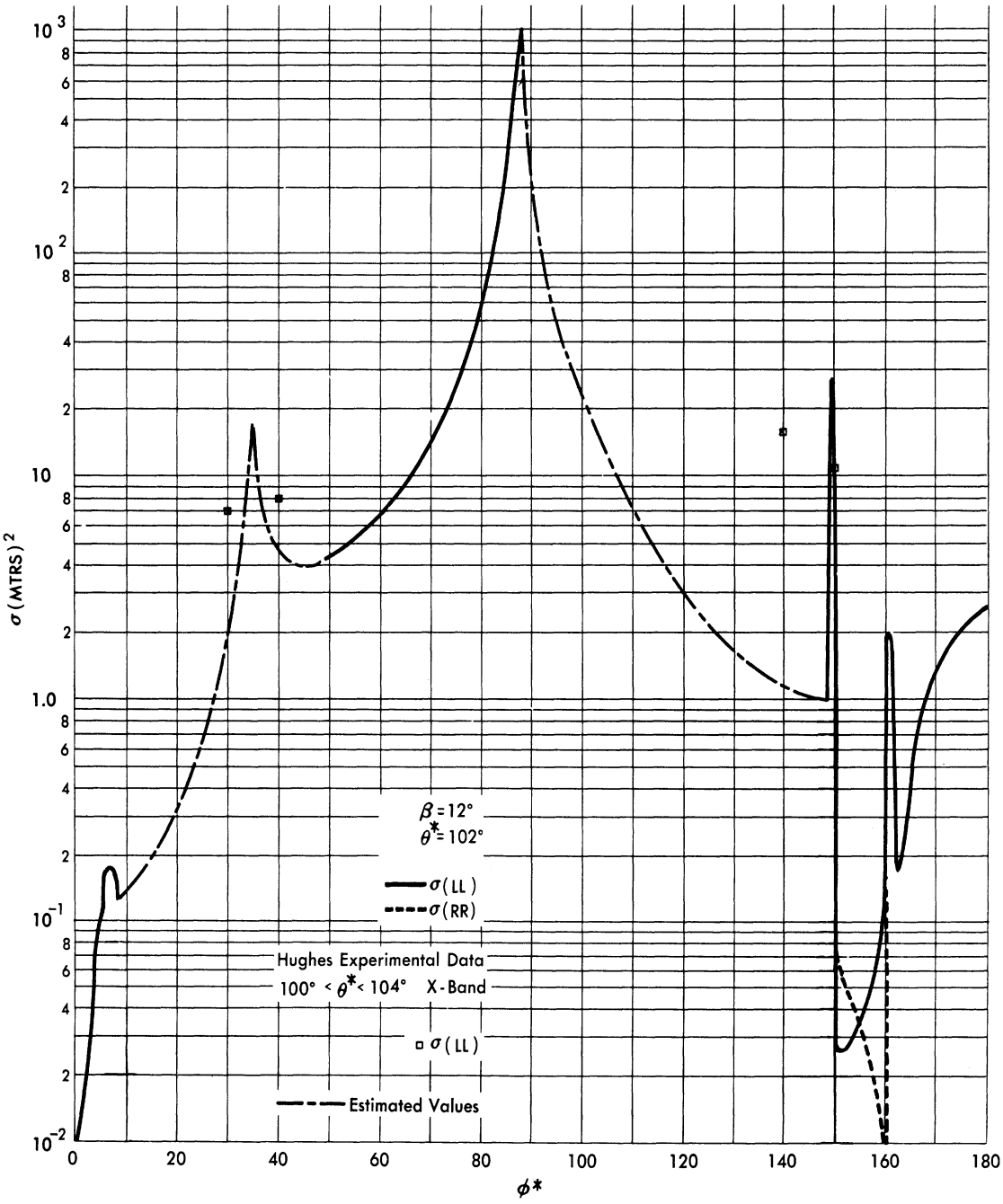

FIG. B-7 COMPARISON OF THEORY vs. EXPERIMENT FOR B-47 CROSS-SECTIONS FOR ELEVATION 12°

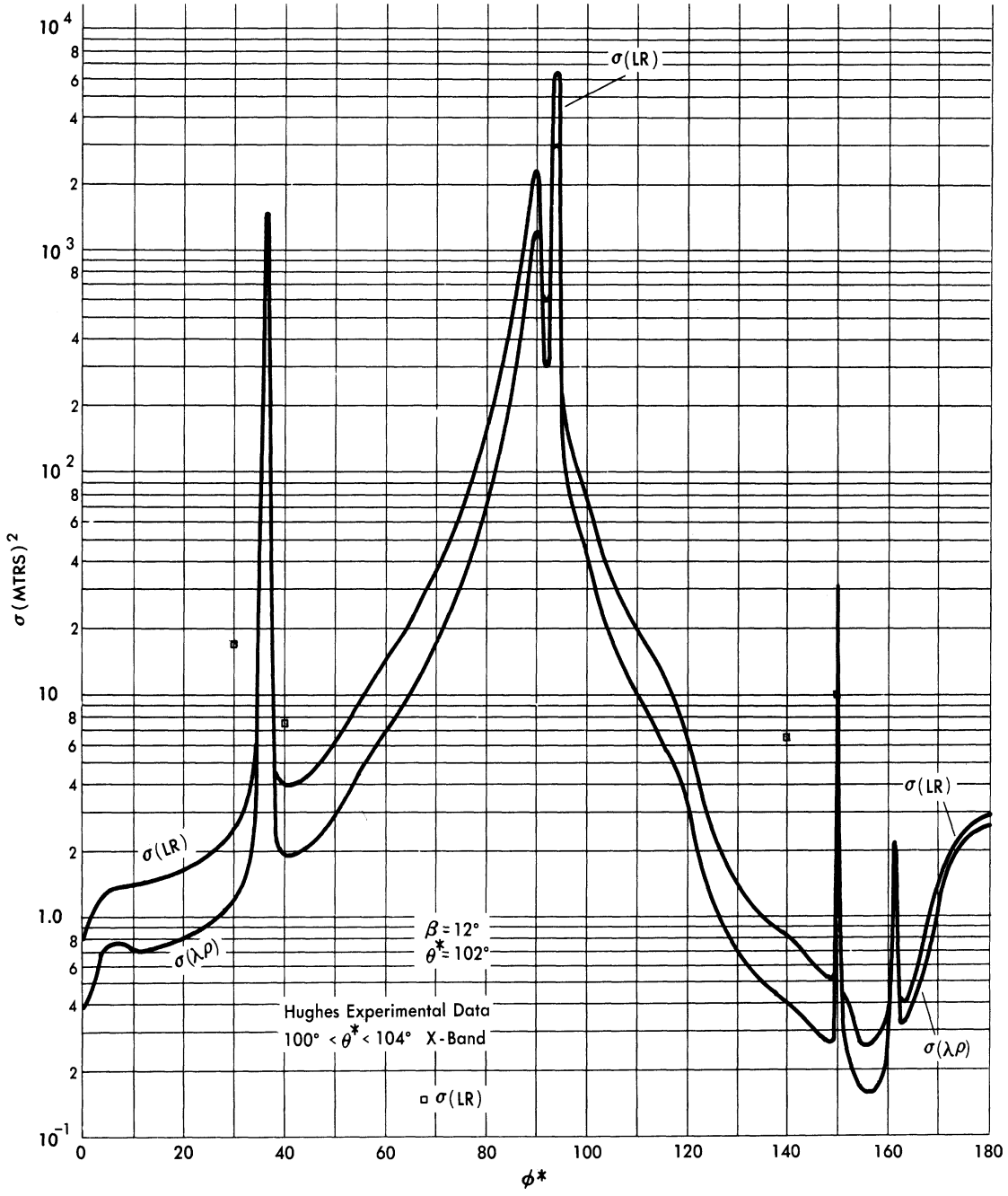

FIG. B-8 COMPARISON OF THEORY vs. EXPERIMENT FOR B-47 CROSS-SECTIONS FOR ELEVATION 12°

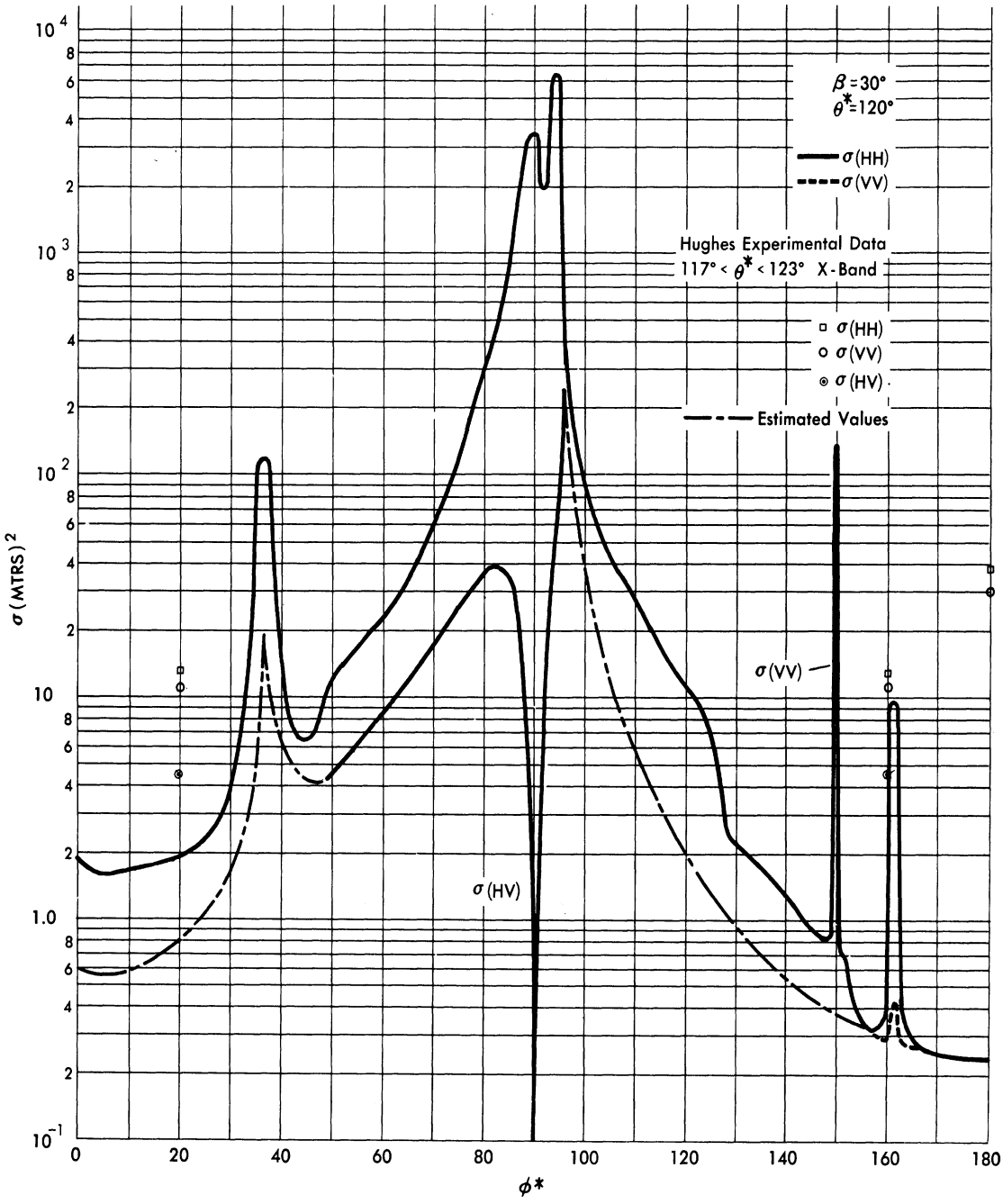

FIG. B-9 COMPARISON OF THEORY vs. EXPERIMENT FOR B-47 CROSS-SECTIONS FOR ELEVATION 30°

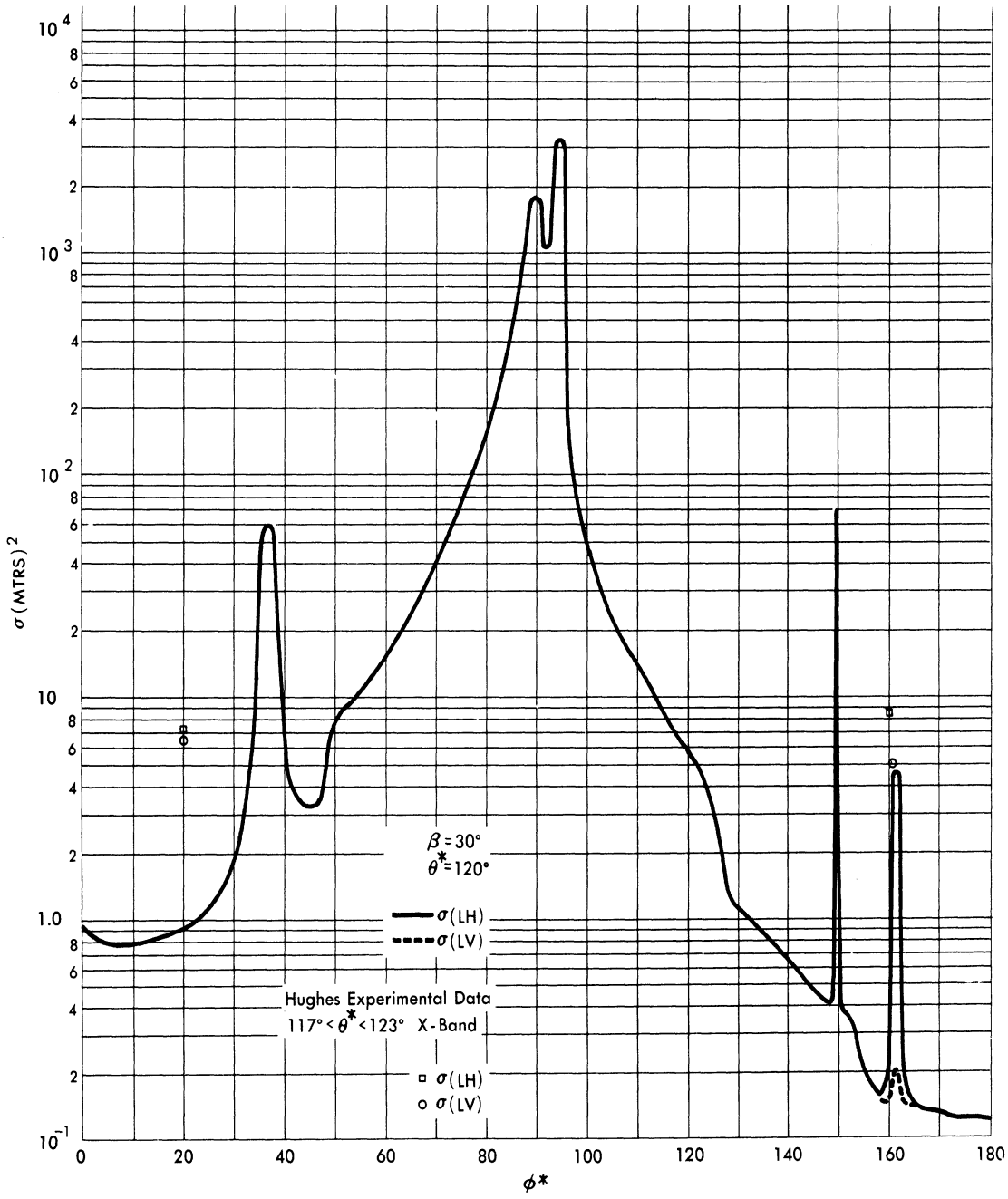

FIG. B-10 COMPARISON OF THEORY vs. EXPERIMENT FOR B-47 CROSS-SECTIONS FOR ELEVATION 30°

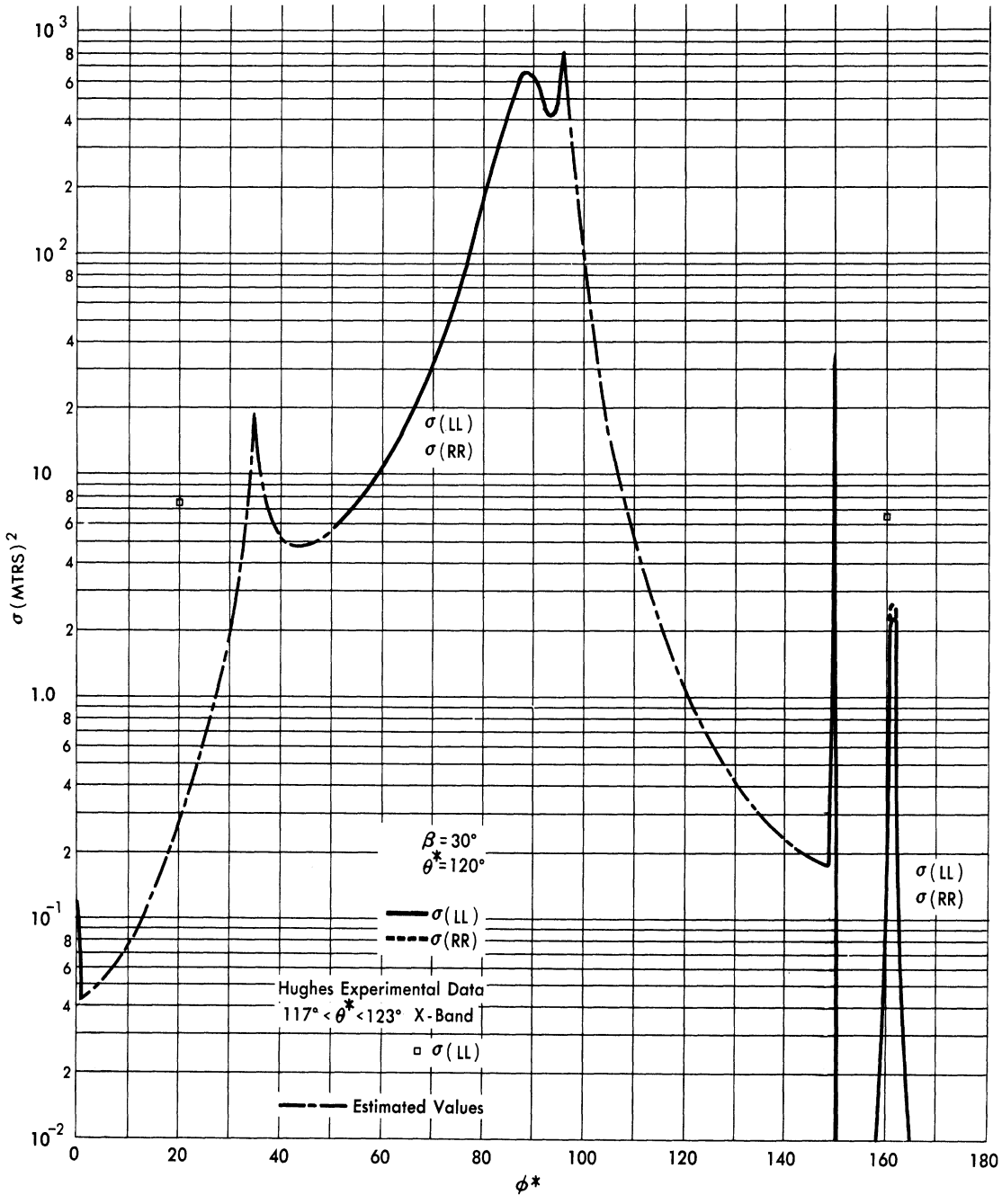

FIG. B-11 COMPARISON OF THEORY vs. EXPERIMENT FOR B-47 CROSS-SECTIONS FOR ELEVATION 30°

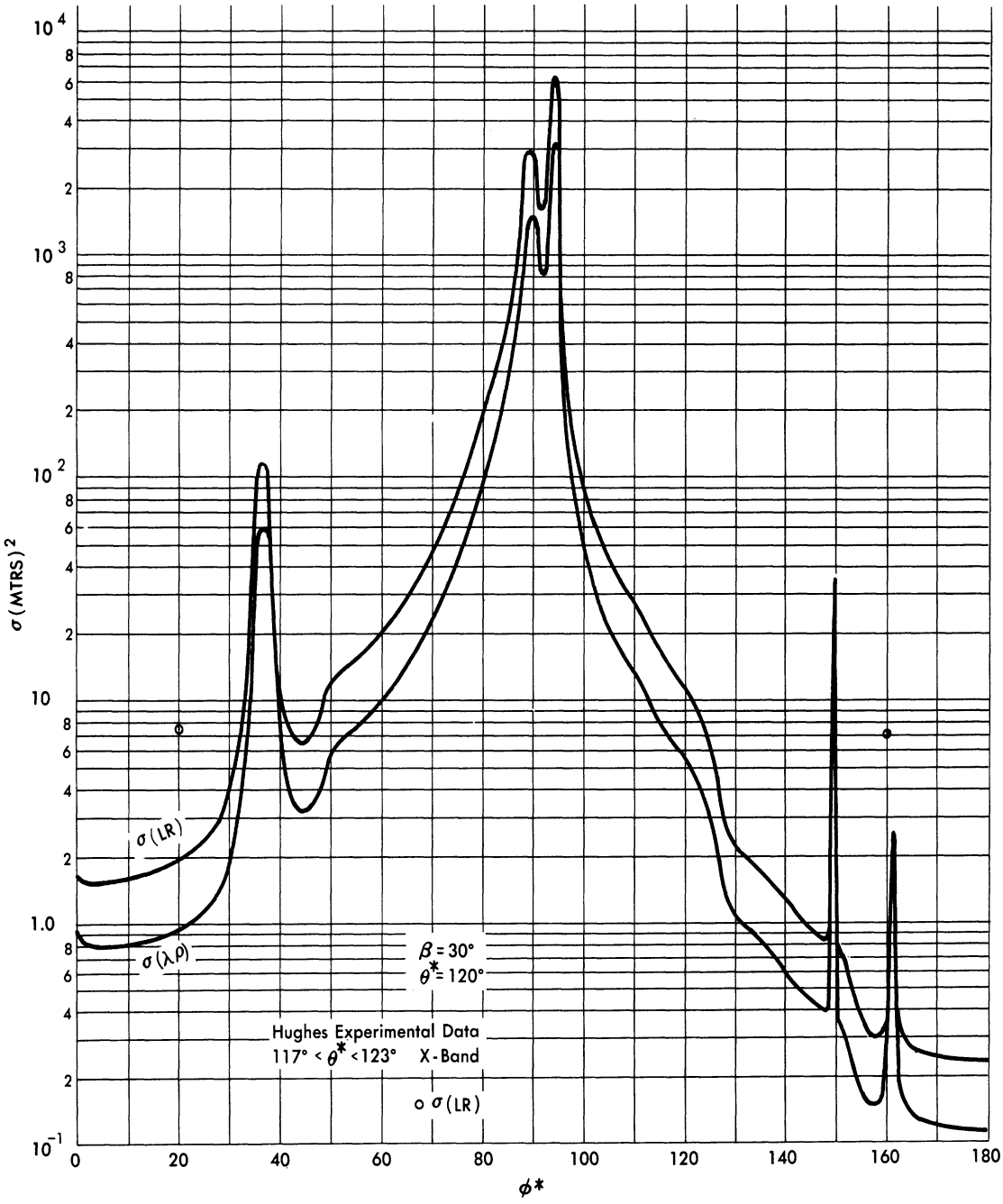

FIG. B-12 COMPARISON OF THEORY vs. EXPERIMENT FOR B-47 CROSS-SECTIONS FOR ELEVATION 30°

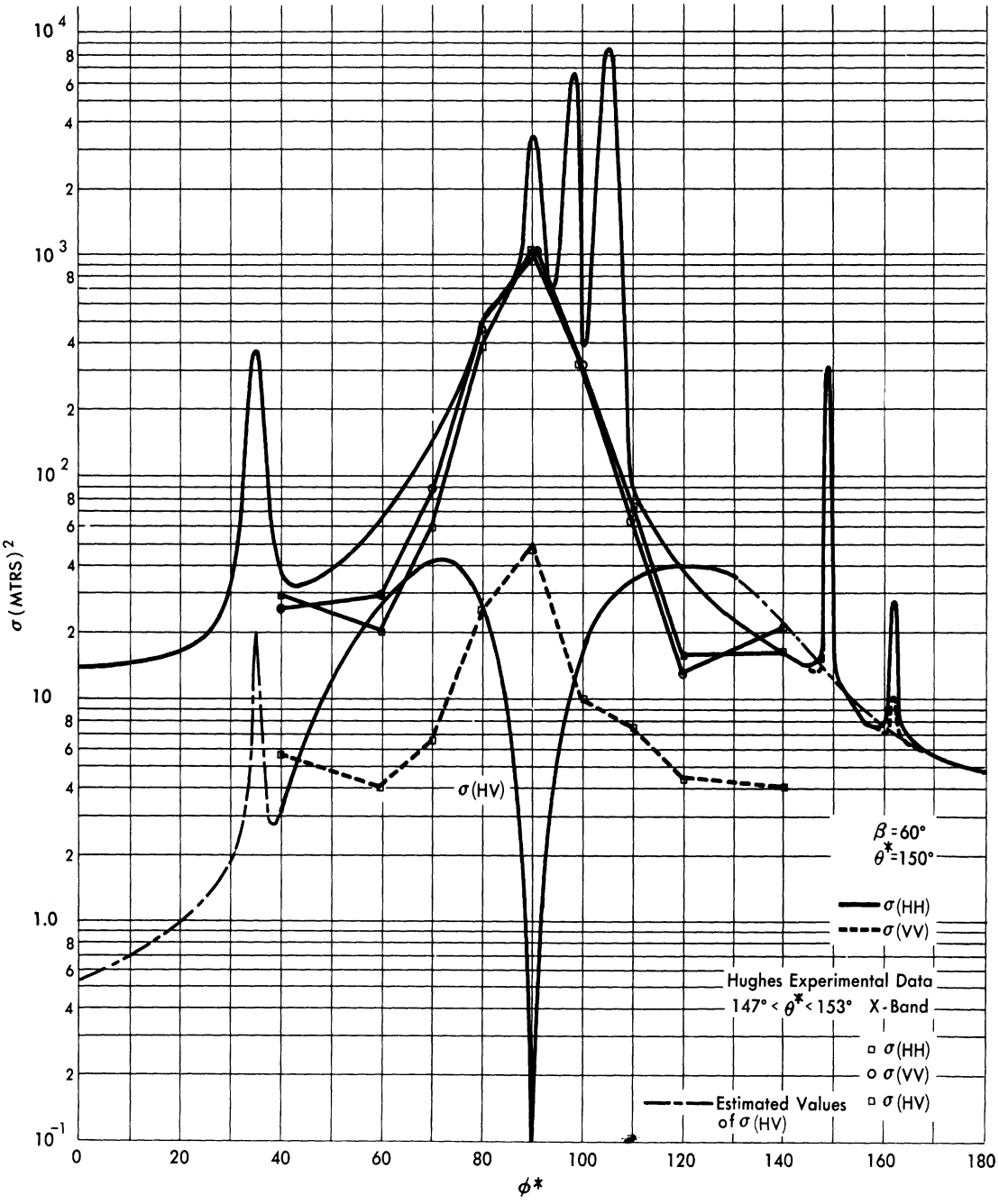

FIG. B-13 COMPARISON OF THEORY vs. EXPERIMENT FOR B-47 CROSS-SECTIONS FOR ELEVATION 60°

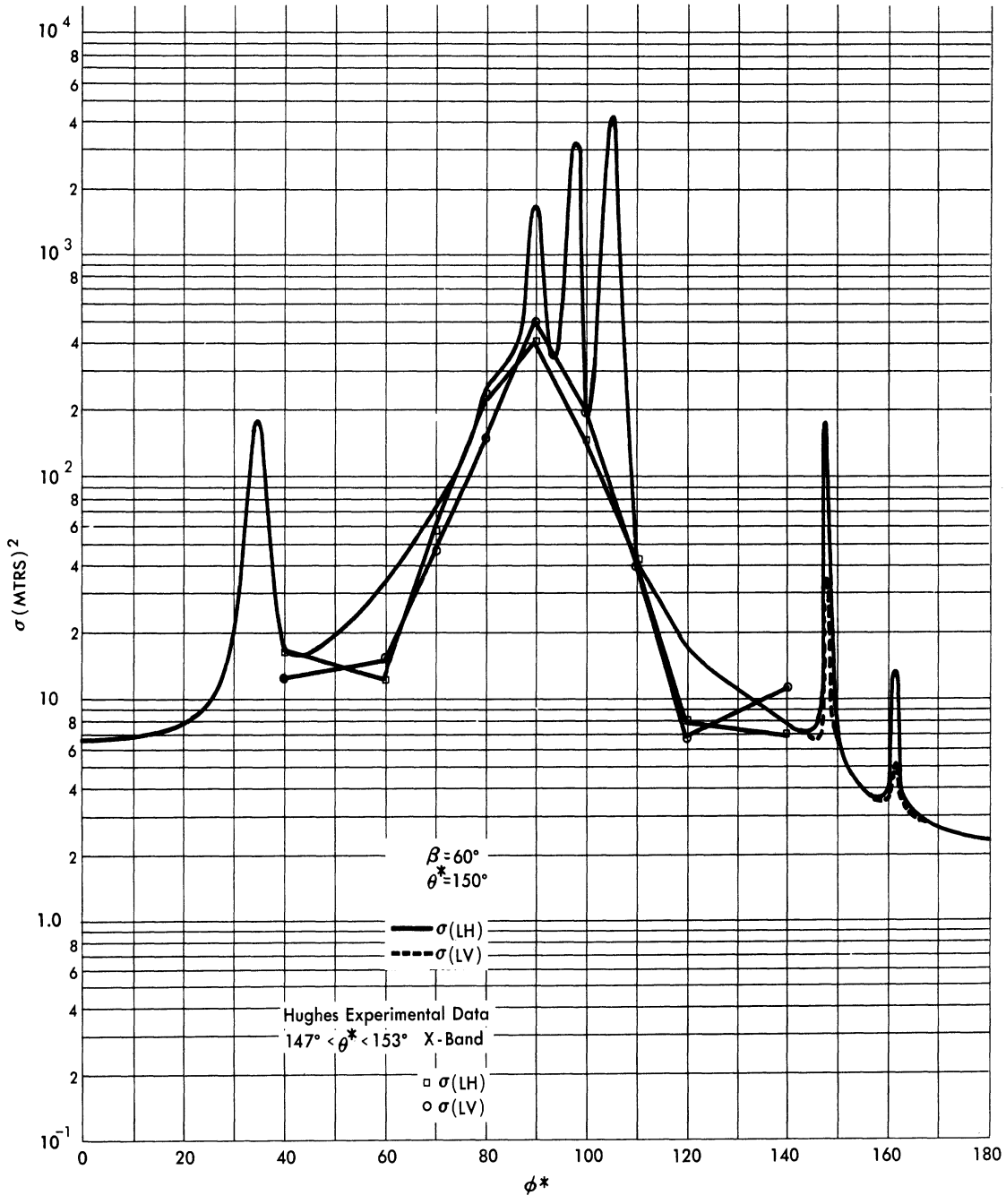

FIG. B-14 COMPARISON OF THEORY vs. EXPERIMENT FOR B-47 CROSS-SECTIONS FOR ELEVATION 60°

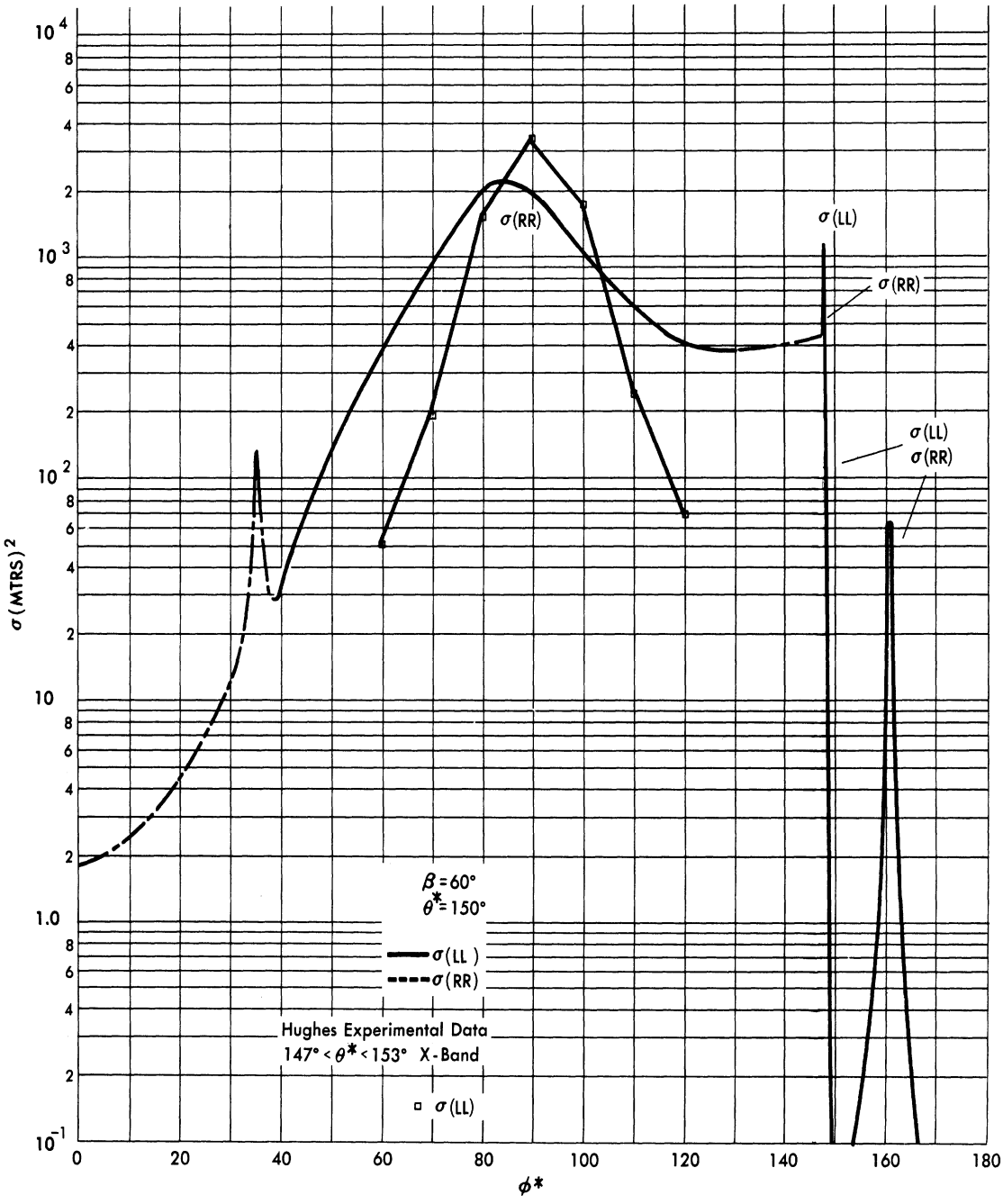

FIG. B-15 COMPARISON OF THEORY vs. EXPERIMENT FOR B-47 CROSS-SECTIONS FOR ELEVATION 60°

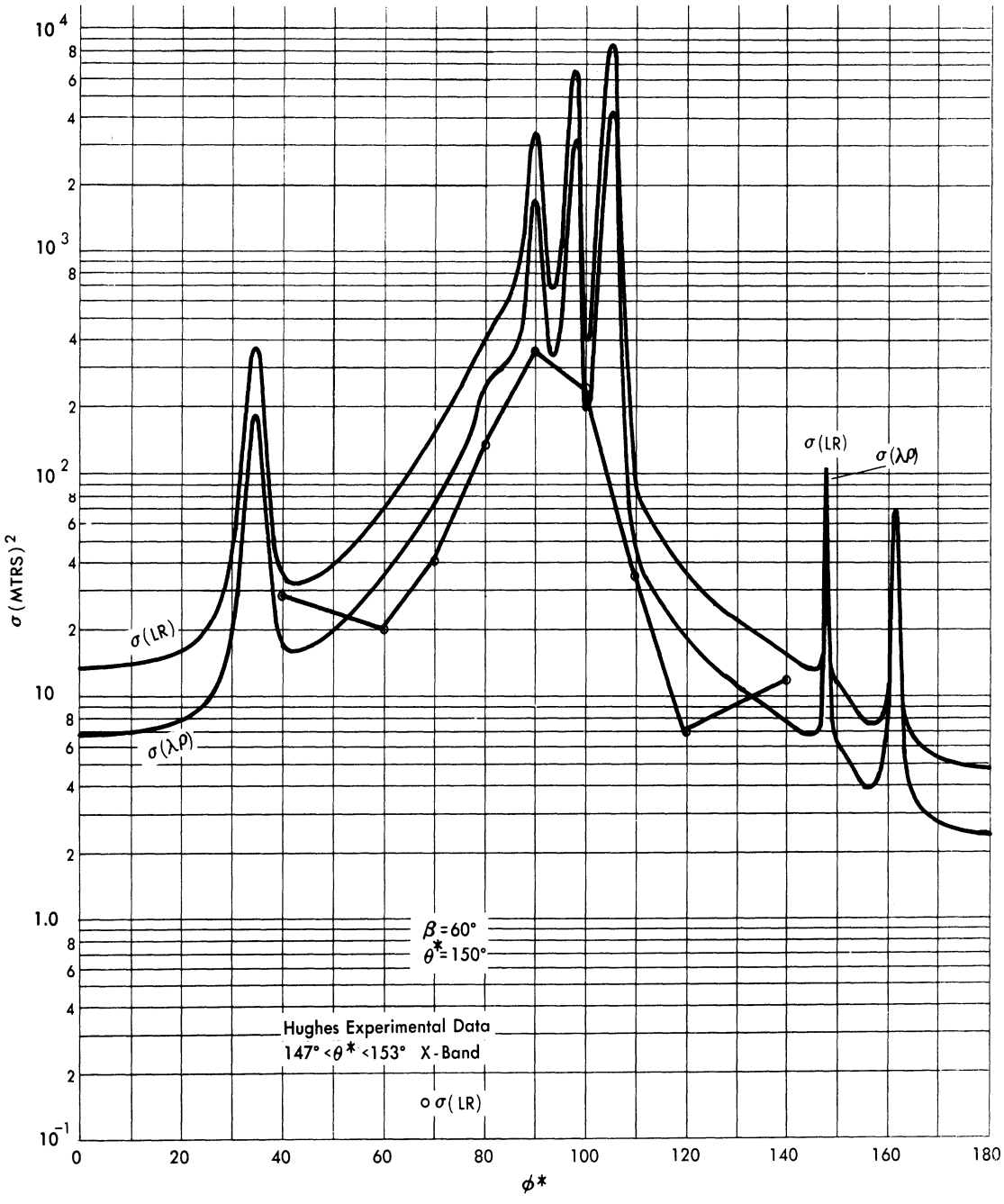

FIG. B-16 COMPARISON OF THEORY vs. EXPERIMENT FOR B-47 CROSS-SECTIONS FOR ELEVATION 60°

C

COMPARISON BETWEEN EFFECTIVE CROSS-SECTIONS WITH CIRCULAR AND LINEAR POLARIZATION

(Confidential)

The usefulness of radar equipment designed to measure the effective cross-sections $\sigma(LL)$ or $\sigma(RR)$ will depend upon the permissible reduction of signal strength as compared with measurement of, say, the cross-sections $\sigma(HH)$ or $\sigma(VV)$. That the reduction in signal strength is not too great has been shown experimentally.

The Group 22 Systems Analysis Section of MIT Lincoln Laboratory has studied weather clutter and, in particular, has investigated the use of circular polarization to reduce this clutter. They have been interested in the relative performance on aircraft targets of a particular radar installation operating in circular and linear polarization modes.

The preliminary results obtained indicate an average apparent degradation of performance for the circular polarization mode of operation compared to the linear vertical mode of only about 1 db. Their results are only preliminary, having been made with only one radar set, and with a radar whose circularity of radiation is, at present, not well established. Furthermore, the received power is not measured directly, but is derived with the aid of blip-scan theory from the probability per scan of obtaining a blip. The relation used is

$$x = e^{-p_{min}/p_{av.}},$$

where x = blip scan ratio, p_{min} = the power threshold of detectability, and $p_{av.}$ = the average signal echo power. While it may not be dependable for yielding absolute power levels $p_{av.}$, since p_{min} is not easily calculable, this expression can be used to obtain relative return-signal power.

It is encouraging that the degradation factor determined from

blip-scan observations from radar PPI's agreed closely with that determined from the slowed-down video scopes. In addition, the degradation parameter did not depend significantly on type of aircraft, altitude, or range. The preliminary results indicate a weather clutter reduction of about 12 db by use of circular polarization.

The same problem was investigated in 1950 by Airborne Instruments Laboratory, Inc., Mineola, N. Y., using an AN/CPS-5 (L-band) radar. A circularly-polarized feed was developed and installed in the test set and observations were made of a heavily traveled portion of the sky near New York City. The degradation was measured as follows:

Successive scans used linear and circular polarization, and photographs were taken of the PPI. The gain for linear polarization was decreased in 5 db steps, leaving the gain for circular polarization unchanged, and each step photographed. The targets in a given range zone on all photographs were counted. Finally, the average degradation was taken to be the difference in gain settings such that the number of targets missed by the circular polarization equipment but seen by the linear polarization equipment was the same as the number of targets missed by the linear polarization equipment but seen by the circular polarization equipment.

The circularity of the radiation was checked carefully, and the difference in transmission and reflection efficiency for the two types of polarization, which was inherent in the circuitry, yielded a correction factor which was applied to the data. On the basis of their data, AIL concluded that target attenuation due to circular polarization is 7 db $\pm$ 1 db. Corresponding to this, they arrive at a net discrimination in favor of aircraft return over precipitation return of 8 to 25 db.

Studies have also been made by the Dalmo-Victor Company (Ref. 14) of the effect of polarization on the return from rain and from ground targets. They worked at X-band and used a variable-polarization feed assembly to produce the desired type of elliptical polarization. Their equipment included set-ups in which a single antenna was used for transmission and reception, as well as separate antennas for transmitting and receiving different polarizations.

The data were filmed with an A-scope pulse-to-pulse-recording camera, the radar system being calibrated for decibel attenuation at the antenna versus video output to the A-scope. The film was then projected on a screen. Extreme difficulty was experienced in reading average values of voltages by this method. Furthermore, the linearity of the A-scope oscilloscope necessitated compression of the 20-30 db range into an inconveniently narrow part of the scale.

It was found that raindrops do scatter isotropically. They yield maximum return with linear polarization and minimum with either sense of circular polarization (the same antenna, of course, being used for transmission and reception). The average return with circular polarization was found to be 24 db below the maximum return with linear polarization.

Some simple ground targets were investigated, and conclusions which have at least qualitative value obtained. The results seem not to pertain to airplanes, the subject of this study. The return from a smooth hill dropped 20 db when polarization was shifted from linear to circular. Several bridges and a drive-in movie screen, all of which resembled flat plates, were used as targets. The greatest attenuation was observed with circular polarization.

The returns from groups of objects were of less well-defined behavior. A group of cylindrical tanks and Alcatraz prison both yielded returns in which some of the objects increased and others decreased in brightness with change of polarization. The greatest decrease in the Alcatraz pattern was 15 db.

The conclusion of the Dalmo-Victor study was that circular polarization yields a smaller return from simple objects than does linear polarization by about 2.7 db. It should still be used, though, since it affords 15 db of discrimination between these objects and rain clutter, on the average. This is a better value than that afforded by linear polarization.

The Raytheon Manufacturing Company of Boston, Massachusetts,

also obtained information about returns of energy from various objects and installations when incident circularly polarized energy was used. Their experiments were arranged so that, when transmitting circularly polarized energy, the percentages of right and left circularly and horizontal and vertical linearly polarized energy received could be calculated.

For example, when transmitting circularly polarized energy at a typical New England town, they found that about fifty per cent of the returned energy was polarized in one circular sense, fifty per cent in the other circular sense; the reception of energy was down approximately 3 db. Indeed, this type of situation prevailed for clutter in general. Exceptions were noted for rain and chaff. For rain, when transmitting circularly polarized energy, 85 - 90 per cent of the returned energy was circularly polarized in the opposite sense. For a twin-jet F-3D, transmitting again with circularly polarized energy, approximately 60 per cent of the returned energy was polarized in a sense opposite to that transmitted.

REFERENCES

Number

1. C. Schensted, J. Crispin, K. Siegel, "Studies in Radar Cross-Sections XV--Radar Cross-Sections of B-47 and B-52 Aircraft," 2260-1-T, Willow Run Research Center, Engineering Research Institute, University of Michigan (1954). CONFIDENTIAL

2. D. Kerr, "Propagation of Short Radio Waves," Volume 13, Massachusetts Institute of Technology Radiation Laboratory Series, McGraw-Hill Book Company (1951).

3. W. D. White, "Circular Polarization Study," Report No. 394-1, Airborne Instruments Laboratory Inc. (1950). CONFIDENTIAL

4. "Effects of Type of Polarization in Echo Characteristics," Second Quarterly Progress Report under Contract No. AF 28(099)-90, The Ohio State University Research Foundation, Antennas Laboratory (1949). UNCLASSIFIED

5. "Quarterly Progress Report," Division 2--Aircraft Control and Warning, Massachusetts Institute of Technology, Lincoln Laboratory (15 August, 1954). SECRET

6. Project Report 389-4, The Ohio State University Research Foundation, Antenna Laboratory, Prepared under Contract AF 28(099)-90 (June, 1950). UNCLASSIFIED

7. K. M. Siegel, H. A. Alperin, J. W. Crispin, H. E. Hunter, R. E. Kleinman, W. C. Orthwein, and C. E. Schensted, "Studies in Radar Cross-Sections IV--Comparison Between Theory and Experiment of the Cross-Section of a Cone," UMM-92, Willow Run Research Center, Engineering Research Institute, University of Michigan (February, 1953). UNCLASSIFIED

REFERENCES (Continued)

Number

8. W. W. Granneman, C. W. Horton, and R. B. Watson, "Diffraction of Electromagnetic Waves by a Metallic Wedge of Acute Dihedral Angle," Presented at the 1954 Austin (Texas) Meeting of the American Physical Society, February 26-27, 1954.

9. V. Fock, "The Field of a Plane Wave Near the Surface of A Conducting Body," Journal of Physics, Vol. X, pp. 399-409 (1946).
"The Distribution of Currents Induced by a Plane Wave on the Surface of a Conductor," Journal of Physics, Vol. X, pp. 130-136 (1946).

10. F. Oberhettinger, "Diffraction of Waves by A Wedge," Communications on Pure and Applied Mathematics, Vol. VII, pp. 551-563 (1954).

11. W. Gröbner and N. Hofreiter, Integraltafel, zweiter teil, Springer-Verlag (1950).

12. W. Franz and K. Depperman, "Theory of Diffraction by A Cylinder As Affected by the Surface Wave," Annalen der Physik, 10, 361 (1952).

13. W. Franz, "On The Green's Functions of the Cylinder and Sphere," Zeitschrift für Naturforschung, 9a, pp. 705-716 (1954).

14. G. Walters, "Final Engineering Report on Effect of Polarization of the Radar Return from Ground Target and Rain," Dalmo-Victor--R-135-697(AF-20926) (30 May 1952). CONFIDENTIAL

15. S. D. Wanlass, G. Tanielian, D. M. Jacob, "X-Band Radar Cross-Section Measurements," Hughes Aircraft Company, TM 371 (1 August 1954). CONFIDENTIAL

REFERENCES (Continued)

Number

16. K. M. Siegel, H. A. Alperin, R. R. Bonkowski, J. W. Crispin, A. L. Maffett, C. E. Schensted, and I. V. Schensted, "Studies in Radar Cross-Sections VIII--Theoretical Cross-Sections as a Function of Separation Angle Between Transmitter and Receiver at Small Wavelengths," UMM-115, Willow Run Research Center, Engineering Research Institute, University of Michigan (October 1953). UNCLASSIFIED

17. R. R. Bonkowski, C. R. Lubitz, and C. E. Schensted, "Studies in Radar Cross-Sections VI--Cross-Sections of Corner Reflectors and Other Multiple Scatterers at Microwave Frequencies," UMM-106, Willow Run Research Center, Engineering Research Institute, University of Michigan (October 1953). UNCLASSIFIED

18. Private communication from Mr. William R. Hutchins, Radar and Missile Division, Raytheon Manufacturing Company, Boston, Massachusetts.

DISTRIBUTION LIST

COPY NO.	
1-2	Commander, Wright Air Development Center ATTN: WCLRE-5, R. Rawhouser Wright-Patterson Air Force Base, Ohio
3-12	Commander, Wright Air Development Center ATTN: WCSG, Major F. Porter Wright-Patterson Air Force Base, Ohio
13	Commander, Wright Air Development Center ATTN: WCLRC-1, G. W. Schivley Wright-Patterson Air Force Base, Ohio
14	Commander, Wright Air Development Center ATTN: WCLGB, A. L. Brothers Wright-Patterson Air Force Base, Ohio
15	Commander, Wright Air Development Center ATTN: WCOSI Wright-Patterson Air Force Base, Ohio
16	Commander, Wright Air Development Center ATTN: WCSB, J. S. McCollom Wright-Patterson Air Force Base, Ohio
17	Commander, Wright Air Development Center ATTN: WCSM, P. R. Doty Wright-Patterson Air Force Base, Ohio
18	Commander, Wright Air Development Center ATTN: WCSM, J. A. Walker Wright-Patterson Air Force Base, Ohio
19	Commander, Wright Air Development Center ATTN: WCSM, J. R. Korosei Wright-Patterson Air Force Base, Ohio
20	Commander, Wright Air Development Center ATTN: WCSP, E. B. Bell Wright-Patterson Air Force Base, Ohio
21	Commander, Air Materiel Command ATTN: ATIAE, R. L. James Wright-Patterson Air Force Base, Ohio
22	Commander, Wright Air Development Center ATTN: WCLRO, Major G. J. Akerland Aircraft Radiation Laboratory Wright-Patterson Air Force Base, Ohio

DISTRIBUTION LIST (Continued)

COPY NO.	
23	Commander, Wright Air Development Center ATTN: WCLRD, G. B. Fanning Wright-Patterson Air Force Base, Ohio
24	Director of Research and Development Headquarters, USAF ATTN: AF-DRD-EL Washington 25, D. C.
25	Commander, Air Research and Development Command ATTN: RDDE, Major D. L. Deal P. O. Box 1395, Baltimore 3, Maryland
26	Commander Rome Air Development Center ATTN: Research Library, RCRES-4C Griffiss Air Force Base, Rome, New York
27	Commander, U. S. Naval Air Missile Test Center ATTN: L. S. Marquardt Point Mugu, California
28	Commander, Air Force Cambridge Research Center ATTN: CRRDG, Ralph Hiatt L. G. Hanscom Field, Bedford, Massachusetts
29	Commander, Air Force Cambridge Research Center ATTN: Electronics Research Library L. G. Hanscom Field, Bedford, Massachusetts
30	Commander, U. S. Naval Air Missile Test Center ATTN: Stanley R. Radom Point Mugu, California
31	Commander, Air Force Cambridge Research Center ATTN: CRRDG, Nelson A. Logan L. G. Hanscom Field, Bedford, Massachusetts
32	Commander, Air Force Cambridge Research Center ATTN: CRRDG, C. J. Sletten L. G. Hanscom Field, Bedford, Massachusetts
33	Commander, Air Force Cambridge Research Center ATTN: CRRDA, R. M. Barrett L. G. Hanscom Field, Bedford, Massachusetts
34	Commander, Air Force Missile Test Center ATTN: A. R. Beach Patrick Air Force Base, Cocoa, Florida

DISTRIBUTION LIST (Continued)

COPY NO.	
35	Commander, Holloman Air Development Center ATTN: Operation and Project Center Alamogordo, New Mexico
36	Research and Development Board, Library Branch Information Offices ATTN: W. H. Plant RE. E1065, The Pentagon Washington 25, D. C.
37	Commander, Rome Air Development Center ATTN: RCECC-1, Louis F. Moses Griffiss Air Force Base, Rome, New York
38	Commander, Air Force Armament Center ATTN: A. J. Wilde Eglin Air Force Base, Florida
39	Commander, Air Proving Ground Command ATTN: Class. Tech. Data Br. D/01 Eglin Air Force Base, Florida
40	Commander, Strategic Air Command ATTN: Operations Analysis Office Offutt Air Force Base, Nebraska
41	Commander, Headquarters Central Air Defense Force Post Office Box 528 Kansas City, Missouri
42	Director, Air University Req. CR-3998 Maxwell Air Force Base, Alabama
43	Commander, Rome Air Development Center ATTN: RCER, Morris Handlesman Griffiss Air Force Base, Rome, New York
44	Commander, Rome Air Development Center ATTN: RCDE, Joseph Vogelman Griffiss Air Force Base, Rome, New York
45	Dr. George Adomian, Member Special Studies Group Analysis and Planning Section, Systems Laboratories Hughes Aircraft Company, Culver City, California

DISTRIBUTION LIST (Continued)

COPY NO.	
46	Director, Naval Research Laboratory ATTN: John E. Meade, Code 5340 Washington 25, D. C.
47	Director, Naval Research Laboratory ATTN: W. S. Ament, Code 5278 Washington 25, D. C.
48	Chief, Bureau of Ships, Department of the Navy ATTN: Code 816 Washington 25, D. C.
49	Chief, Bureau of Aeronautics, Department of the Navy ATTN: Electronics Division Washington 25, D. C.
50	Bureau of Aeronautics, Central District ATTN: Electronics Division Wright-Patterson Air Force Base, Ohio
51	Chief, Bureau of Ordnance, Department of the Navy ATTN: Code AD-3 Washington 25, D. C.
52	Chief of Naval Operations, Department of the Navy ATTN: OP-42-B2 Washington 25, D. C.
53	Commanding Officer and Director U. S. Navy Electronics Laboratory San Diego 52, California
54	Commander, U. S. Naval Air Development Center ATTN: Electronics Laboratory Johnsville, Pennsylvania
55	Commander, U. S. Naval Ordnance Laboratory Silver Spring 19, Maryland
56	Commander, U. S. Naval Ordnance Test Station, Inyokern China Lake, California
57	Commander, Rome Air Development Center ATTN: Harry Davis, Technical Director - RCT Griffiss Air Force Base, Rome, New York
58	Chief Signal Officer, Department of the Army ATTN: Engineering Technical Division Washington 25, D. C.

DISTRIBUTION LIST (Continued)

COPY NO.	
59	Department of the Army, Office of Chief of Ordnance ATTN: ORDTU, Capt. W. O. Fuller Washington 25, D. C.
60	Massachusetts Institute of Technology Project Lincoln, Lincoln Laboratory ATTN: V. A. Nedzel Post Office Box 73, Lexington 73, Massachusetts
61	Hughes Aircraft Company Research and Development Laboratories ATTN: C. H. Wilcox Culver City, California
62	Cornell Aeronautical Laboratory, Incorporated ATTN: R. Kell Buffalo, New York
63	Commander, Signal Engineering Laboratory ATTN: Technical Documents Center Fort Monmouth, New Jersey
64	Cornell Aeronautical Laboratory, Incorporated ATTN: George Richmond Buffalo, New York
65	Document Room, Project Lincoln Massachusetts Institute of Technology ATTN: Ethel R. Brans P. O. Box 390, Cambridge 39, Massachusetts
66	Massachusetts Institute of Technology ATTN: Dr. Dan Dustin, Lincoln Laboratory P. O. Box 73, Lexington 73, Massachusetts
67	Massachusetts Institute of Technology ATTN: I. Shapiro, Lincoln Laboratory P. O. Box 73, Lexington 73, Massachusetts
68	Commander, Air Defense Command ATTN: Major Richard J. Lloyd Colorado Springs, Colorado
69	Ohio State University Research Foundation ATTN: Dr. A. Fouty 310 Administration Building, Ohio State University Columbus 10, Ohio

DISTRIBUTION LIST (Continued)

COPY NO.	
70	Radiation, Incorporated ATTN: M. Cox Melbourne, Florida
71	The University of Texas Electrical Engineering Research Laboratory ATTN: Dr. A. W. Straiton Box 8026, University Station, Austin 12, Texas
72	Franklin Institute Laboratories 20th St. Benjamin Franklin Parkway ATTN: Dr. S. Charp Philadelphia 3, Pennsylvania
73	Boeing Airplane Company ATTN: R. H. Jewett Seattle 14, Washington
74	Hughes Aircraft Company Research and Development Laboratories ATTN: D. Adcock Culver City, California
75	Hughes Aircraft Company Research and Development Laboratories ATTN: Dr. L. L. Bailin Culver City, California
76	Hughes Aircraft Company Research and Development Laboratories ATTN: Dr. N. Begovich Culver City, California
77	Hughes Aircraft Company Research and Development Laboratories ATTN: R. S. Wehmer Culver City, California
78	The Rand Corporation ATTN: Dr. John L. Hult 1500 4th Street, Santa Monica, California
79	The Rand Corporation ATTN: Dr. Sidney Bertram, Electronics Division 1500 4th Street, Santa Monica, California

DISTRIBUTION LIST (Continued)

COPY NO.	
80	Ramo-Wooldridge Corporation ATTN: Dr. F. S. Manov 8820 Bellanca Ave., Los Angeles 45, California
81	Stanford University ATTN: Professor L. I. Schiff, Physics Department Palo Alto, California
82	University of Tennessee ATTN: Professor F. V. Schultz Knoxville 16, Tennessee
83	University of California ATTN: Professor Samuel Silver Electrical Engineering Department Berkeley 4, California
84	Philco Radio Corporation ATTN: B. D. Steinberg--Project Engineer Philadelphia 34, Pennsylvania
85	Electronics Defense Laboratory ATTN: Dr. V. Twersky P. O. Box 205, Mountain View, California
86	Bell Telephone Laboratory ATTN: Dr. Allen B. Currie Whippany, New Jersey
87	Ramo-Wooldridge Corporation ATTN: Dr. S. Ramo 8820 Bellanca Ave., Los Angeles 45, California
88	Ramo-Wooldridge Corporation ATTN: Dr. B. Wieland 8820 Bellanca Ave., Los Angeles 45, California
89	Cornell Aeronautical Laboratory, Incorporated ATTN: Dr. Robert A. Wolf Buffalo, New York
90	Georgia Institute of Technology State Engineering Experimental Station Atlanta, Georgia
91	Standard Rolling Mills, Incorporated ATTN: Vincent Lane 196 Diamond Street, Brooklyn 22, New York

DISTRIBUTION LIST (Continued)

COPY NO.	
92	The Johns Hopkins University ATTN: Dr. D. D. King--Radiation Laboratory 1315 St. Paul Street, Baltimore, Maryland
93	The Johns Hopkins University ATTN: E. M. Glaser--Radiation Laboratory 1315 St. Paul Street, Baltimore, Maryland
94	Massachusetts Institute of Technology Research Laboratory of Electronics ATTN: Dr. L. J. Chu Cambridge, Massachusetts
95	Lockheed Missile System Division, Dept. 75-31 7701 Woodley Ave., Van Nuys, California
96	Ryan Aeronautical Company ATTN: J. R. Giantvalley Lindbergh Field, San Diego 12, California
97	Convair, A Division of General Dynamics Corporation ATTN: Orison Wade--Engineering Department San Diego, California
98	Operational Research Group ATTN: G. R. Lindsay Defense Research Board Ottawa, Ontario, Canada
99	McGill University ATTN: Professor G. A. Woonton Eaton Electronics Laboratory Montreal, Quebec, Canada
100	Sylvania Engineering Laboratory ATTN: Dr. L. S. Scheingold 70 Forsythe Street, Boston, Massachusetts
101	William R. Hutchins Raytheon Manufacturing Company Missile and Radar Division Hartwell Road Bedford, Massachusetts
102	Dr. R. S. Elliott Research and Development Laboratories Hughes Aircraft Company Culver City, California